AUTOMATED ASSEMBLY OF LARGE COMPOSITE PREFORMS FOR REINFORCEMENT APPLICATIONS IN AEROSTRUCTURES

A thesis submitted for the degree of Doctor of Philosophy

bY

Tarik Mohamed Tewfic

Department Of Design and Systems Engineering
Brunel University

January 2004

PAGE NUMBERING AS ORIGINAL

Abstract

There is considerable interest in the use of textiles, which are known as dry fabrics, for the construction of structural preforms of varying complexity.

Cost reduction is a key factor in the future expansion of textiles and this can, to a great extent, be achieved by automation of the preform assembly process. Non-Crimp-Fabrics (NCF) offer significant potential for the process automation, due to an increased deposition rate and high structural performance.

This work is focused on the development of a novel methodology which can be used to generate a fully integrated automation cell to produce three-dimensional (3D) components.

Aautomation technique has been developed, which enables large reinforcement structures of I,C,J, and T shape to be readily produced for subsequent forming into required shapes when loaded into the mould. The preform is produced as a single piece, to reduce associated assembly and handling times.

The proposed technique has been realised in design and implemented as a novel tool for forming the three-dimensional components in a single stroke for the aerospace applications. The resulting tool has been integrated into a fully automated manufacturing cell, providing an opportunity for a successful proof of principle application of such a device.

The automated manufacturing cell has an integrated by robotic tacking device (RTD) which helps to produce preforms with a high degree of accuracy, where the fabrics are arranged in the required format to match the service loading of the component. Mechanical tests and numerical analyses have been conducted on a typical I-beam section to investigate the effects of both tacking position and the loading conditions on the consolidated product. Numerical analyses investigations have produced largely encourage results.

Acknowledgements

All praise be to Allah

The author is very thankful to Professor M. Sarhadi for his supervision, guidance and great support through the course of this project. The author is also very grateful to Dr. H. Bahai, for his assistance and advice during this research.

Thanks are also expressed to the members of the systems engineering department, especially Mrs L Edgecock, Mrs L Hedges and Dr. B greives for their help during this project. The author also wishes to acknowledge the help of the technical staff in the systems and Mechanical engineering departments, especially Mr. B shaw and Mr Keith for their great assistance through the project.

The author's gratitude must also be expressed to all his friends and colleagues who have provided help and a friendly atmosphere through these years.

I would also like to express my deepest appreciation to both my father and mother for their endless prayers and support. I am also extremely grateful to all of my brothers, sister and my wife for their continuous encouragement and support.

Finally, to my wife, my daughter and my son for their support and patience through this work, my indebtedness is great.

Nomenclatures

AN	Acrylonitrile
CAD	Computer Aided Design
DMC	Dough Moulding Compounds
FE	Finite Element
FEA	Finite Element Analysis
FOSSIL	FOlding Shuttle for Shape Inclusive Lay-up
MDS	Material Delivery System
NCF	Non Crimp Fabric
NS	Non Stitched Samples
PAN	Polyacrylonitrile
PMC	Polymer Matrix Composite
RTD	Robotic Tacking Device
RTM	Resin Transfer Moulding
S	Stitched Samples
SEM	Scanning Electron Microscopic
SFS	Shape Forming Shuttle
SMC	Sheet Moulding Compounds
STD	Standard Deviation
TCP	Tool Centre Point
UAZ	Ultrasonically Assisted Z-fibre

Table of contents

List of figures

CHAPTER 4

CHAPTER 5

CHAPTER 6

CHAPTER 7

CHAPTER 9

List of tables

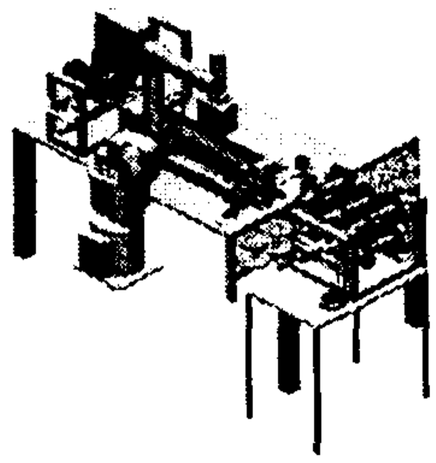

Chapter 1 Introduction

1.1 Background

Composite materials have a long history; among the earliest composites must surely be the simple straw and mud brick that continues to be used even today. The higher tensile strength of the straw binder overcomes the limitations of the friable clay matrix to give a durable building block.

Composites are different from metals. They are combinations of materials differing in composition or form. The constituents retain their identities in the composites and do not dissolve or otherwise merge completely into each other although they act together. Reinforced concrete is an excellent example of a composite structure in which the concrete and steel still retain their identities. The steel bars carry the tension loads and the concrete carries the compression loads. In aircraft construction the term composite structures refers to fabric resin combinations in which the fabric is embedded in the resin but still retains its identity.

Over the last two decades, the materials research community has experienced fast development and wide recognition of composite material technology. As a result, the potential adaptation of composite materials is moving beyond the boundaries of aerospace, as shown in, Figure1, and automobile industries. For example, composite materials are now being considered in taking a part in the role of structural materials for civil infrastructures. However, the development of a low cost, high volume, high quality fabrication process is a major issue that must be resolved before a composite material can be used as load carrying structural components in such applications. This issue implies that the application of composite

materials cannot be justified solely upon their superior material properties over those of traditional engineering materials. Rather, the advantages must be accompanied by proof of cost effectiveness.

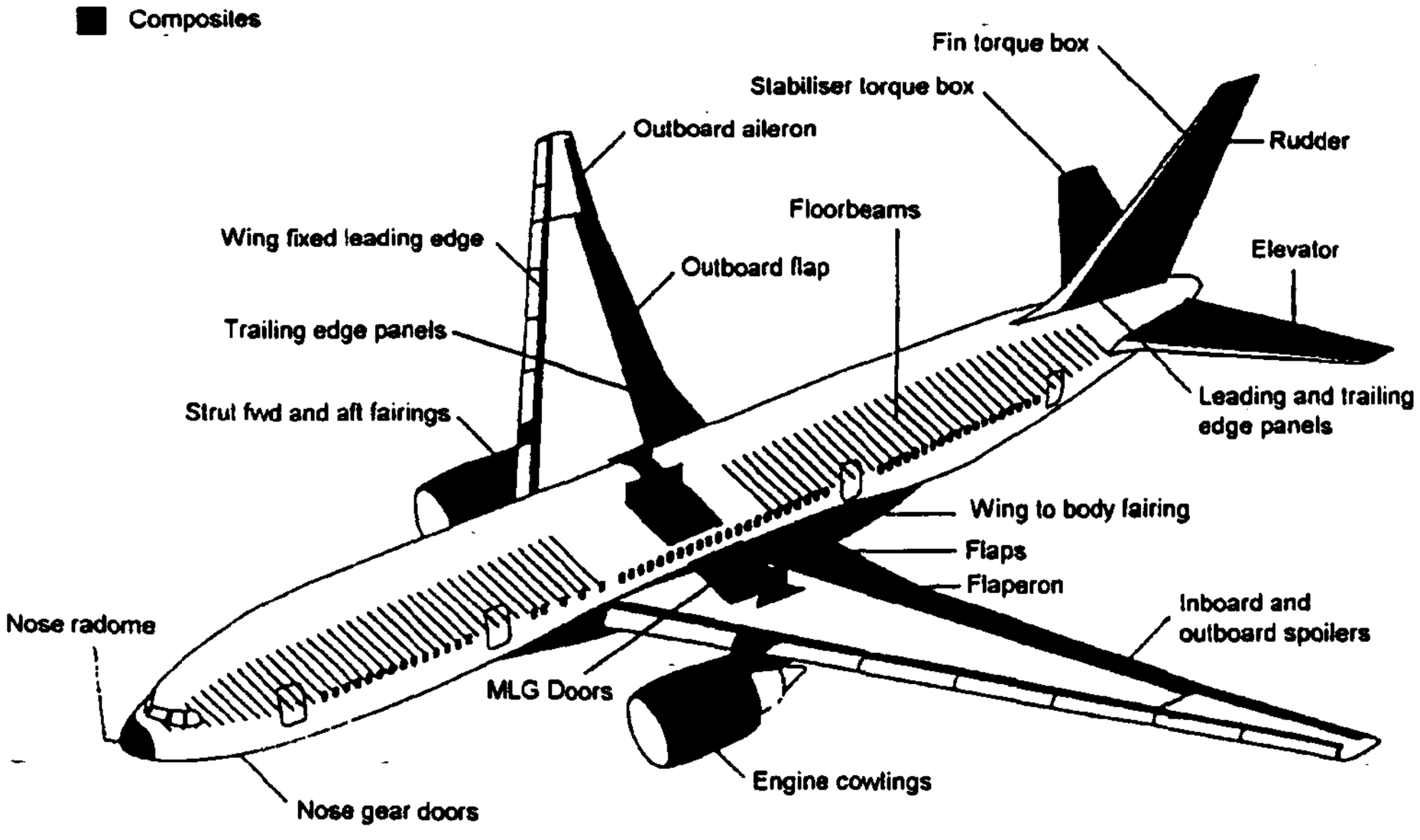

Boeing B777

Figure1.1 Diagram illustrate the various components of the Boeing B777 aircraft made of composite materials.

1.2 Advanced composite material

Carbon fibre reinforced epoxy resins are the most significant of all current composite materials, accounting for more than 90% of all composites presently specified for aircraft construction **[Middleton, 1990]**. This type of composite offers new design, fabrication and enhanced mechanical properties, which enables it to have wider applications in the future **[Smichumacher, et al., 1998]**. The aircraft manufacturers began to show increased interest in stitching as a way to achieve damage tolerance composite structures. This work presents a highly automated process that can be used to improve damage tolerance of the dry fabric, which known as non-crimp fabric (NCF). The developed automated cell utilises NCF material and this will create a potential benefits in the perform that include; reduce the material and assembly labour costs through the automated fabrication of the preforms; reduced machining and material scrap through use of near net

shape preforms; elimination of cold storage requirements and limits on shelf. Fast deposition rates with two or four layer formats and no need to remove backing paper; the drapability of the fabric can be influenced by the z-direction stitch type and material density to enable lay-up of components with severe or complex curvature **[Chestney, et al. 1996]**. The resulting composite component has near unidirectional performance, comparable to woven fabric **[Bibo, et al., 1997]**.

1.3 Problem definition

High performance composite components have been increasingly used in the aircraft industry. The European Fighter aircraft project has a projected utilisation of 35% composite components, whilst a weight saving of 800 kg has been achieved in the Airbus 320. The fin, tailplane, wing and rudder sections of these aircraft will all be manufactured from carbon composite materials.

The manufacture of these components involves the manipulation and lay-up of large size composite fabric pieces to a high degree of accuracy. Manual lay-up is the most extensive technique used for producing these components. Producing high volume fractions with this method requires debulking every five to ten layers adding considerable time to the lay-up process, 'Vacuum bagging' problems are also among the largest contributors to high scrap rates in composites **[Sarhadi, et al 1999]** and **[Ridell, 1987]**. Manual lay-up is independent of the skin structure, and requires the use of a mould tool. The consolidated structures are then bonded to the skin to produce the final composite structure.

Mould tools are expensive and are under utilised because of the lengthy lay-up process. There is an increasing interest in the use of Resin Transfer Moulding (RTM) method, especially with larger components, Figure1.1, (tailplanes, wing, bay doors). RTM is a lower cost approach, can produce a moulded finish on all faces of the component, and allows single process

moulding of complex components. RTM process employs resin-free materials (dry fabrics).

A range of technologies has been developed for cutting, handling and fixing **[Sarhadi, et al 1996], [Sarhadi, et al 1999]**, but a purely technological solution is insufficient when dealing with three-dimensional (3D) components; a methodology for implementing the technology for dry fabric preforms is required. This methodology should allow jigless manufacture of flat preforms, which can subsequently be formed into three-dimensional shapes when loaded into the mould. Furthermore, this should enable producing complex components as a single perform; reducing both preform production and moulding times.

This work is focused on the development of a novel methodology which can be used to generate a fully integrated automation cell to produce three-dimensional (3D) components.

1.4 Aims and Objectives

1.4.1 Aim

The aim of this project is to develop a novel methodology to enable preforms for 3D components to be produced and stored flat and introducing the shape only when the preform is loaded into the mould. The Ultimate aim is to apply the newly developed methodology to the design and implementation of a novel forming tool and integrate it into an automated manufacturing cell to enable the production of reinforcement structures for aerospace applications.

1.4.2 Objectives

In order to achieve the aims of this project the following objectives must be fulfilled:

1. To gain an up-to-date knowledge of the state of the art in the research topic by conducting a critical literature review.

2. To determine criteria for creation of a configurable devices and identify any limitations.
3. To develop a novel methodology which enable performs for 3D components to be produced and stored flat and introducing the shape only when the perform is loaded into the mould.
4. To carry out modelling and simulation tasks for the proposed manufacturing cell to achieve the right sequences for the cell elements and to determine the cycle time for the process.
5. To devise an effective automated manufacturing cell based on the developed methodology, allowing low cost, reliable performance to be achieved from configurable devices.
6. To conduct optimisation tasks to all cell components that would achieve the optimal cell performance.
7. To examine the mechanical properties of the cell final product.
8. To conduct numerical analytical studies using finite element analysis (FEA) to study the effect of joining technique that has been used on the reinforcement structure produced by the automated cell.
9. To verify the cell accuracy, reliability and repeatability using statistical analysis.

1.5 Introduction to thesis

Chapter 2: Provides a critical literature review for composite materials and all the techniques and technologies that have been used to produce products from these materials.

Chapter 3: Summarises the existing methods for fibre joining techniques used in composite materials to assess their suitability, as they stand, or modified, for joining structural components. The rest of the chapter discussed the methodologies used in the development of the forming tools. The various methods considered for manipulation and control of the material have been stated.

Chapter 4: Before the manufacturing cell is developed, a simulation has been done to study the performance of the manufacturing cell. The individual parts have been modelled and arranged as a manufacturing cell, to carry out the required tasks.

Programs for the robot and machines have been developed and written, to enable integration in the modelled cell. The modelled cell conducted with the programs for each element of the cell to simulate the manufacturing processes which will be later carried out by the real manufacturing cell.

Chapter 5: Presents the novel methodology that have been developed and applied to produce a new flexible manufacturing cell for composite preforms into which the novel forming tool is integrated. This is followed by a description of all the design and control aspects.

Chapter 6: Examines the capability of each component in the manufacturing cell in performing the required task(s) and offer appropriate modifications to achieve optimal cell performance.

Chapter 7: provides a statistical analysis studies to verify the accuracy, repeatability and reliability of the manufacturing cell. Uncertainty of measurement was conducted to eliminate the errors in the results.

Chapter 8: Provides details of experimental studies on examining the mechanical characteristics of the final product. Numerical analysis studies for the various reinforcement structures that have been produced from the automated manufacturing cell are provided. This is followed by a description of a generic modelling strategy for predicting the behaviour of such structural components. Finally Investigations of the effect of the stitching characteristics on the overall behaviour of the structural components are provided.

Chapter 9: Provides details of the conclusions drawn from the research work, and suggests potential areas for future research work. The results achieved are discussed in relation to the original objectives for the research.

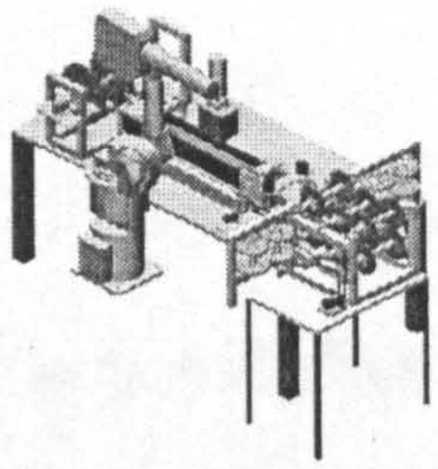

Chapter 2 literature survey

2.1 Introduction

The term composite refers to a material system consisting of two or more phases on a macroscopic scale, whose mechanical performance and properties are designed to be superior to those of the constituent materials acting independently. Modern composite materials constitute a significant proportion of the engineering materials market ranging from everyday products, such as steel reinforced concrete for buildings through to sophisticated niche applications like high performance ceramic armor designed to resist explosive impacts. Each type of composite brings its own performance characteristics that give it favors in selected applications. Most notably for fibre reinforced polymers they can be tailored to give high strength coupled with relatively low weight, corrosion resistance to most chemicals, and offer long term durability under most conditions of environmental exposure.

Composite materials can no longer be considered as exotic materials suitable only for niche applications where the performance demands justify very high prices, such as in aerospace or premium sporting goods markets. Today composite materials are starting to challenge that most ubiquitous of engineering materials, steel, in everyday applications as diverse as automobile bodies and civil infrastructure. It would be naive to suggest that it will displace steel from its dominant role; however, continuous advances in the manufacturing technologies and performance of composites have intensified the competition in a growing range of applications leading to significant growth in market acceptance, Figure 2.1.

2.1.1 A brief history of composite materials

The concept of composite materials is very old. Many historical references mentioned that the ancient Egyptians reinforced mud with straw to build straw-brick houses. Nature also provides us with a very versatile fibrous composite like wood, which has characteristics similar to those exhibited by modern advanced composite materials. Wood has been used for thousands of years as a structural material and at the beginning of this century engineers learned how to design aircraft structures using its unidirectional properties aligned in the direction of loading. Laminated plywood is typical of a composite with unidirectional fibre layers aligned in different directions to carry the loads applied.

The introduction of modern composite materials in manufacturing started in the beginning of the twentieth century with the production of phenolic resin reinforced with asbestos fibres. The first fibre glass boat was made in 1942. The development of the modern composites carried on and the emergence of high strength-to-weight continuous fibres expanded. The first boron and high strength carbon fibres were introduced in the early 1960s, with applications of advanced composites to aircraft components by 1968. Starting in the late 1970s applications of composites expanded widely to the aircraft, automotive, sporting goods, and biomedical industries. The 1980s marked a significant increase in high modulus fibre utilization. Now emphasis is being placed on development of newer carbon/carbon composites, for aircraft and aerospace structures, automotive components and many other products designed to have high mechanical performance and/or environmental stability coupled with low weight.

2.1.2 Advanced Composite Materials

The introduction of newer polymer resin matrix materials and high performance reinforcement fibres of glass, carbon and aramid has enabled a steady expansion in applications and volume. With increased volume has

come an expected reduction in costs. Composite materials can now be found in such diverse applications as the fuel cylinders of natural gas vehicles, the blades of wind-powered turbines, industrial drive shafts, the support beams of highway bridges and even paper making rollers. An examination of the diversity of some of these newer applications and the social and commercial pressures that underpin their introduction gives an instructive insight into the future place of Composite material.

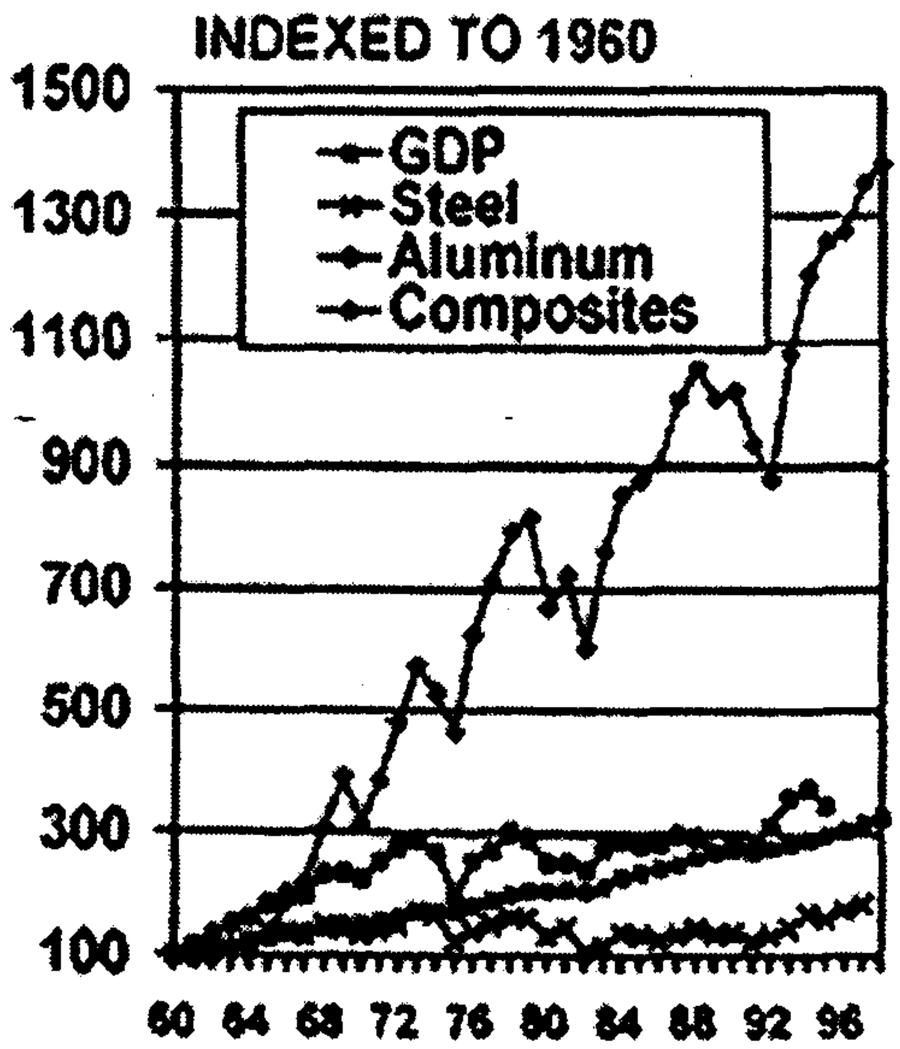

Figure 2.1 US Growth in composite shipments compared with aluminum and steel **[Long, 1998]**.

2.2 Composite Hybrids

Hybrids are made by the addition of some complementary material such as fibre glass or kevlar to the basic carbon fibre/epoxy matrix. The added materials are used to obtain specific material characteristics such as greater fracture toughness and impact resistance, and should be considered for areas subject to foreign object damage. The addition of carbon / epoxy to fibre glass structure is used to provide additional stiffness.

2.3 High Performance Fibre Reinforced Composites

Fibre Reinforced Composites combine the properties of two materials that retain their respective chemical and physical characteristics when combined together ,table 2.1, they allow the properties of each to be utilised to their greatest effect. The fibres discussed below are the main reinforcements being actively used today in high performance structures.

Table 2.1: Type of Composite Materials

Matrix type	Fibre	Matrix
Polymer	E-glass S-glass Carbon (graphite) Aramid (Kevlar) Boron	Epoxy Polyimide Plyester Thermoplastics (PEEK, polysulfone,etc.)
Metal	Boron Borsic Carbon (graphite) Silicon carbide Alumina	Aluminium Magnesium Titanium copper
Ceramic	Silicon carbide Alumina Silicon nitride	Silicon carbide Alumina Glass-ceramic Silicon nitride
Carbon	Carbon	Carbon

2.3.1 Glass Fibre

First manufactured in the United States in 1938. The fibres are produced by drawing molten borosilicate glass through 204 bushings at a time at a speed of 2 miles/minute; the bundle of 204 filaments, each filament being .0004"

diameter, is known as a 'fibre end'. The fibres are treated with a chemical size immediately after drawing to prevent mechanical damage and also act as a coupling agent to the plastic matrix in the finalised composite. There are two main types of glass fibre in use today:

2.3.1.1 E glass

The first glass developed specifically for the production of continuous fibres, and found adaptable and effective in a great variety of processes and products ranging from decorative to structural applications, E glass has become known as the standard textile glass.

2.3.1.2 S glass

A high strength glass with tensile strength 33% greater and modulus of elasticity 20% greater than E glass. Significant properties of S glass for aerospace applications are its high strength to weight ratio, its superior strength retention at elevated temperatures and a good fatigue limit, it has been applied to rocket motor cases, high performance aircraft parts and other areas where mechanical performance is a primary concern.

The main characteristics, which make glass fibre a good composite reinforcement, are:

- Perfect elasticity, deflection is directly proportional to load, i.e. it obeys Hooks Law.
- Good thermal proportion retains 50% of its strength at 350°C.
- Excellent moisture and corrosion resistance.
- Excellent dimensional stability.
- Low cost compared with other high strength fibre.

One main disadvantage glass fibre exhibits is its relatively low modulus of elasticity (approximately half that of aluminium alloys) when made into a composite, this feature has limited its application generally to secondary

structures as primary high performance structure are usually designed for stiffness as well as strength ,table 2.2,.

The low stiffness of glass fibre has led in recent years to the development of higher stiffness fibres, viz., boron, carbon, and kevlar49.

Table 2.2 Fibre reinforcement properties

Material	Density g/cm^3	Tensile Strength (MPa)	Elastic Modulus (GPa)
Carbon	1.75	3500	290
Kevlar	1.44	3500	131
E-glass	2.60	3400	72.5
S-glass	2.49	4480	85.6
Boron	2.60	3400	300

2.3.2 Boron Fibre

Was the first manufactured in the United States in 1950. It is produced by vapour plating boron onto a 0.0005" diameter tungsten filament giving a final diameter of 0.004". Boron fibre was the first high modulus, high strength fibre to be produced in quantity for aerospace applications but the cost was and still very high compared with other fibres, it has similar strength and stiffness properties to carbon fibre as shown in ,Table 2.2,.

Some advantages of boron over the other stiff fibres are its good toughness properties and its compatibility with some metals, and boron/ aluminium composites have shown good impact properties and tolerance of concentrated point loading. However these composites are expensive to fabricate and require sophisticated equipment. Machining of boron reinforced materials has proved very difficult and this, coupled with its high cost and other processing problems has lead to many composite material application

developments programs to change to carbon fibre with its similar stiffness properties.

2.3.3 Carbon Fibre

Carbon fibres are derived from one of two precursor materials:

1. Polyacrylonitrile (PAN) precursors.
2. Pitch precursors.

Acrylonitrile(AN), which is chemically produced, is used as raw material for manufacturing PAN. Today, approximately 90 percent of all commercial carbon fibres are produced from a PAN precursor fibre. Normally, PAN is copolymerized with a small amount of another monomer, such as methylacrylate, to lower its glass transition temperature and control its oxidation rate.

Normally, the conversion of PAN to carbon fibres is made in four continuous stages: -

- Oxidisation: In air at 250° C under tension to align the molecules.
- Carbonization: At temperatures ascending from 450 - 1100° C.
- Heat Treatment: To further align the molecules and give the desired stiffness and strength properties.

Surface Treatment: A chemical etching which improves the fibre to matrix bond, (this treatment is still under development as treated fibre composite possess a brittle characteristic which gives low impact properties, and a sensitively to stress concentrations).

PAN based carbon fibres are under continual development and are used in composites to make materials of great strength and lightness.

A Pitch can be produced by the thermal or catalytic polymerization of a suitable petroleum or coal tar Pitch. When a highly aromatic pitch, such as a decant oil Pitch, is heated to temperatures of 400 to 450° C for approximately 40 hr, 45 to 65 percent of it will transform from an isotropic material to an optically anisotropic liquid crystal. A free radical mechanism is believed to be responsible for polymerization of the carbonaceous material. Pitch based

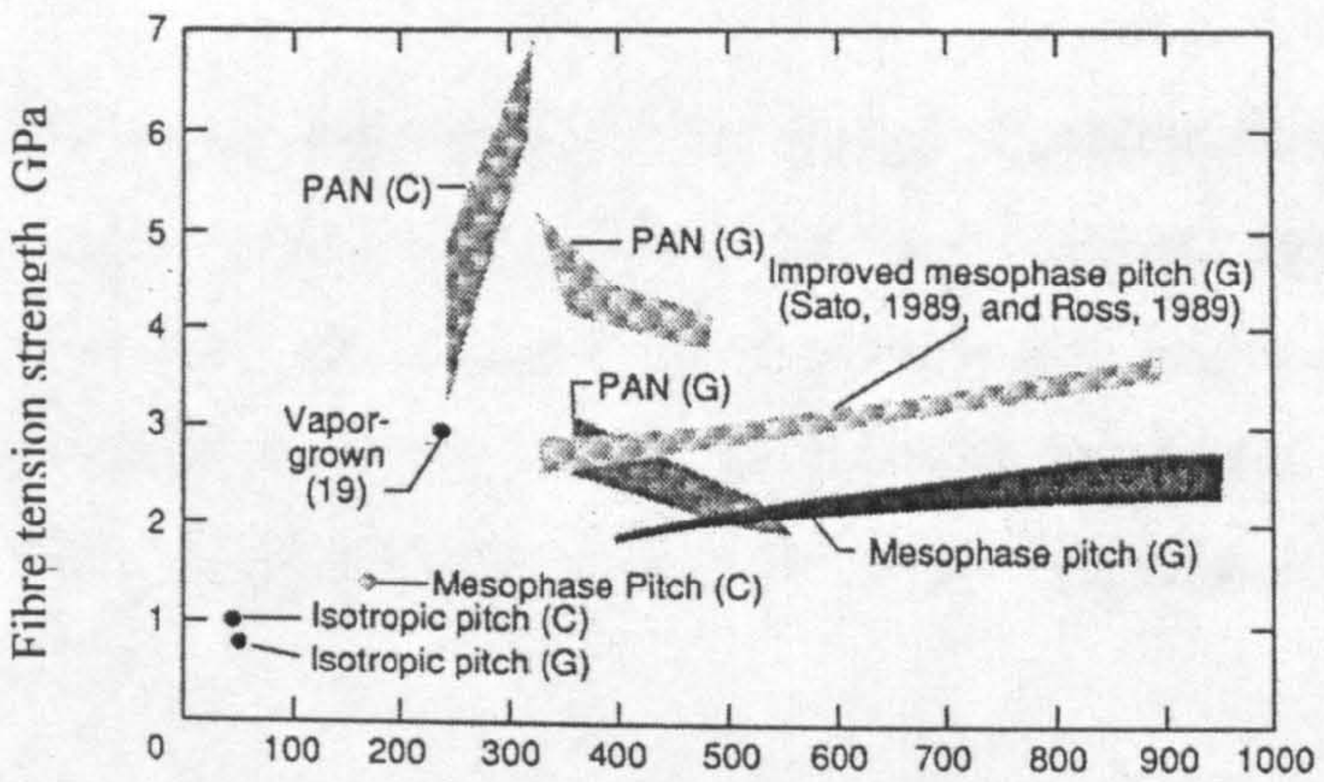

Figure 2.2 Tensile strength and modulus of various types of carbon fibres **[Tibbetts, 1990].**

carbon fibres ,Figure 2.2, have lower mechanical properties, therefor rarely used in critical structural applications **[Tibbetts, 1990].**

2.3.3.1 Carbon Fibre Properties and Applications

The properties, which make carbon fibre a very attractive reinforcement for high performance application, are:

- High modulus, some four times that of glass fibre.
- High strength.
- Good thermal properties, both temperature resistance and thermal conductivity.
- Excellent fatigue properties.
- Excellent dimensional stability.
- Fibres are electrically conductive.

- Moderate cost compared with other high modulus fibres.

Carbon fibres find extensive use in the many applications, this is due to the unique properties of such type of fibres, the use of lighter materials in aircraft construction allows for fuel savings or a greater payload, Carbon fibres are used extensively in both military and civil aircraft structures **[Bibo, et al, 1997].**

Carbon fibres are also unique in the range of properties that can be found, in this one generic type of material. As most carbon fibre manufactures are working in a state of constant development and improvement, the range of fibres now available to the structural engineer is always changing ,Table 2.3, present four classifications that have been reported by the manufacturers **[Edie, 1987]**.

In addition, because of their improved friction performance and high wear resistance, carbon fibres are used in high-performance brakes of aircraft and racing cars. Using the carbon/carbon composites in brakes of passenger cars and trucks were being evaluated in mid 80s **[Arnold, 1986].**

2.3.4 KEVLAR 49

A new aramid organic chemically produced fibre first in the United States in 1971, it is a middle of the road fibre with a stiffness twice that of glass and half that of carbon fibre. The tensile strength is much the same as glass and carbon fibre, Table 2.2, it has lower density (some two thirds of glass fibre) and very good toughness properties.

The use of kevlar fibre combined with glass and carbon fibres gives composites with much improved impact properties. It is very versatile fibre and has been used for interior panels and structural aircraft parts, facings for automobile clutch plates, for belts in tyres, cut resistant and bullet-proof clothing for military and police use, in combination with other fibres in boat hulls, skis and pressure vessels.

Table 2.3 Development of the range of carbon fibres **[Edie d. 1987]**

Type	Precursor	Density g/cm^3	Tensile Strength (MPa)	Elastic Modulus (GPa)
Low modulus	Pitch	1.8-1.9	1030-1380	140-170
Intermediate modulus	Pan	1.7-1.8	3100-3790	210-240
High Modulus	Pan	1.8-1.9	2210-2760	340-390
High Modulus	Pitch	1.9-2.0	1720-2070	340-380
Ultra High Modulus	Pan	1.9-2.0	1520-1860	480-520
Ultra High Modulus	Pitch	2.0-2.1	1720-2070	480-520
Ultra High Modulus	Pitch	2.1-2.2	1720-2070	690-724

The main property characteristics of kevlar 49 fibre are:

- High thermal stability with low combustibility.
- Low density compared with glass fibre.
- Good dielectric properties.
- High modulus and strength.
- Good fatigue properties.
- High cut resistance and toughness.
- Good dimensional stability in seawater, oils, solvents and other environments.

Its disadvantages are a low compressive strength and degradation in ultraviolet light, these problems are overcome by hybridisation with other fibres and the use of ultraviolet protective coatings or matrices **[hashim Z. 1983].**

2.4 MATRIX MATERIALS

In order to make a composite material the reinforcing fibres are combined with a matrix material, which must be compatible with the fibre, be easily processed, and offer good mechanical properties so as to maximise the potential fibre strength. Thermosetting polymers such as polyester and

epoxide resins, thermoplastics such as nylon and also metal are used as matrix materials for structural applications the thermosetting resins are commonly used.

2.4.1 Polyester Resin

This is the most widely used resin for glass reinforced plastics especially in the commercial field, and has the lowest cost, applications are numerous and include boats, large chemical engineering structures, storage tanks, aircraft panels and fairings. Composites using this resin have good corrosion resistance and dielectric properties, and are capable of withstanding temperatures up to 120°C. However, polyester resin has a high shrinkage during the moulding and curing cycle, which can give built in stresses and this together with a brittle nature lowers the fatigue capability for high performance applications.

2.4.2 Epoxide Resins

These resins possess several important properties, which make them unique; although some other resin types exhibit certain outstanding properties, none has the combination available in epoxides:

Curing conditions: Cure rapidly or slowly depending on the hardener system chosen or at any temperature from 5 to 180°C.

Low shrinkage: unlike polyester resins the epoxides exhibit very low shrinkage during cure (in the region of 1%).

Toughness: some six times tougher than polyester resins.

Mechanical Properties: high compared with other resins with excellent adhesive properties, good chemical resistance and dimensional stability.

Thermal Stability: show good temperature resistance and can be used at temperatures in the order of 200°C.

The combination of properties makes epoxides an ideal matrix for high performance composite material applications, and they are used for most glass, carbon, boron and Kevlar composite structures in aerospace applications. The composites produced with this resin exhibit good mechanical properties with excellent fatigue resistance and dimensional stability.

Despite their merits, resin matrices still inhibit the potential strength of composites, as they are an order of magnitude lower in strength than the reinforcing fibres. This relatively low matrix strength makes the introduction of point loading or a multiplicity of load connections to a composite structure difficult to achieve without addition of material and therefore weight, such weight increases negate the advantages of using the composite material.

2.4.3 Metals

In order to overcome the problem of the relatively weak matrix, efforts are being made to incorporate the fibres into light weight metal matrices, however processing difficulties have caused development to lag. In the United States primary emphasis has been on the development of boron aluminium composite, because the main problem (oxidation and degradation of the fibre during the high process temperature involved) has been easier to overcome with boron.

The method employed is to coat the boron fibre with silicone carbide, which make it insensitive to degrading reactions up to 1100°C in air and 600°C in aluminium alloys, this coated fibre know as BORSIC aluminium permits more flexibility in the fabrication techniques. Also a technique for producing a monolayer of equally spaced fibres on a backing of alloy foil bonded together by a plasma spry coating of the matrix alloy has been developed in the United States. The fabrication of shaped parts can be accomplished either by diffusion bonding or by a braze foil.

Although manufacturing costs for metal matrix composites are still high, development is continuing as also is research fibre reinforced in carbon fibre reinforced aluminium and other light weight metals.

2.4.4 Thermoplastics

Thermoplastics such as nylon and acetal resins have been successfully reinforced with short length (2.0 mm or less) glass and carbon fibres; the advantage for these materials is their ability to be injection moulded at a high production rate, i.e. tens of moulding per hour. However the properties of these materials are not in the same class as the other previously mentioned. Certain applications where the straight thermoplastic material showed a lack of stiffness or strength can now be met by these fibre reinforced materials.

2.5 Material Forms Available

2.5.1 Resins

Polyester and epoxide resins are supplied in liquid form and mixed with hardening agent prior to use. Hardening can be carried out to room temperature, but for most high performance types it is performed at elevated temperatures. The shelf life of most unmixed resins is in excess of a year.

2.5.1.1 Pre-Impregnated Fibre Sheet (Prepreg)

A combination of resin and fibre known as prepreg is now widely used in the aerospace industry.

The fibres that are preimpregnated with matrix resin and become ready to mould in sheet form or to wind in roving form, which may be cloth, mat, unidirectional fibre or paper impregnated with resin and stored for use. The dominant type of prepreg is tape which serves to hold the fibre together on the backing material. In aerospace applications automated machinery is most effective and plays a lead roll in production of the composite material, many of

these machines were designed to use tapes. The tapes have two unique techniques, unidirectional and multidirectional tapes, these types of prepreg have merits over the other types of prepreg fabric that they are not crimped or distorted as in others. ,Figure 2.3, Show the typical tensile property translation differences between tape and fabric prepreg.

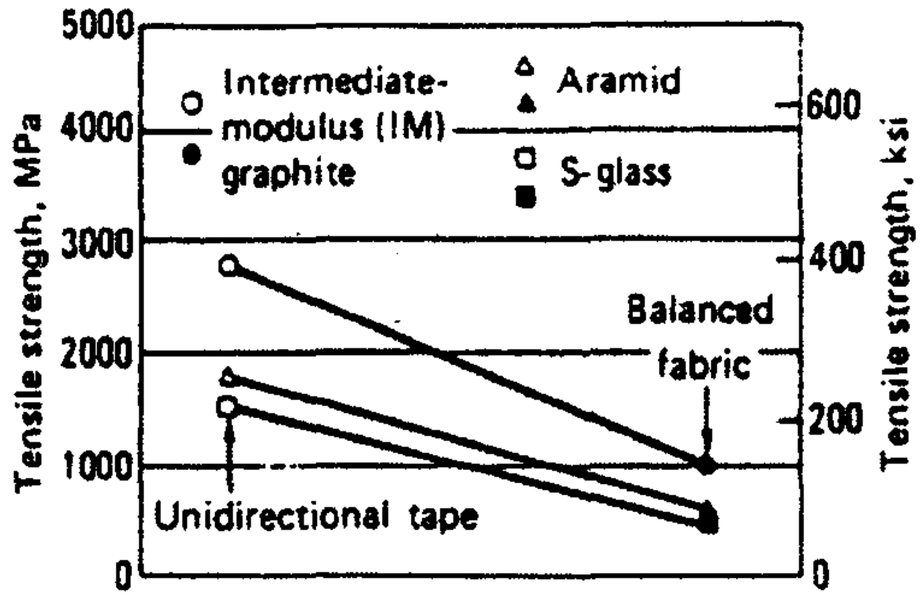

Figure 2.3 Tensile strength comparison - fibre-epoxy tape versus fabric

2.5.1.1.1 Unidirectional tape

Unidirectional tape is considered one of the most effective techniques used in composite material applications. This fabric is prepared by bringing a number of spooled tows into a collimated form then the prepreg operation of the tows starts by passing the tows in a heating material resin to obtain low viscosity and creating a well-dispersed fibre-resin mass. The amount of fibre can be controlled via the number of tows brought into the prepreg line, the resin can be cast onto the substrate paper through the prepreg line, the finished product, a thin sheet of fibre reinforced resin is packed and stored.

Unidirectional tape has the flexibility to use with many manufacturing processes like hand lay-up, machine-cut patterns and automatic machine lay-up. Numerically controlled automatic tape-laying machines found a good response in aerospace industry, presently programming it to lay down plies of tape in the quasi-isotropic patterns required by most design applications. In addition to being able to lay-down plies in a little time and with reduced scrap, the use of robotics in the process can increase the consistency of the

pressure of the lay down and ply-to-ply separations. These advantages of automation play a major role when considering future technologies associated with manufacturing of composite products.

The advantages of automatic tape laying machines technology have major effect in two important factors, the first one is the product life of unidirectional prepreg tape and the second is economical effect, cheaper forms of composite material can be achieved.

The automated of the manufacturing technology will play a leading roll to reduce the overall manufacturing cost. **[Agarwol, et al, 1980],[Dexter,et al, 1996].**

2.5.1.1.2 Multidirectional tape prepreg

Multidirectional tape prepreg might be considered as special case of unidirectional tape, basically it is manufactured from layers of unidirectional tape, these layers oriented depending on the use of final product. These tapes are available in the same width and package size as unidirectional tape, but in a multidirectional tape up to four or five layers of tape are plied together to produce the end product. ,Figure 2.4, show the difference between the two types of tape. A key advantage of using the multidirectional tape, is a substantial reduction in the lay-up cost. **[lubin, 1982]**

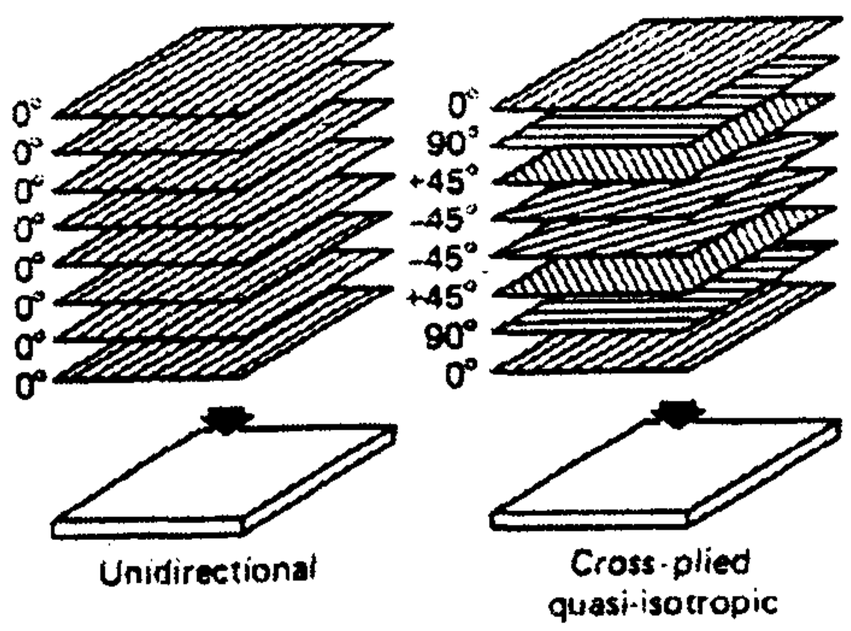

Figure 2.4 Unidirectional versus quase-isotriopic lay-ups

2.5.1.2 Fibre filled thermoplastics materials

Such as nylon 6.6 reinforced injection moulding compound; the methods employed for their use are identical to those for the basic thermoplastics material.

2.5.1.3 Sheet moulding compounds (SMC)

These are sheet materials composed of short length fibre preimpregnated with polyester or epoxide resin and partially cured; the sheets are cut roughly to size and loaded into a steel die where they are moulded under heat and pressure **[Hull, et al,1996]**.

2.5.1.4 Dough moulding compounds (DMC)

These are similar to sheet moulding compounds except that the material is supplied as impregnated dough or flock for moulding in a steel die under heat and pressure **[Mathews, et al 1994].**

2.5.2 Textile Material Forms

Textile material forms that have shown the highest potential for application to airframe structures. ,Table 2.4, indicates the properties of textile materials include: **[Dexter, 1996],[Bibo, etal, 1997].**

- 3-D woven Fabric
- 2-D braided preform
- 3-D braided preform
- low Crimp Uniweave
- 2-D woven Fabric
- multiaxial Warp Knit (NCF)

a. Unstitched

b. Stitched

2.5.2.1 Knitted fabric

The labour intensive requirements of manufacturing unidirectional prepreg tape laminates led to search for automated processes that give all the specifications of the unidirectional prepreg tapes technique but with reduced cost and high-volume production. One of such techniques that offer automated high volume production is the textile process. The sort of textile, which has a particular interest in these investigations, as mentioned before in chapter 1 is non-crimp fabric (NCF). Non-crimp fabric are produced by two methods:

1 weft knitted process.

2 warp knitted process.

2.5.2.1.1 Weft knitted fabrics

Weft knitted fabrics are produced by intermeshing loops under computer control substantially across the width of the fabrics. It mostly consists of 4-plies with ply orientations of (0°,90°,$\pm\theta$) with θ ranging from 30° to 60°, the machine which used to produce the weft knitted fabric can produce fabrics up to 1.6m wide at rate of 45 m/h **[Ko, et al, 1988]** The unique features of weft knit fabrics are the flexibility when additional reinforcement is needed in the 0° and 90° directions. The most problem with the Weft knitted fabrics structures is their bulkiness, which leads to reduced of the volume fraction compared with other fabric preforms **[Ko, et al, 1986]**

2.5.2.1.2 Warp knitted fabrics

Warp knitted fabrics are also produced by intermeshing loops under computer control but substantially along the length of the fabrics. The warp knitted fabrics system consists of warp, weft and bias (0°, 90°,$\pm\theta$) with θ ranging from 30° to 60°. It can produce in variety of structures such as uniaxial, biaxial, multiaxial yarns. This textile system is unique since it is utilising polyester or aramide yarns that bind the individual plies of the fabric together, thus yielding an equal quantity of fibre in the bias directions. The major distinction of these

Table 2.4 Textile reinforced composite materials for aircraft structures

Textile Process	Advantages	limitations
3-D Woven Fabric	Moderate in-plan and out-of-plan properties. Automated Preform fabrication process. Limited Woven shapes possible.	Limited tailorability for off-axis properties. Poor drapability.
2-D Braided Preform	Good balance in off-axis properties. Automated Preform fabrication process. Well suited for complex curved shapes. Good drability.	Size limitation due to machine availability. Low out-of-plane properties.
3-D Braided Preform	Good balance in in-plane and out-of-plane properties. Well suited for complex shapes.	Slow preform fabrication process. Size limitation due to machine availability.
Low Crimp Uniweave	High in-plan properties. Good tailorability. Highly Automated Preform fabrication process.	Low transverse and out-of-plane properties. Poor fabric stability. Labour intensive ply lay-up.
2-D Woven Fabric	Good in-plane properties. Good drability. Highly Automated Preform fabrication process. Integrally woven shapes possible. Suited for large area coverage.	Limited tailorability for off-axis properties. Low out-of-plane properties.
NCF (Unstitched)	Good tailorability for balanced in-plane properties. Highly Automated Preform fabrication process. Multi-layer high throughput material suited for large area coverage.	Low out -of-plane properties.
NCF (stitched)	Highly Automated process. Provides excellent damage tolerance and out-of-plane strength. Excellent assembly aid.	Small reduction in in-plane properties. Poor accessibility to complex curved shapes.

fabrics are the linearity of the bias yarns, the number of axis and the precision of stitching process **[Shaurt, 1985], [Raz, et al, 1990],[Lyer, 1992].**

The development of non crimp fabrics has attracted major interest from the manufacturer. Three different techniques are now available for manufacturing its. Two of them are known as Karl Mayer system, Figure 2.5, and the third is Liba (Hexel), Figure 2.6.

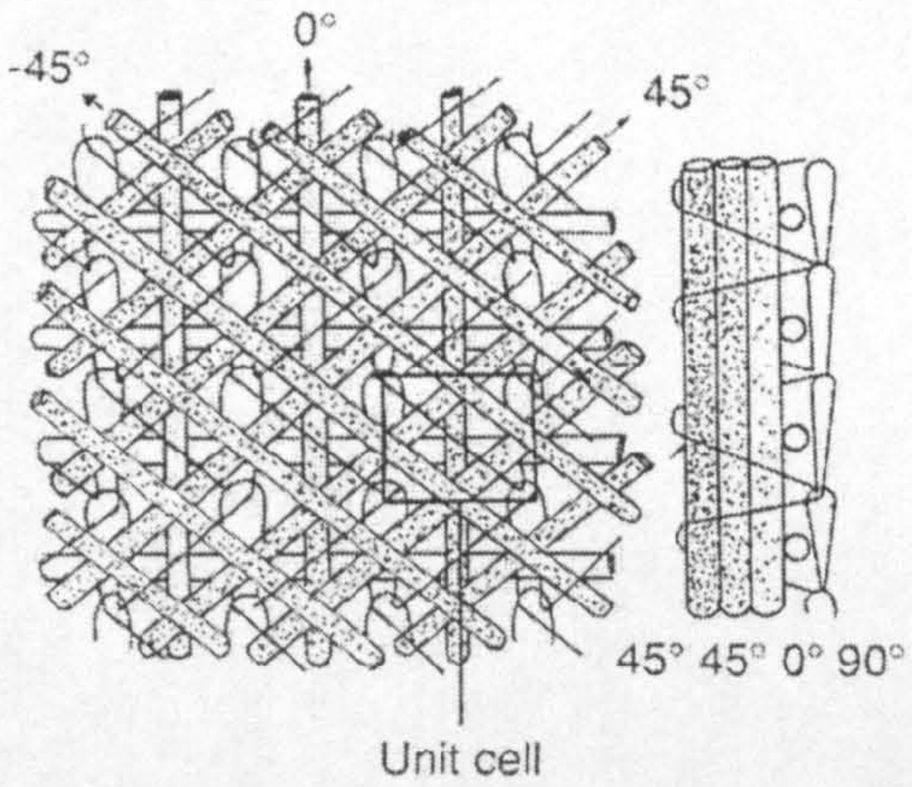

Figure 2.5 Multiaxial warp-knit fabric (stitched & unstitched) **[Dexter, 1996]**

These systems have almost similar methods with subtle differences between the two techniques. In both systems the pointed compound needles have to pierce through the different yarn layers to form the stitch structure to hold them together, whilst in the Mayer system, the needles do not damage the filaments, as they are laid in between the needles in an orderly manner. In the Liba technique the threads in the weft and diagonal directions are laid absolutely parallel and at fixed angles to one another **[Lyer, 1992], [Dexter, 1996].**

Non crimp fabrics exhibit improved mechanical properties compared with prepreg technique ,Figure 2.7,. The moduli for the NCF with E90sl resin are

slightly higher than those of prepreg tape laminates. These variations are attributed to volume fraction variations.

Compression stress of NCF laminates are compared with those of the prepreg laminates in ,Figure 2.8, NCF laminates exhibite compression stress about 25% lower than those of prepreg tape laminates. This reduction attributed to fibre waviness, fibre damage, and gaps between carbon fibre tows .The analytical results indicated that fibre waviness is a major contribution to initiation of fibre microbuckling under compression loading. However, NCF laminates exhibited compression after impact stress up to 80% higher than those of prepreg tape laminates as shown in, Figure 2.9, **[Dexter, and 1996a].**

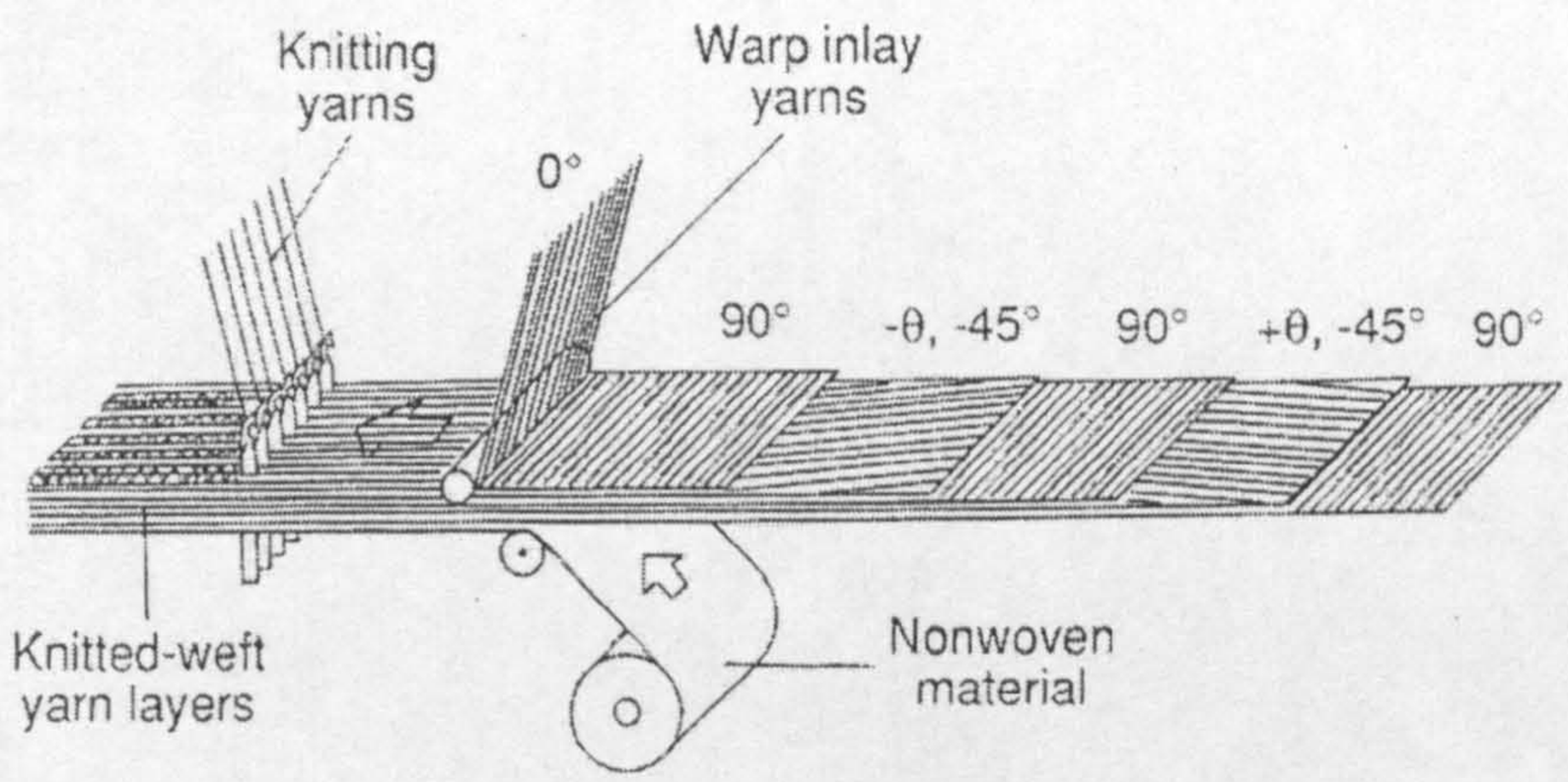

Figure 2.6 LIBA Multiaxal warp-knit fabric **[Ko,et al 1986]**

2.5.2.2 Chopped Fibre Matt

Continuous fibre is chopped into lengths in the order of 2" which are then deposited in a random manner with a resin compatible binder to form a matt, this gives material with an equal but reduced planer strength in all directions.

2.5.2.3 Chopped Fibres
These are available in a variety of lengths for reinforcement of thermoplastic and thermosetting plastic materials.

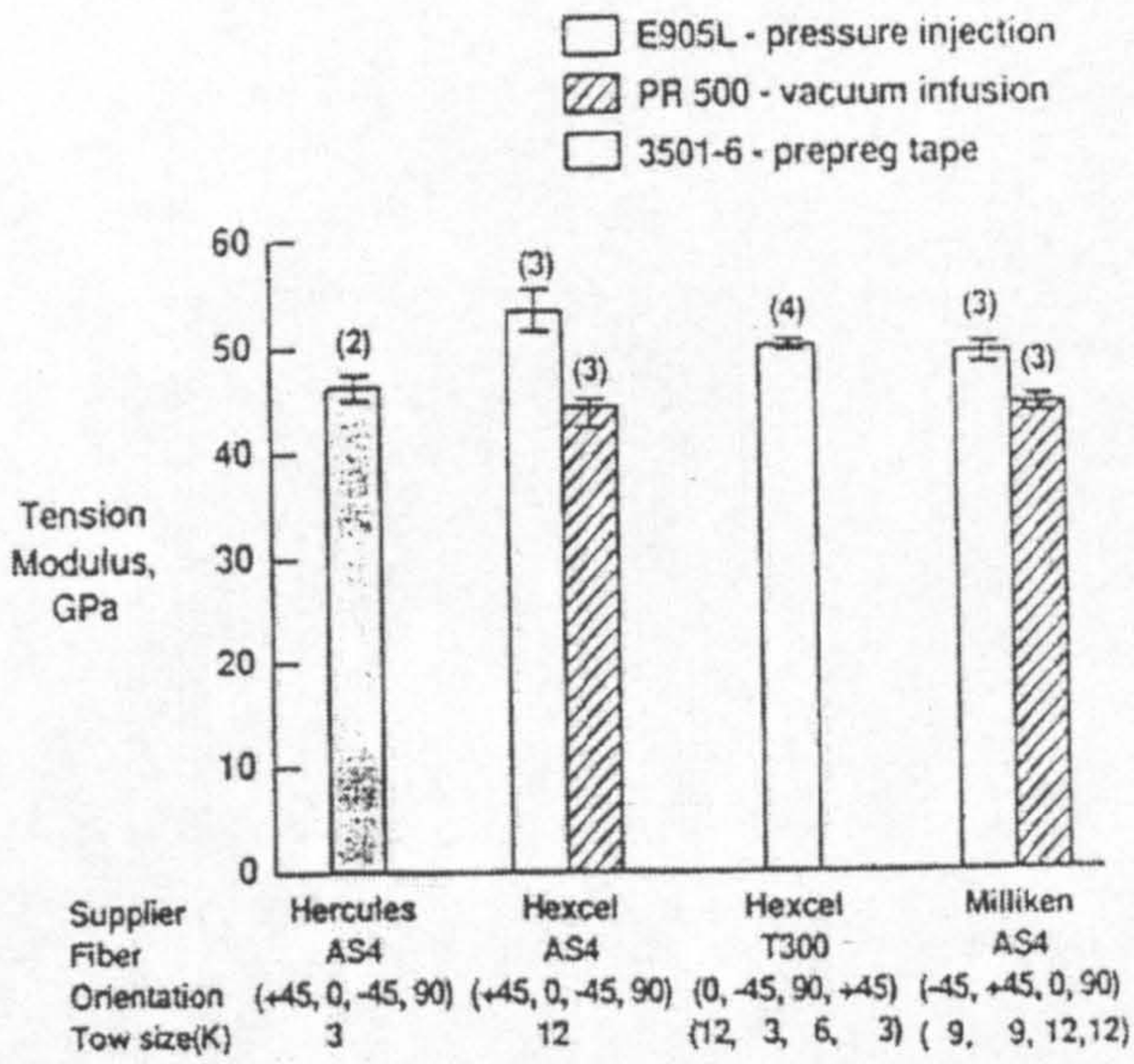

Figure 2.7 Tension moduli of NCF composites and prepreg tape laminates **[Dexter et al, 1996a]**

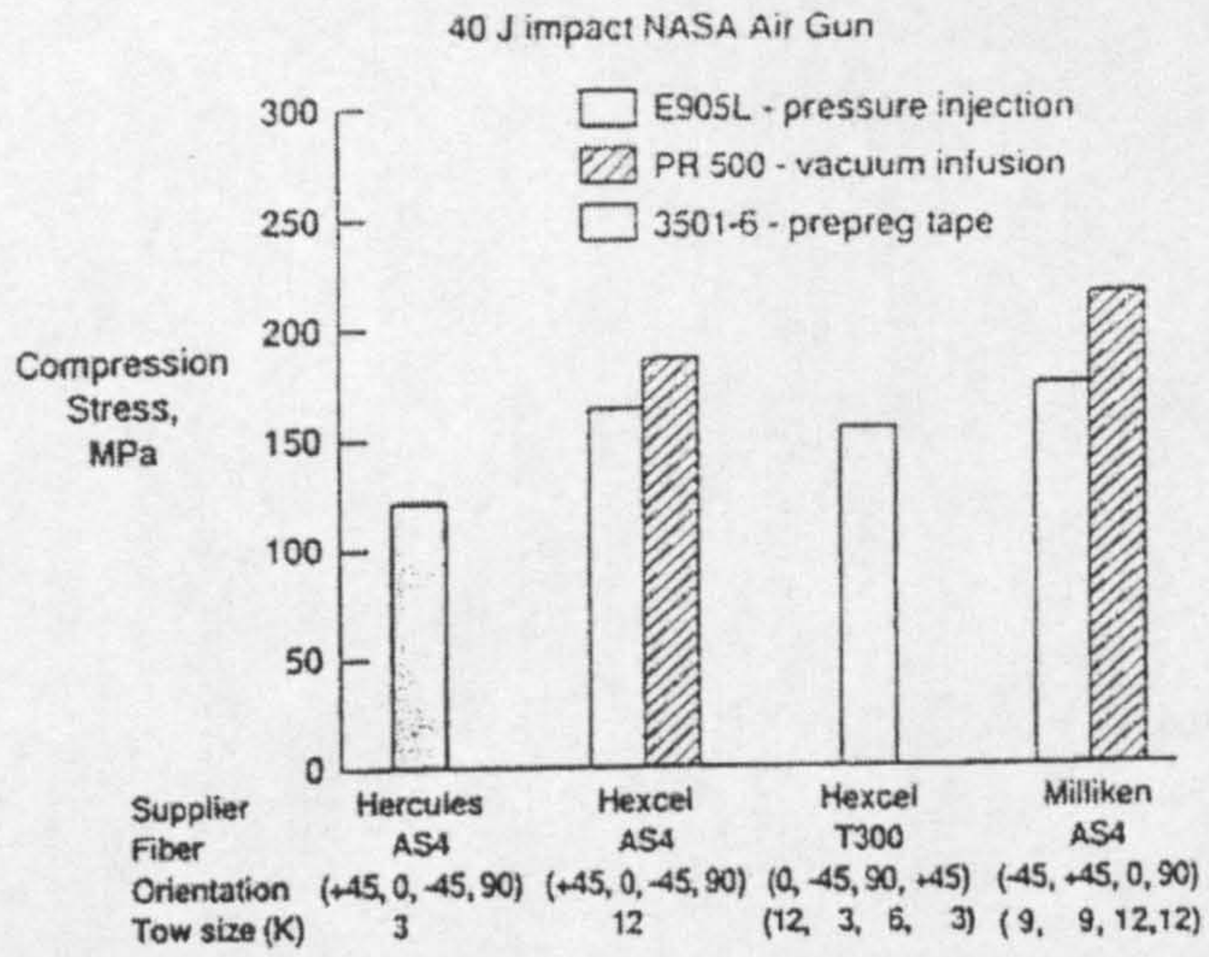

Figure 2.8 Compression stress of NCF composites and prepreg tape laminates. **[Dexter et al, 1996a]**

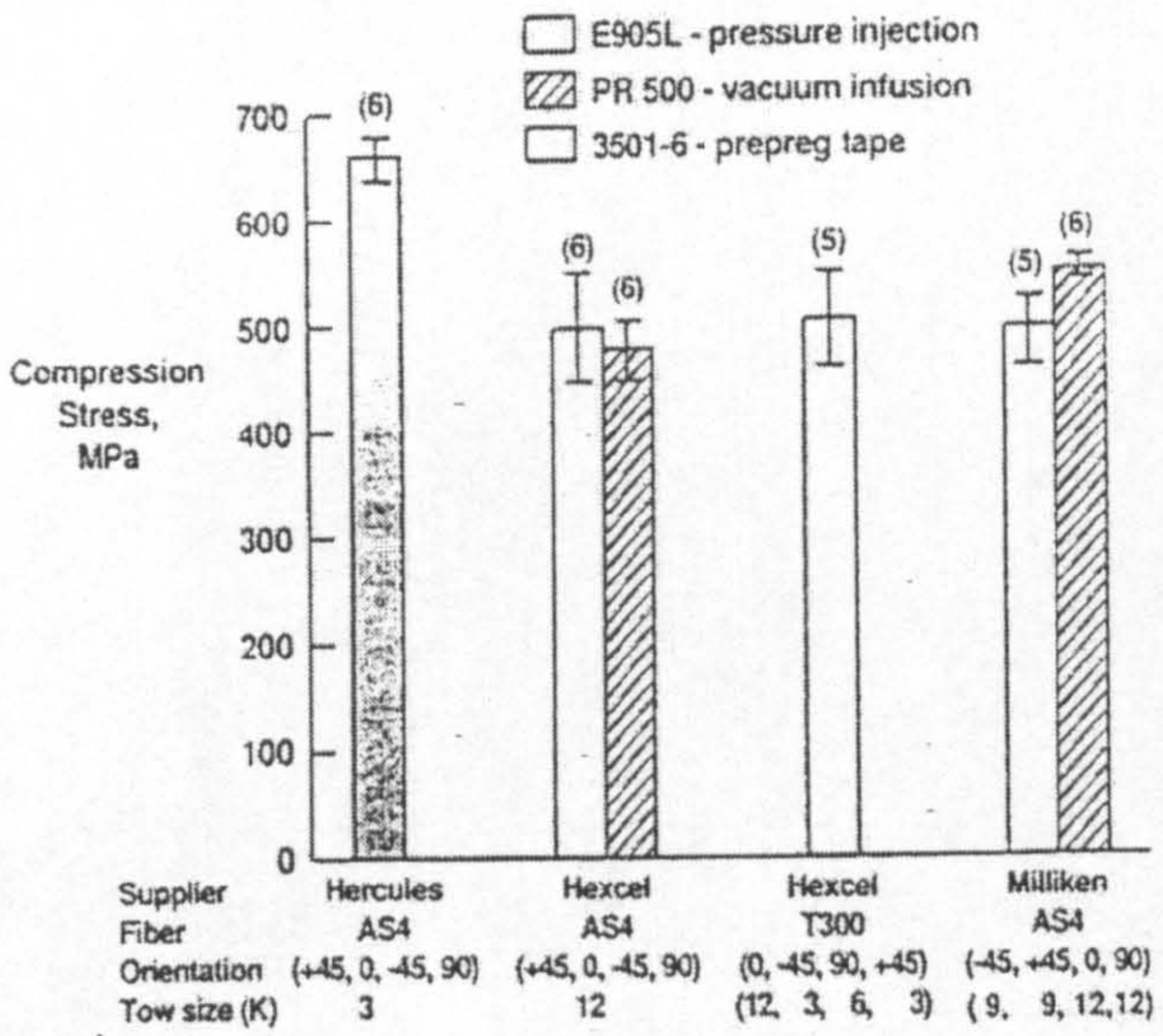

Figure 2.9 Compression after impact stress of NCF composites and prepregtape laminates **[Dexter et al, 1996a]**

2.6 Composite Material Manufacturing Processes

There are several techniques employed for manufacture of composite materials. The most common automated techniques and manual lay-up to fabricate are described below:

2.6.1 Filament Winding

This technique utilises continuous fibre, which may be dry or pre-impregnated with resin; the method is confined to circular or similar components such as pressure cylinders and tanks.

Winding is carried out on a machine similar to lathe but specially constructed for this purpose. If dry fibre is used it is first passed through a resin bath and tensioning device and then onto a rotating mandrel or former. Winding is carried out to a predetermined pattern, which may be helical or polar or a combination of both; the winding pattern is controlled on the latest machines by taps programming. Should pre-impregnated fibre be used the fibre goes straight through a tensioning device and then onto a rotating mandrel. This method of manufacture can be highly mechanised and good quality may be

achieved. One of the main problems of this method, the winding machines is expensive.

2.6.2 Bag Moulding

This general process of bag moulding can be divided into two basic methods; vacuum and autoclave. For bag moulding prepreg materials are usually used, laminated onto a former or mould and covered with release film and a flexible membrane or bag, the material is then cured and consolidated by vacuum and heat, either a heated mould or an oven can be used. In the autoclave process the vacuum bag is still used but the whole assembly is inserted into an autoclave pressure cylinder, pressure and heat being applied by steam or hot air. The main advantage of bag moulding is that tooling is relatively inexpensive and the basic autoclave equipment can be used for unlimited variety shaped parts. The process is recommended for prototype parts small production runs, extremely large parts, and production of complex parts, which are practical to make with matched dies.

2.6.3 Compression Moulding

This method utilises prepreg SMC or DMC materials which are laminated into preforms and then formed and cured in steel moulds mounted in an electrically or steam-heated platen press ,Figure 2.10,. Press mould parts are of high quality and the process is readily mechanised with good quality control, however, tooling costs per part can be high especially for short production runs **[Hull, et al 1996].**

2.6.4 Vacuum Resin Injection

The resin injection technique uses dry cloth reinforcement which is made into a preform of the part, the layers being sewn of heat bonded together with a binder; the preform is put into a closed mould and sealed. Resin is then introduced into the mould vacuum pressure, and impregnation of the preform takes place. Cure is carried out in an oven or using heaters embedded in the

mould. The injection method advantages are low tooling cost, the materials used have long shelf lives and the method can be readily mechanised with good control.

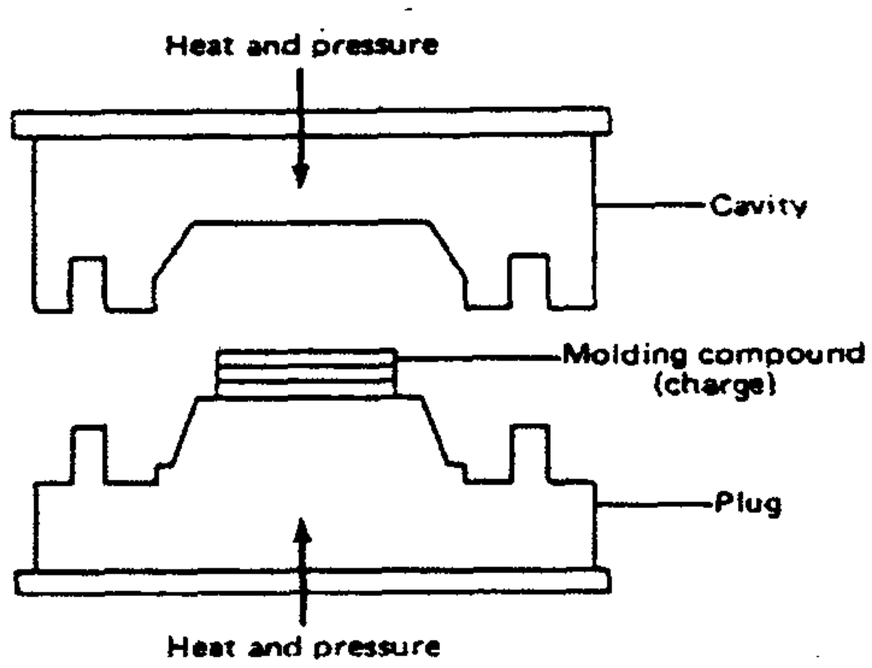

Figure 2.10 SMC Moulding Operation

2.6.5 Injection Moulding

Short fibre reinforced thermoplastic pellets are used with standard injection moulding machines ,Figure 2.11,. The material is fed from a hopper into a rotating screw which drives the material via a preheating section through a heated nozzle into oil or water heated die; after injection the die is rapidly cooled to allow part ejection. The whole process is now electrically controlled and parts can be produced in seconds, however the expensive tooling and machinery requires large batch quantities for economic operation **[smith, 1999].**

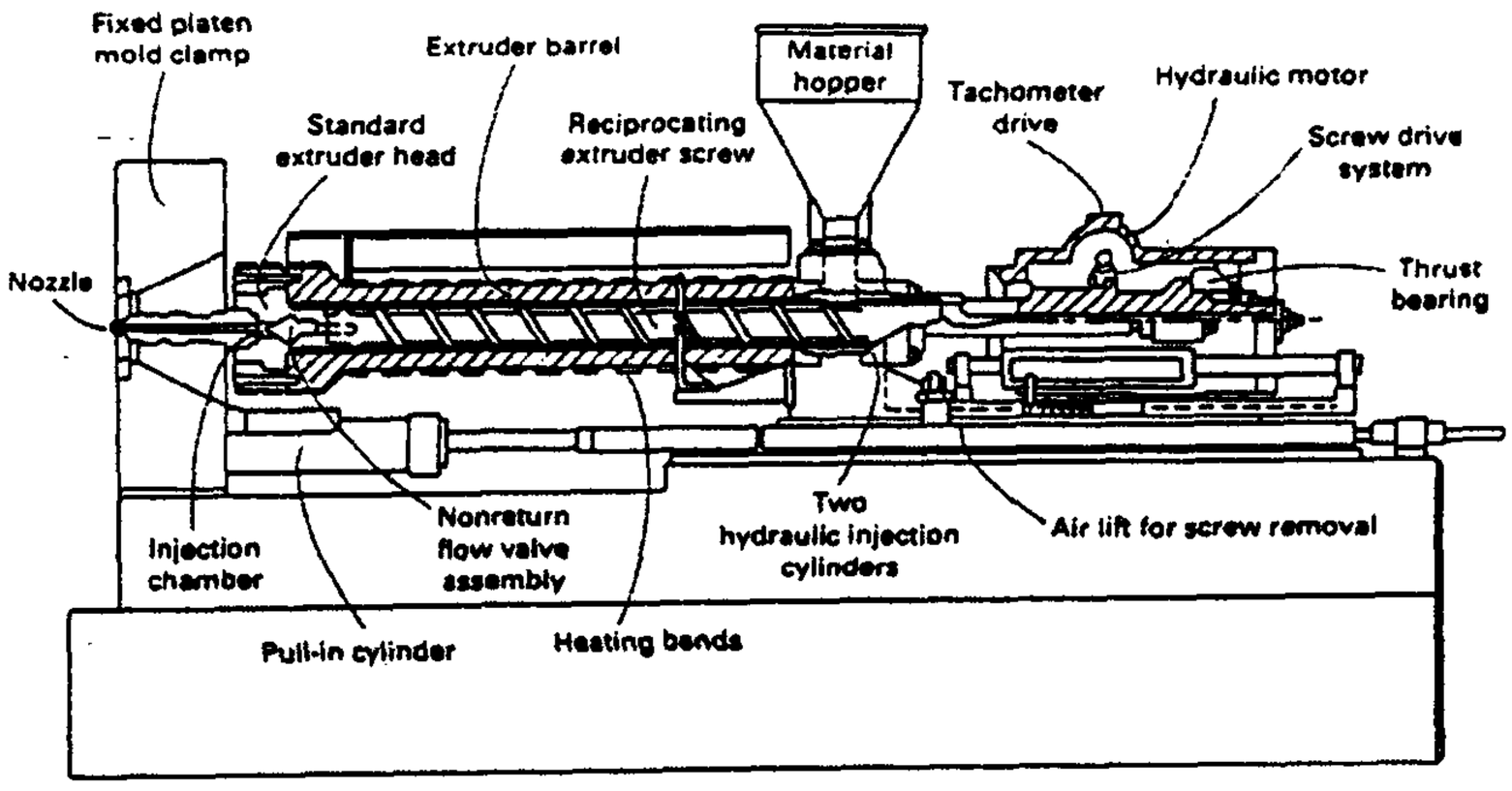

Figure 2.11: Injection End of a Reciprocating Screw Injection

2.6.6 Resin transfer moulding (RTM)

Resin transfer moulding, Figure 2.12, is a closed-mould low-pressure process in which resin is injected into a mould cavity filled with a fibrous preform. RTM process allows the fabrication of composites ranging in complexity from simple, low-performance to complex high-performance articles and in size from small to very large. The process is different from the other moulding processes in that the dry reinforcement and the resin are combined within the mould cavity to form the composite component. The process has the potential to produce low-cost, high quality and geometrically complex parts.

Resin transfer moulding (RTM) is becoming the most effective fabrication technique for composite materials which is gaining favour in the aircraft industry as a result of its superior dimensional control and its ability for parts consolidation and reduced cycle time compared with the other processes. The resin transfer moulding is used not only in the aircraft industries but also in many other applications like automotive industries. Ford Motor Company completed a concept study in which the entire 90-piece steel front structure of an Escort automobile was replaced by a 2-piece when using a resin transfer moulding process **[johnson, 1986]**.

2.6.6.1 RTM process

The first step in the RTM process consists of placing the dry fibre reinforcement in the mould cavity. It is usually constructed from woven or stitched fibre mats or three-dimensional weaves, constructed from continuous-strand fibres of glass, Kevlar, or carbon. Once the mould has been sealed, a polymeric resin matrix is injected into mould cavity via a controlled pumping mechanism, and through capillary action, resin permeates the fibre form.

When complete saturation has occurred and any air present expelled, resin will be visible through vent lines strategically placed in the mould. The mould

is then heated up to the required temperature for a specified time and the curing reaction is initiated. Usually after complete filling of the mould cavity, and the part solidifies. The finished composite product can then be removed from the mould **[Bickerton, et al ,1997], [Johnson, et al, 1986],[joseph, et al, 1998].**

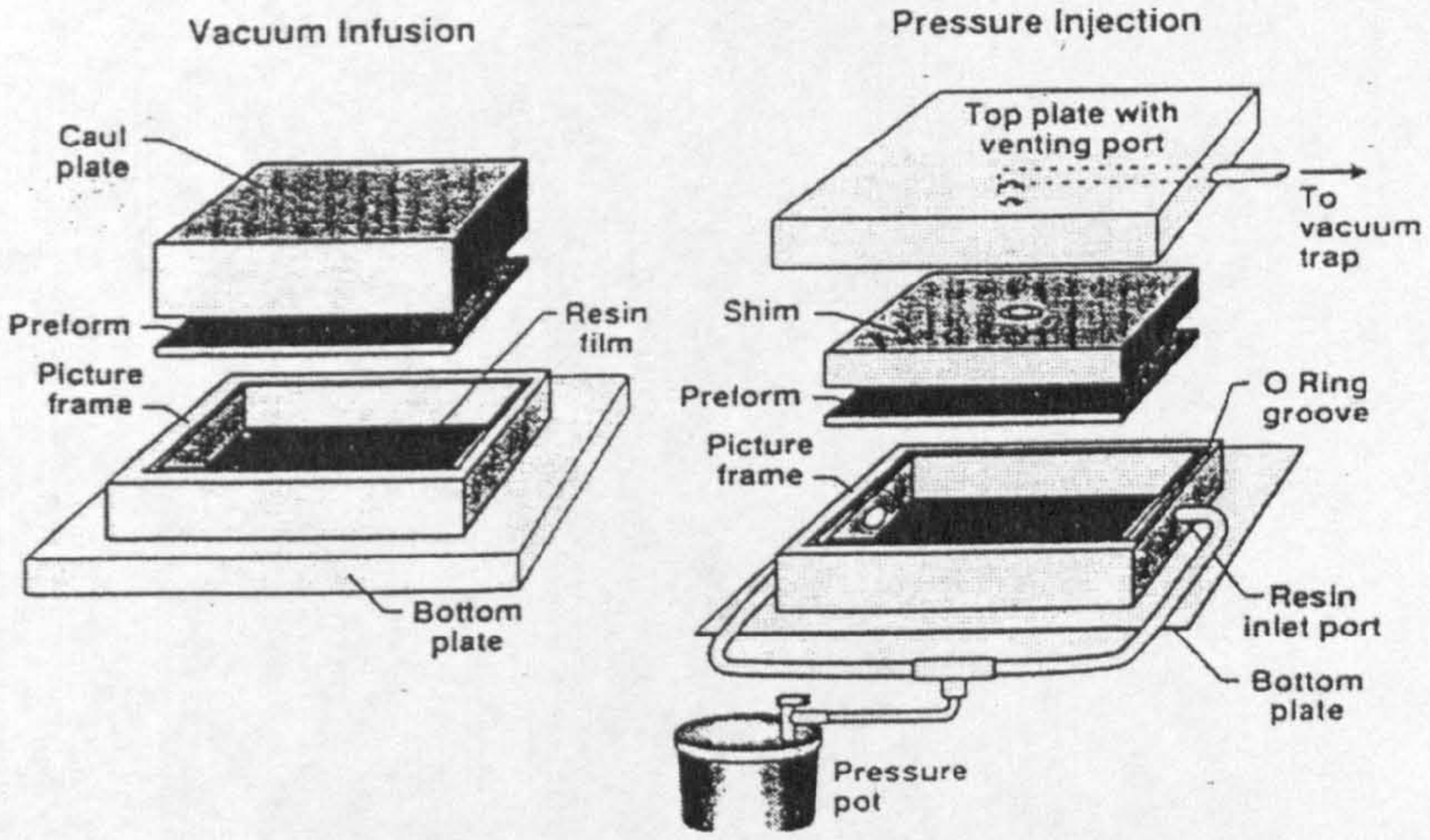

Figure 2.12 Vacuum infusion and pressure injection resin transfer moulding **[Dexter, 1996a].**

2.6.6.2 Factors affecting the process

1- There are many factors affect in the successful of the RTM process, the most critical factors are shown in, Figure 2.13, some of these factors will be briefly discussed in the following sections.

2.6.6.2.1 Mould Design

The first element of these factors is the mould design. The mould design has been fully discussed in **[Michael, et al, 1982],[El-amin, 1981]**. They have reported that the mould itself may be broken down into five major areas:

- The injection ports
- The air vents.
- The guide pins.

- The mould cavity.
- The gasket.

The injection ports and air vents provide resin access to the mould and a means for removing volatile and trapped air from the part. The guide pins ensure the proper alignment of the mould halves. The mould cavity imparts the desired shape to the part, while the gasket seals the mould and restricts resin flow out of it. Two other important considerations in mould design and construction are surface finish of the mould cavity and temperature control.

2.6.6.2.2 Fibre preform

The second element is fibre preform. Primary areas of concern related to fibre preform are proper orientation and fibre volume. In the preform lay-up process to ensure that cure should be taken correct orientation and fibre volume are maintained. The manner in which preforms and fabrics are made and held together is also important, particularly in high-volume production.

2.6.6.2.3 Resin system

There are several key characteristics specific to the selection of a resin system. The term resin system refers to everything needed to make the system suitable for the desired processing and for the end-use application. This includes the resin, curing agent, catalysts, fillers, pigments, promoters, and inhibitors. In general, resin systems that are most suitable for the process have a long pot life (at least 2h) and low viscosity at the temperature used to transfer the resin, a short gel time at the curing temperature (less than 1h), and low levels of outgases, volatile, and cure by-products **[Sayers, et al, 1985]**.

2.6.6.3 RTM simulation

Recently much effort has been directed towards modelling and simulation of the RTM process. Such simulations usually model the filling of RTM moulds as flow through porous media. At present, significant research effort is being

expended on the development of numerical simulations of the RTM process. The common aim is to develop a comprehensive code, simulating both filling and curing stages. Such a simulation would represent an invaluable design tool for industrial applications, allowing for full exploitation of the RTM benefits. These simulations will ensure that an injection scheme can be found to minimise defects and production costs, before the expensive process of mould fabrication is considered **[Fracchia, et al, 1995],[Young, et al,1991],[Voller, et al,1995].**

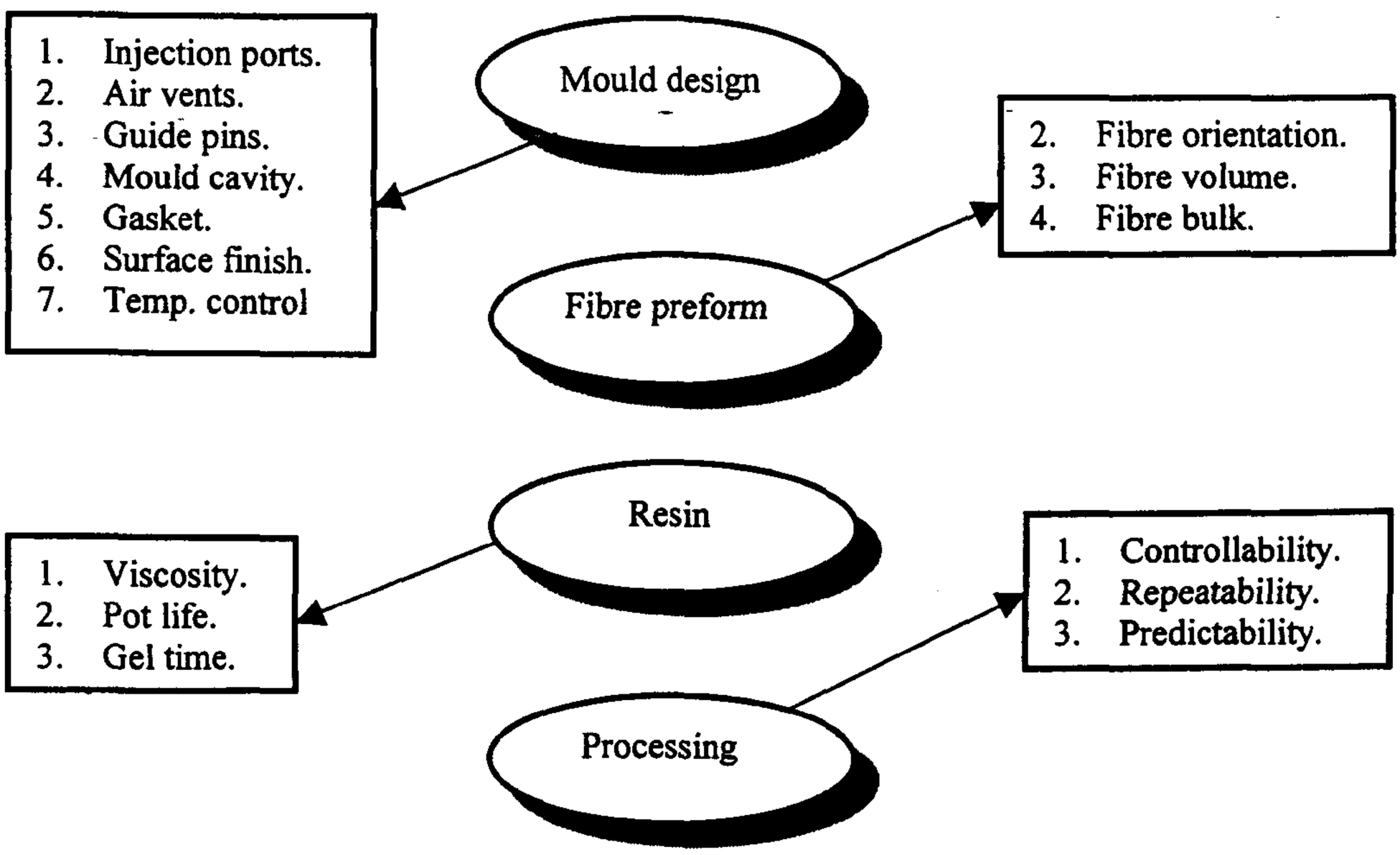

Figure 2.13: Factor affecting of the RTM process

2.6.6.4 Cost Analysis

Once the material has been specified with respect to their properties, compatibility, and cost, the process to produce the required parts must be cost-competitive with other available fabrication techniques. The economics of RTM versus other moulding techniques and hand lay-up are shown in

,Table 2.5, 2.6**[Grigoropoulos, 1985],[Tabei, 1983].** As can be seen in ,Table 2.5, the cost advantages of RTM over hand lay-up are predominantly in the areas of part fabrication and labour. However, when compared to other moulding techniques that have much lower manufacturing and labour depreciation costs than the hand lay-up technique, RTM becomes less economical with respect to these factors ,Table 2.6,. The advantages of RTM compared to other moulding techniques are the types of parts that can be manufactured and the generally lower tooling costs. Improvements in the RTM process that can be made in order to further reduce part cost include the use of automation, assembly lines, multiple tools, and better resin systems **[Bickerton,1997],[Michaels, et al, 1982].**

Table 2.5: breakdown of costs of RTM versus hand lay-up **[Tabie, 1983].**

	Resin transfer moulding	**Hand lay-up**
Product weight Kg	30	33
Production rate pieces/month	1000	1000
Direct labourers	14	30
Material cost		
Resin	28.4%	27.4%
Glass fibres	27.7%	26.4%
Others	0.3%	2.7%
Subtotal	56.4%	56.5%
Depreciation cost		
Mould	9.0%	3.0%
Equipment	1.8%	0.7%
Subtotal	10.8%	3.7%
Scrap	1.6%	0.0%
Manufacturing cost	14.4%	39.6%
Gel cost	0.0%	0.2%
Subtotal	16.0%	39.8%
Total	83.2%	100.0%

Table 2.6: Breakdown of costs of RTM versus other moulding techniques [Grigoropoloulos, 1985].

	Resin transfer moulding	Sheet moulding compounds	Injection moulding
Process Operation			
Production volume	5000-10 000/press	25 000/press	30 000/press
Labour	High	Moderate	Moderate
Skill dependency	Considerable	Very low	Lowest
Operation	Movements/intersection	Flowing,neat	Flowing,neat
Product			
Complexity	Preform limit	Yes	Best
Size	Big parts for low invest.	Big parts if flat	Not very big
Tolerance	Good	Very good	Very good
Cores/inserts	Possible	Not easy	Possible
Strength	Moderate	Best	Very good
Material usage			
Raw-material cost	Lowest	Highest	High
Handling/applying	Skill dependence	Easy	Automated feed
Precision	Skill dependence	Very good	Automated feed
Waste	<3%	Very low	Attention runner
Mould			
Initial cost	Moderate	Very high	Very high
Cycle life	3000-4000 parts	Years	Years
Preparation	In-factory	Special shop	Special shop
Maintenance	In-factory	Special tools	Special tools
Reinforcement			
Flexibility	Yes	No	No

2.6.6.5 Manual Lay-up

This is the most common fabrication method used in the commercial field for producing boats, Chemical process equipment and a variety of other components. Resin is applied to the open surfaces of a mould conforming to the outside shape of the component, a pre-cut reinforcing layer of dry glass matt of cloth is laid onto the wet resin and air is worked out by brush or roller. When impregnation is completed subsequent layers are built up to the required thickness before curing. Components produced by this method have a rough finish on one side and have relatively high resin content, quality control is difficult as the process is left very much in the hands of the operator. However the method utilises inexpensive reinforced plastic tooling and is ideal for one and short run production of complex shaped parts.

2.6.7 Honeycomb

Honeycomb is a series of hexagonal or rectangular cells, nested together to form panels similar in appearance to a cross-sectional sliver of a beehive. Composite honeycomb sandwich structure have been used extensively on commercial airplanes for fairings, control surfaces, radomes, and leading to lower cost, composite honeycomb has found its way into aircraft primary structures. The Beech Starship, the first all carbon fibre airplane, was designed to take advantage of the benefits of sandwich construction with an essentially all carbon fibre honeycomb airframe. In fact, the main fuel tank and the control surfaces were the only parts not of honeycomb construction.

The properties of honeycomb composites enable the design of aerospace structures, which have excellent potential for reduced manufacturing cost based on lower part count and elimination of joints and subassembly operations. The benefits of modern composite sandwich construction are obvious: low weight, high bending stiffness, and the ability to fabricate very large structures with compound curvature. These may be cured in a single

piece, eliminating parts, joints, sub-assemblies, and associated inspection costs **[Ric, et al, 1998].**

The honeycomb core is rigidly attached between two faces of a sandwich panel. Many types of honeycomb are available (appendix I), the polypropylene honeycomb, Figure 2.14, is available in different thickness, different diameter cells, and features a non-woven polyester scrim thermofused to each of the core faces. This polyester scrim provides resin migration to the cells. The resulting structure is capable of the highest strength-to-weight and rigidity-to-weight ratios presently obtainable by ordinary design methods.

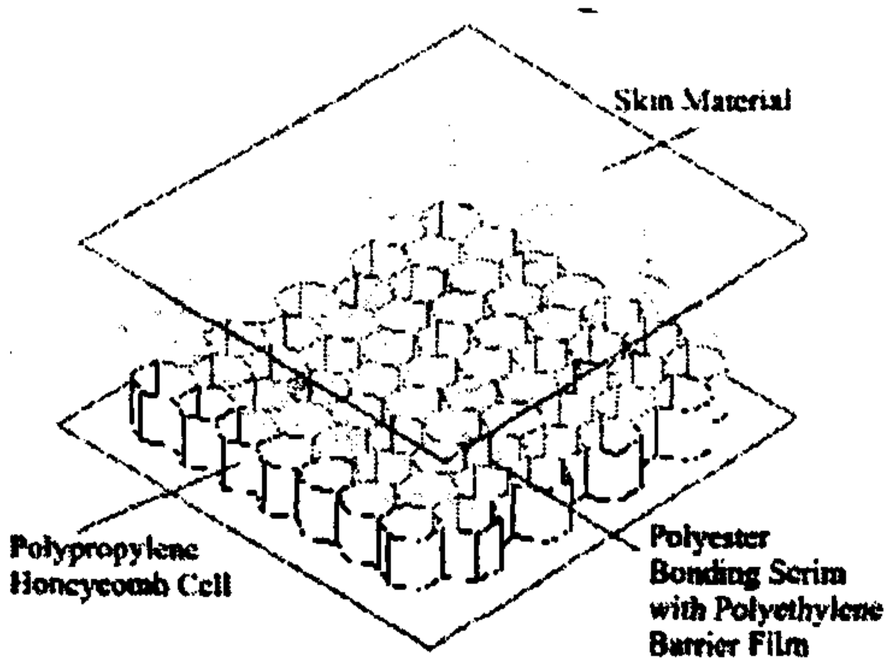

Figure 2.14 Honeycomb cell

Due to its superior strength, rigidity and lightweight compared to the materials it replaces, specifically in the aerospace industry, a growing interest has developed in the use of honeycomb sandwich for a broad range of commercial applications. These range from production master tools, subway, marine, racing cars, railway car components and military fields to exterior curtain walls for high-rise buildings. The flexibility and versatility of sandwich structures can solve many design problems. Honeycomb is also ideal material for energy absorption uses such as bumpers/fenders and elevator shaft

bases. ,Figure 2.15, shows the fast ship manufactured by honeycomb technique.

2.6.7.1 Mechanical properties

The mechanical properties of honeycomb constructions can be compared to I-beams as shown in, Figure2.16. The skins of the sandwich panels correspond to the flanges which take up the bending stress (tensile and compression stress). The honeycomb core corresponds to the stem which bears the shear loads (thrusts) as a brace and which prevents the deflection of the skins **[Martin, et al, 1996].**

2.6.7.2 Constructing consideration

Due to the properties of these structure elements essentially two factors are to be considered when constructing:

1. An optimum mode of panel operation will be only guaranteed if the active loads on the panel are induced in both skins. This is very important in the case of bending and shear stress.
2. The honeycomb core of the sandwich panel should be protected. This will be achieved by a "panel suited" construction design of the bearer frame or joining extrusions.

Finally, one problem associated with the manufacture of honeycomb sandwich structure is core crush. Historically, the origins of this defect were not well understood and its occurrence was often unanticipated. In commercial production, several techniques such as internal optimization and tool modification through grit strips are used to mechanically restrain the core crush, have produced no fundamental understanding of the underlying process or mechanism **[Martin, et al, 1997].**

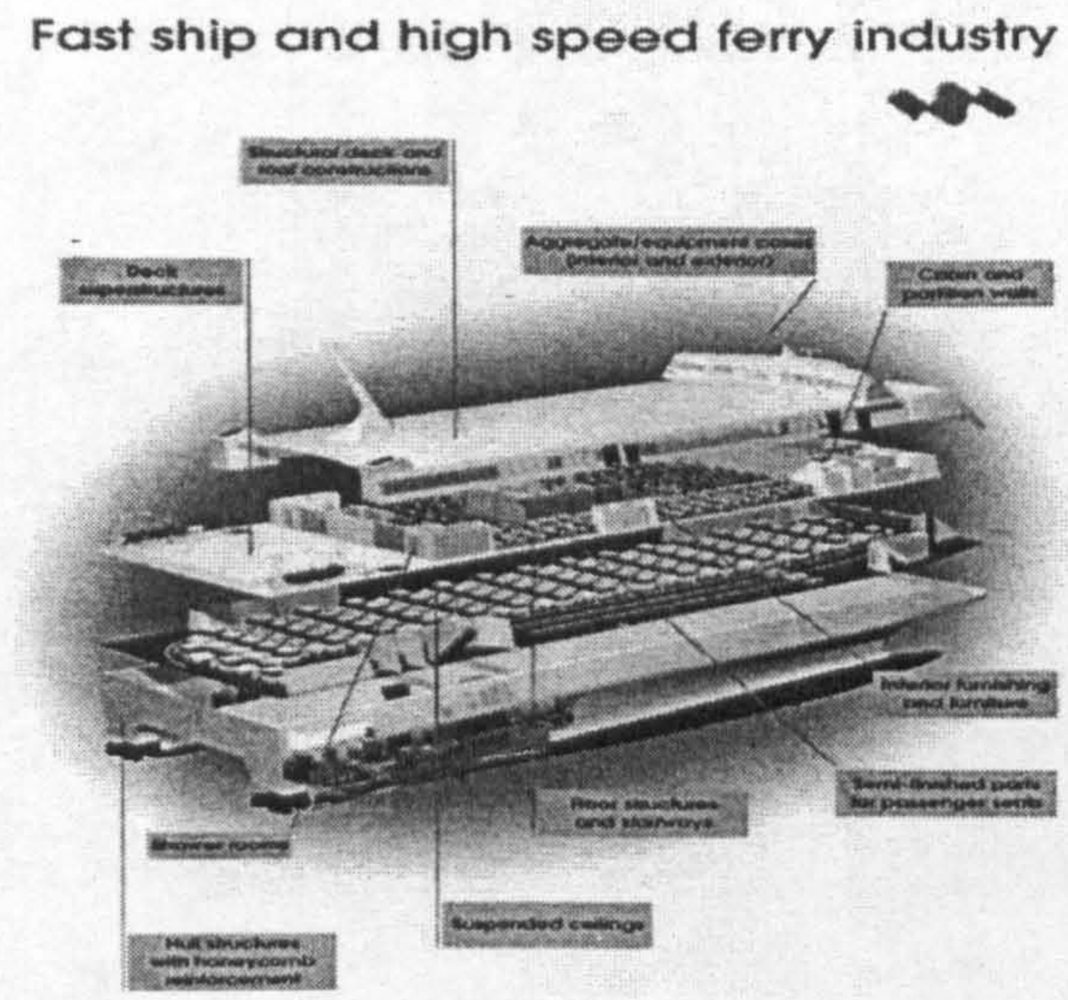

Figure 2.15: Fast ship and high speed ferry

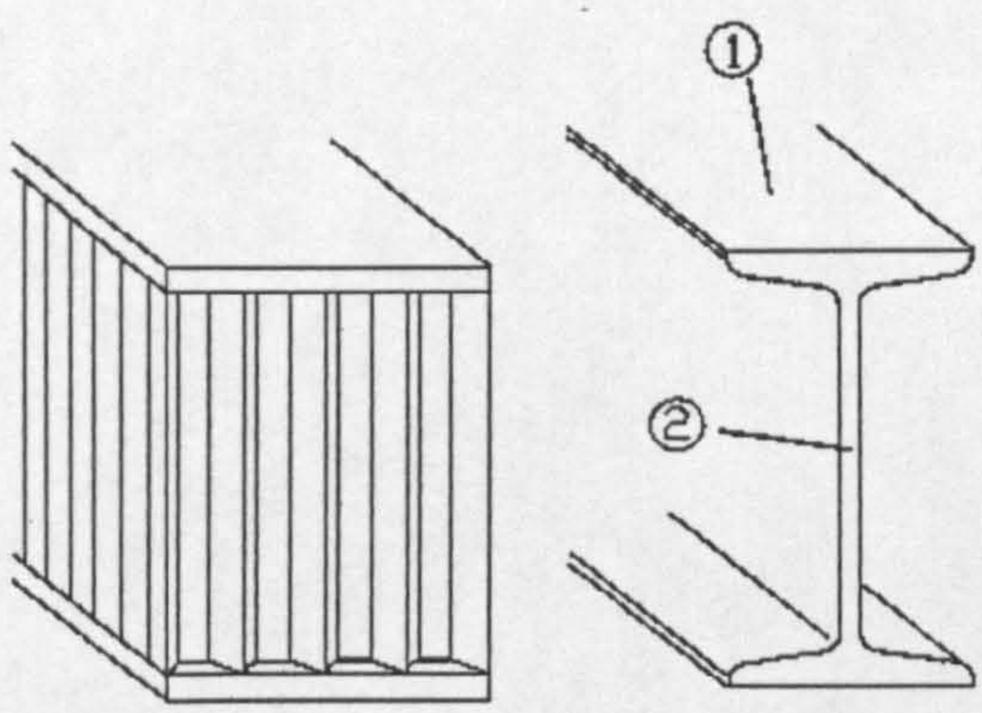

Figure 2.16 Mechanical properties of honeycomb

2.7 Composite Repair

At present, construction and aerospace industries have been plagued with repair or replacement of aging structural components. Most of these problems were not anticipated at the time of initial design, dating many years back. Consequently, this has caused great concern over the cost effectiveness of existing structural systems and the adaptation of new engineering material

systems. It is believed that the complete design of a composite structure needs to address load-carrying capability, health monitoring synthesis, and a refurbishment strategy. In other words, the design of a composite structure must consider the consequences of its entire life cycle. This life cycle design process must rely on the development of design/construction guidelines, non-destructive inspection techniques, synthesis of damage evolution (based on material properties database), and structural health assessment through reverse mechanics. Many of these issues have been studied for years with substantial achievement already made. However, these topical issues must ultimately be integrated together to form a close loop synthesis so that the state of health and loading conditions of a composite structure are under control at all times.

Boeing Company has developed a number of cutting tools specifically designed for use with composite materials, which provide superior performance at substantial cost savings. Repairing composite materials requires drilled holes of precise depth to fill with resin delaminating, cracks, or voids. Boeing Company has developed, demonstrated, and implemented composite repair approaches for polymer matrix composite (PMC) material. These technique augments bolted repair approaches and can repair delaminating that would ordinarily cause scraping of the hardware. The approaches address repair of delaminating caused by impacts, routing, drilling, and fastener installation/removal in cloth and unidirectional reinforcements of carbon, glass, or Kevlar. The Boeing Company-developed method involves drilling holes at appropriate locations and injecting resin, filling the delaminating ,Figure 2.17, This method is superior to vacuum and syringe techniques that are currently state-of-the-art. This successful repair technology consists of evaluating rejection criteria, delaminating cause, part materials and part features. Usable resins for repairs are dependent on the specific application and program requirements, this repair equipment is usable for almost all delaminating regardless of size or location.

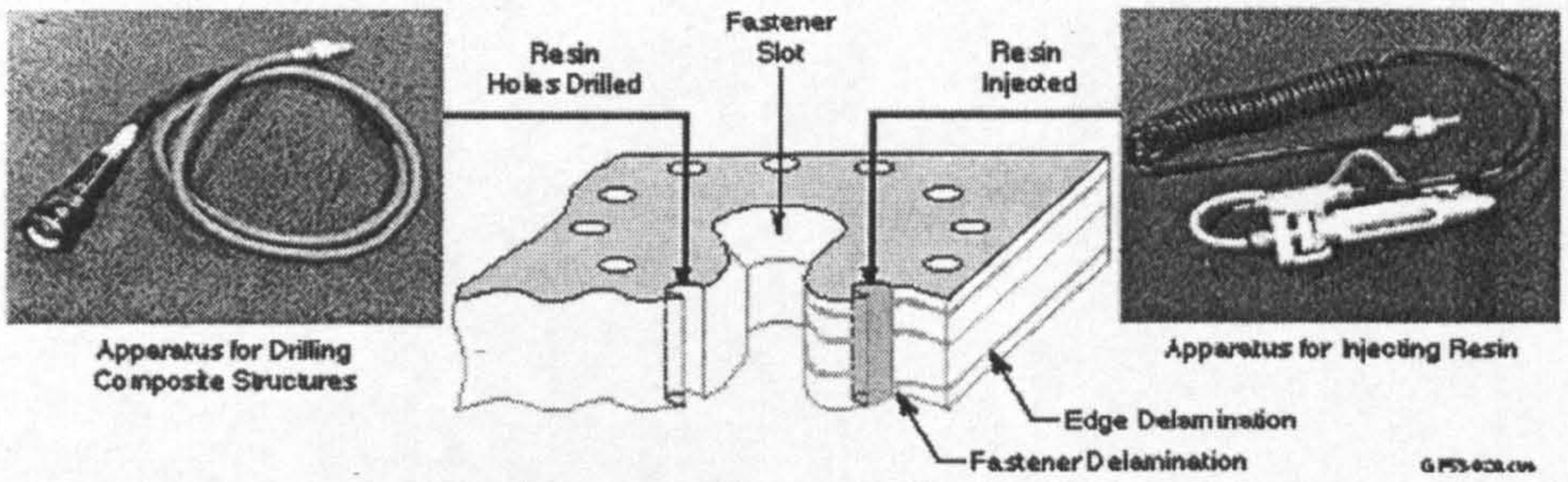

Figure 2.17: Apparatus for repairing composite.

This repair approach has yielded greater than a 90% success on structures for the AV-8B, F-18C/D, and F-18E/F compared to less than 30% for commonly used approaches. The success of this repair approach allows for greater use of composites by improving maintenance reliability. With reduced composite assembly acquisition costs and demonstrated life cycle cost improvements, PMC has been used increasingly in all aerospace sectors. On fighter aircraft, use of PMC has increased to approximately 40% of the structural weight for reasons of increased performance.

Boeing Company has also developed a superior cutting tool adapted for delivering lubricating and cooling fluid to the cutting portion of the tool ,Figure 2.18,. The tool is used in connection with a hydraulic depth-sensing device to control the depth of fastener holes and countersinks in contoured surfaces, such as composite aircraft wings, where the flushness of the fastener head is critical.

A device related to The Boeing Company's various cutting tools is the Chip Extraction Apparatus. The device extracts chip "swarf" produced when drilling composite and metallic materials. The invention contributes to achieving improved surface finishes within the hole, better hole size consistency, and reduced entrance side delaminating for holes made in composite materials.

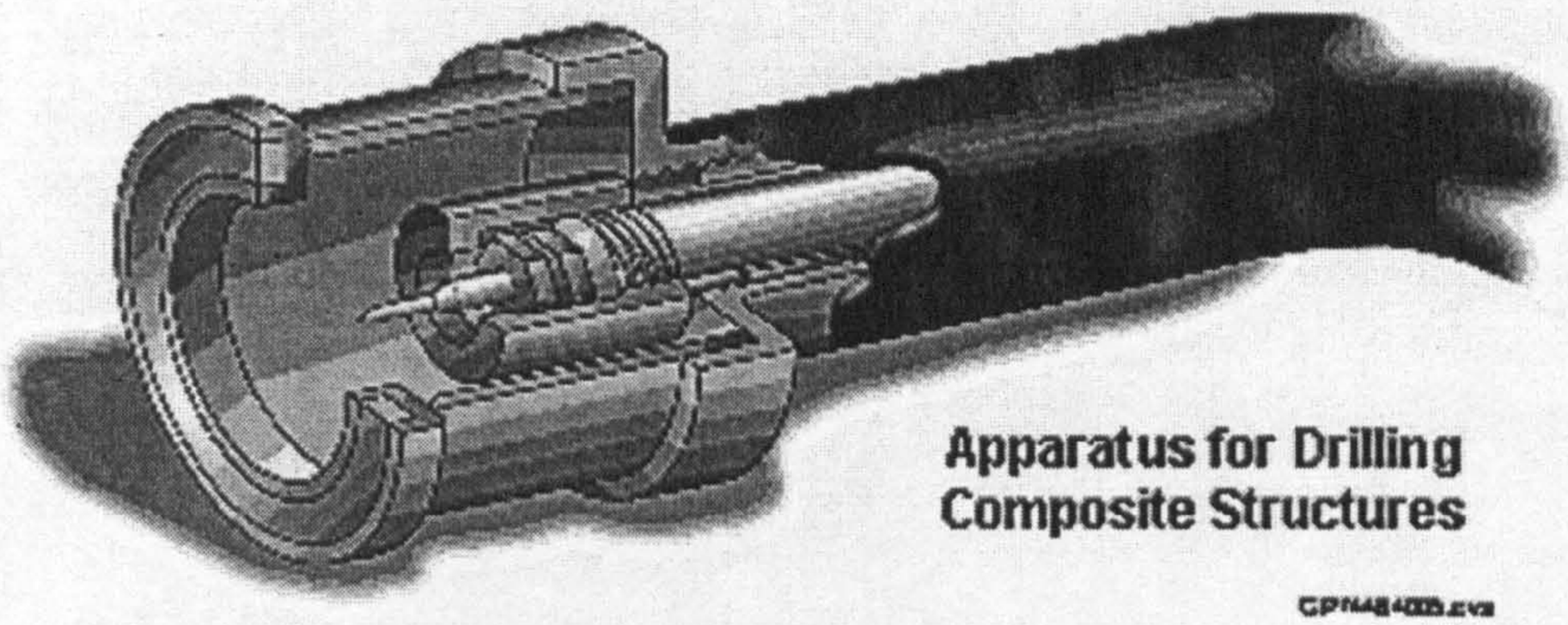

Figure 2.18 Apparatus for drilling composite structures.

2.8 Composite Material Properties

The mechanical properties of the fibres and composite materials described earlier showed that all composites exhibited excellent properties compared with conventional metallic materials. Their full potential may be recognised by comparing their specific strength and modulus ,figure 2.19, where it is explained that for a given weight these materials are the strongest and lightest known today.

The main advantages to be gained from composite material compared with metallic materials are:

- Lower weight.
- Better fatigue resistance.
- Better vibration damping.
- Excellent corrosion resistance.
- The material can be tailored to suit the loading on the part.
- Lower production cost (in some cases).
- Ability to tune resonant frequencies (very important in rotating parts such as fan blades and propeller blades).

- Complex shapes can be produced without machining.

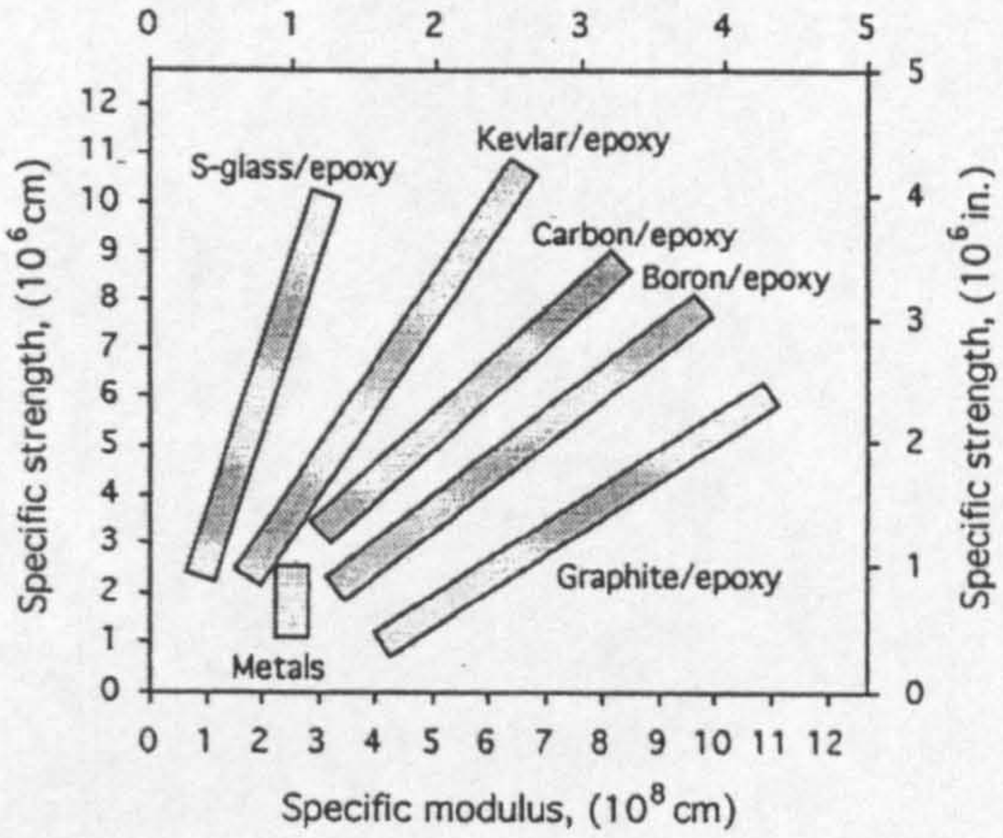

Figure 2.19 Performance map of structural composites**[Bunsell, 1988]**.

Properties, which need careful consideration when selecting composites for a particular application, are:

- The coefficients of expansion which are different in the fibre longitudinal and transverse directions.
- The low thermal conductivity compared with metallic materials.
- The strain to failure which effects their compatibility when being joined to other materials.

2.9 Conclusion

From the above investigations it can be concluded that composite materials have excellent structural properties, and where their application is correctly selected a much improved product from the fatigue, corrosion and weight aspect is achieved.

Advanced composite materials have an increasing application in aerostructures mainly due to their weight reduction potential that cannot be

achieved with the metal materials, thus appropriate industrialised fabrication techniques have to be developed and implemented, to allow complex part manufacture at low cost. In this work automated production concepts have been applied that can contribute to this task.

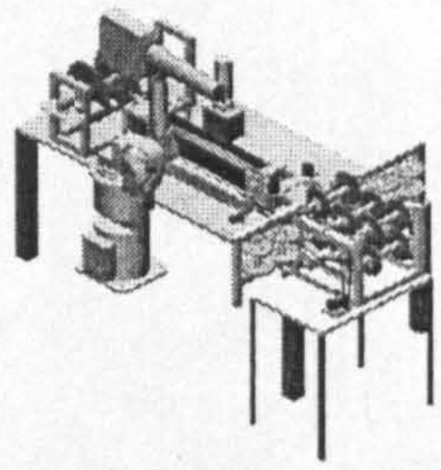

Chapter 3 Fibre Joining Techniques

3.1 introduction

The number of the plies in the stack of the fabric must join at any number of points on the surface of the top ply and at any position generally remote from the edges. This requirement implies that any fixing method must be implemented and manipulated from the upper surface of the top ply.

In the assembly of dry carbon fibre preforms, a number of approaches can be adopted to join plies together in the stack. It is possible to use mechanical fasteners to join composite structures, or to attach composite structures to metal ones. Specially designed rivets and fasteners are available for use in composites, as using rivets designed for metal may damage the composite material. Standard bolts also may be used, but (as metal fasteners) galvanic corrosion of the fasteners must be prevented, such as using specially coated fasteners.

A large number of specialist items are available for making attachments to composites. This chapter covers the various methods discussed for attaching the different components of the reinforcement structures together. A full assessment of the properties, advantages and disadvantages of each method has been investigated.

The study has been made of the existing methods, to asses their suitability, as they stand, or modified, for joining structural components. Those methods include sewing, fusion, tagging, barbing, stapling and knotting procedures.

The rest of the chapter discusses the methodologies used in the development of the forming tools. The various methods considered for material

manipulation and control of the material through the tool have been stated. Some of these methods were modelled at Brunel.

3.2 Means of Attachment

There are two basics form which may be adopted for the fixing member namely; a rod or dowel and a 'U' shape staple either upright or inverted. These forms may be used in groups of dowels or on linked multiples of staples.

The fixing may be retained in the plies by the following methods:

3.2.1 Friction

Various textile threads, thought likely to exhibit the higher surface frictional properties, were inserted into sets of two pads over the range of fabrics supplied using a hand sewing needle. Neither straight dowels nor inverted staples offered any sensible retaining force.

3.2.2 Adhesion

It is obviously possible to apply an adhesive to a dowel or staple which is then inserted into preform holes in the plies to become cemented in place. However, applying adhesive to minute fixings, together with a high probability of gummed-up works, is unattractive.

Alternatively, a solvent based adhesive could be injected into a preformed hole in the plies to form a dowel on solidification. However, control of the spreading of the extrudate within and between the plies is seen as a major difficulty **[Davis and Bennett, 1993]**.

3.2.3 Fusion

Fusion bonding generally refers to the heat activation of a binder material which is added to the dry fabric. Fixing could no doubt be established by extruding molten polymer into the plies but would be prone to the some difficulties envisaged for the solvent bases adhesive. The fixing can be

applied either in the fabric manufacturing process or during the preform assembly **[Wilcox and Sarhadi, 1994]**.

Fusion bonding can be implemented in a number of ways. These include resistance heating, infrared heating, microwave heating, ultrasonic welding, induction heating and laser heating **[Benatar et al 1986]**. The main drawback with fusion bonding is that it does not allow any inter-ply movement **[Dewing et al 1999]**.

3.2.4 Geometry

A retaining geometry may be implemented by the following methods:

3.2.4.1preform inserts

It is clear that the initial shape of a staples or dowels can be engineered so that it tends to hold the two plies of fabric together mechanically. This class of fixing, as illustrated in, Figure3.1, includes:

a. zigzag,
b. helices,
c. screws,
d. ring nails,
e. diabolos,
f. tags,
g. barbs.

It is thought that barbed staples probably represent the optimum design in giving the maximum grip for the minimum material. Such staples would have to be produced by injection moulding in a multi-impression tool giving a string of linked staples which would be cropped off as they were inserted into the fabric.

Experiments with available tags **[Benatar et al 1986]** showed that almost all the retaining bar could be cut away before the tag could be pulled through the fabrics.

The remaining shapes, see ,Figurer 3.1, whilst offering some scope for effective fixing, are seen as over-massive and likely to introduce an intolerable burden of foreign inclusions into the lay-up.

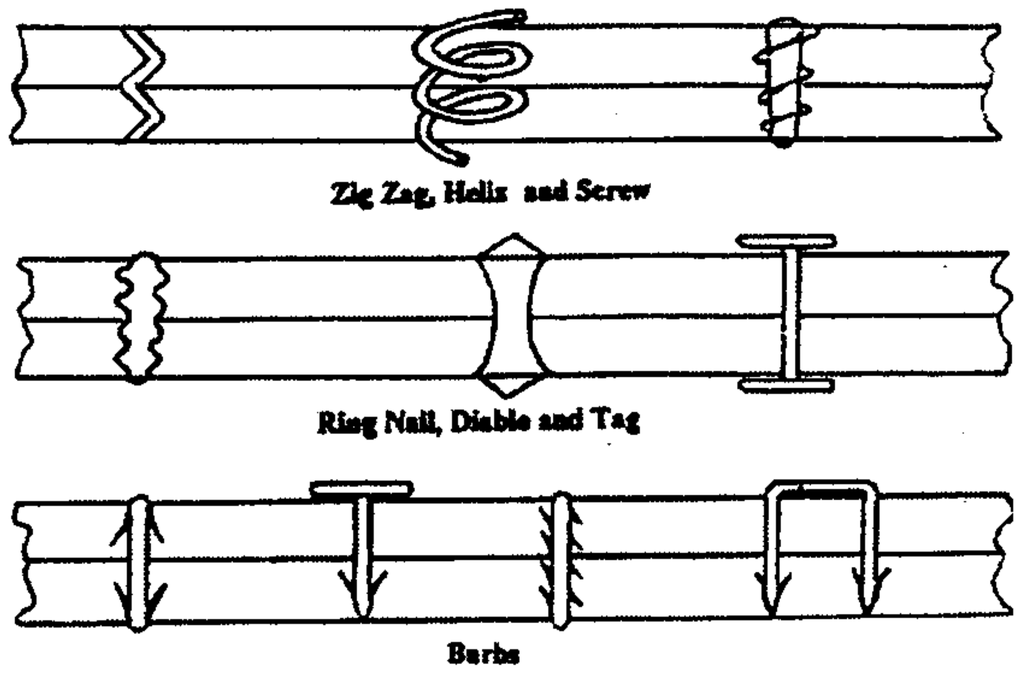

Figure3.1 Illustrations of performs insertions

3.2.4.2 Dispositional attachment

Polymer pins could be used for fixing structural fabrics but their use would require the plies to be puckered to enable their insertion. However, slightly curved pins or group of straight pins inserted at various inclinations to the normal overcome this difficulty as shown in, Figure3.2.

The drawback with this approach is being the fabric in somehow able to slip free during handling and it was apparent that, for the method to work, both fabric and insert would have to be very stiff.

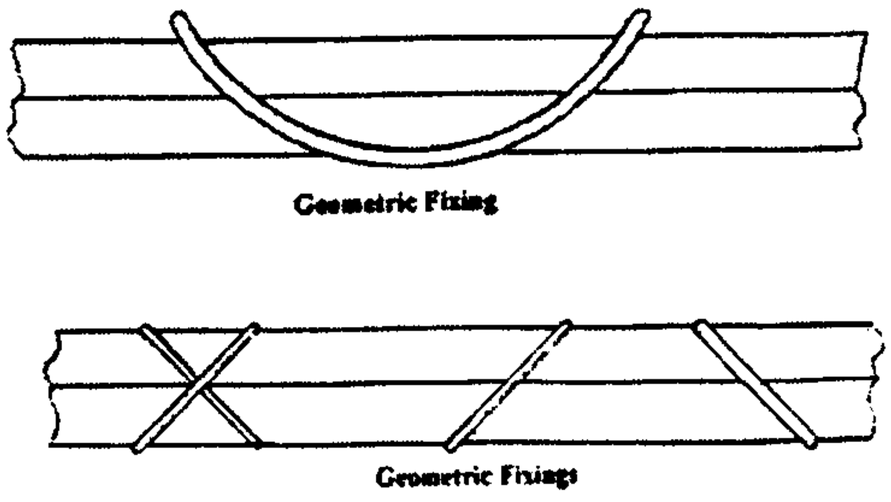

Figure3.2 Illustrations of dispositional attachment

3.2.4.3 Rivets

Secure riveting of plies was achieved by heat beading the ends of dowels and inverted staples in polypropylene and polyester as shown, Figure3.3, the size

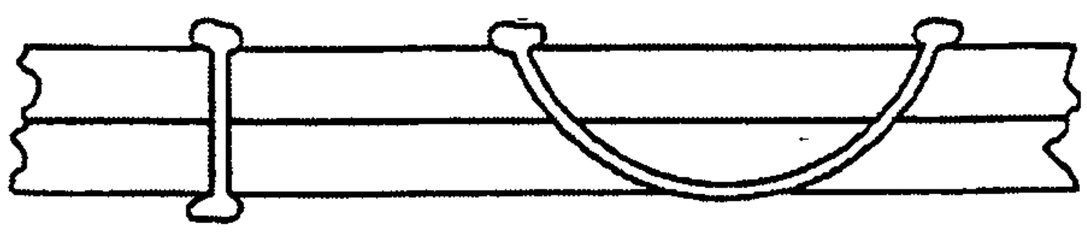

Figure3.3 Bead rivets

And neatness of the fixing could be controlled to a large extent of the protrusion of the inserts prior to heating.

From the exploratory work done the technique is considered to be very promising particularly as only small amounts of foreign material is necessary for a satisfactory fixing **[Dewing et al 1999]**.

3.2.4.4 Stapling

The method of stapling the plies together was thought of during the initial discussions on the development of the tool. Stapling is a proven technology in the paper/stationary industry, but whether this kind of attachment could be incorporated into the attachment methods of NCF composite components is still being investigated.

The initial idea was to use a standard stapler to conduct trials, but variations were considered due to the fixed depth that the staplers could achieve. An example of how the staple would look through the NCF is shown in ,Figure3.4.

If a controllable method could be found, the depth that the staple holds could be controlled in such as way as to produce the correct depth for the composite after the moulding process has been carried out.

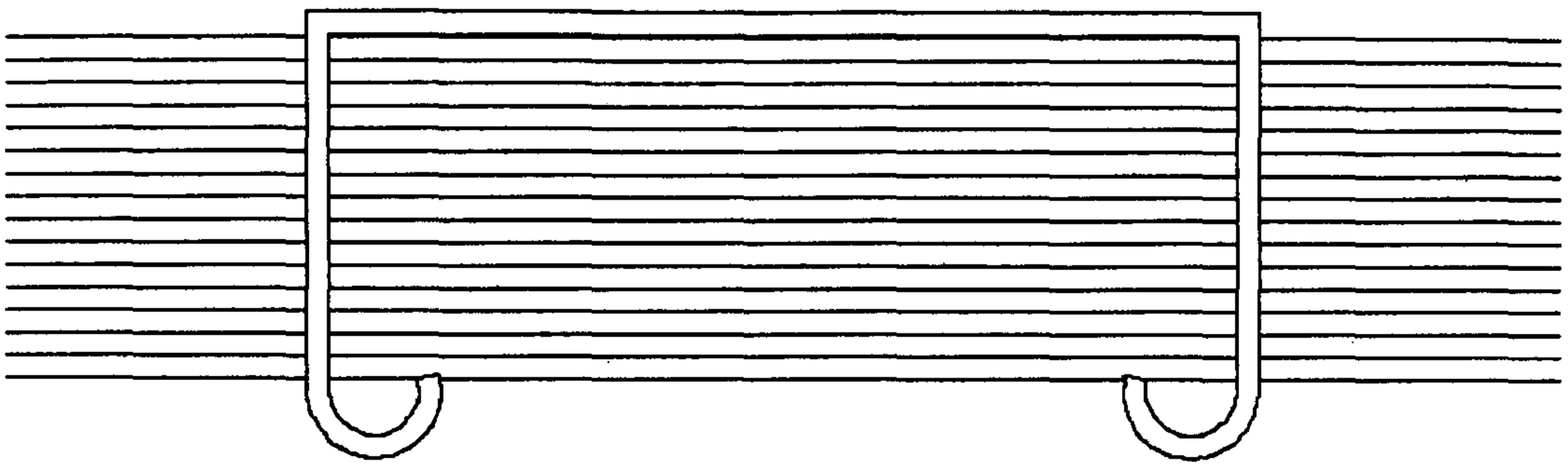

Figure3.4 Staple through a ply stack-up

3.3 Other Methods of Attachment

Some other methods were discussed, each idea was thought of as a solution to only having access to one side, of the lay-up.

The first idea was Ultrasonically Assisted Z-fibre (UAZ) process, this method use small solid cylindrical pins to join the structures, these pins, typically 0.25 to 0.5 mm in diameter.

UAZ employs a basic Z-fibre perform (composite or metallic pins) which is partially compacted, in the first stage of the process, under forces applied by an ultrasonic horn. The residual foam layer is then removed and a second pass is made with the ultrasonic horn to set the pin ends flush with the part surface as shown in ,Figure3.5, **[Glenn et al 1997]**.

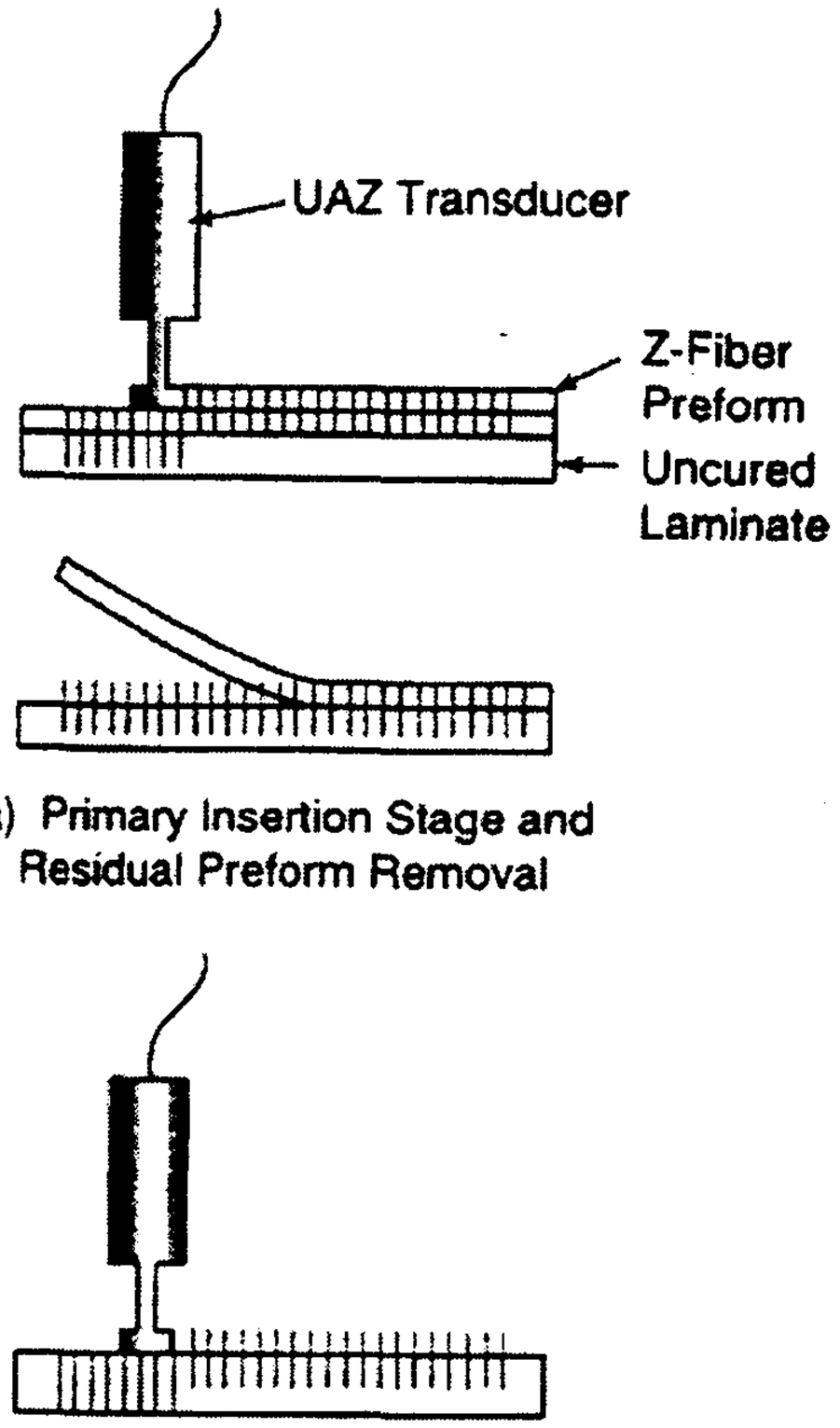

a) Primary Insertion Stage and
Residual Preform Removal

b) Secondary Insertion Stage

Figure3.5 schematic diagram of UAZ operation

The second method was the use of a hollow pin inserted into the lay-up. A secondary piece of the pin is then pushed through the hollow section. The lower section of the inner pin is split and sprung, therefore when it leaves the hollow section it spreads out, gripping the material surrounding it. A sketch is shown in, Figure3.6.

Another idea was the use of a roller formed staple. This would use a staple forming anvil to produce a coiled staple that would have sufficient force to loop around inside the material. A larger roller would then roll over the staple to form the finished staple, whilst matching the thickness of the staple to that of the ply stack. A simple sketch is shown in ,Figure3.7.

This type of attachment device would a lot of research into the type of material used for the staple, the forming method, and the control of the roller when finishing the staple. A big assumption of this concept was that the underlying material (the wing skin and the stringer) was supported by hard tooling of some kind.

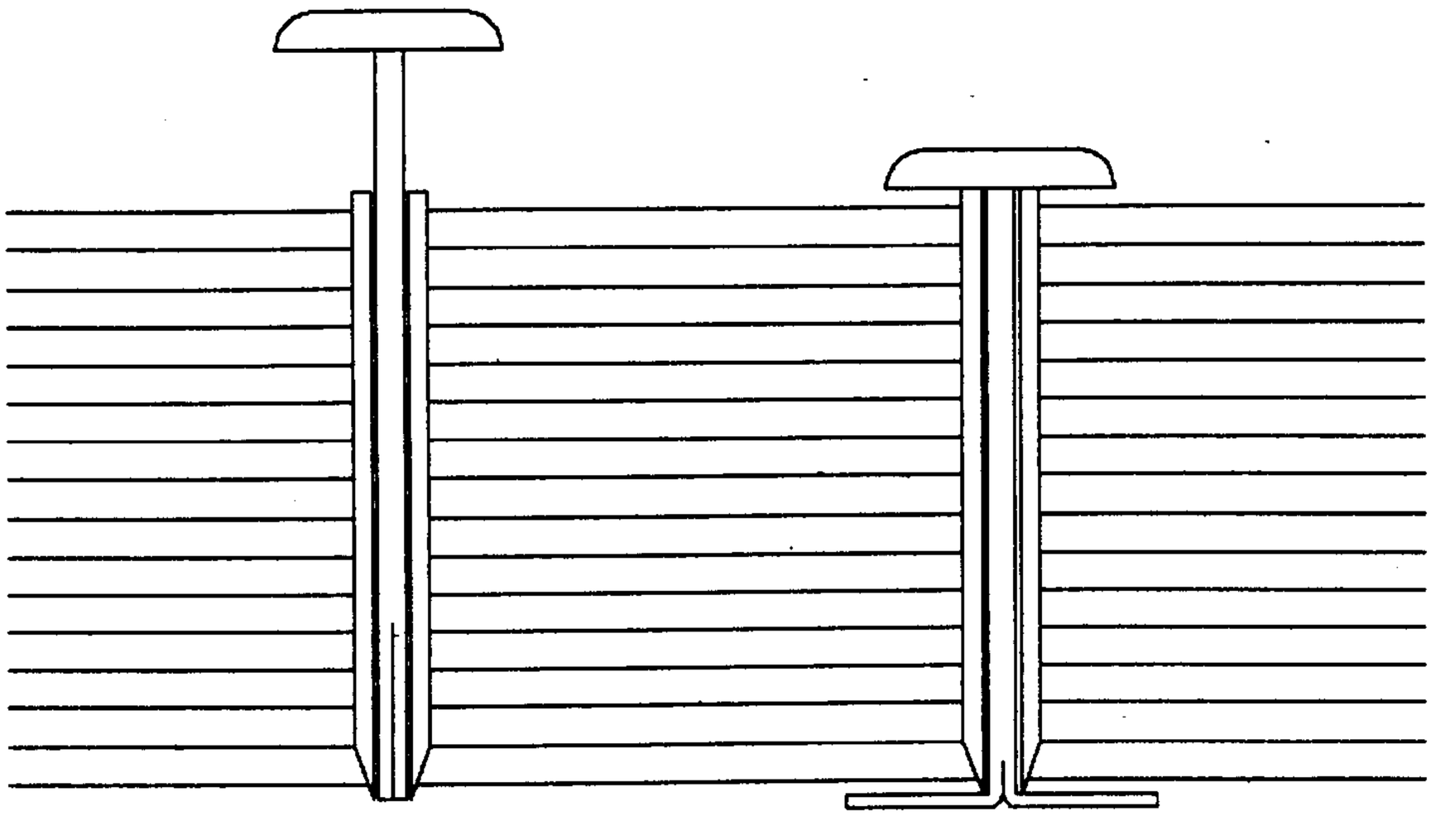

Figure 3.6 Two-piece Push Pin

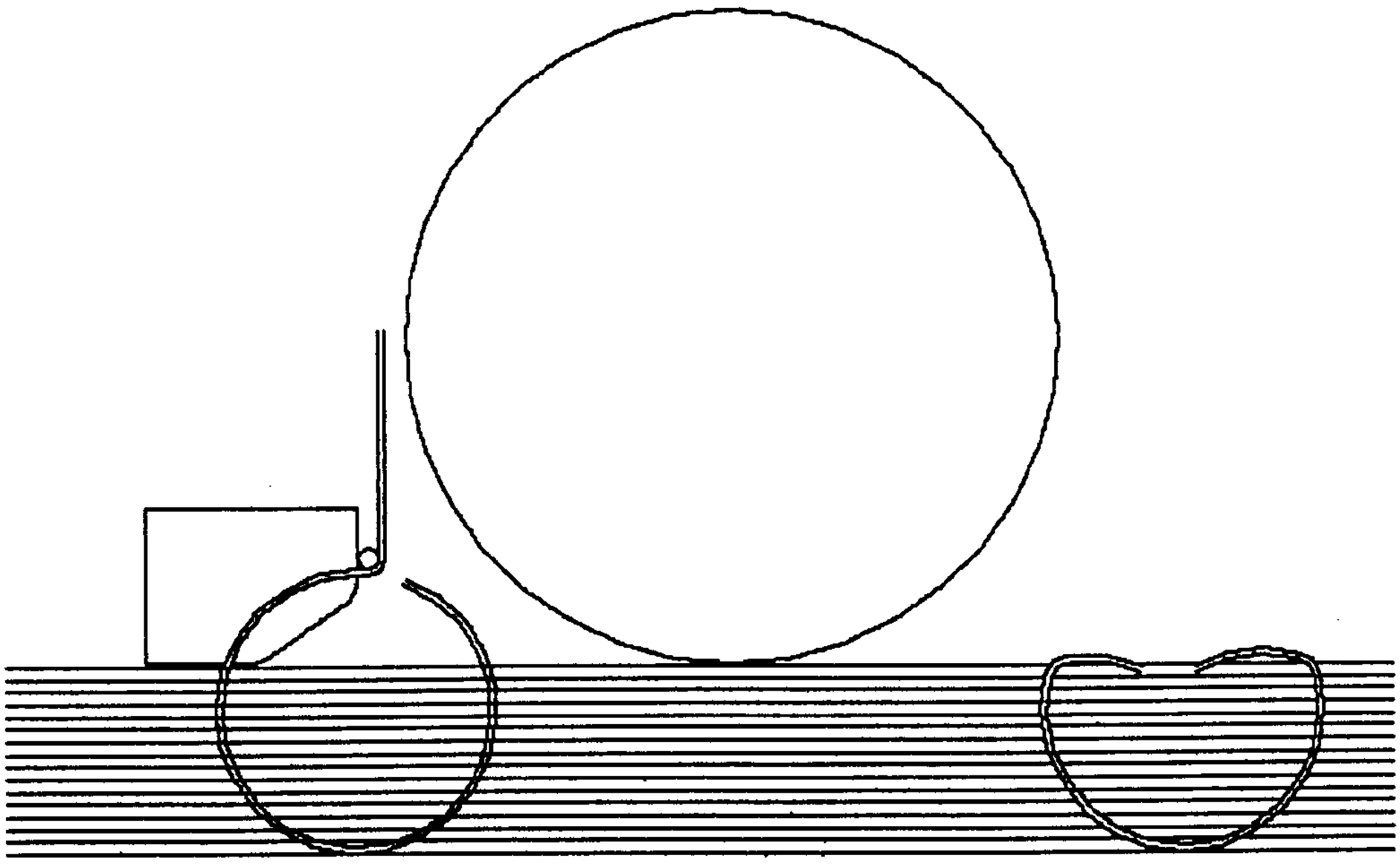

Figure 3.7 Pressure Formed Staple

3.4 Sewing

Sewing stitches in general consist of a series of staples interlinked above and below the fabrics they join together. There is an extensive range of stitch patterns which in almost all instances requires mechanical activity both above and below the fabrics being sewn.

3.4.1 Conventional stitching

With a normal sewing machine, the machine can be used to stitch through the thickness of the lay-up to give extra strength to the ply, as well as providing an effective means of attachment. An example of a series of stitches through the NCF stackup is shown in, Figure3.8.

A sewing machine could be adapted to stitch both through the web, with some slight modifications **[MPhil thesis 2002]**.

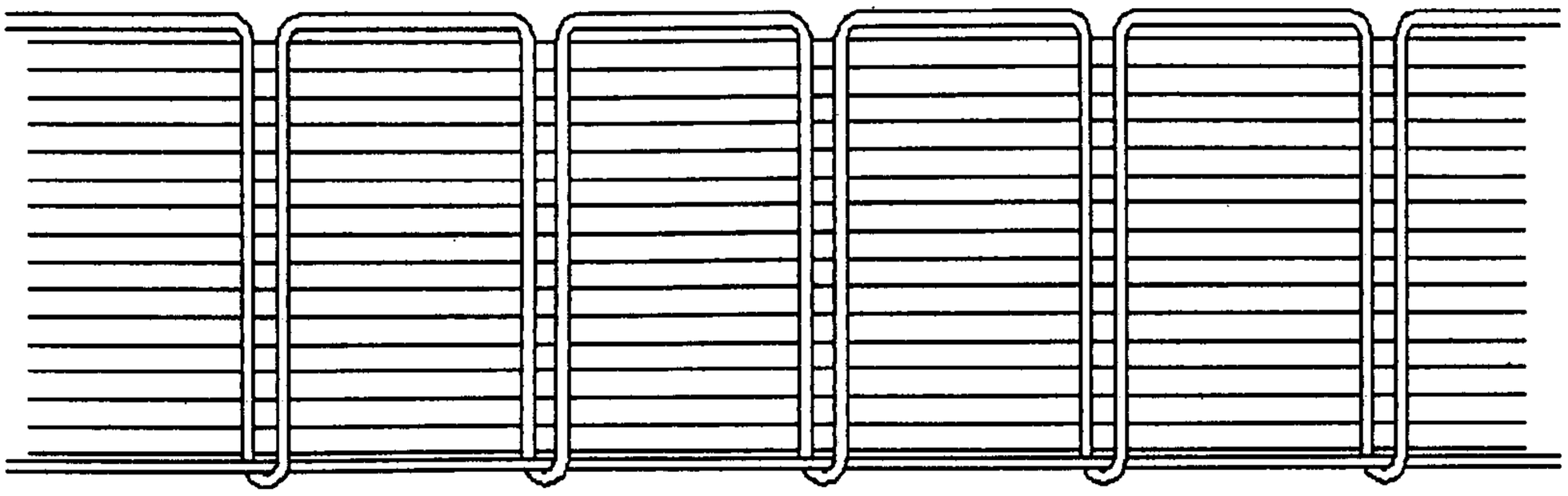

Figure 3.8 Stitching Through-the-Thickness

3.4.2 Blind stitch

From the previous illustration the need of a novel technique to integrate with the cell to join the structures in safe way becomes essential. The use of blind stitching to join the composite structures is an idea that has been adopted and developed to generate a creative robotic tacking device (RTD) which has been integrated in the automated cell to form a series of stitches to join the composite structures. In this method a curved needle is used which, having penetrated the fabrics, re-emerges at the upper surface. Before the needle

retracts a loop is hooked from it to be carried over to the next point of entry of the needle where it becomes interlinked with the new stitch as shown in ,Figure3.9, (full details of the operation in chapter 5).

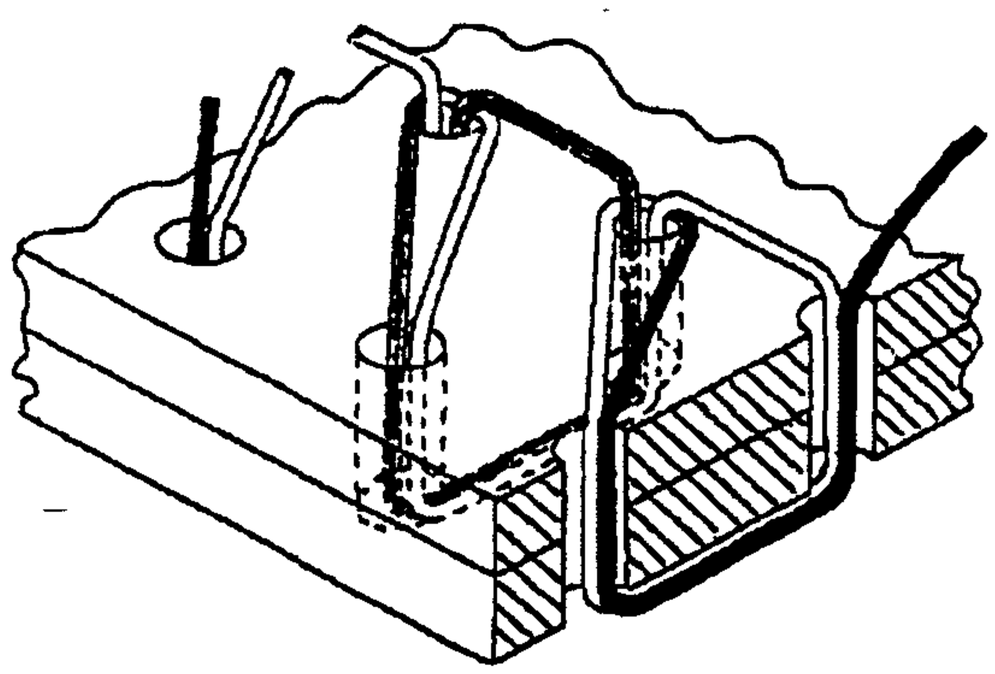

Figure 3.9 RTD chain stitches

3.5 Ply Manipulation

The section presents the most important part of the skin stiffener tool design; namely the means of manipulation. Various designs that have been considered for forming a range of shapes from flat plies into 3-D structures (I,C, J,T) will be reviewed; with regards to their advantages and limitations.

The section concludes with a proposal of a multi-purpose forming tool that encompasses all the aforementioned shapes. This tool, which overcomes most the obstacles encountered in the previous designs, has been adopted in this project.

3.5.1 FOlding Shuttle for Shape Inclusive Lay-up (FOSSIL)

The first design considered was similar to that produced by **[Chesney et al 1995]** during the development of the Brunel 'FOSSIL' (**FO**lding **S**huttle for **S**hape Inclusive **L**ay-up). This design was based on the shuttle being a robotic end effector, which is used to manipulate a flat piece of material already laid-up on a flat surface. The device was designed to 'pick-up' the

material and run along the edge, thereby initiating a fold. A second piece of material was then placed on top of the folded edge prior to being attached and placed in a mould. A picture of the original FOSSIL is shown in ,Figure 3.10.

This design utilised the folding of one piece of material around a single tight radius along the centre of the fossil.

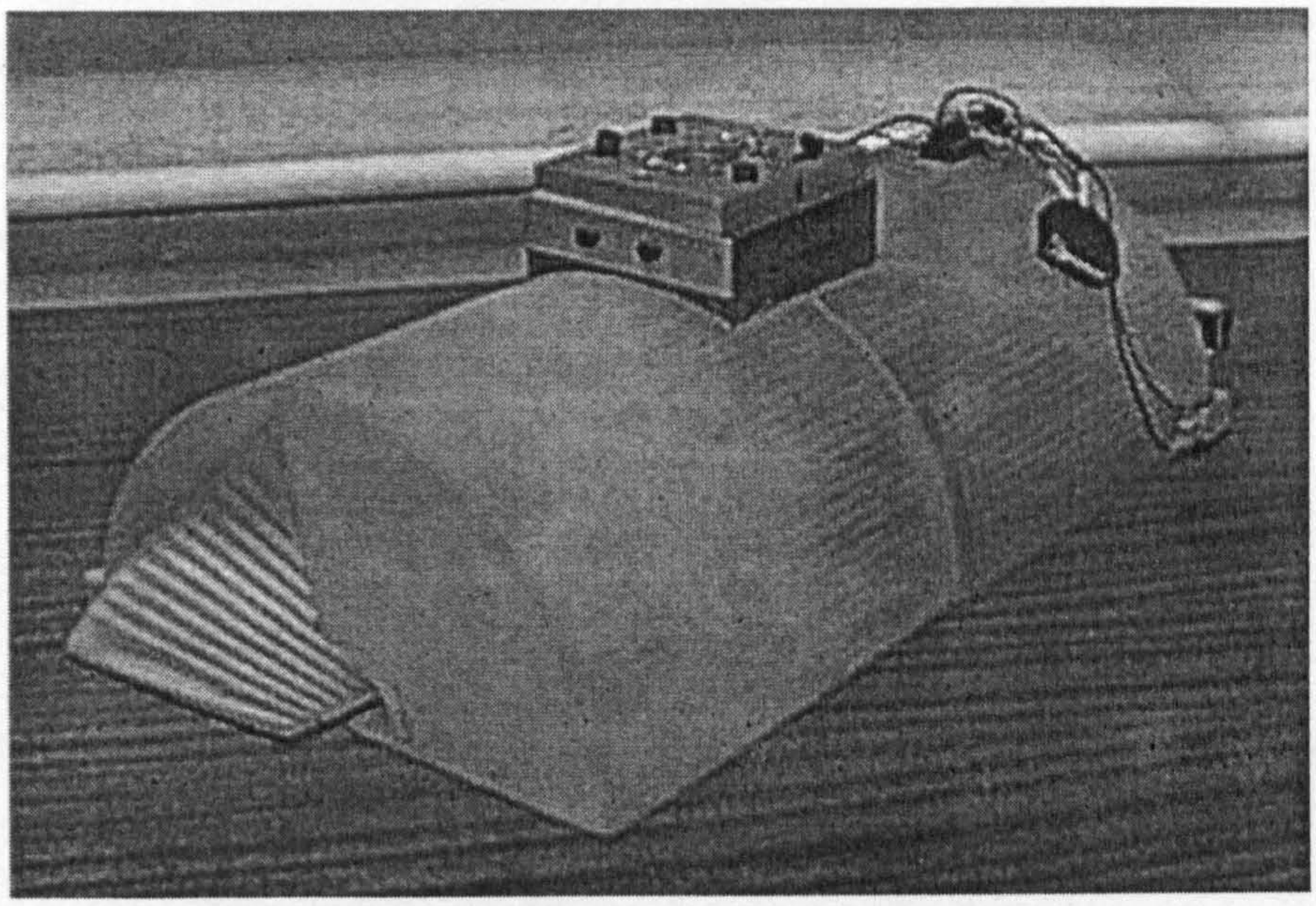

Figure 3.10 The original FOSSIL Developed at Brunel University

A model was developed at Brunel, based on the fossil method, to establish the minimum length the estimated material thickness could be folded in, and also to establish the internal radius of the bend. This tool could be manipulated by the use of a series of collars with basic 'rollers' on them to control the material through the bend with minimal friction between the material and the rollers. As ,Figure 3.11, shows there were forty of these rollers around the centre rod, each one able to be set to give a profile for the entry of a new tool.

Results from this model showed that the fossil fold could be induced over a shorter length, because once the material had been picked up by the FOSSIL, the first third of the fossil was not in contact with the material. This would

allow a much shorter fossil to be developed, making the tool much more compact, thus allowing more room for other parts of the system.

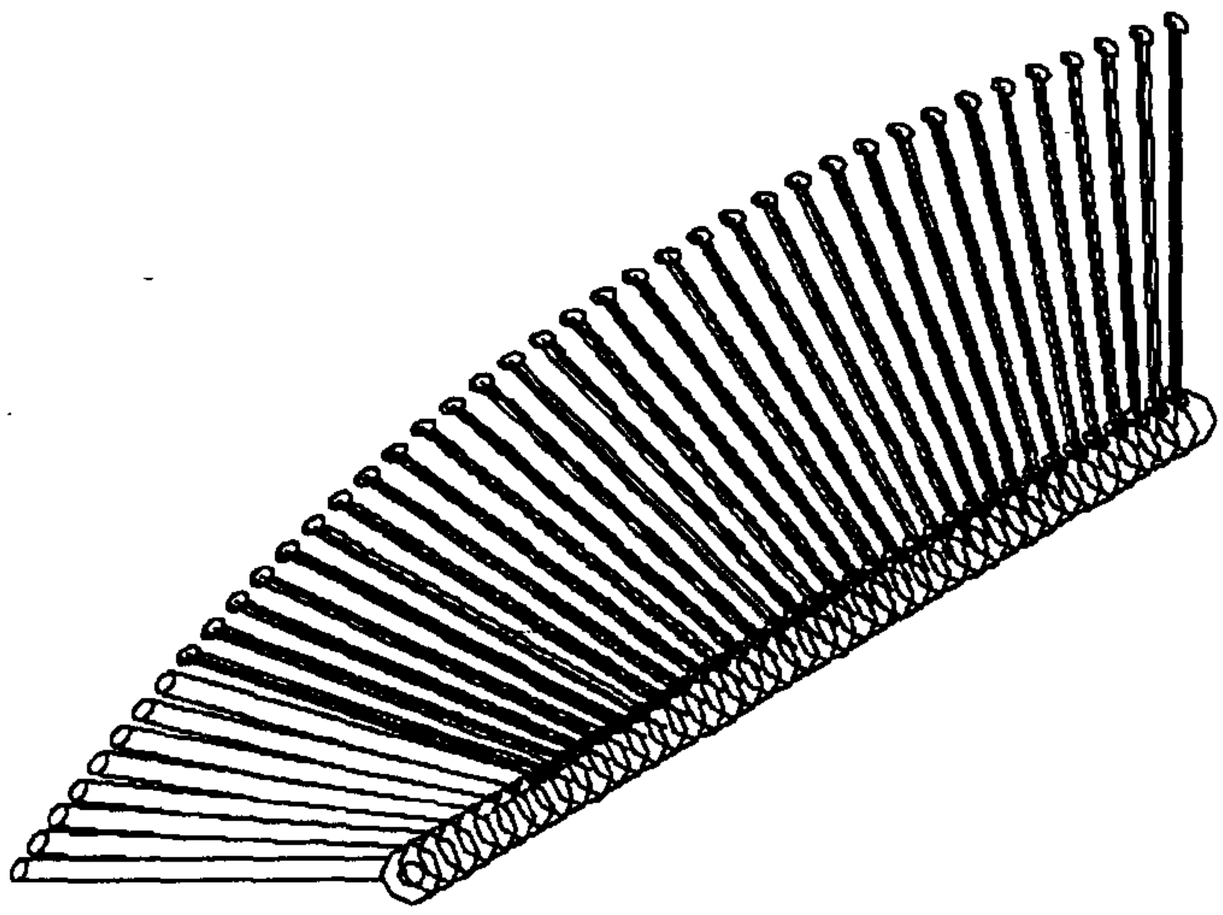

Figure 3.11 Fossil Prototyping Device

The first parts of the designs considered for single ply manipulation was developed around a single pass along the span. This was to take some NCF and manipulate it into a single stringer for attachment to the skin as individual stiffeners. The stringer would look something like the drawing shown in ,Figure 3.12.

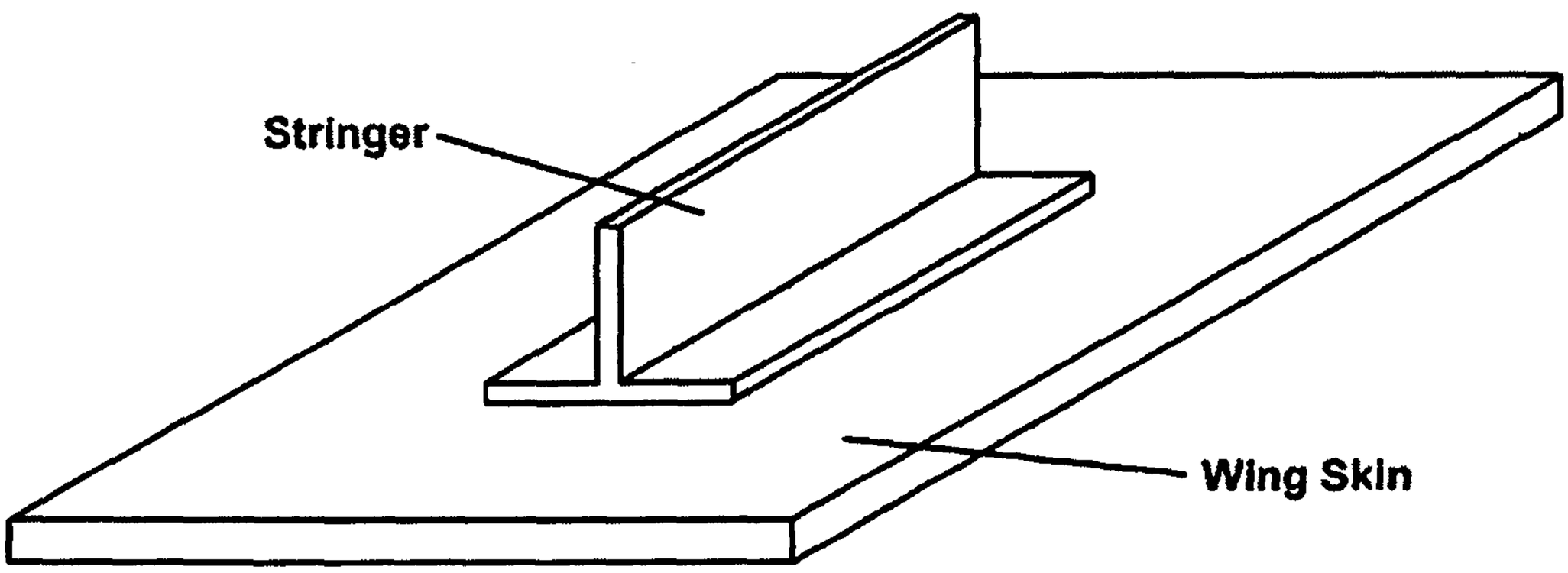

Figure 3.12 Stringer mounted onto skin

Two different methods were considered, the first was to take two pieces of material, fold them into 'L' shapes, and then stitch them through the thickness in the web, and also attach the stringer to the skin.

The second method considered was to take a single piece of material and manipulate it into the stringer shape, as shown in, Figure 3.13. The device was developed at Cranfield University for prepreg materials **[MPhil thesis 2002]**.

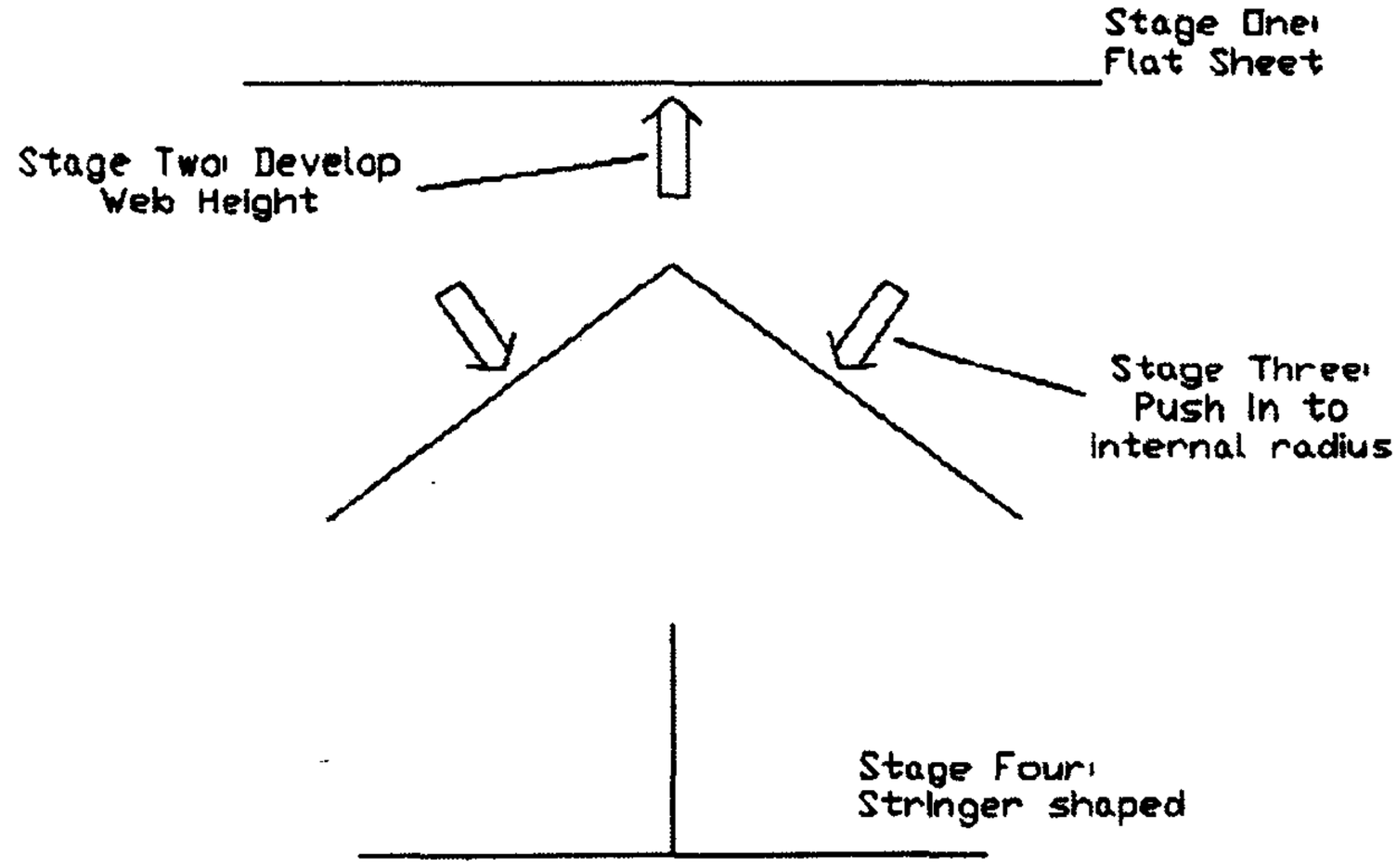

Figure 3.13 Single Sheet Manipulation into Stringer

3.5.2 The Semi-Fossil

This design was an adaptation of the original fossil shown in, Figure3.10. However, the Brunel Fossil induced an 180° fold, which had already been proven on previous Brunel research, and was, at the final stages of the project, deemed unsuitable for the final design of the tool being developed.

This design was supposed to be two 'half' fossils used to manipulate the material into the desired shape. The Semi-Fossil concept is shown in ,Figure 3.14.

Figure 3.14, shows the internal surface of the semi-fossil, which shows the edge of the material being lifted from a horizontal to a vertical position. The internal radius of the material would be controlled by an internal face of the tool, with sections in the vertical face being removed for the through-the-thickness attachment method.

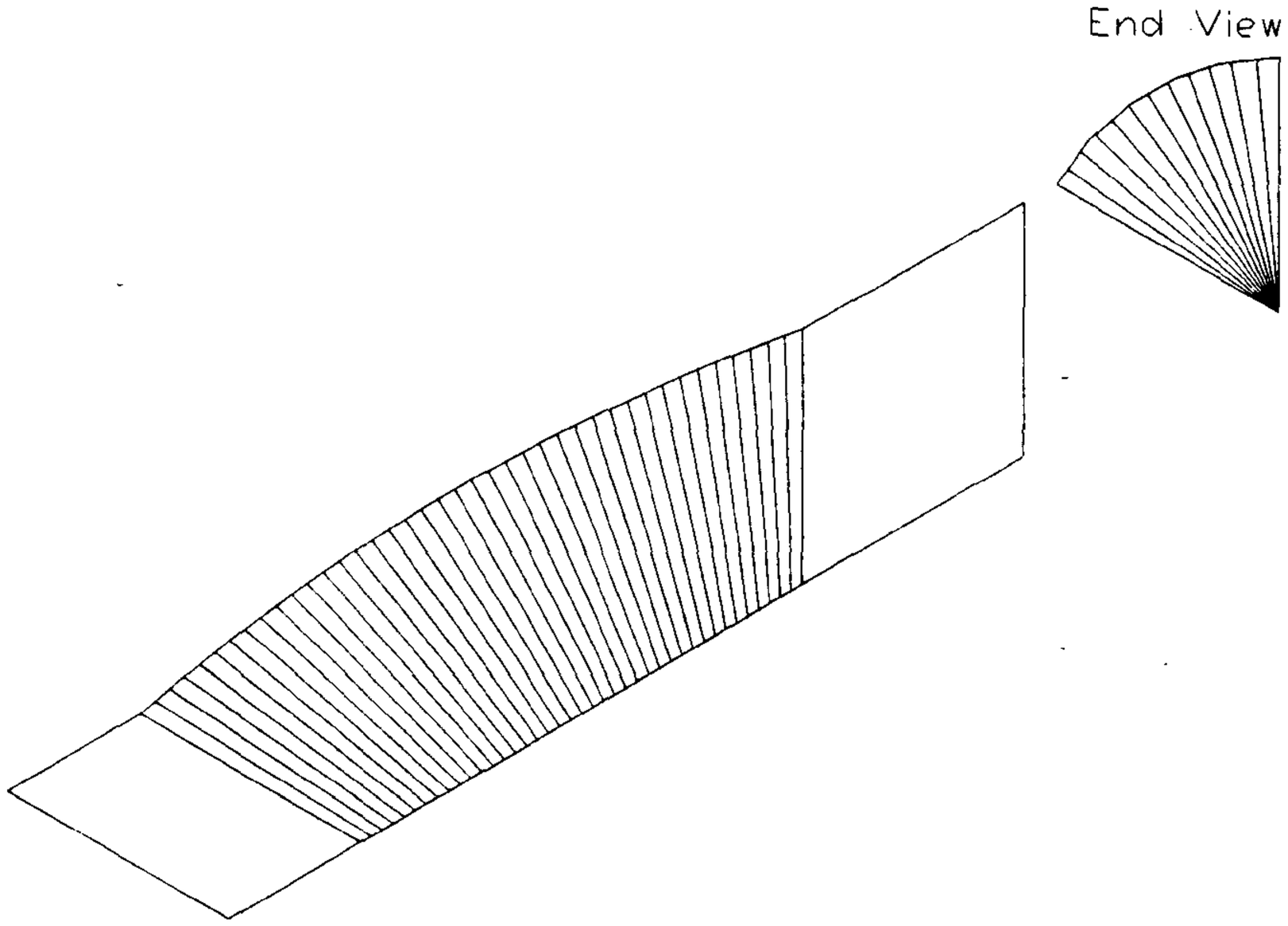

Figure 3.14 'Half' Fossil Concept

3.5.3 The Wire Forming Method

This method was first considered as a control surface for the semi-fossil. However, while the semi-fossil lifts the material to the vertical position, there is still the need to induce the internal radius of the stringer vertical section. This method was a way of inducing this parameter into the tool.

Following discussions, it was determined that this method could be utilised on it's own, with fewer control surfaces on the shaping part of the tool.

A simple model was built at Brunel to test the theory, and, using simple tests, the method worked quite well, however, due to the in-built flexibility in the wire, the method was unable to produce reliable results.

Different variations in the shape of the wire were also tried, but the method shown in, Figure 3.15, seemed to give the best forming of the radius. With more investigation, this method could be an alternative way of introducing a fold, especially where the internal radius is a critical factor.

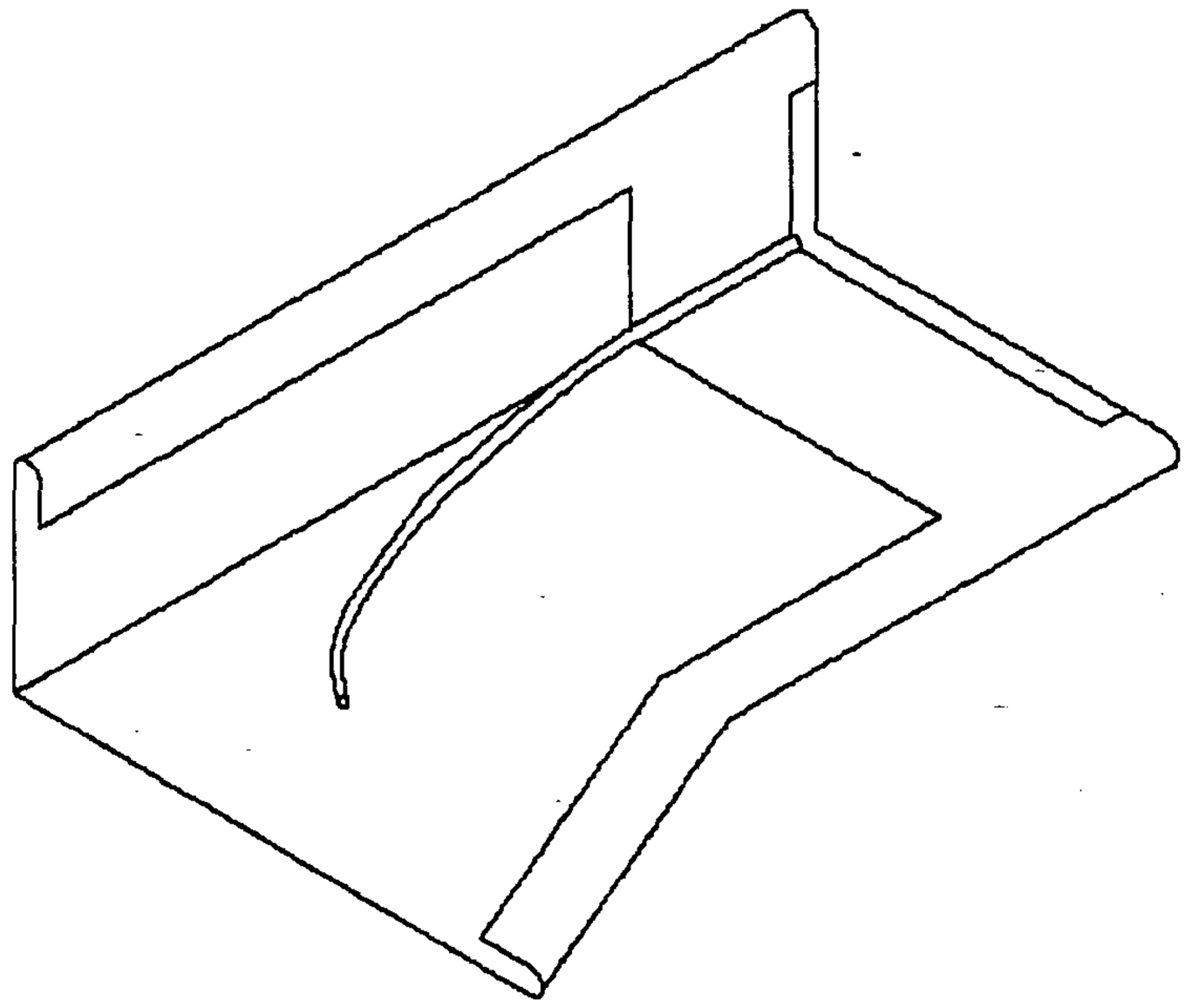

Figure 3.15 the Wire Forming Method

3.5.4 The Shape Forming Shuttle

The shape forming shuttle (SFS) was taken from the 'shuttle' design used in the wire forming method. The idea was to take the flat piece of material and control it exactly through a specially designed forming tool. This tool was flat at the front, where the material was picked up, and shaped to the correct dimensions at the rear, where the material is attached to the skin. A sketch of the SFS is shown in ,Figure3.16.

With a lot of today's low friction materials, a shuttle of this type could be used to shape the flat lay-up into the required L shape. However, the usefulness of this type of shuttle in a development environment would limit the number of design iterations due to cost and lead-time for the component.

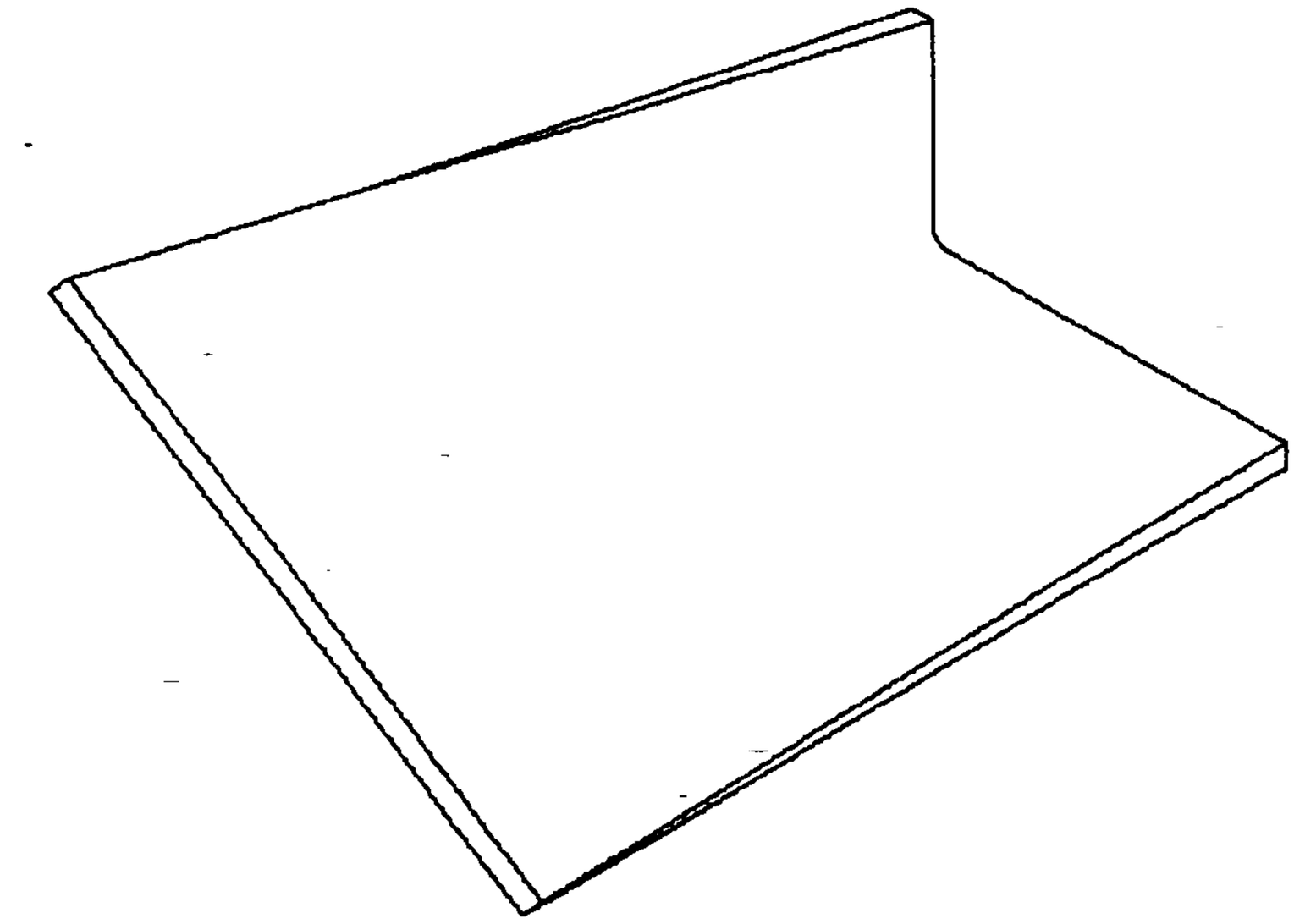

Figure 3.16 The Shape Forming Shuttle Sketch

3.5.5 Ply Forming Across the Cord

With the final planned use of the tool being a single pass along the wing box, covering both span and cord of the wing, methods of duplicating the process across the cord of the wing were considered. ,Figure3.17, shows one method considered for duplicating the half fossil folding shuttle across the cord of the wing.

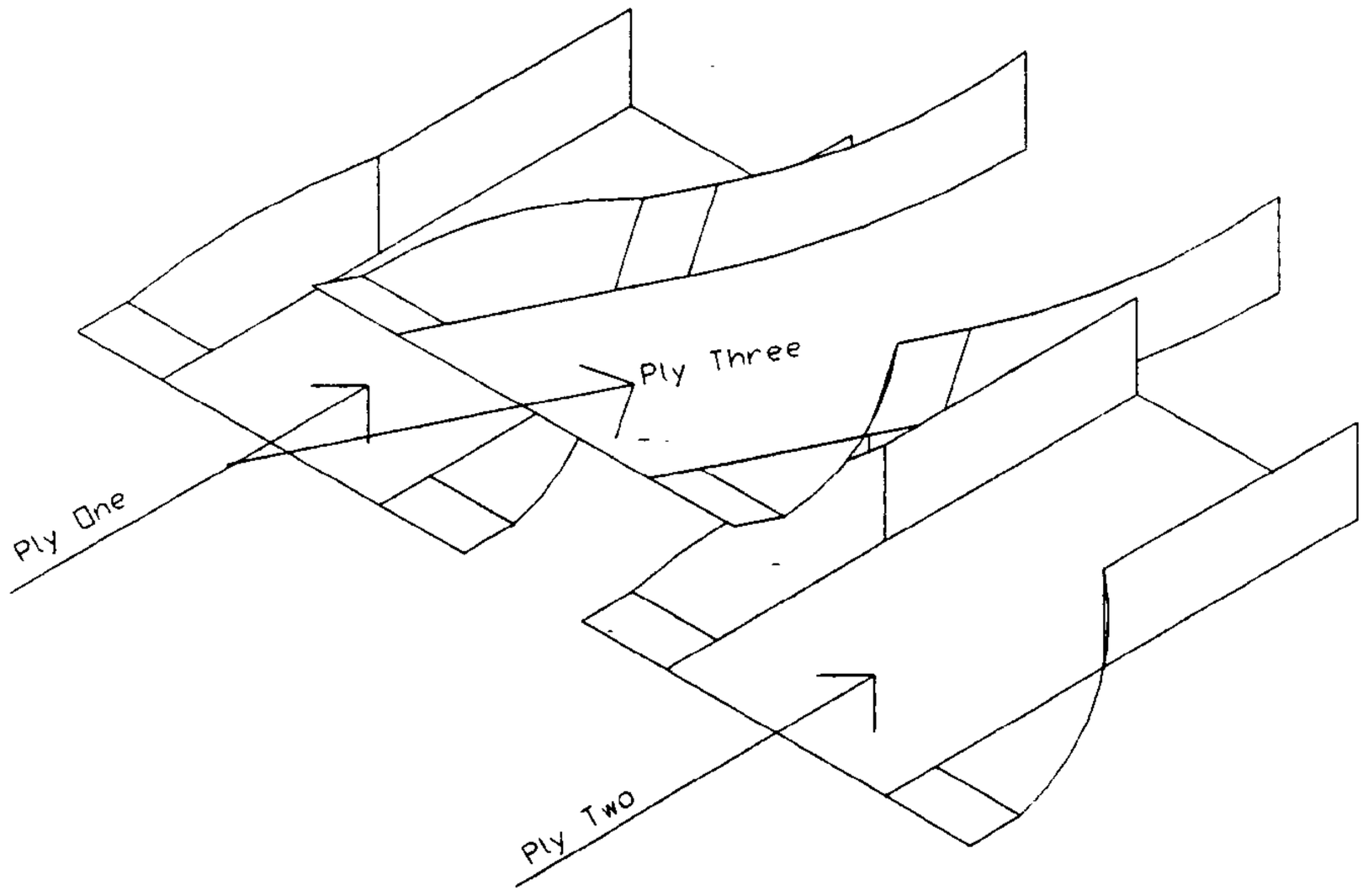

Figure 3.17 Semi-Fossil for Placement of Stringer Across Cord of Wing

It can be seen from, Figure3.17, that the middle 'U' section (Ply Three) of the stringer has a higher material collection (leading) edge than the two parts (Ply One and Ply Two) on the bottom. This is due to the material exiting the semi-fossil at the same level, allowing the web to be attached prior to the attachment to the wing skin.

This type of shuttle would be modified slightly, allowing the extra NCF for the web to be fed into the shuttle, on the same level as Ply One and Ply Two, at the same time as the two 'U' sections. This allows greater flexibility when selecting the means of attachment, as all the material can be manipulated into the correct shape prior to attaching the material together through the web. This method of attachment does not need the extra flexibility for the Brunel RTD head when stitching, as there is clear access to both sides of the component being stitched.

3.5.6 Tool Material Manipulation Method

This method, Figure 3.18, utilises a forming shuttle to control the edges of the material as it passes from the entry as a flat sheet into the L forming process, attachment through the web, and attachment to the skin. This method gives a high degree of control on the edges of the dry fabric lay-up. But it is not flexible tool, only introducing a certain T section is possible.

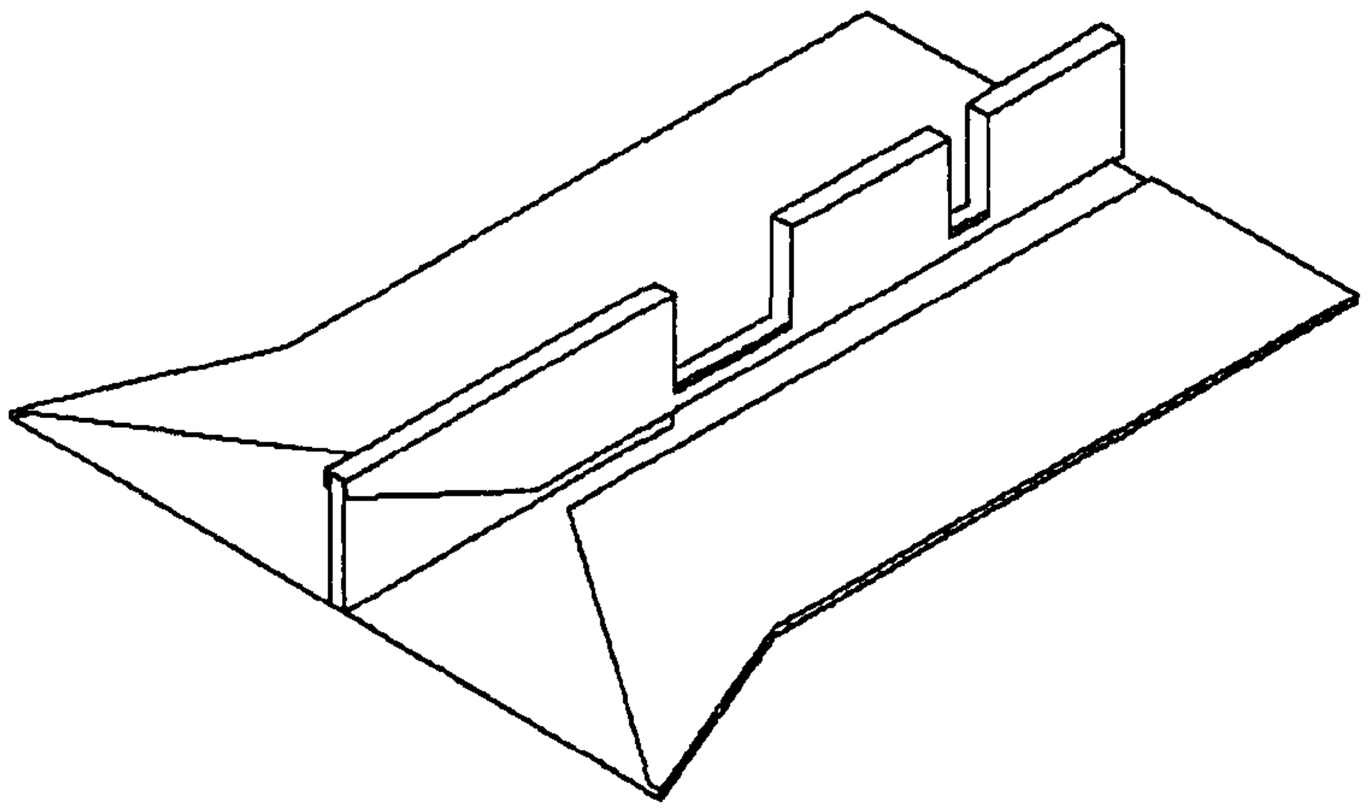

Figure 3.18 Folding Shuttle for Tool

3.6 Ply Control

This section discusses various methods and models for controlling the ply as it passes through the forming process, and into the attachment stage of the process. This section is split into two areas, means of moving the material and means of controlling the material.

3.6.1 Vertical Pinch-Rollers

This is a relatively simple method of controlling the ply through the shape forming section of the tool. A pair of rollers, driven from the same source so their speed is identical, are used to grip and pull the material through the forming process. ,Figure3.19, shows how the rollers are mounted.

The pinch rollers are mounted in a frame on the stringer tool. The speed of the rollers is maintained so that the speed of the motor is sufficient to only pull the material when the material is being manoeuvred by the sewing machine. This reduces the material damage that may have been caused by the speed (rotation) of the motor being too high.

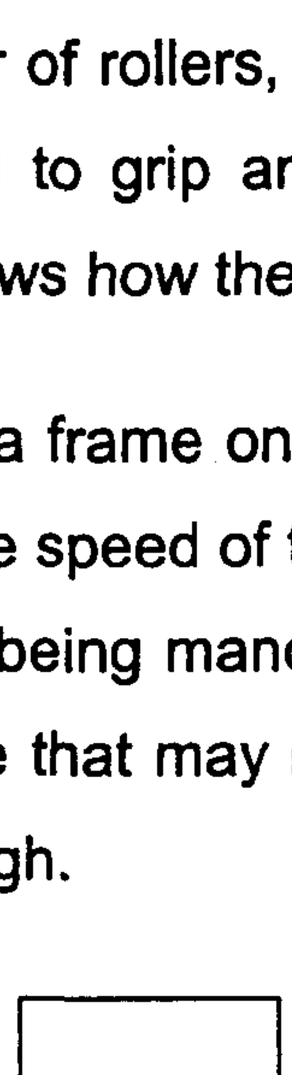

Figure 3.19 Vertical Pinch Rollers

This type of roller could be used on flange portion of the stringer to pull, or push, the material through the stringer manufacturing section of the tool.

3.6.2 Horizontal Rollers

The horizontal rollers, Figure 3.20, would be used to control the material in the horizontal plane of the material as it was passing through the tool. The rollers would also be driven from the same motor, and therefore their speeds would match.

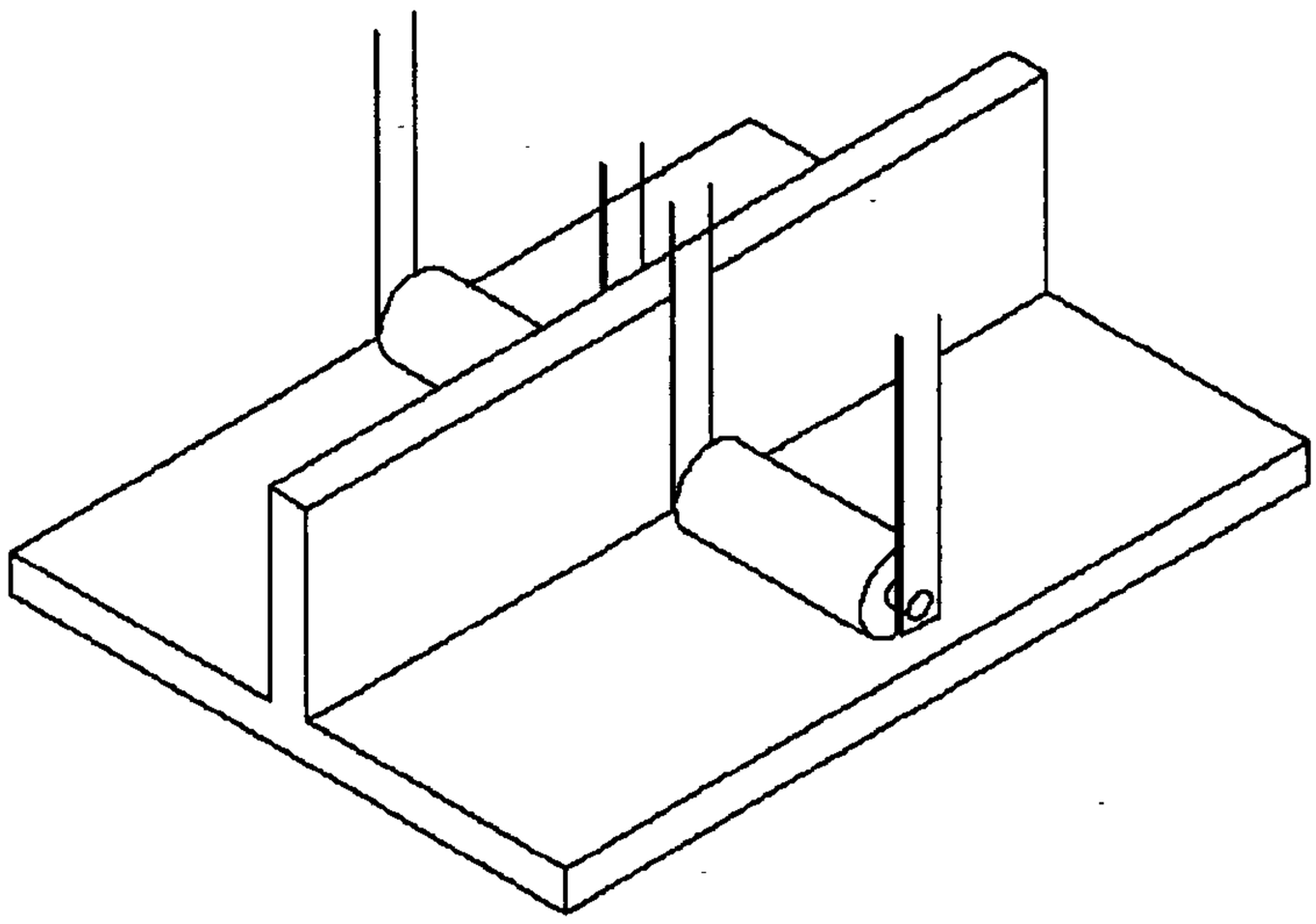

Figure 3.20 Horizontal Rollers

The mechanism for driving two rollers was never developed as a single roller, developed under a different project, at Brunel proved to be too difficult to control the material, and the addition of another roller would create more problems.

Some of the problems experienced were due to the roller's interface with the material that caused the material to locally deform. The two rollers had to be exactly in line, and exactly parallel to the material, or the material was subjected to a shearing force at the rollers contact point that caused the material to deform.

3.6.3 The 'Pulley' Rollers

The system that was considered, Figure 3.21, the pulley is driven at both ends of the pulley, using a single motor and a gearing system, to drive material on

both sides of the web. The width of the system could be varied both horizontally and vertically to increase the control of the material being moved through the tool. As with the previous method, the control mechanisms for this type of small roller system would need to be extremely accurate, and manufactured to the tightest tolerances, in order for this type of system to work.

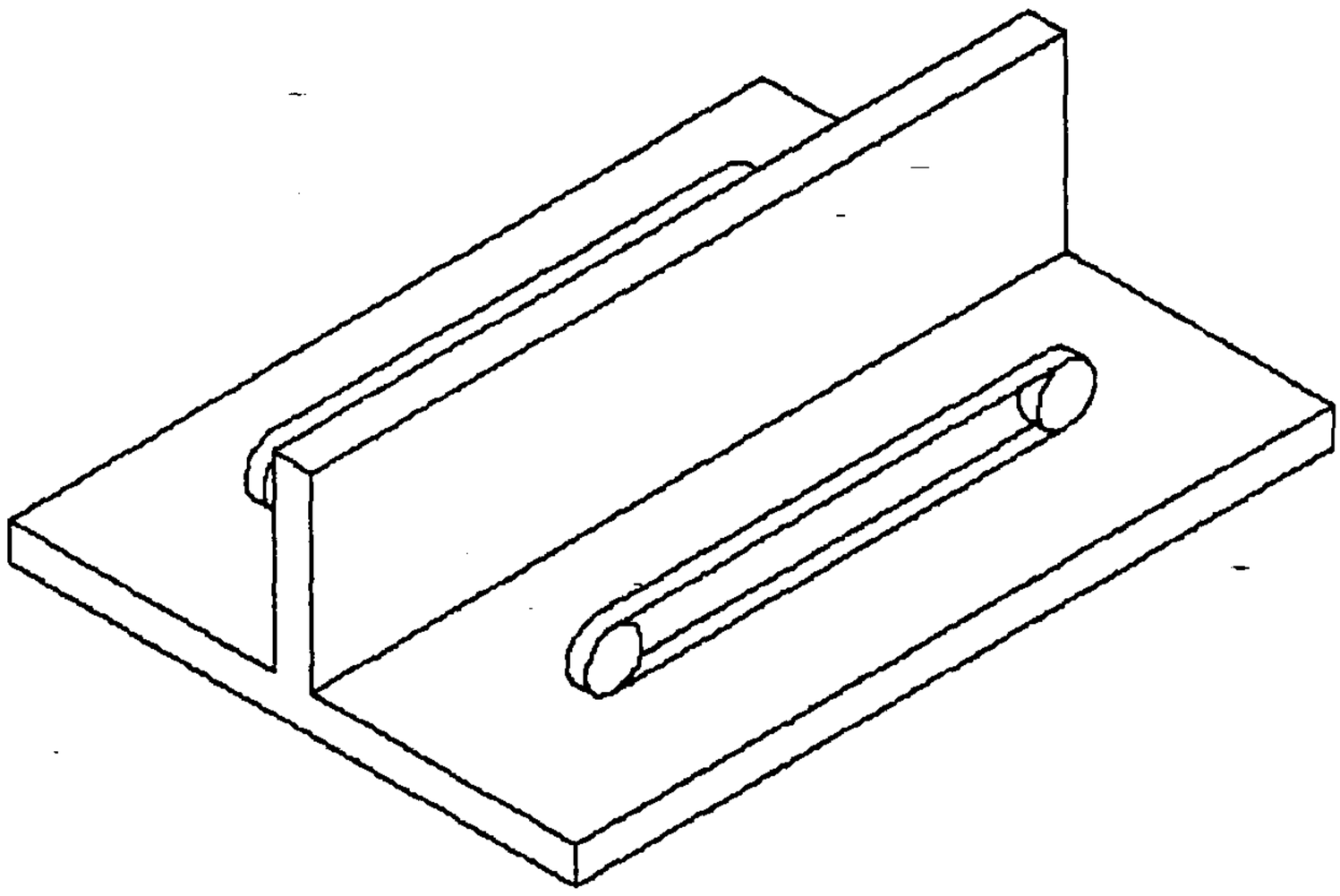

Figure 3.21 'Pulley' Rollers

3.6.4 The Corner Rollers

This type of material control system was thought of as both a material control and a material forming system. This could be used in the material forming method. A sketch of the rollers is shown in ,Figure 3.22.

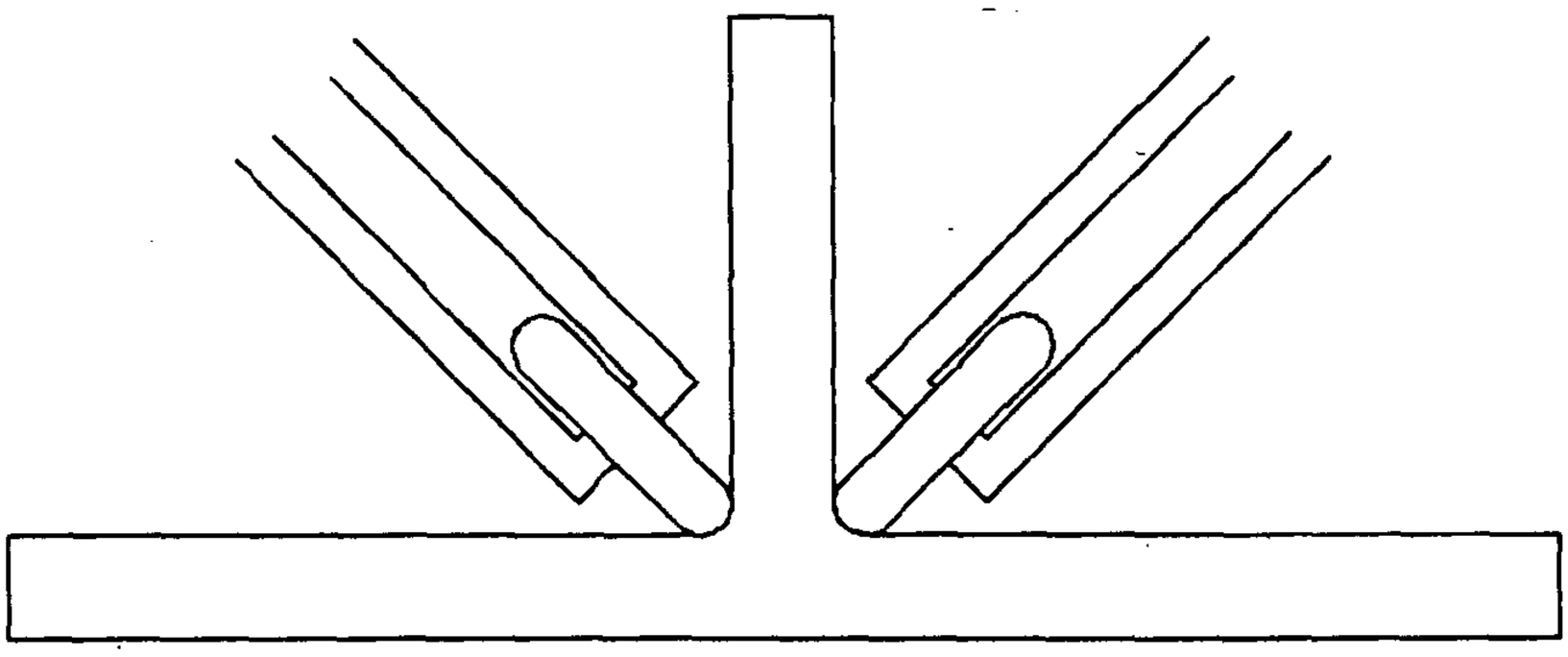

Figure 3.22 Corner Roller System

This method could have been used on an NCF designed stringer to push the material into the correct radius prior to the skin attachment and through the web attachment. However, it would be much more suited to use on a prepreg material where the material can be heated prior to manipulation so it becomes 'tacky' and would hold the radius much better.

3.6.5 The Large Single Roller

The large single roller was conceived to try to reduce the control problems associated with the two smaller horizontal rollers. The principle is similar, except the roller is a single roller with a channel cut in the centre to allow the web to pass through.

Figure 3.23a, b shows the large single roller in front and isometric view on the stringer. This method had the advantage of giving a larger surface area, due to the larger radius, to contact the material. Again, any small angular error in mounting the roller could cause problems within the material when attaching to the skin.

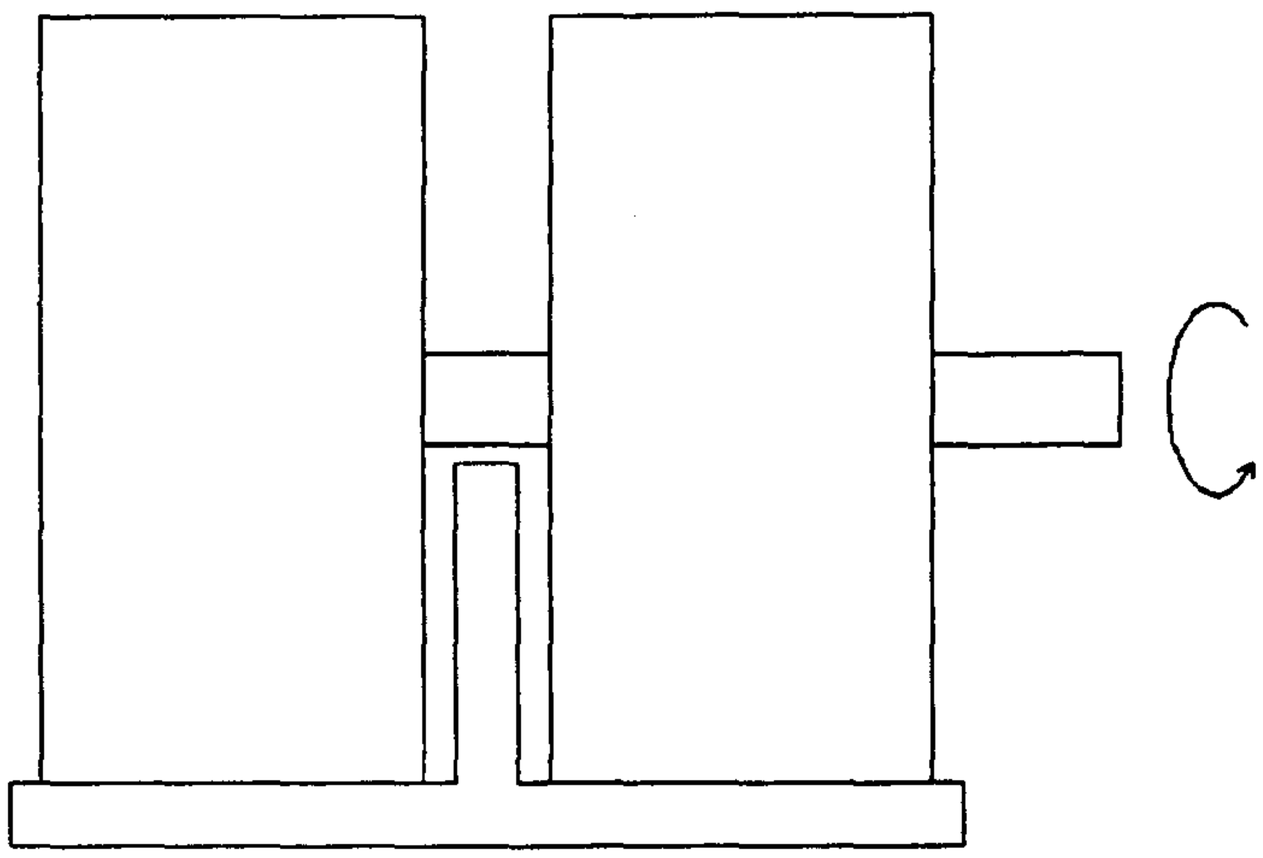

Figure3.23a Front View of Large, Single Roller

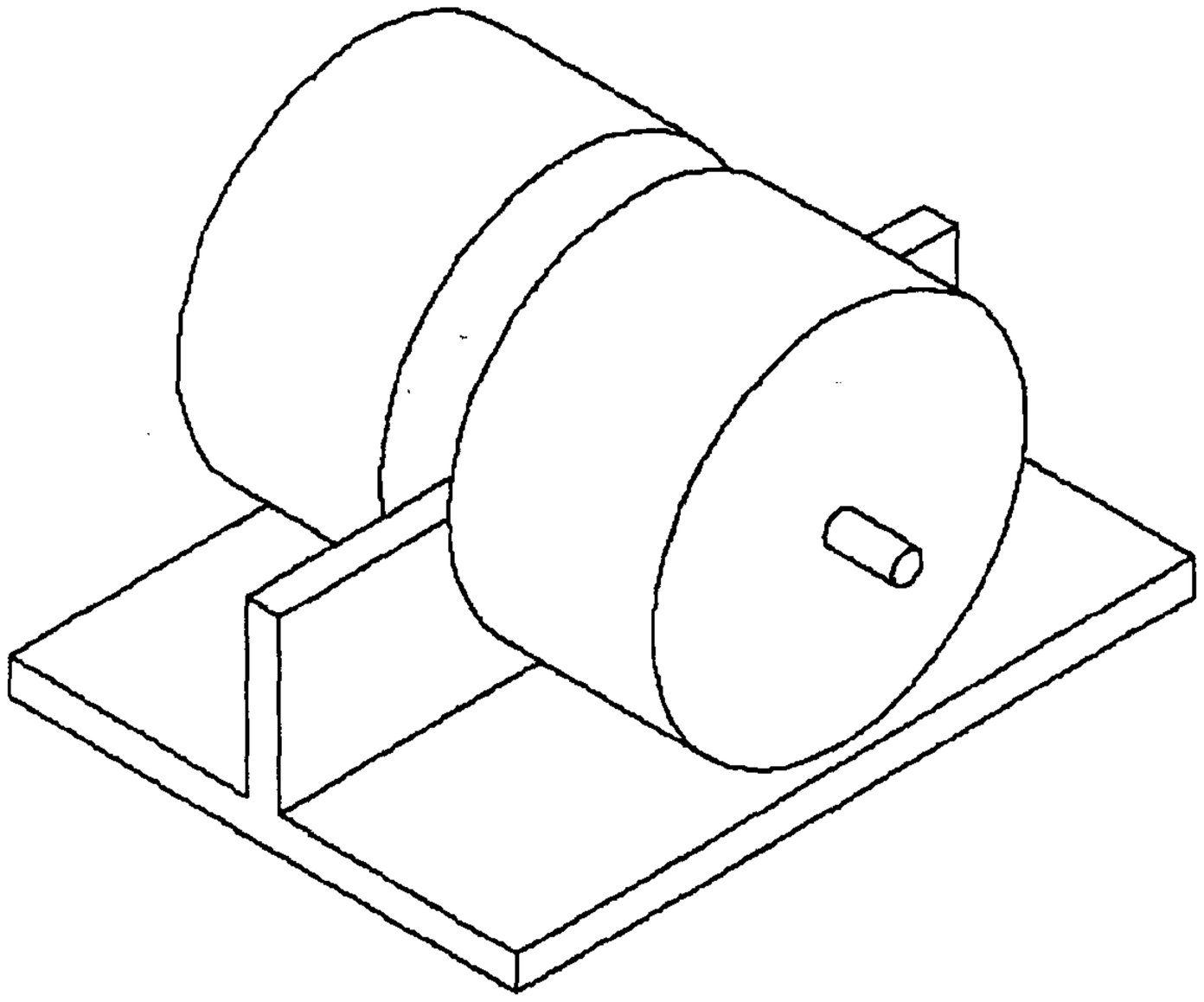

Figure 3.23b Large Single Roller

These rollers could be driven from a single stepper motor, giving accurate control of the speed of the material through the shaping process.

3.7 All in one forming tool

The previous investigations showed that the need for flexible tool to manipulate with dry fabric, introducing the various composite structures, is desperate. Figure 24a, b shows the novel technique that has been adopted in this project. The forming tool is integrated into a fully automated cell to allow the tool to introduce the various shapes of structural components with various dimensions in one single shot. The forming tool was built so that the inner surfaces matched the exact dimensions required for the finished stitched component. Full details of the construction and integration of the forming tool as given in chapter 5.

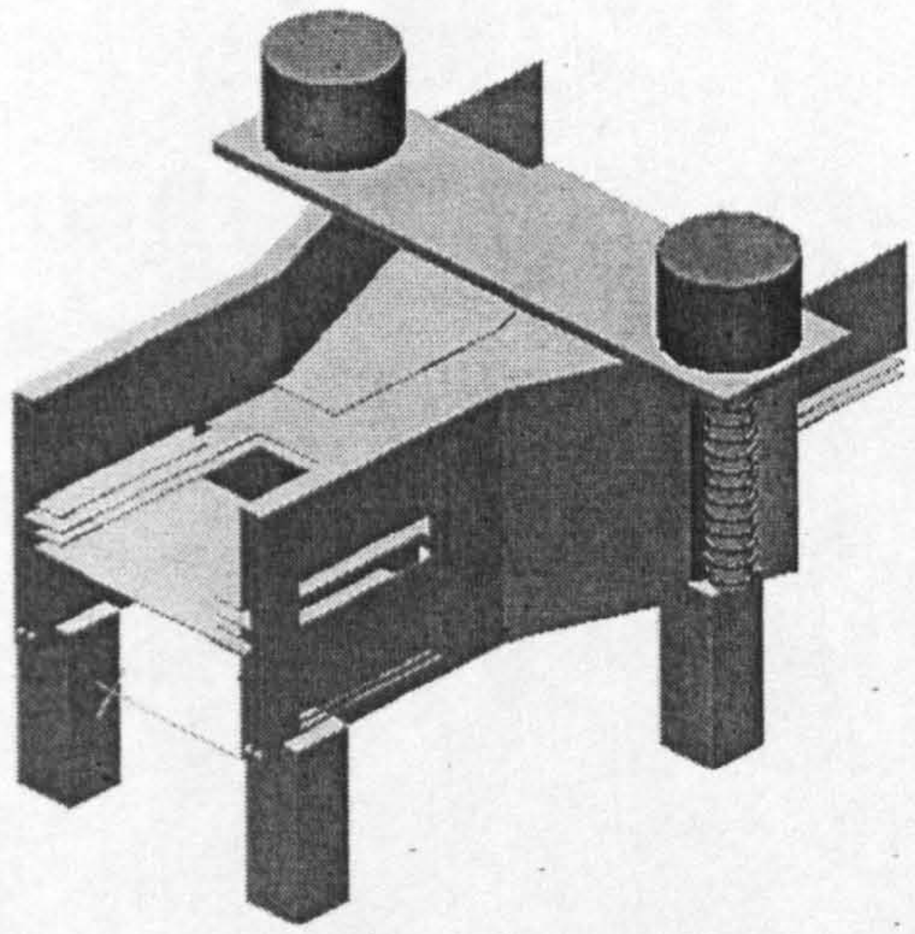

Figure 3.24a front view of the novel forming tool

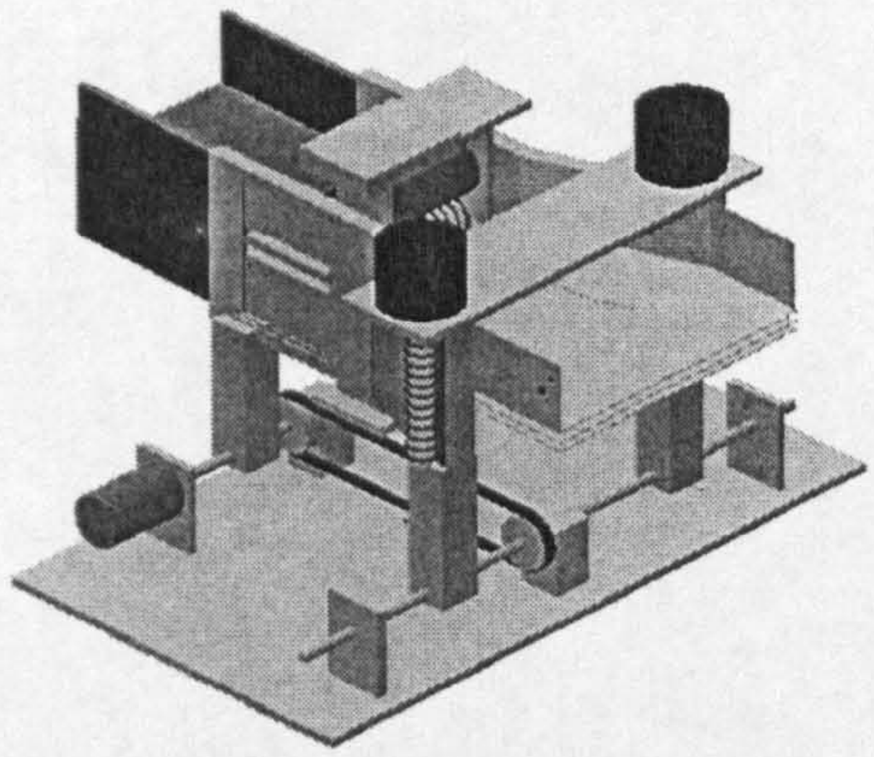

Figure3.24b back view of the novel forming tool

3.8 Conclusion

This chapter discussed a number of approaches to join plies together and make attachment to the reinforcement structures. A full assessment of the properties, advantages and disadvantages of each method has been investigated.

The means of manipulation is the most important part of the skin stiffener tool design. Various designs for forming a range of shapes from flat plies into 3-D structures (I, C, J, and T) have been proposed in the literature. A critical

review of these designs has been undertaken; with particular emphasis on to their advantages and limitations.

Finally, a proposal of a multi-purpose tool for forming a range of reinforcement structures has been suggested. This tool, which overcomes most the obstacles encountered in the previous designs, has been adopted throughout this project.

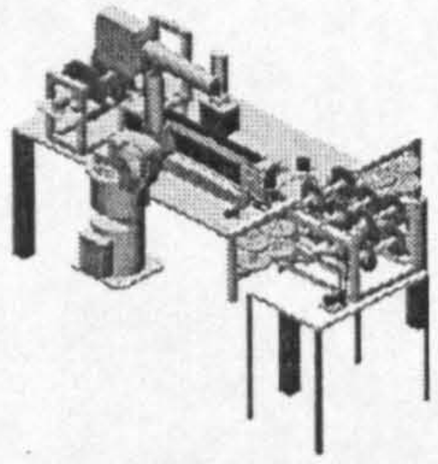

Chapter 4 Modelling and Simulation of the Manufacturing Cell

4.1 Introduction

Before the manufacturing cell is developed, a simulation was undertaken to examine the cell. The individual parts have been modeled and arranged as a manufacturing cell, which is able to carry out the required tasks. Different cell layouts have been created and each of them examined to determine the most appropriate solution for the cell layout. Necessary modification of the cell arrangement can be made immediately, without any difficulties. In addition clash detection can be carried out in advance to avoid unfavourable motions and robot configurations.

Grasp 2000 was used, which has the facilities for demonstration animation and off-line programming. Off-line programming offers a couple of advantages compared to on-line programming.

For example programs can be written for new applications even if the robot is still used in an order task. So, periods of robot standstill are avoided while the new robot program is generated and systems start faster because of reduction of program time.

Each part of the manufacturing cell has been modeled and then arranged in the workplace according to the proposed design. Afterwards the required robot motions, which are necessary to carry out the task, have to be determined. Programs for the robot and machines have been developed and written, and subsequently integrated in the modeled cell. Finally the modeled cell should be able to simulate the manufacturing processes which will be later carried out by the real manufacturing cell.

4.2 Simulation objectives and plan:

First of all an identification of the required objectives has to be carried out. It is advisable to work out these goals carefully and all the boundaries and limits of the entire process should be considered. Modification or changes are much more time consuming and often impossible to realise at later stage.

In the second stage the modeling of the machines, robot, manipulators and all other items of equipment has to be done. Normally it is one of the most time consuming parts. But the Grasp 2000 offers facilities to reduce this expenditure by using CAD interface. Predefine objects can be easily imported and sufficient accuracy of the models is guaranteed.

The next stage is creation of tracks, which contain all the required commands for driving the robot and the rest of the cell. In the beginning the modeled entities have to be arranged in the work environment and different types of paths have to be defined. Next the required tracks have to be created considering the communication between the single systems.

After that an optimization of the entire program may be carried out and workplace modification can be done. This is one area in which the Grasp 2000 has obvious advantages compared to the real world. To move robot and machines is easy in the Grasp 2000, whereas in reality the relocation of a machine takes a lot of effort and time.

When the whole system is optimised and performed in the required way, the final output may be used for off-line programming, clash detection examination, cycle time determination also video and slide creation and for production of plots and hard copies (appendix A).

4.3 Simulation aims:

- Determine the cycle time for the process
- Create the right sequences for the cell elements.
- Identify and prevent the collision among the moving elements.
- Design off-line programs to run the cell, which will be very easy to make any required modifications.
- Calculate the required area for the automated cell
- Create impressive and effective demonstrations and run repeated 'what-if' scenarios to evaluate different solutions for the cell equipment.

4.4 Simulation overview

The Grasp 2000, which used in this work, is an advanced robot Grasp 2000 using the latest computer technology. In contrast to usual simulation applications, where different software tools are necessary to model the environment and run a simulation, the Grasp 2000 contains both a 3-D solid modeling module and a generalised kinematic modeler so there is no interface is necessary to transfer data from a CAD system to the simulation program.

The Grasp 2000 has the facility to generate a task with two different methods for interacting between user and system. On one hand there is the more sophisticated textural file input, and on the other hand the fully interactive user interface allowed entering commands by picking them from the screen using the mouse. In addition a mixture of both methods may be used which is the most common way of designing and creating a task for normal applications.

The Grasp 2000 also offers the feature of robot off-line programming. After designing the manufacturing cell and creating all the required movements the Grasp 2000 generates a neutral high level program which includes all the necessary positional and logical information required by the robot.

4.5 Modelling of the manufacturing cell

4.5.1 Manufacturing cell

The manufacturing cell comprises of a laser cutting table (AXON A201), articulated robot (GMFanuc S-10), tacking device, lay-up table, material bank, material delivery system (MDS), folding device, transporter and storage. The tacking device is attached to the robot and it is used to tack the stacked layers together. Both devices can be easily dismounted.

All the entities have been modeled and stored in a single file. Frequently a mixture of textural input method and interactive application were used to model the objects. In the last stage all these files were imported and arranged accordingly to the layout of the manufacturing cell.

In the following sections the modeling of each object and the final arrangement of the manufacturing cell are described, and in the final section the manufacturing cell is created.

4.5.2 Modeling of the tools

4.5.2.1 Modeling of the laser cutter

The Axon A201 laser cutter consists of two axes which can move either in x-direction or y-direction. The Grasp 2000 offers two ways to model the laser cutter, either auxiliary axes within a robot file or a single robot. The base of the Axon laser cutter consists of the frame of the machine, which is built up of four bars and the vacuum table. The object co-ordinate systems of the base and the modeled laser cutter are coincident and placed at the top corner. The arrangement of the joints is illustrated in ,Figure 4.1.

The first joint is shifted 50 millimeters along x- and y-axis and performs a transnational movement in x-direction. The sledge, which is situated on the base and consists of four bars arranged in a cubical way, belongs to the first

joint. The joint is able to drive 2500 millimeters by a maximal velocity of 1000 mm/sec and an acceleration of 0.67 mm/sec^2.

The second joint is shifted 45 millimeters along y-axes and lifted 200 millimeters along z-axes relatively to the first joint. This joint performs a translational movement in y-direction by a velocity 1000 mm/sec and an acceleration of 0.67 mm/sec^2. It is able to drive 1250 millimeters. The laser head, consists of %BOX1 and %BOX2, is connected to joint 2.

Joint 3 is on the same height as joint 2, and is only shifted 700 millimeters in the x-direction, it performs no translational or rotational movement and no objects are linked to it. Joint 4, 5 and 6 coincide and shift 170 millimeters in negative z-direction. They are also fixed and immovable and only a cylinder is added to join 4. The laser cutter is modelled using the solid object method as shown in, Figure 4.2.

4.5.2.2 Tacking device (RTD)

The tacking device consists of four main parts: an adapter, which is necessary to attach the tacking device to the TAP (tool attachment point) of the GMFanuc S-10 robot, and small components such as steel needle, yarn and cutting device as shown in, Figure 4.3. These details are not relevant for simulation. They only increase the required time for modeling the tacking device and enhance the required memory space and calculation time. Hence, it is advisable to override the modeling of the details and concentrate on the creation of the main parts.

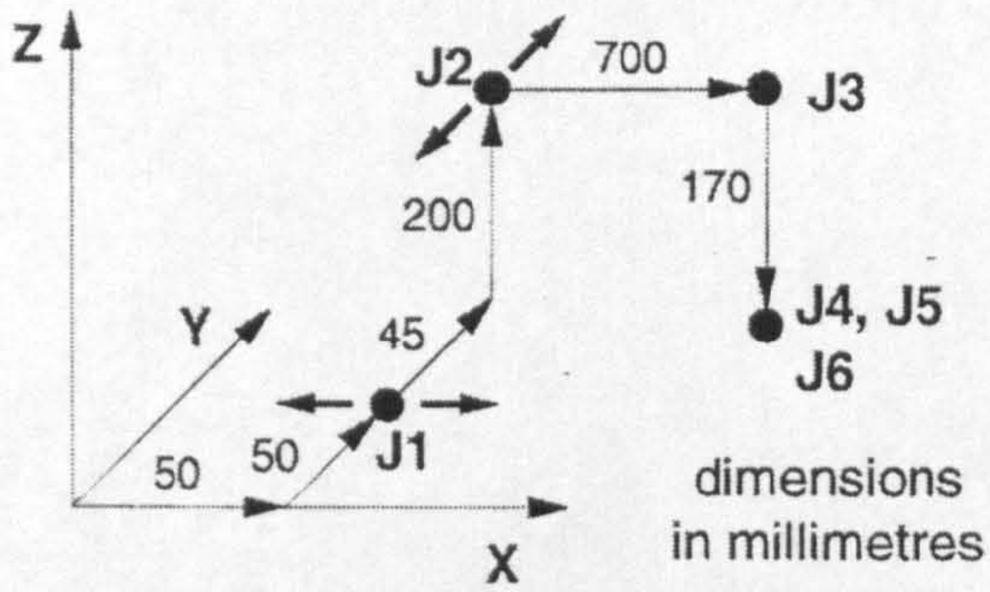

Textural Input File:

```
ROBOT LASER NEW TYPE AXON
        JOINT1 (SHIFT X 50 Y 50   ) PRISMATIC X
        JOINT2          (SHIFT Y 45  Z      200) PRISMATIC Y
        JOINT3 (SHIFT X 735       ) PRISMATIC Z
        JOINT4 (SHIFT Z- 170      ) PRISMATIC Z
        JOINT5                      PRISMATIC Y
        JOINT6                      PRISMATIC X
        TAP      (SHIFT Z –25)
        MINIMUM            0  -40  -15  -15  -15  -15
        MAXIMUM     3095  1955 -15  -15  -15  -15
        INITIAL              0   40   0    0     0     0
        PARK    0    40   0    0     0     0
        VELOCITY       1000  1000   0    0     0     0
        ACCELERATION 667    667  0    0     0     0
        MAXIMUM_LINEAR_SPEED  1000;
```

Figure 4.1 Joint arrangement of the AXON A201 laser cutter

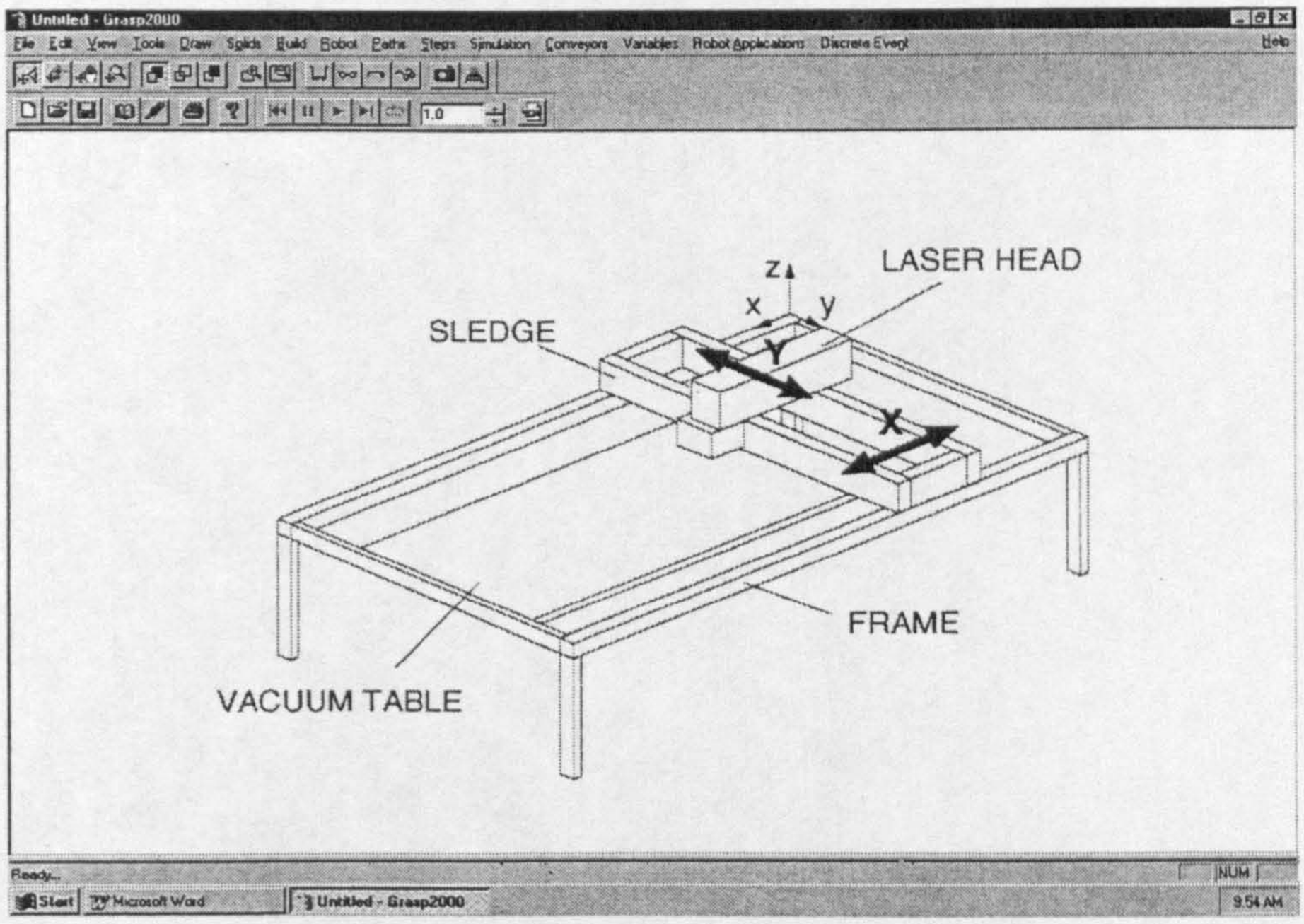

Figure 4.2 Modelled laser cutter

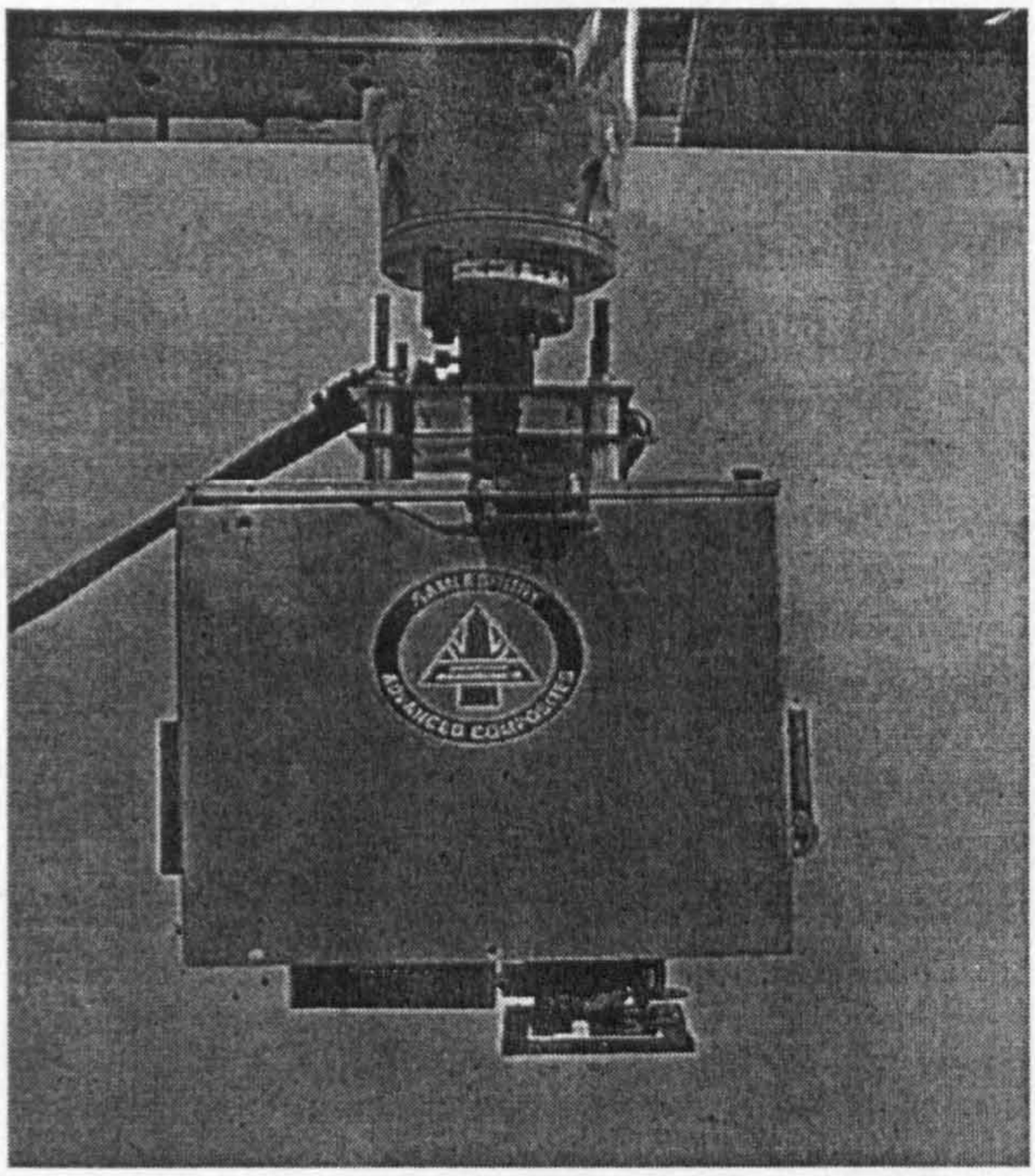

Figure 4.3 Robotic Tacking Device

Later the whole-modeled tacking device has to be attached on the GMFanuc S-10 robot. This will be achieved by integrating the created RTD-file into the robot file. Figure 4.4, shows the four main parts of the tacking device:

In the first step the four single main parts are modeled using temporary names (BOX1, BOX2, BOX3, TUBE). These temporary names are marked through the % sign. Then these modeled objects are moved in the right position according to the real tacking device. In addition a new TCP is created and moved to the working center of the tacking device.

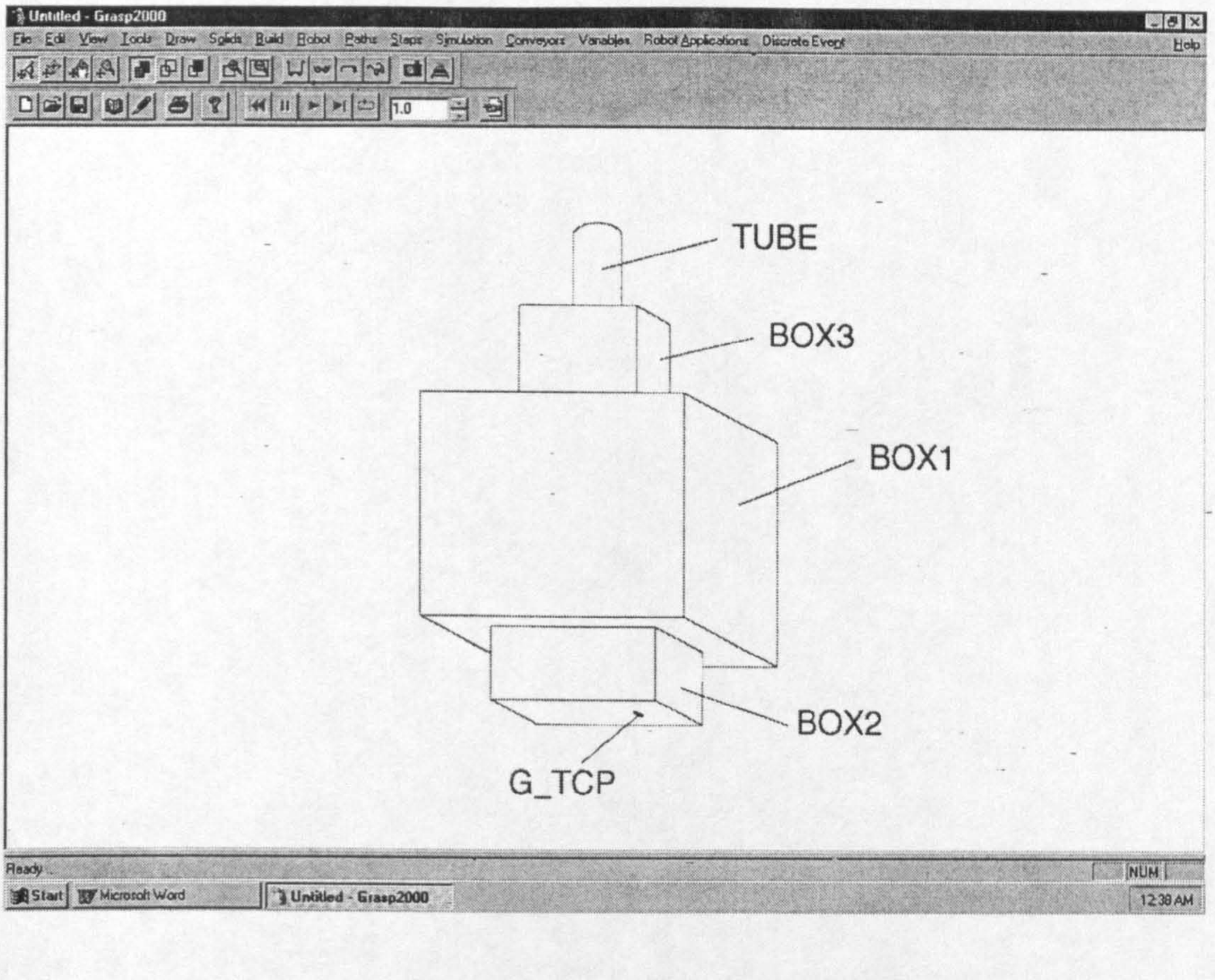

Figure 4.4 Main parts of the tacking device

4.5.2.3 Modeling of GMFanuc S-10 robot

The GMFanuc S-10 robot has six joints able to perform rotational movement. All joints are arranged sequentially and the robot provides a working envelope similar to toroid. The modeled GMFanuc S-10 robot and its joint arrangement are illustrated in, Figure 4.5.

As shown the first joint coincide with the base of the robot and performs a rotation around the z-axis. The second joint is shifted 220 mm in positive x-direction and is able to rotate around its y-axis. The following link (joint 3) is lifted 700 mm and revolves around its y-axis as well.

Joint 4 is shifted 110 mm in positive z-direction and 157 mm in negative y-direction in relation to the previous joint. Lastly joint 5 is moved 600 mm in x-

direction and 120 mm in y-direction, while joint 6 and the TCP coincide and are moved 115 mm in positive x-direction relative to joint 5.

The entire robot is modeled using the robot option of the Grasp 2000. It offers the opportunity to model the robot exactly.

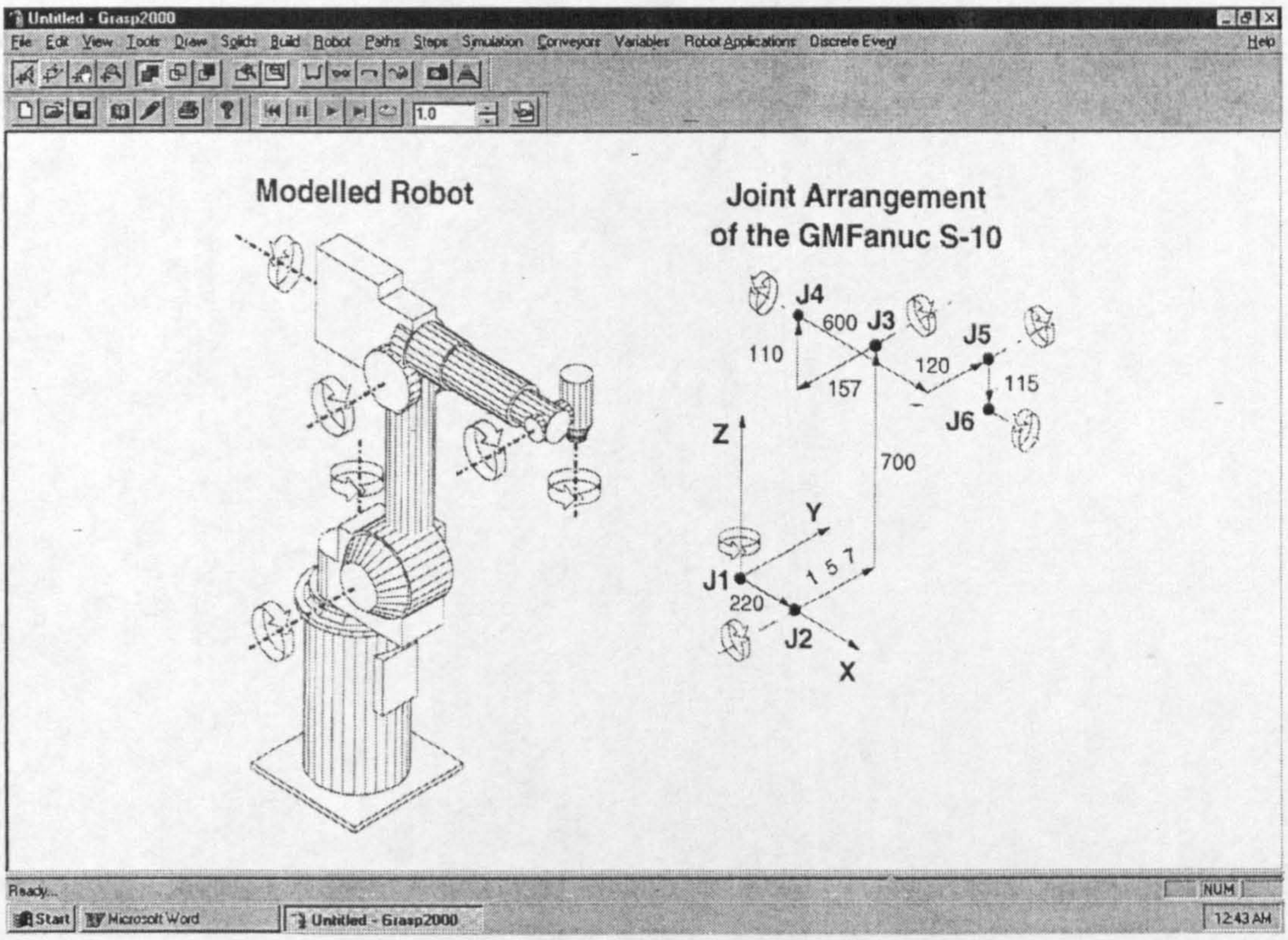

Figure 4.5 Joint arrangement of the fanuc S-10 robot

4.5.2.4 Modeling of the folding device and MDS

Modeling of the folding device and MDS requires the same condition as for the tacking device. It is not necessary to model all the details. First, it is sufficient to create the base of the set and attach the MDS to it as shown in ,Figure 4.6.

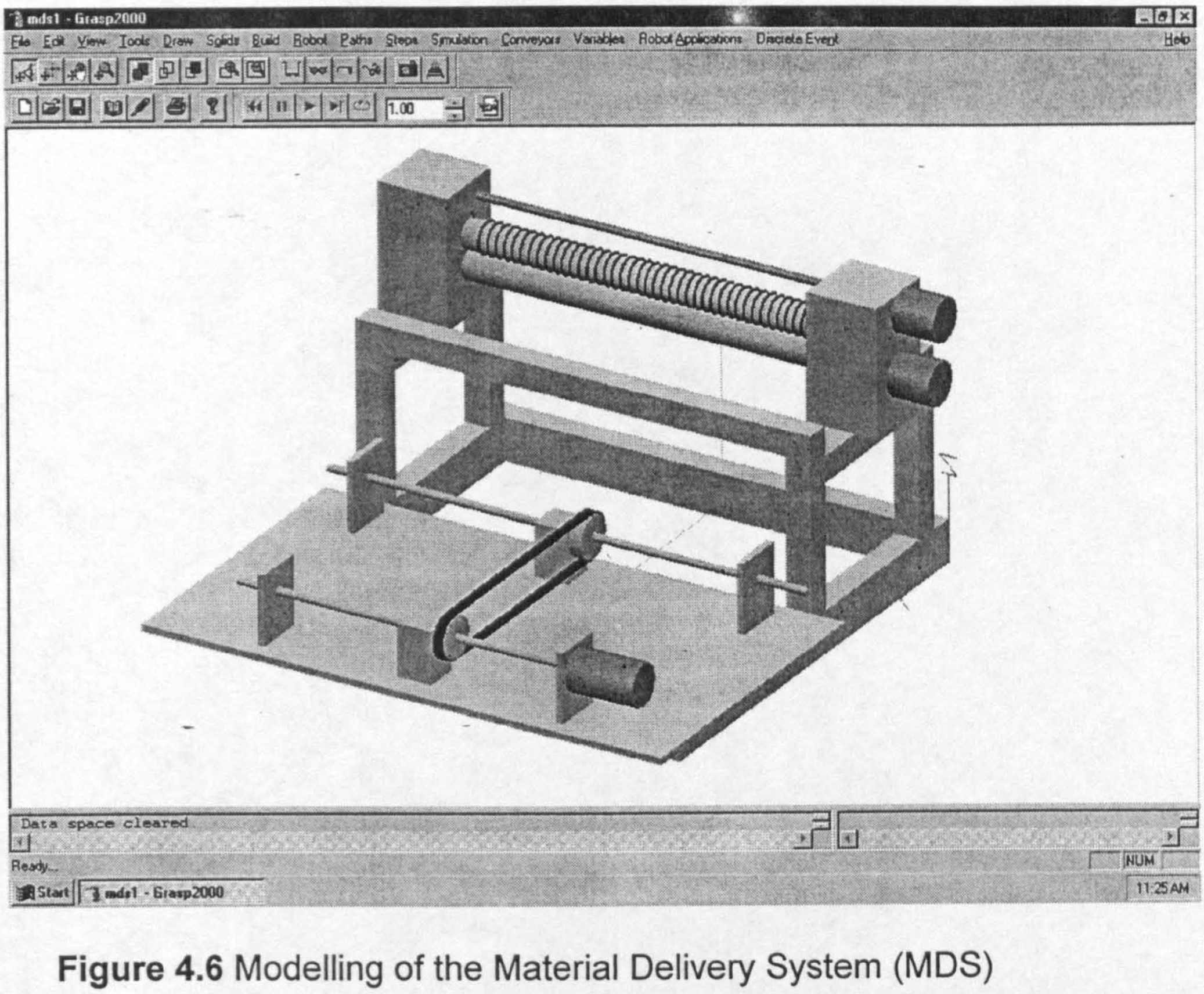

Figure 4.6 Modelling of the Material Delivery System (MDS)

Second, model the outer frame of the folding device, The stepper motors, holders and rollers have been done and attached to the base, Figure 4.7.

The folding device performs movement in x-direction, which only needs one axis to model. The required joints have been defined and arranged. The whole model integrated as single robot.

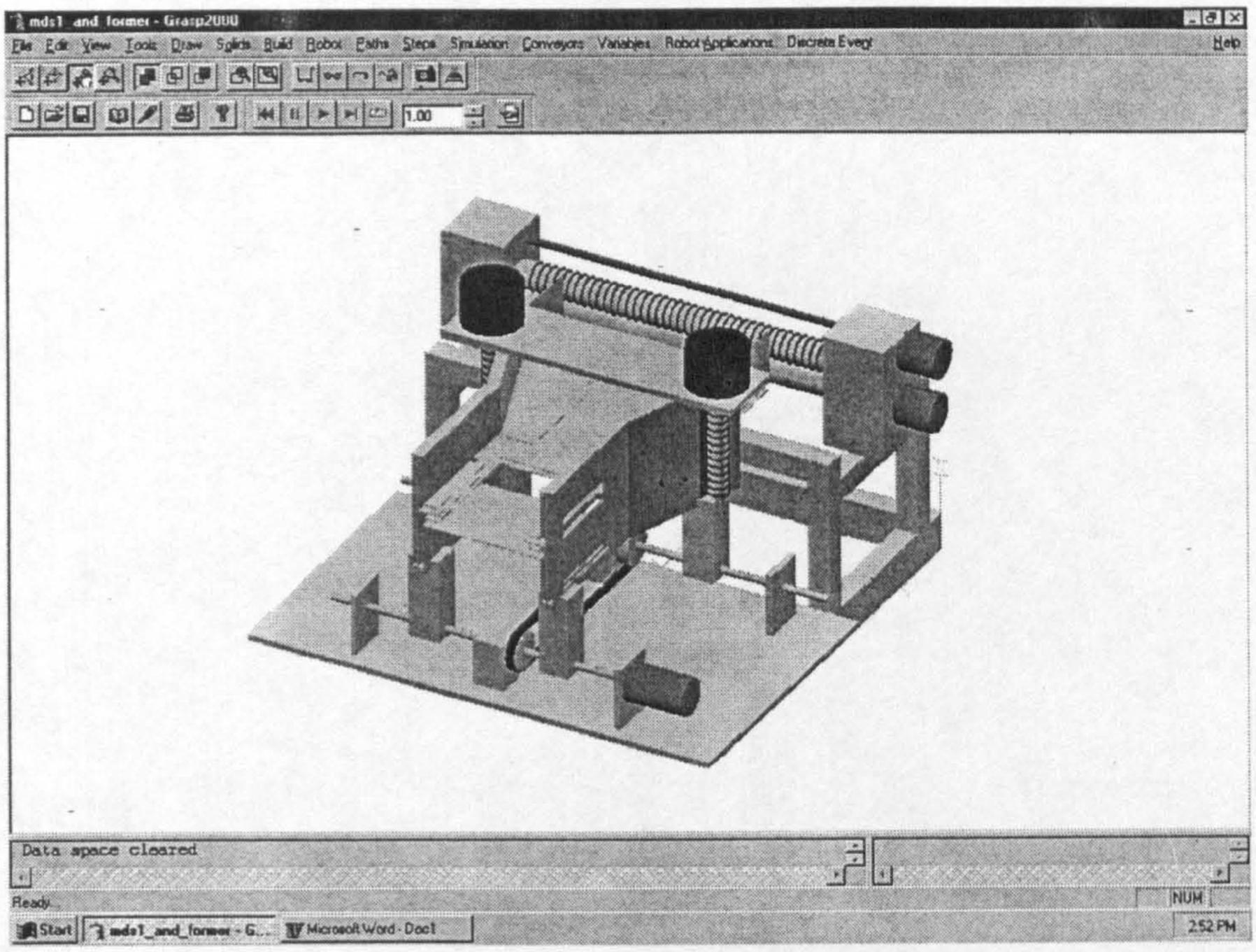

Figure 4.7 Assembly modelling of the Material Delivery System (MDS)

4.5.2.5 Modeling of the transporter and gripping system

The transporter and gripping system are modeled as two joint robot, joint 1 is moved 760 mm in x-direction which is responsible for controlling the horizontal movement of the transporter. The second joint is shifted 50 mm in z-direction and able to move 35 mm in the same direction, this movement is used to control the stroke for the gripper as shown in ,Figure 4.8.

Before the values for the initial joint has been configured, maximum and minimum limits, velocities, accelerations and park position are defined.

4.5.2.6 Modeling of the environment

The environment of the manufacturing cell consists of the lay-up table, the controllers of the machines and surrounding walls and floor.

4.5.2.6.1 Lay-up table

The lay-up table consists of four legs and a tabletop. All entities can be easily modeled out of cuboids and the co-ordinate system is located at the corner of the tabletop, Figure 4.9, shows the modeled lay-up and the cell components.

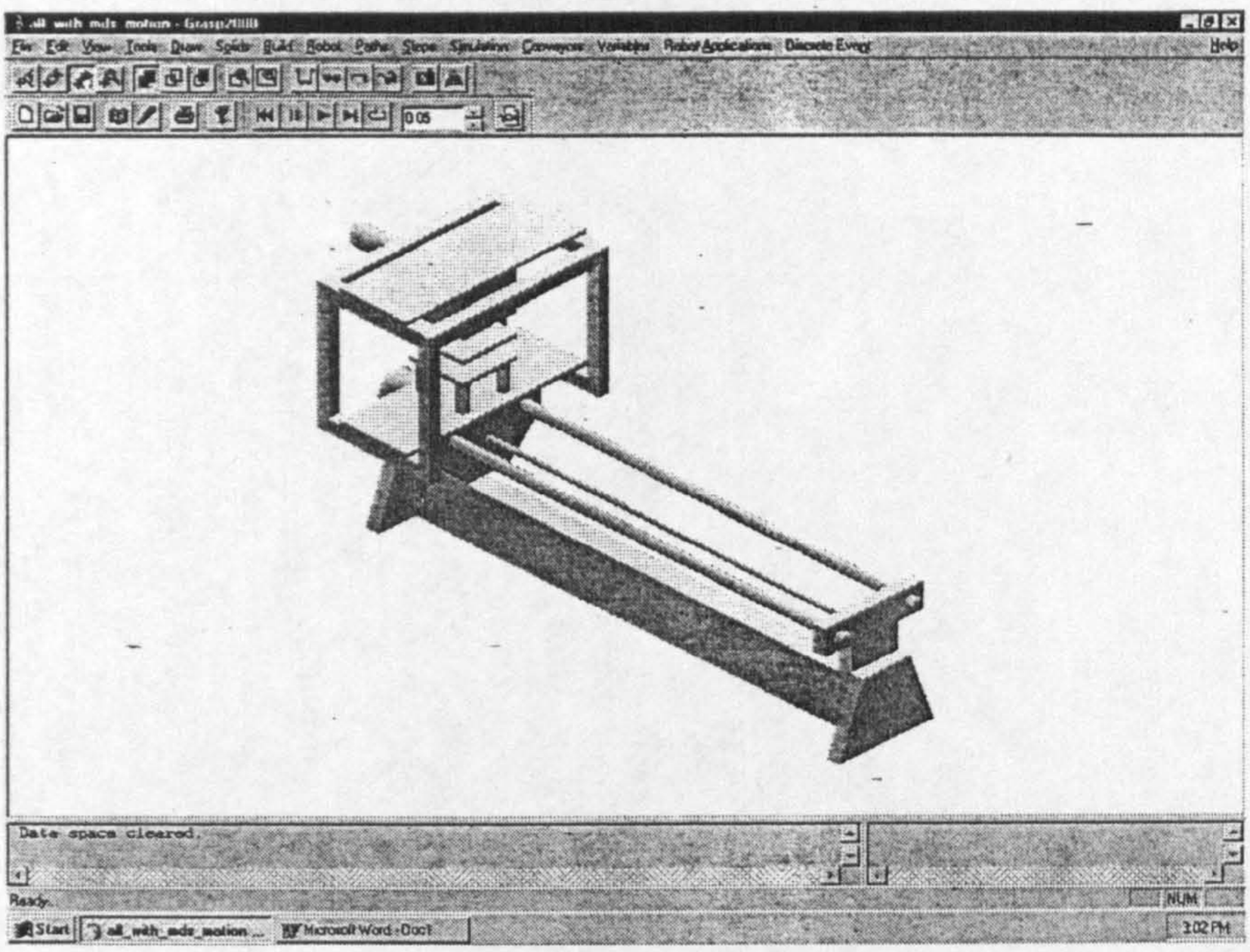

Figure 4.8 Modelling of the gripping and linear track system

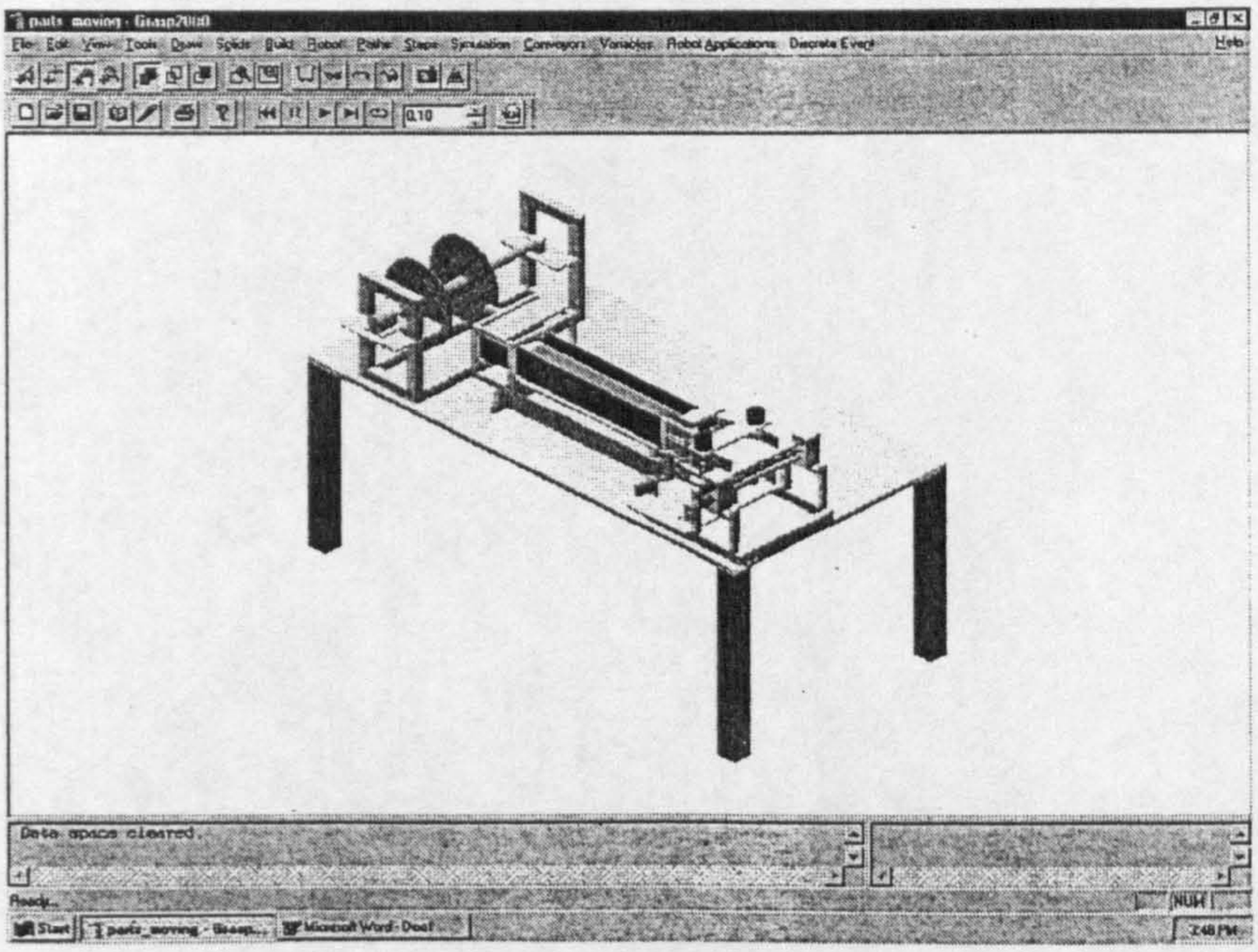

Figure 4.9 Lay-up table

4.5.2.7 Material bank and the Storage

Figures 4.10 & 4.11,show the detailed modeling of the material bank and the storage.

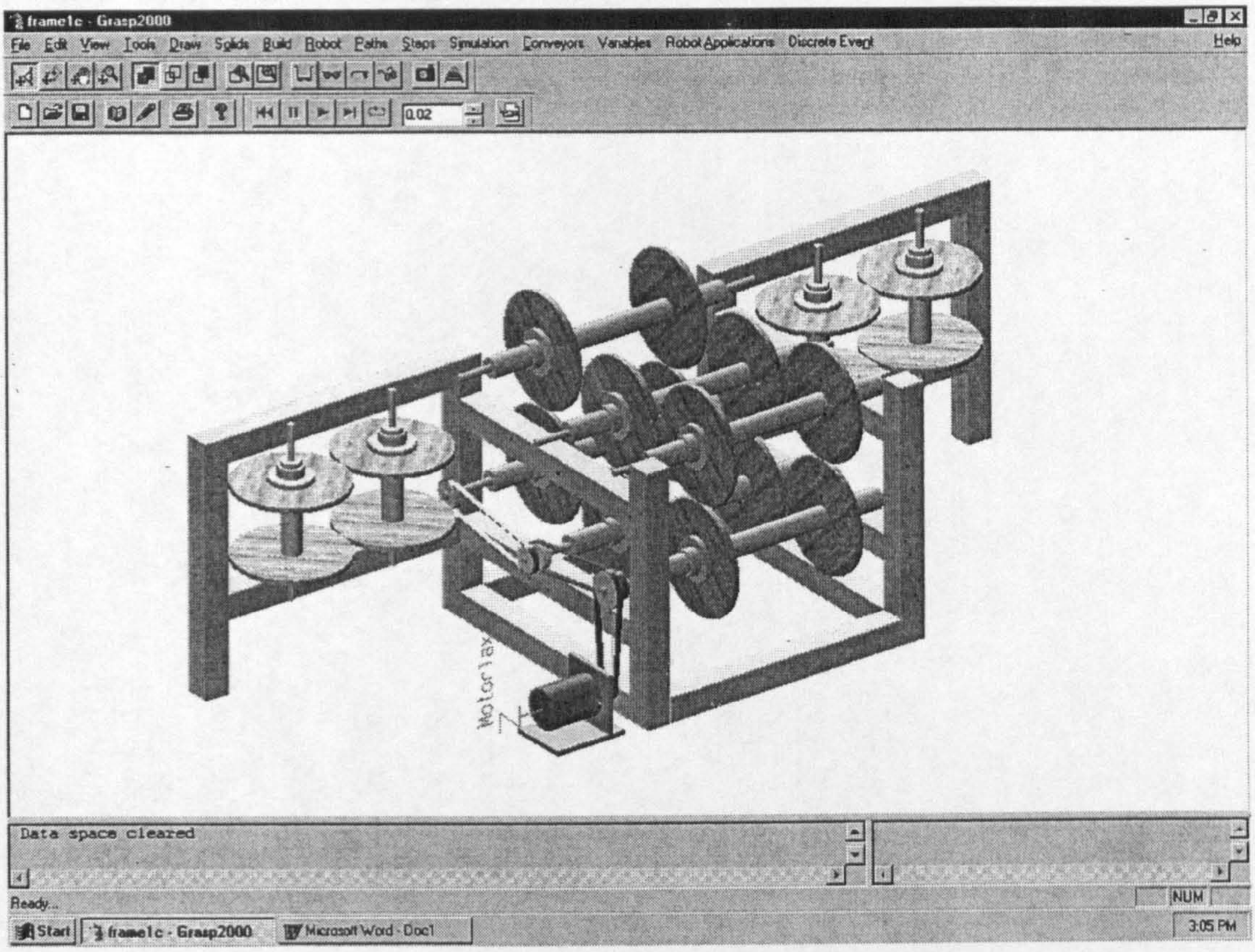

Figure 4.10 Material bank

4.5.2.8 Surrounding

The surrounding file includes the surrounding walls and the floor on which the complete manufacturing cell is arranged. The individual parts are modeled out of cuboids and aligned to the global co-ordinate axis.

The floor is aligned to the plane created by the x-y axis, and the walls are aligned to the x-z and y-z axes. The co-ordinate system of the surrounding object is located where the three planes intersect each other. In the final stage

the object co-ordinate system of the surrounding will be used as global co-ordinate system for the whole manufacturing cell.

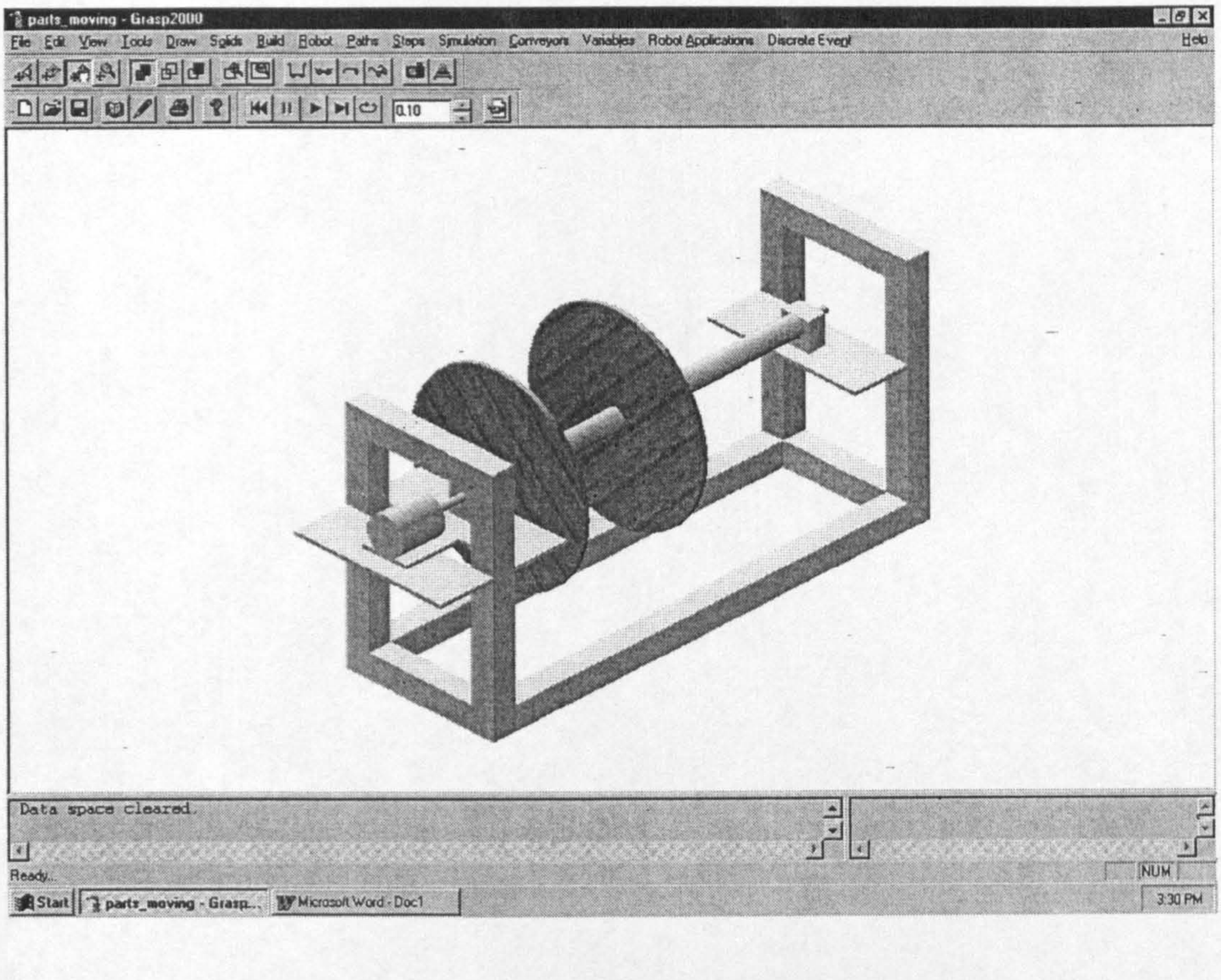

Figure 4.11 Modelling of the storage

4.5.2.9 Modelling of the complete manufacturing cell

The complete manufacturing cell ,Figure 4.12, is created by putting together the above modeled files as the same sequence of the real cell. After a new session is started, the predefined files imported sequentially into the program and they will belong to the workplace and arranged as appropriate to the real cell layout. Therefore it is sufficient to move only the bases of the models, as all the other parts of an object are associated with the base they will carryout the same movement. The diagram in ,Figure 4.13, illustrates the file structure of the manufacturing cell.

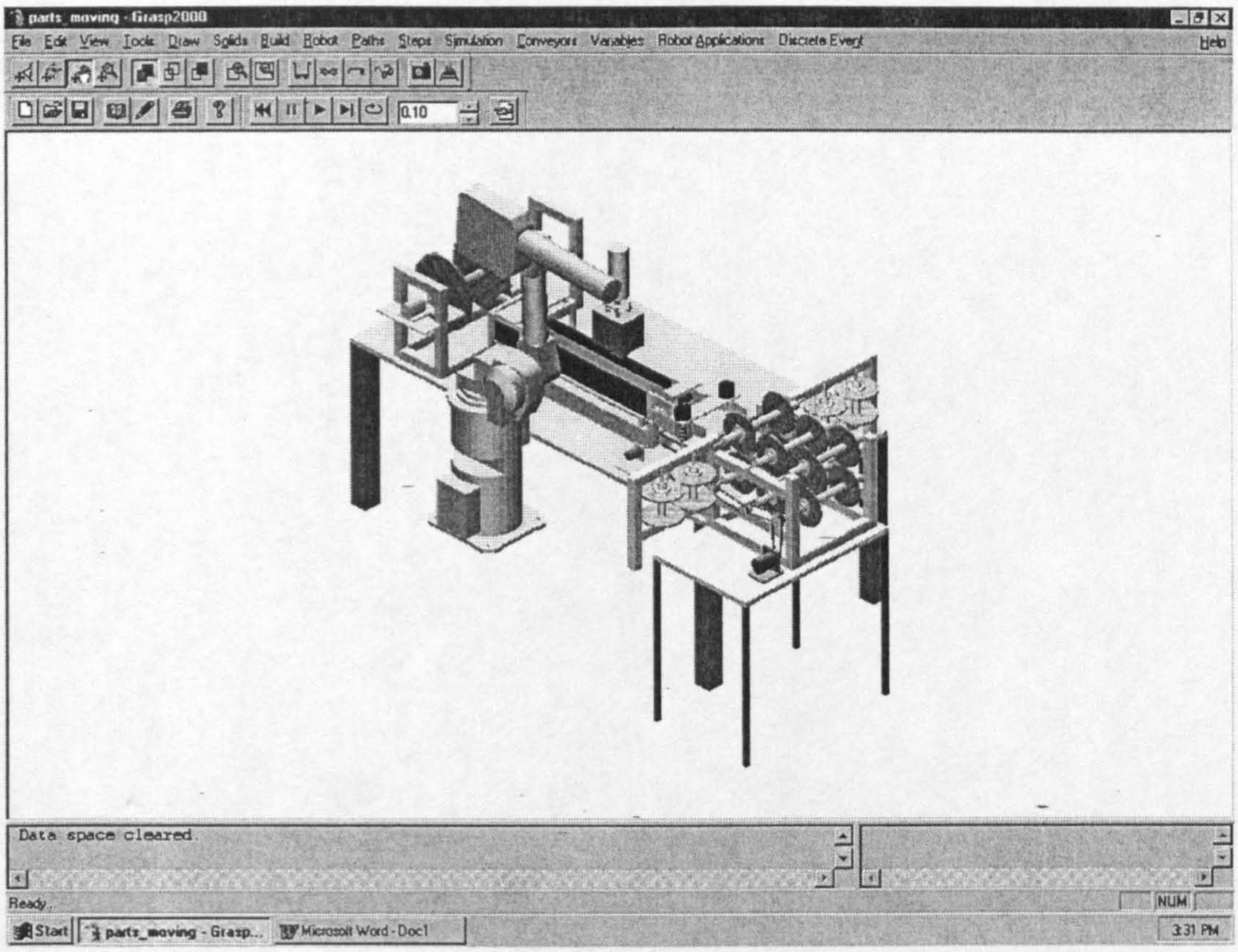

Figure 4.12 The Manufacturing cell

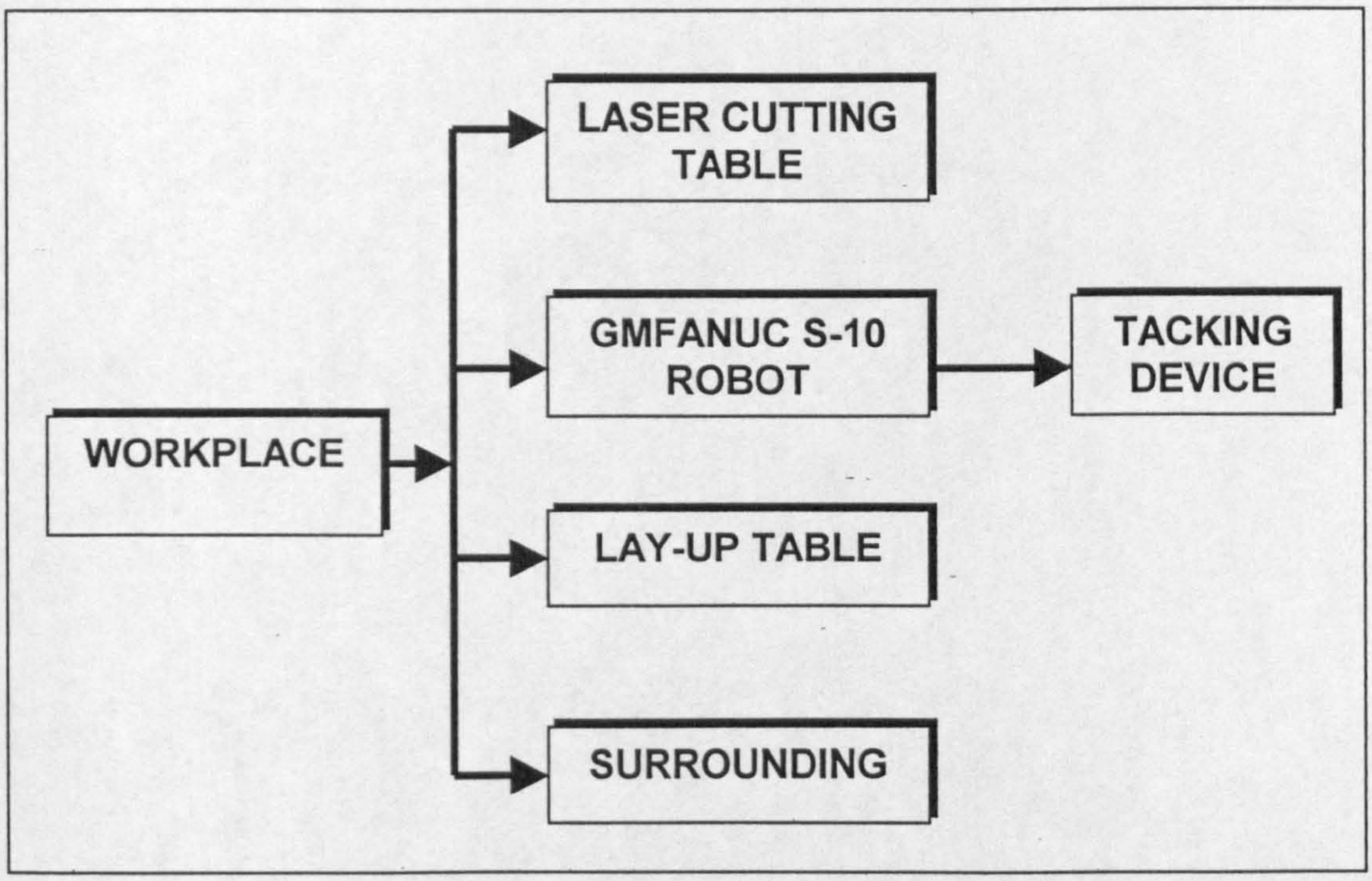

Figure 4.13 File structure of the manufacturing cell

4.6 Track generation

After the material is safely fed into the folding device through the material delivery system (MDS), the GMFanuc S-10 with attached tacking device, begins to stitch the lay-up together. First, it searches for the first tacking point. Then it moves to the selected position and lowers the tacking heads slowly onto the surface of the top play.

The first stitch is formed in approximately three seconds. The tacking operation is repeated four times. Each time the tacking device is lifted, shifted about three millimeters and again lowered. After the tacking procedure is finished the GMFanuc S-10 moves to the next position to perform the second tack. These steps are repeated until the last tacking point is finished, and the robot return to its home position and waits for the rest of the cell to generate a new stitch area.

Clearly there are operational requirements which should be kept in mind when programming the working task. The robots should work simultaneously when simulating the manufacturing process. This also offers the opportunity to visualise and detect potential clashes. It is very important for simulation to be performed at different velocities.

In addition to these requirements, limitations of the Grasp 2000 should be considered when creating the track. The Grasp 2000 is only able to drive one robot with each track. If more than one robot has to be moved within a task simultaneously, one track can be used as a current track, called foreground track, and the residual tracks have to be driven as background tracks.

4.7 Definition of path type

To simulate the manufacturing process realistically reality, different path types for each entity have to be defined. For example, the GMFanuc S-10 robot moves in three different ways, but all movements in a straight line. The

movements on a higher level are carried out at a speed of 100 mm/sec. The approach onto the surface of the plies is carried out at 30 mm/sec, and the final moves until touching the surface, as well as the shifting between the stitches are performed at 3 mm/sec. In all these cases the accelerations are very low and can be neglected.

Sometimes it is difficult to follow the movements of the TCPs' of the robots while running a simulation of the performed tracks of individual joints. These trajectories have to be defined before a simulation is running. Or they can be integrated in the programmed tracks.

To define such a track it is necessary to name the new trajectory, determine the item for which a trace is required, state if the trace should be shown for the time or only after determined time intervals, indicate if the trace is switched on or off and input the owner of the defined trace. If required, the shape and the colour of the trajectory path may be defined and altered.

4.8 Conclusion

The aim of this chapter was to model the manufacturing cell and simulate the movements of each machine (production sequence). For that purpose the robot Grasp 2000 was used.

The complete manufacturing cell has been developed and currently used for automatic manufacture of the aerospace component. It consists of Axon A201 laser-cutter, GMFaunc robot, prototype of the tacking device, MDS, folding device, transporter, material bank, and lay-up table.

In the first stage of the work, the single objects of the cell was modeled and subsequently stored in an individual data file. The two-axis laser cutter was also modeled as robot, the first two joints carry out the translation movements, while the residual joints are fixed and maintain their current orientation. by the

same manner, the residual of the cell were modeled and arranged as the reality. Finally the tacking device was attached to GMFaunc S-10.

In the next stage the manufacturing cell was measured, and afterwards the individual data file of the modeled objects was imported and arranged accordingly to the measured cell layout. In addition appropriate reference objects were defined for the following track generation. The simulation identified and prevented the collision among the moving components of the cell. It also provided the means to calculate the required areas for the automated cell. The simulation output, which consists of the running time for each component to provide various reinforcement structures, can be presented for each run.

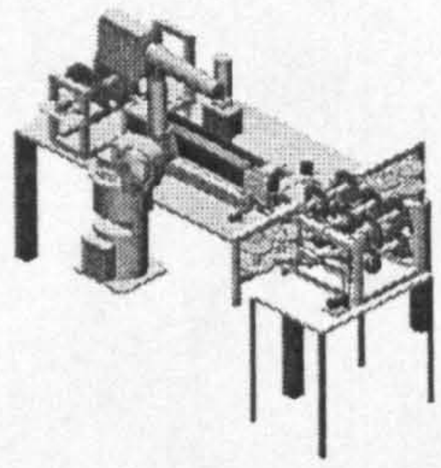

Chapter 5 Description of the Manufacturing Cell

5.1 INTRODUCTION

Fibre-reinforced composites offer potential advantages to the automotive and aerospace industries, including design flexibility, weight reduction and reduced manufacturing costs.

The manufacture of such components involves the manipulation and lay-up of large size composite fabric pieces to a high degree of accuracy. Manual lay-up is the most extensive technique used for producing these components. Producing high volume fractions with this method requires debulking every five to ten layers adding considerable time to the lay-up process, 'Vacuum bagging' problems are also among the largest contributors to high scrap rates in composites **[Zhang and Sarhadi, 1999],[Ridell, 1987].**

A range of technologies has been developed for cutting, handling and fixing **[chestney and zhang 1994]**, **[zhang and sarhadi 1997]**, but a purely technological solution is insufficient when dealing with three-dimensional (3D) components; a methodology for implementing the technology for dry fabric preforms is required. To this end, the cell, which used to produce 3D components, should have a capability to manufacturing a generic range of components without tooling in the lay-up process. This work has been directed towards one particular approach, which involves the requirement for a technique to produce the three-dimensional (3D) components and integrated this technique in fully automated cell.

The concept created allows jigless manufacture of flat preforms, which can subsequently be formed into three-dimensional shapes when, loaded into the

mould. An added advantage is that complex components can be produced as a single preform, reducing both preform production and moulding times.

5.2 THE MANUFACTURING METHODOLOGY

A new manufacturing methodology, termed shape inclusive lay-up has been developed which, enables preforms for 3D components to be produced and stored flat, introducing the shape only when the preform is loaded into the mould. Very limited linear variation can be incorporated into the cross-section dimensions with a combination of ply geometry and angled fold paths. Components with varying degrees of complexity can be manufactured using this methodology.

5.2.1 The requirements for the shape-inclusive preforming are:

- Fabric flexibility: a drapable material is required for reinforcement structures (e.g. NCF) which enable the preforms to conform to the mould.
- Loose-coupling mechanism: to allow inter-ply movement for shape conformity, plies within the preform are required to be secured by a localised loose coupling (e.g. stitching).
- Folding: to enable the production and integration of the 3D components, ply-folding mechanism should be incorporated within the manufacturing cell.

5.2.2 The advantages of Shape-inclusive performing include:

- Flat storage of preform is possible.
- Preforms have infinite shelf life (since dry-fibre materials are used).
- Parts integration are drastically reducing the number of the moulding cycles and eliminating the need for bonding.
- Reduction in manufacturing cost and time can be achieved.
- Reinforcement structures and skin can be co-cured or co-bonded.

5.2.3 The capabilities of shape-inclusive preforming include:

- Production of a number of reinforcement structures: C,I,T and J structures.

5.3 CELL HARDWARE

A prototype robotic manufacturing cell has been designed, implemented and assembled, Figure 5.1, and cell control has been developed for operation directly from CAD design data.

Briefly, the cell comprises the following components:

- **An automated cutting table:**

  In the cell, ply profiles are cut from the material roll by laser, to an accuracy of 0.25 mm with minimum heat effects.

- **Material Bank** :

  After the dry carbon fibre has been cut for the required size of the reinforcement structures, material bank has been designed and implemented with a set of pulleys connected to stepper motor through single reduction gearbox to collect the fabric and feed it safely to the material delivery system (MDS).

- **A ply folding mechanism**:

  Methods have been devised to perform ply folding. A novel device has been designed and incorporated with the cell. The mechanism is very flexible to produce a wide range of aerospace components **[T.Tewfic and M. Sarhadi, 2001]**.

- **Material delivery system (MDS)**:

To grab automatically the dry fabric preform from a material roll, feed and lay it up in an accurate way through the folding device; the MDS has been implemented and integrated into the cell to fulfil these requirements

- **Transporter :**

  After the material has been formed through the folding device, it was essential to have an appropriate device for delivering the material safely to the final device of the serial line, for this reason, transporter has been implemented to grab and drag the material to the final stage.

- **Collector:**

The final reinforcement structure should be collected and stored accurately for introducing the structures when the preform is loaded into the mould. For this stage the collector has been designed and implemented and integrated into the automated cell.

- **Automated insertion of loose couplings**:

A robotic tacking device inserts a series of blind stitches **[Dewing, et al 1999]**, requiring access to one side only. The tack allows forming to occur without excessive fibre distortion or losses in positional accuracy during handling. The main components are described in more detail in the following sections.

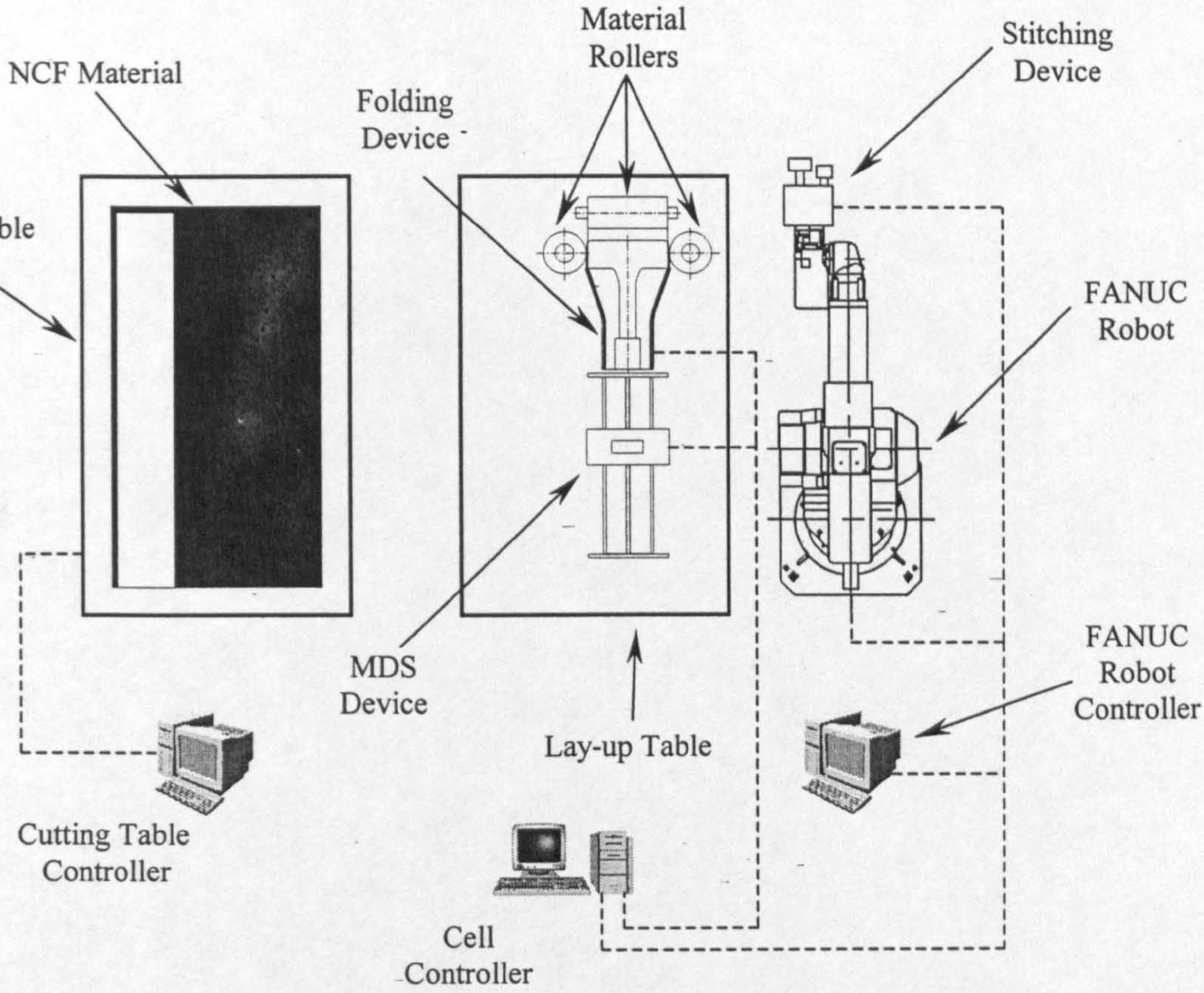

Figure 5.1 Block diagram of the automated cell

5.3.1 Laser Cutting Table

The task of the cutting table is to cut the required ply shapes from a roll of the appropriate material. The cutting table is basically a two-axis gantry robot, fitted with a CO_2 pulsed LASER which performs the cutting as shown in ,Figure 5.2, **[Mitchell, et al. 1994]**. The parameters of the system (i.e. cut speed, LASER power, etc.) can be adjusted depending on the material to be cut. The table is controlled by a software package called DNC3 running on a PC connected to the table via an RS-232-C link. The geometry of each ply in the component is designed using CAD packages. DNC3 imports the data files generated by AUTOSKETCH. The position of cut plies on the table can be defined in AUTOSKETCH. The cutting has an active area of 2.5 by 1.25m, and cutting speeds approaching 6m/min have been achieved with some

materials, following optimization of the laser parameters. The cutting table has been fully integrated into the manufacturing cell.

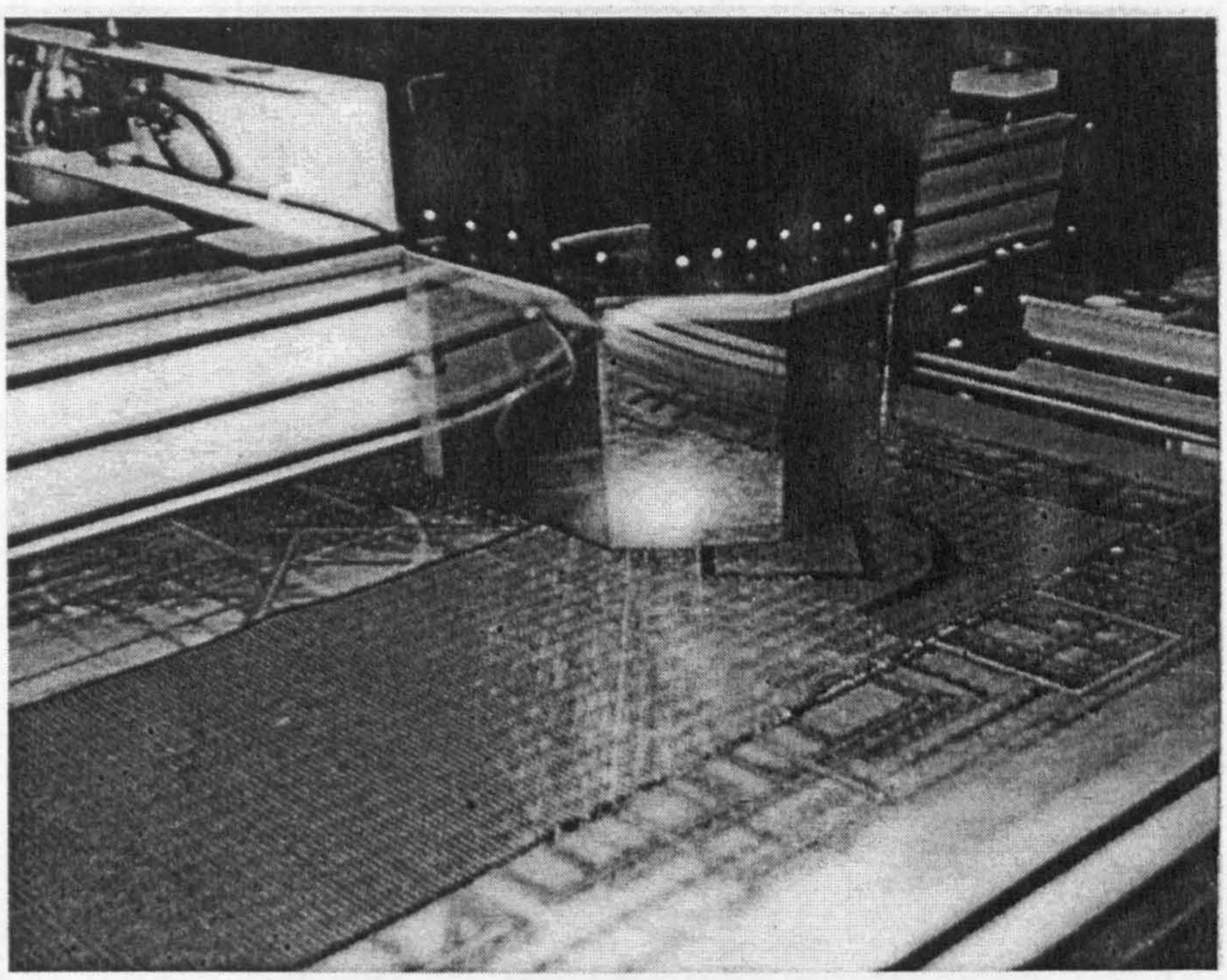

Figure 5.2: Laser cutting table

5.3.2 Folding Device

5.3.2.1 Design of a Novel Folding Device

Effort was directed towards producing a generic solution for including folds within the dry fabrics **[Chestney, et al 1995]**. The selected solution should allow scaling up and could be applied to other components that could be generated from folding. For this reason, the concept should not depend on the present prototype cell, thereby enabling it to be integrated into any manufacturing cell.

5.3.2.1.1 Automated Consideration

- During the folding operation, the positional integrity of the preform should not be compromised.
- Complexity, with respect to function and integration of the device, should be minimized.
- The function of the other cell components, especially the tacking device, should not be hindered.

5.3.2.1.2 Material properties

NCF material is dissimilar to typical fabrics or engineering materials, and consequently poses unique problems.

- NCF material will return to its initial unfolded state, once the means of folding have been removed.
- Ply thickness is typically 0.8 mm for two layers NCF, considerably thicker than the majority of fabrics.
- The NCF ply is susceptible to damage on two levels.

  A. Microscopic level - any damage to the continuous fibres will cause a reduction in load transfer efficiency.
  B. Macroscopic - cut plies can loose their geometry if handled manually.

5.3.2.1.3 Fold generation

To generate a fold, in any material, the standard approach is to fold about a fixed point. Initial trials involved laying plies on to a support plate and rotating it to produce the fold. The mode of fold generation is simple, however, it has a severe limitation, manufacturing and controlling a long thin ply presents some serious design problems; rigidity and positioning. To overcome these drawbacks, a novel approach to folding has been developed.

5.3.2.2 Novel folding concept

The novel concept relies on gradually folding the ply with a device similar to that used in extrusion processes. The plies are pulled through the folding device, as shown in, Figure 5.3 and 5.4, with an external gripping force. The concept of gradually creating the fold enables the device to be incorporated into the cell, creating the fold in the ply by the linear travel (that takes place by the MDS system) of the ply through the device.

The folding device results in a 90° fold on a ply as it passes through it. By passing a number of plies through the specified holes in the folding device the final reinforcement structure could be achieved, then the tacking can take place to assemble the formed plies together. This technique reduces any stresses on the material and results in minimum damage to the fibre.

Moreover, the process in this form is considered to be easily applicable to any number of plies and a range of shapes often found in reinforcement structures. The resulting dry carbon fabric composite when tacked will preserve its shape until it is further processed with RTM. The cell can be used for manufacturing various sizes of the reinforcement structures, which are ready to assemble and store flat.

One of the main advantages of the folding system is that it can be used to produce different shapes of reinforced structures (I, J, C and T sections) as shown in ,Figure 5.5, Moreover, the dimensions of the spar can be altered using variable width mechanisms for the generated reinforcement structure.

This is useful in multiple spar size production, which adds to the economical aspect of the proposed device as it saves the cost of fabricating various folding devices for various dimensions. The change of the spar size is performed using stepper motors controlled by the cell controller computer.

The desired dimension is first entered in the preliminary data on the CAD system of the cell computer.

5.3.3 Material Delivery System (MDS)

In order to improve the manufacturing cell in relation to producing large aircraft components, it is clear that a fixed manufacturing cell (fixed robot and tables) could not provide this with a limited working area. To fulfil these requirements a prototype of the MDS has been designed and tested ,Figure 5.6. The first aim of the MDS is to automate this process in laying-up fed material on the stitching area of the folding device. Also by means of the MDS it is necessary to grab automatically the dry fabric preform from a material roll, feed and lay it up in an accurate way through the folding device.

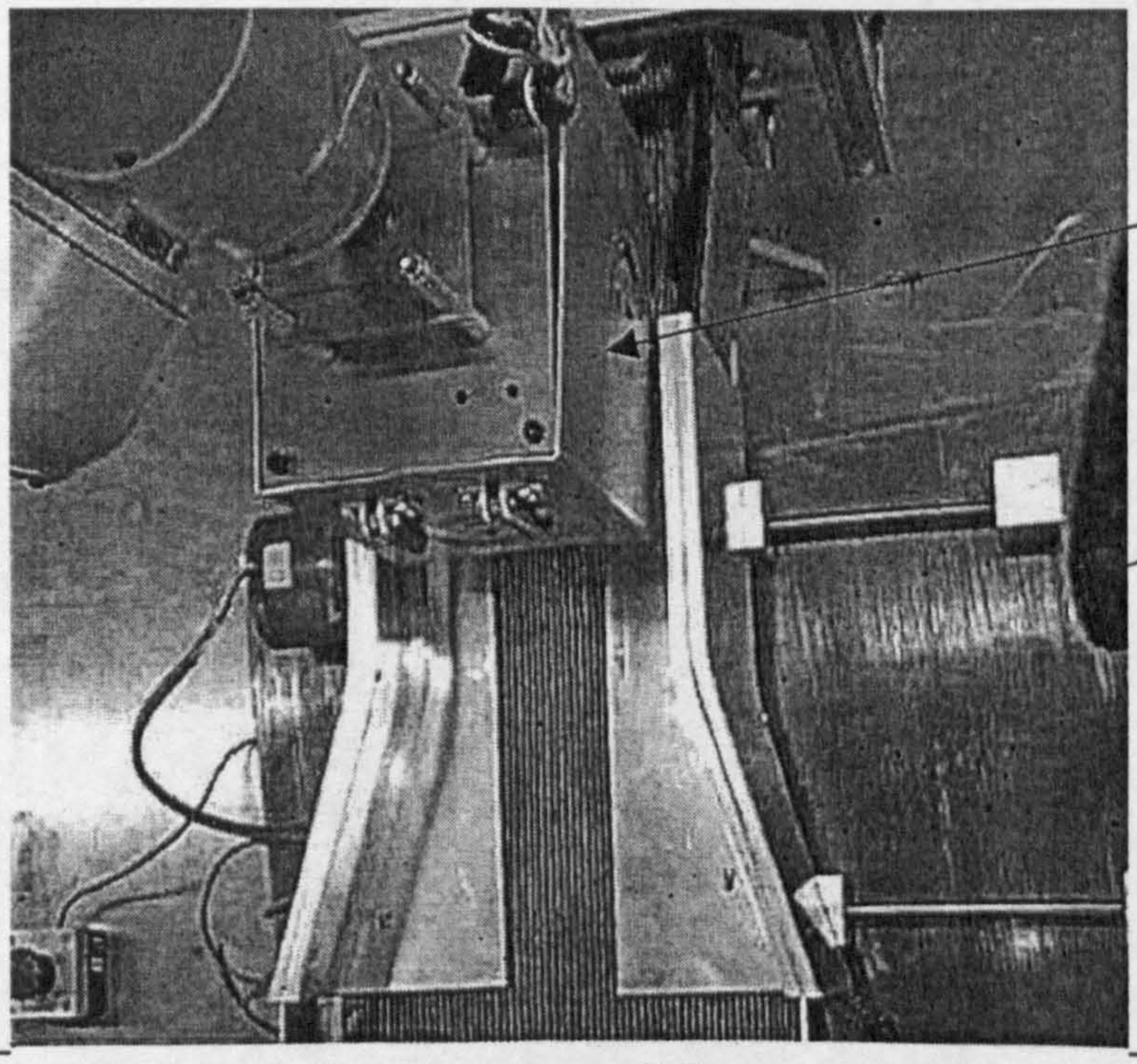

Figure 5.3 Folding device and stitching robot arm (top view)

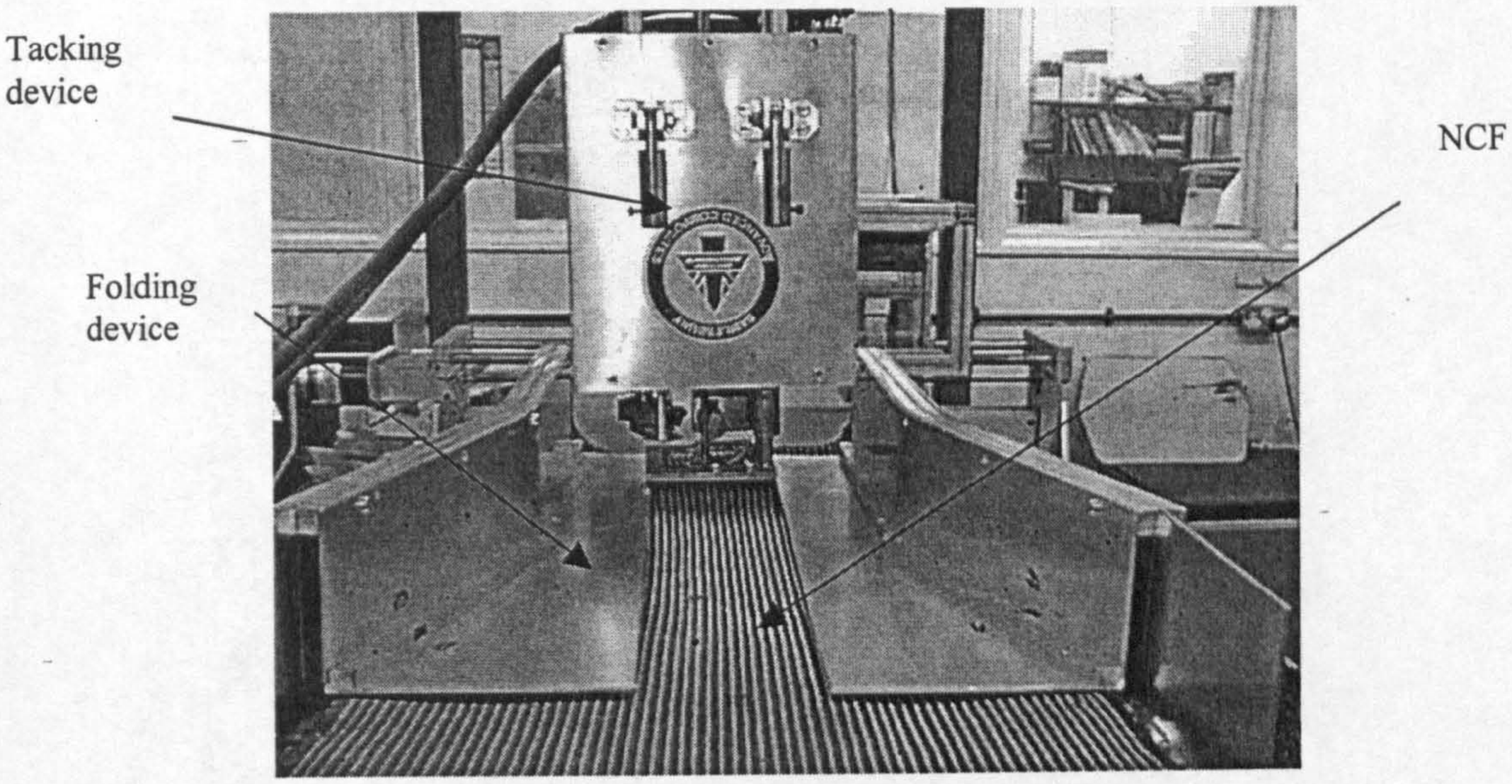

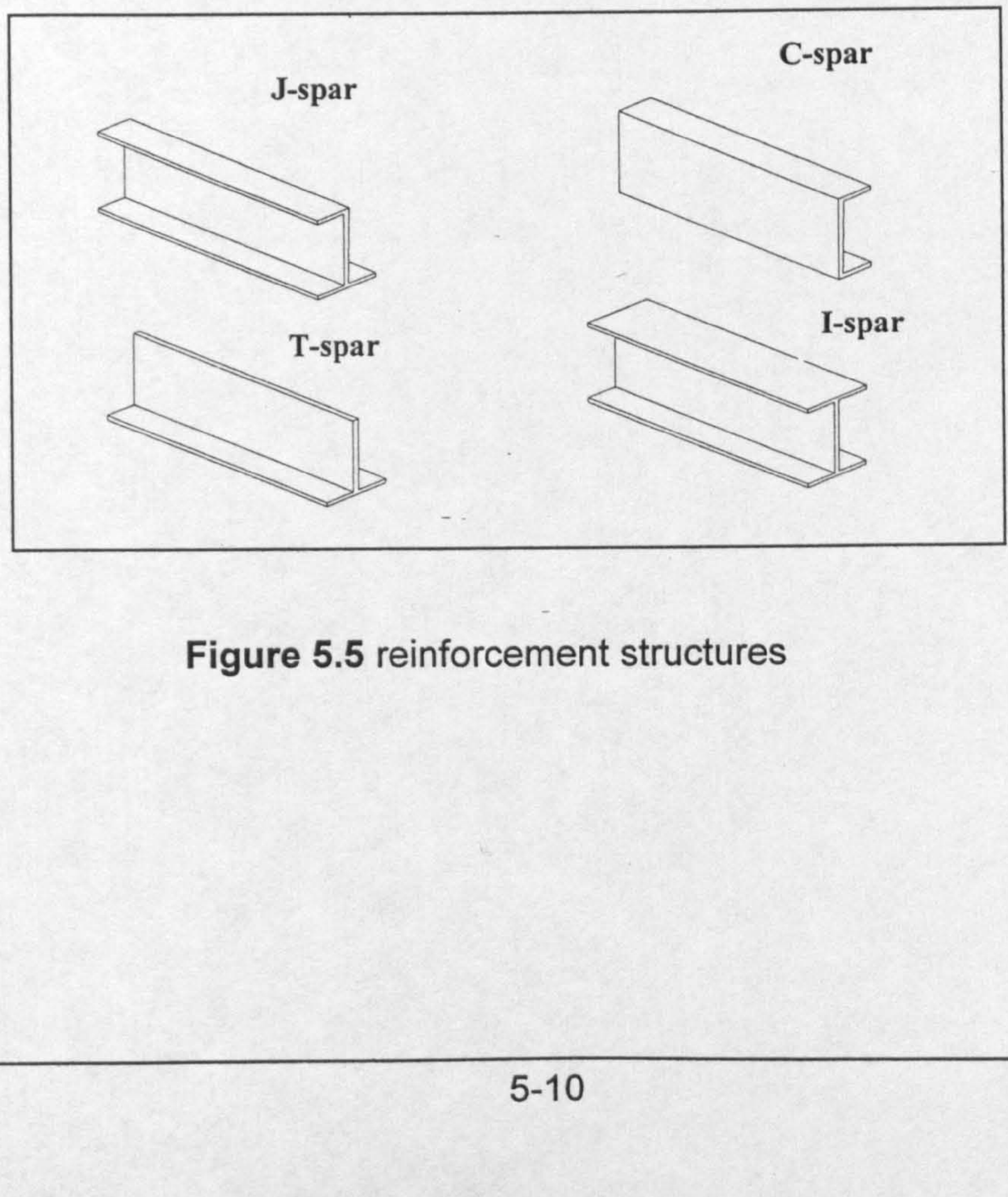

Figure 5.5 reinforcement structures

5.3.3.1 Design of MDS

Dry fabrics are subjected to damage in microscopic and macroscopic levels, as described in section 5.3.2.1.2. MDS has been designed and implemented to enable the fabric to travel safely through it.

Design of the MDS should fulfil the following properties:

- Automated control of gripping the material
- Automated the lay process

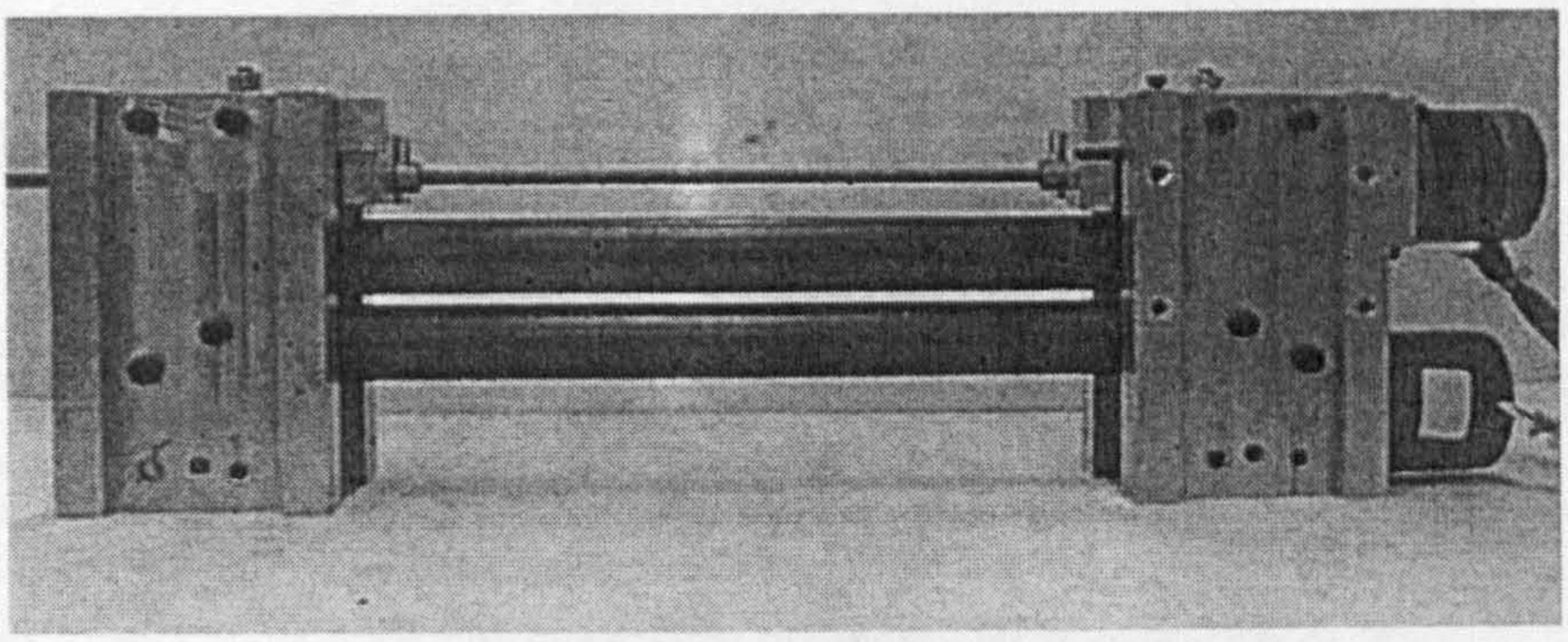

Figure 5.6 Material Delivery System

- Accurate control of dragging the material

5.3.3.1.1 Constituent element s of MDS

a. Rubber rollers:

The rubber roller ,Figure 5.6, consists of metal shaft surrounding by rubber, the rubber is coated with a high grip coating. It is, precisely the high grip coating, in contact with the shifted material and the necks of the metal rotate in bearing that have to act as supports and serve to couple the roller to the drive.

It is possible to determine the pressure between two cylinders in a line contact with Hertz's equations. These equations can be used as long as a line contact between the rollers exists.

B.Rigid frame

The rigid frame ,Figure 5.7, is completely manufactured out of aluminium. The U-profile tracks were milled out of aluminium solids and screwed to the blocks. For an accurate fitting the blocks fit exactly in the U-profile of the tracks.

C. Solids and rollers

The solids ,Figure 5.7, also are manufactured out of aluminium and fitted into the U-profile of the tracks. The fixed ones are screwed to the tracks. The rubber rollers are mounted in self-lubricating bronze bushes. For driving one rubber roller it was necessary to connect the roller to the stepper motor via a shaft that runs through one of the fixed solids. A pair of worm gears and wheels was chosen to fulfil the requirements of automatic adjustment of the rubber roller to guarantee that the composite material is fed in a straight way over a long distance.

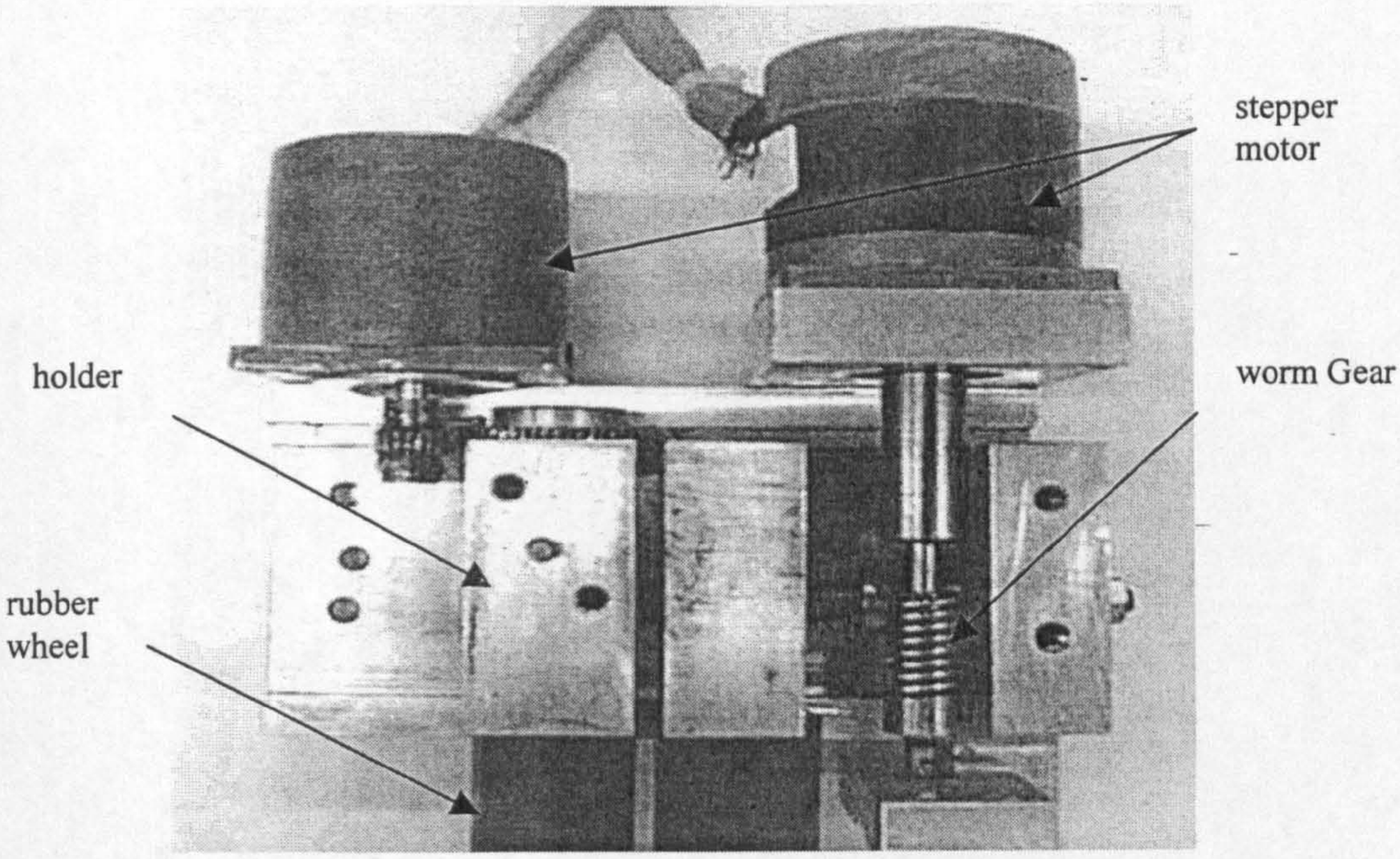

Figure 5. 7 Material delivery system (MDS)
rigid frame and solids

5.3.4 Transporter

5.3.4.1 Linear tracking system:

The linear track system ,Figure 5.8, is built with two stands on each side held together by a hollow rectangle profile screwed to the stands. On the top of the stands are the holders for the steel bars screwed to the stands. Moving table is mounted in linear bearing and driven by a multi-start lead screw via a 6.5 A. stepper motor, it is able to move a distance of 760 mm along the bars.
The lead screw provides a high transmission ratio that is determined in the following equation.

$l_{lead\ screw}$ = pitch * number of starts = 5.2 mm * 5 =26 mm / $motor_{revolution}$

Number of steps / $motor_{revolution}$ = 26 mm / $motor_{revolution}$ = 200(full-step)/ $motor_{revolution}$

$\Rightarrow$ 1 mm linear distance $\approx$ 8 steps
$\Rightarrow$ 1 step $\approx$ 0.125 mm linear distance.

5.3.4.2 Gripping system

Because of the properties of the dry fabric, the material has to be delivered very carefully under the condition that it can not be pulled or pushed on a single point. Therefore it was decided to design the gripping system ,Figure 5.8, from two flat metal parts, with rubber coat, to grab the material and exercise a pulling force based on a large flat area in order to avoid the damaging effect of point pressure application. One of the flat parts is fixed on the moving table and the other part is driven by a D.C. motor to apply the pressure on the material to be dragged.

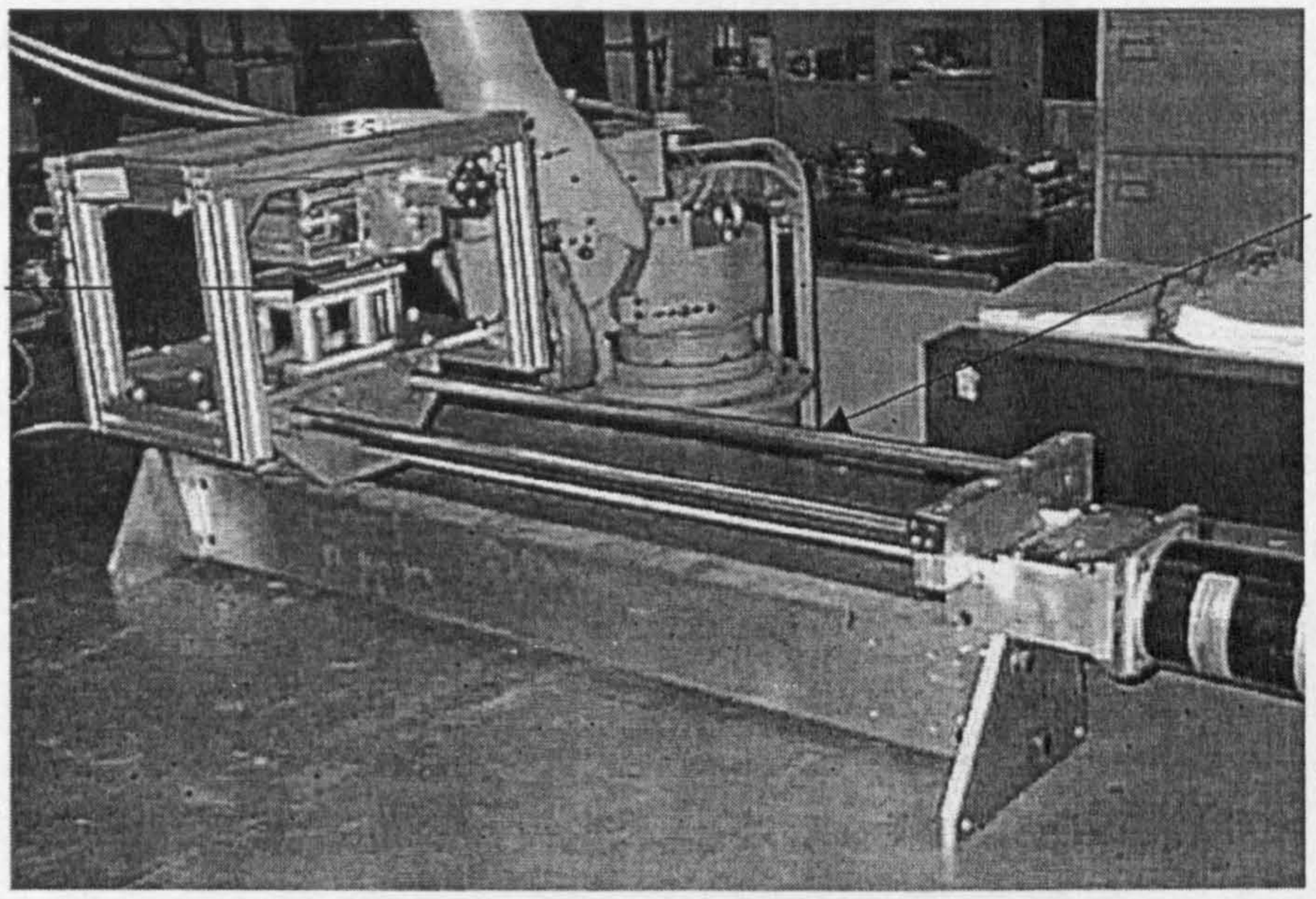

Figure 5.8 Transporter (linear track system and gripping system)

5.3.5 Robotic Tacking Device

Stitching of dry fibre preform is currently an area of interest in the aerospace sector **[Glenn, 1997], [Dewing 1999],[Harris, 1991],[Thompson, 1994],[Mitchell, 1993]**. The principal problems with tacking a dry fiber lay-up are

threefold: there should be no movement of the lay-up induced by the tacking process; there is only access to the upper side of the preform stack, and the lower side is directly contacted the surface of the forming tool. The material of interest, dry fabric, is relatively thick, dense fabric with z direction stitching, which increase the density of the fibres further in the stitch area and creates a barrier that is difficult to penetrate.

5.3.5.1 Requirements specification

The following points are the requirements of the tacking method for this application:

1. There are conflicting requirements for the tack. The tack must allow enough inter-ply movement to satisfy the requirement for loose-coupling in the finished preform, yet the strength of the tack must be sufficient to prevent any undesirable movement during the lay-up process itself and to allow the finish preform to be handled without any significant ply movement.
2. The tacking process must not cause any fiber damage.
3. Any ancillary materials or processes used to attach the fabric layers together must be fully compatible with the intended end use of the preform.
4. The tacking head should be in the form of a robotic end effector for maximum flexibility.
5. The system should be capable of handling all common forms of 'dry' fabric materials used in the aerospace manufacture.
6. The system should have the capability to tack into a contoured tool.
7. The head should preferably not weigh more than 15 kg as it would require an expensive robot to handle a large mass.
8. Since there is no access to the base of the preform stack, the fixing method must be capable of being implemented from the top.

5.3.5.2 The tacking process

A chain stitch is used in this application. Figure 5.9, gives a diagrammatic representation of the stitch type, which has a 'bite' of approximately 10 mm in this instance. The bite is the distance between the needle entry and exit point, which gives the overall width of the stitch. Chain stitching has several advantages over a lock stitch for this application.

A chain stitch may allow for some stretch of the tack. It does not require a secondary thread, including its bobbin and shuttle, to be passed through the loop in the thread, generated at the eye of the needle.

The bobbin would also require loading and unloading. Thus increasing downtime **[Coughlin, 1988]**, **[Gerald, 1985]**. In the case of the chain stitches, this is not required and the spearing of the loop is performed by a looper, which also draws out and suitably positioned the loop so that it becomes intertwined with the next stitch.

In both cases the loop is extended far beyond the size required for the finished stitch and much of it is pulled back after completion of the stitch. Because of this, lengths of the thread are passed back and forth through the eye of the needle and the fabric several times and the thread is distorted in to extreme sharps. These activities place great demands on the thread, particularly when sewing carbon fibre; therefor a very tough thread is required, which must also satisfy the inclusion requirements.

Various thread materials were tested and the one found most suitable was a filament yarn made from Nomex, an aramid, developed by Du pont for applications requiring good dimensional stability and excellent heat resistance. It is readily available in a suitable form and in an acceptable inclusion in the lay-up. Nomex has similar flex and abrasion resistance to polyester and nylon and is superior to that of the acrylic fibers **[Dewing, 1999]**.

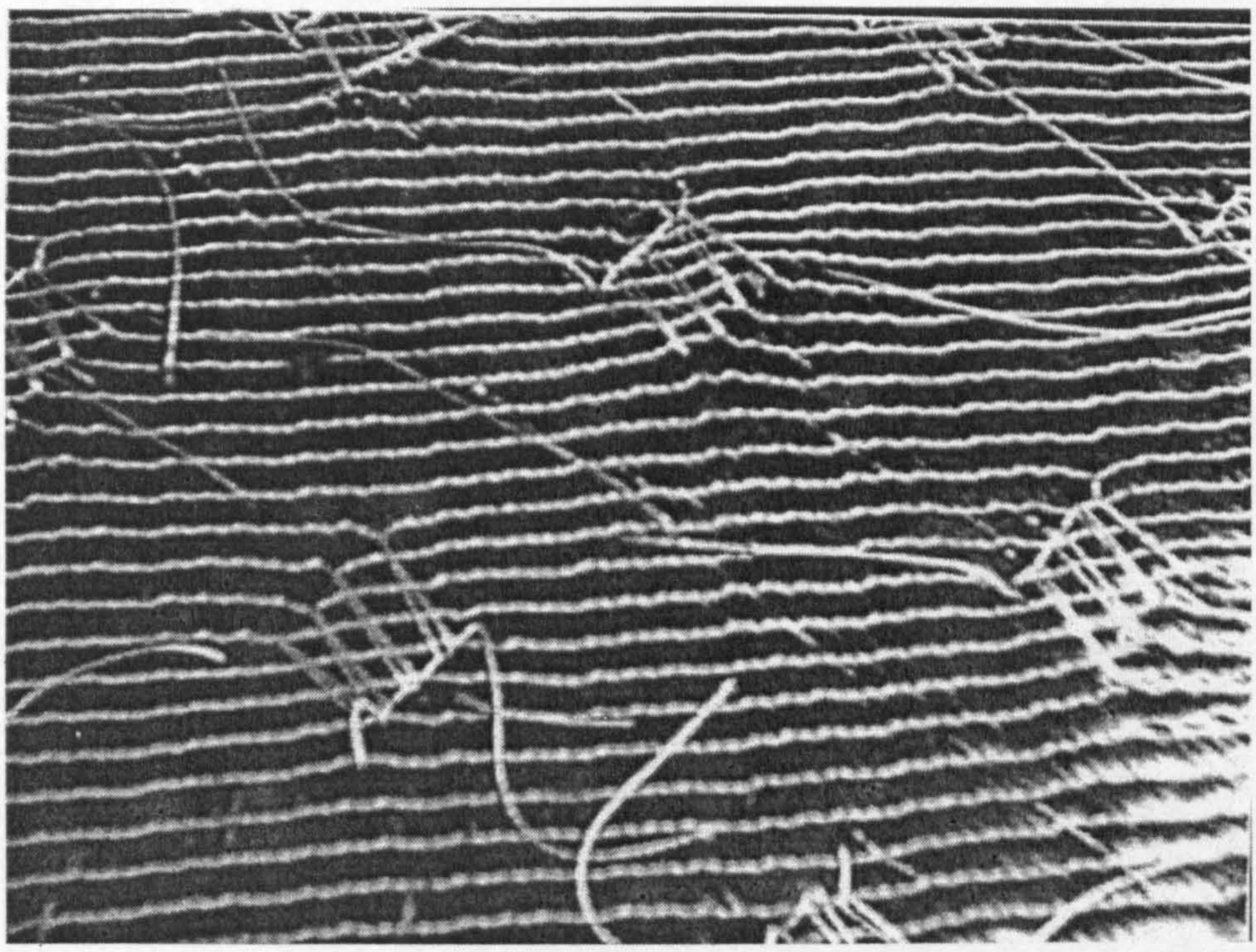

Figure 5. 9 Chain stitch implemented by RTD

5.3.5.3 RTD design

To make the blind chain stitches of the type described, a curved needle is obviously required. In order to implement the stitch a machine was designed which consisted of two primary elements (the needle and the looper) and two secondary elements (the gripper and the cropper). For ease of depiction only the primary element are shown in ,Figure 5.10a, the secondary elements are shown separately in Figure 5.10b. The gripper comprises a rotating arm incorporating a catching vee and a spring-loaded device that clamps the free end of the thread. The cropper is a rotating diamond wheel against which the thread is brought by the rotating arms catchment vee at the end of a tack. The operation of cutting and clamping is performed concurrently.

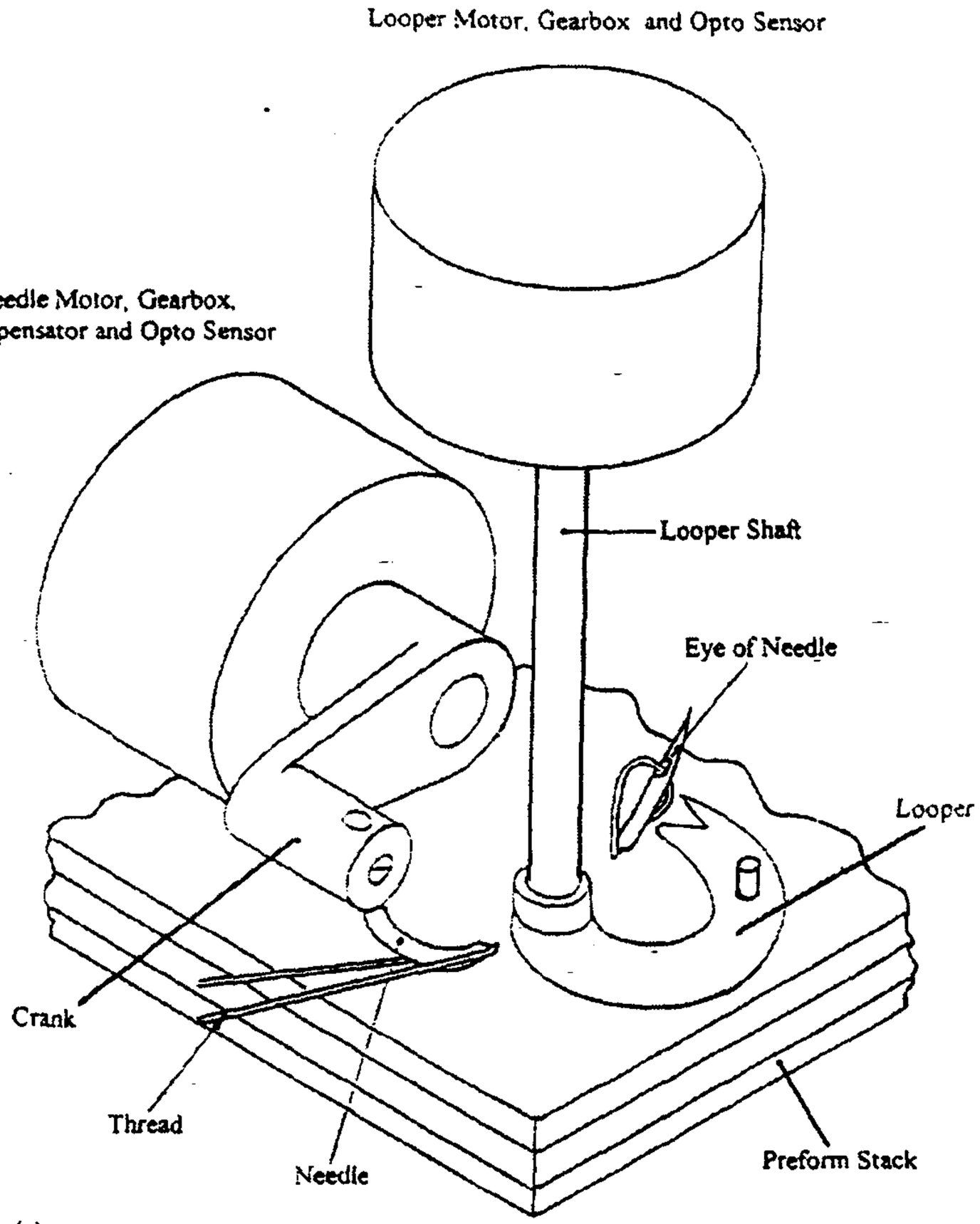

(a)

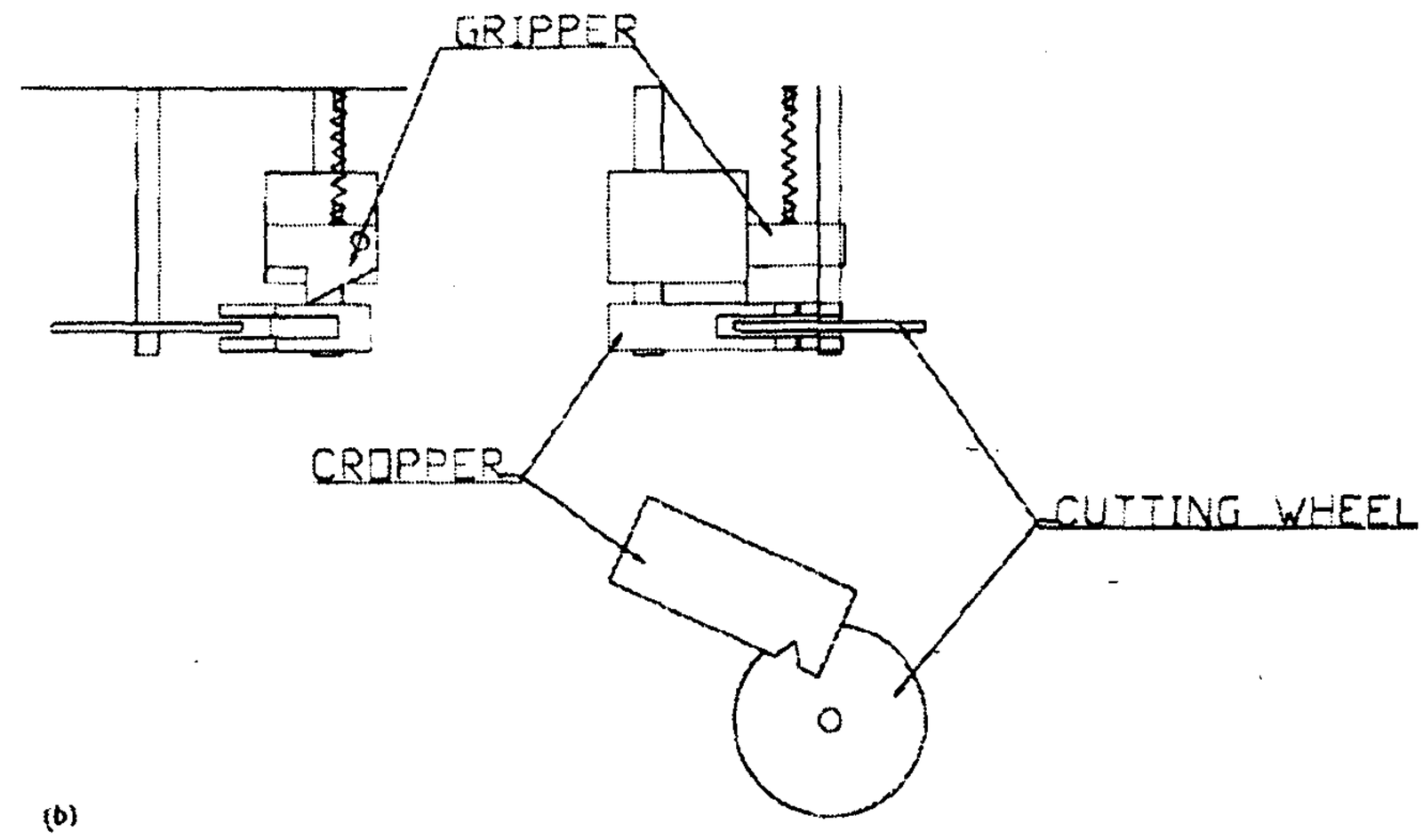

(b)

Figure 5.10 schematic of (a) primary and (b) secondary elements o
RTD

For tacking structural plies together without puckering, the curvature of the needle chosen was such that a reasonably compact bite is made while reaching to a depth of the thickness of the two plies. To cope with the stresses imposed on it in the course of a stitch sequence the needle must have high mechanical performance. To this end, commercially available curved needles were used, ensuring consistent needle quality.

The design of the other components was therefor based on a given needle geometry. The needle drive and the looper drive both use gear reduction systems and have adjustable motor speed controls. The needle drive also incorporates a spring-loaded rocker mechanism (compensator) which allows adjustment of the force exerted on the needle before a fault condition is signaled which will abort the stitch. Final needle drive is via a crank, which encompasses a needle depth control. The thread gripper and cropper are driven directly by their respective motor shafts.

5.3.5.4 RTD operation

The RTD ,Figure 5.11, is mounted on the arm of a six-axis articulated robot . The robot controller and the RTD controller are integrated with the host computer for the manufacturing cell. From an integration viewpoint, the operation of the RTD can be summarized as follows. The needle and looper drivers, under local control, insert a single stitch in the preform.

After each stitch a signal is sent to the cell controller. If required, the cell controller then moves the robot (and hence the RTD) to the next location. After the required number of stitches has been performed, the controller initiates the 'end-of-tack' routine (controlled locally by the RTD). This involves cropping of the thread running between the eye of the needle and the end of the last stitch by a rotating diamond wheel. After this operation is completed, a signal is sent to the controller and the robot is then free to move the stitching head to a new tacking site.

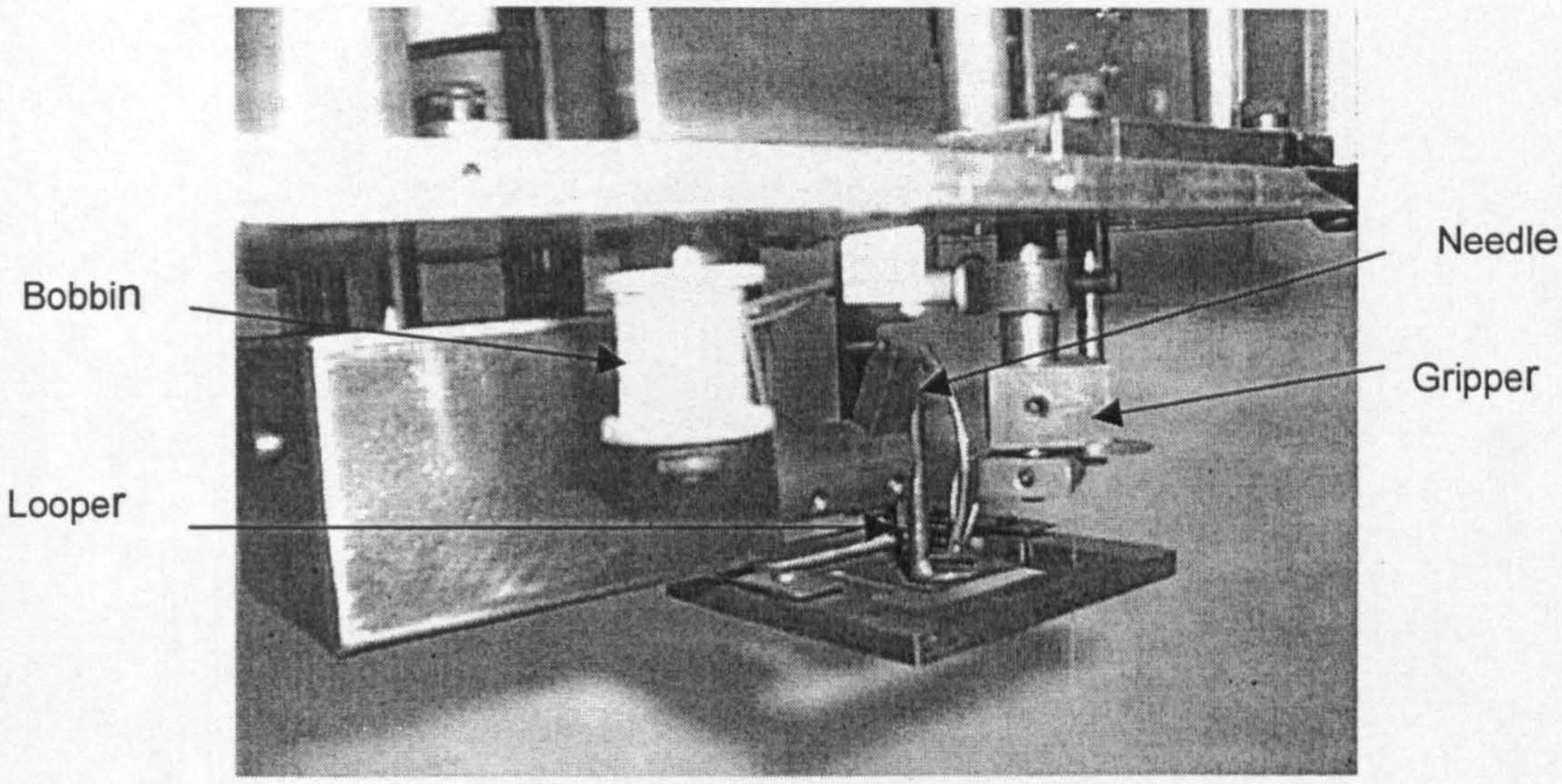

Figure 5.11 The needle and looper

5.3.5.5 Stitch-forming operation

- A curved steel needle and thread ,Figure 5.12, enters the two layers of the dry carbon fibre from the top, and after penetrating the lower layer the needle eye protrudes through the top layer (Movement 1-2)

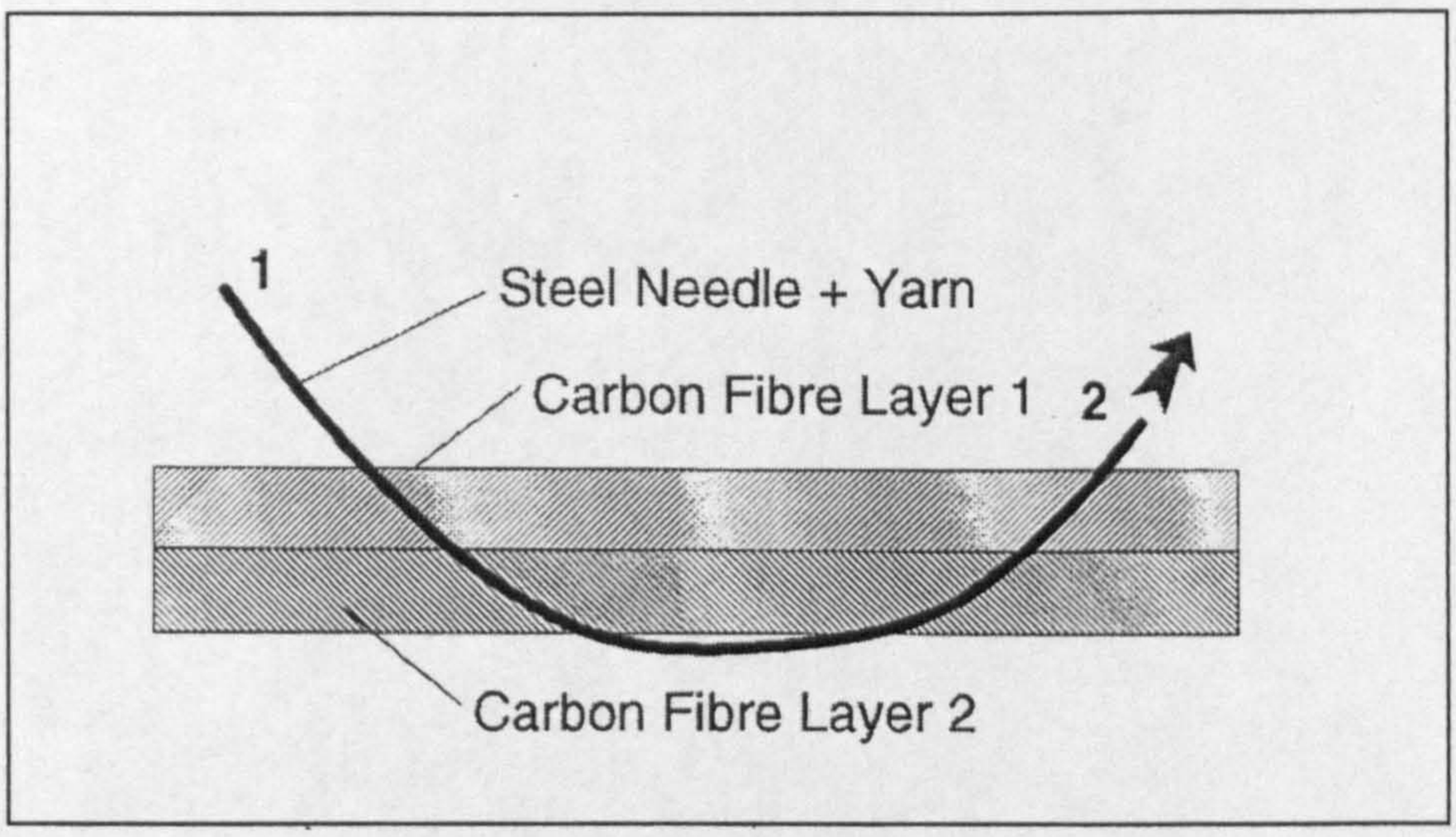

Figure 5.12 tacking procedure (movement 1-2)

- After reaching position 2 the needle withdraw by a small amount, which creates a loop in the yarn at the eye of the needle ,Figure 5.13.
- The looper, which acts parallel to the surface of the carbon fibre, then picks up the loop in the yarn and rotates through approximately 180 from position 3-4 ,Figure 5.14.

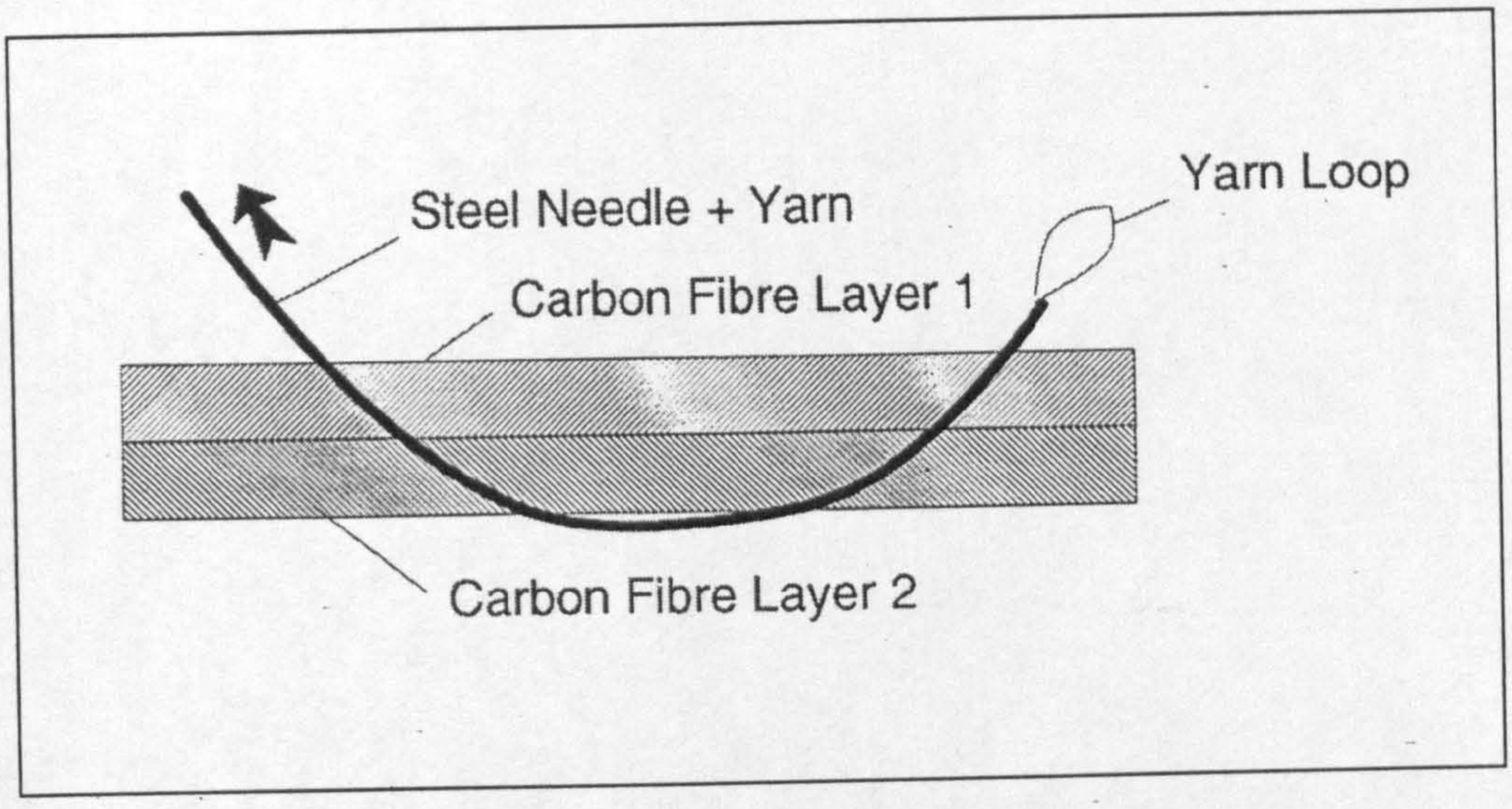

Figure 5.13 Tacking Procedure (Needle moves backwards)

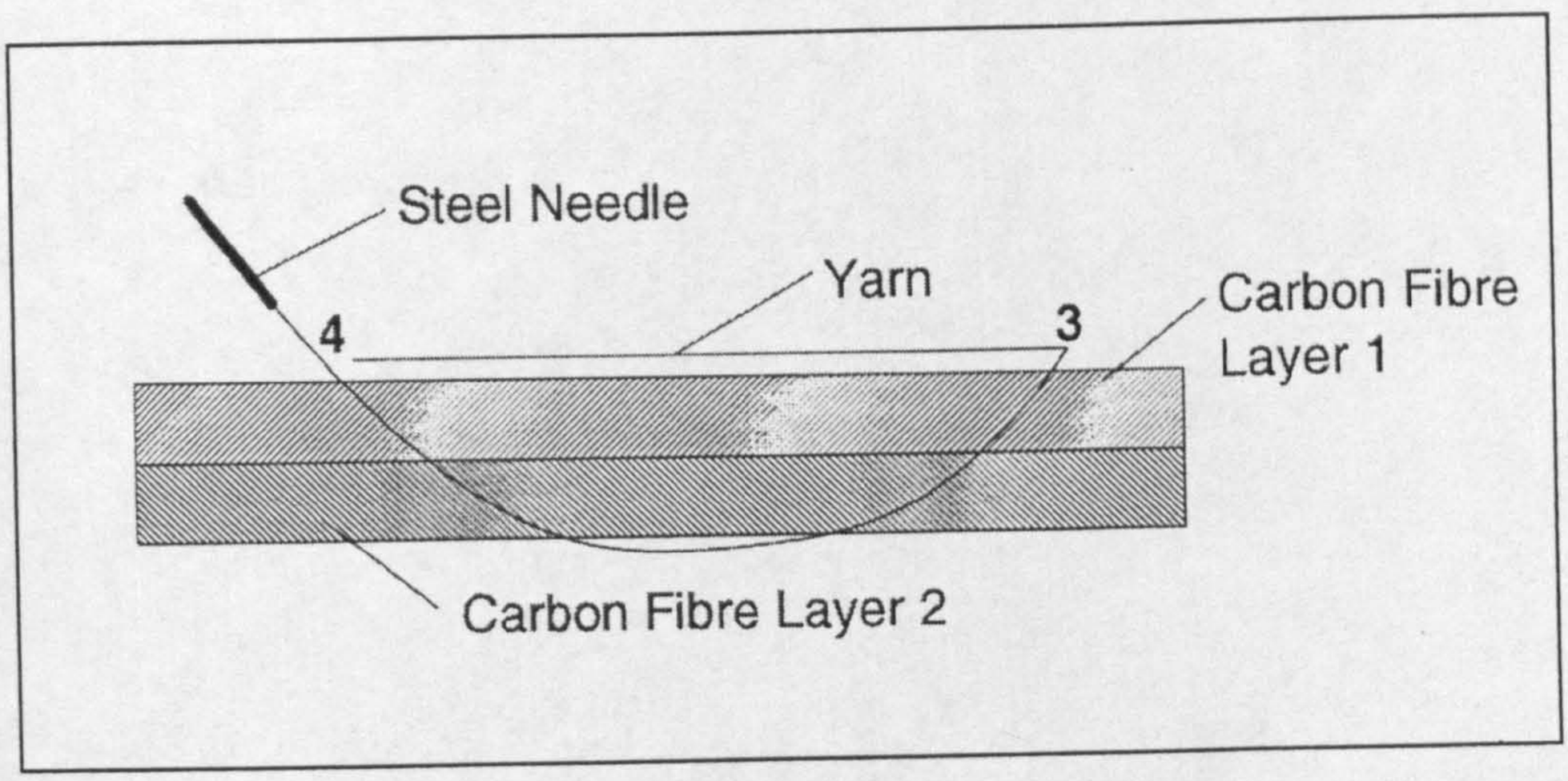

Figure 5.14 Tacking Procedure (Looper performs circular move)

- The needle then withdraws from the material to its home position and the looper rotates through another 20-30. This creataes a triangle configuration in the yarn as shown in ,Figure 5.15.

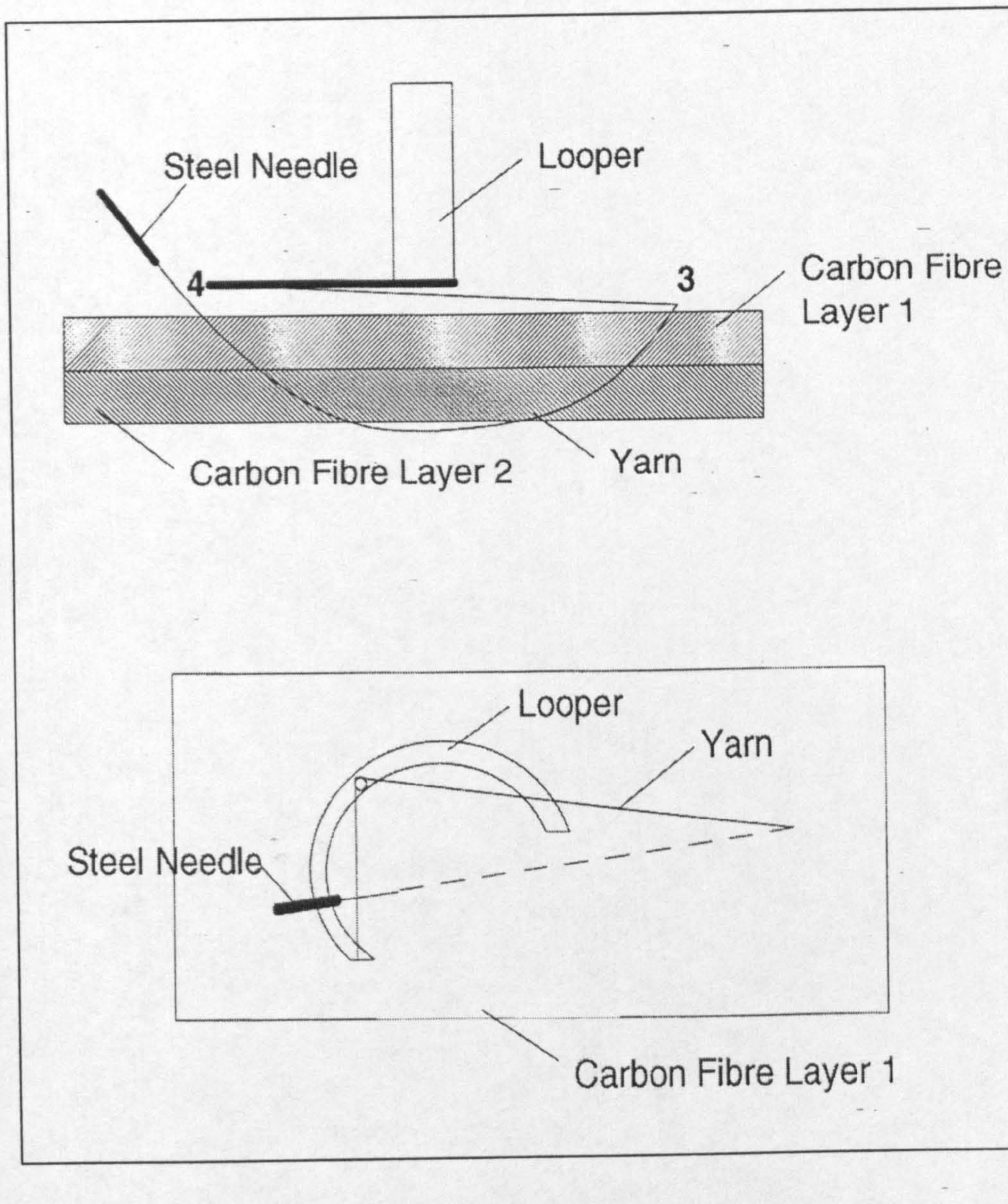

Figure 5.15 Tacking Procedure (triangle Configuration)

- The robot then lifts the RTD a few millimeters of the surface of the carbon fibre and indexes along a pre-set amount in the direction of tack.

- The RTD is then lowered onto the top surface of the material. The needle just penetrates the top layer of the carbon fibre, the looper withdraws to its home position and the whole process is repeataed.
- On the final stitch of the tack the yarn is cut with an automated cutting device (Gripper and Cropper Device) and RTD is then moved to another site to perform another set of stitches.

5.4 The Cell Controller and operation

5.4.1 Cell controller hardware

The cell controller hardware is a PC linking all components of the cell. The main tasks performed include generation and control of data files for each component, robot control, tacking device, folding device and MDS.

A centralized emergency-stop system has also been incorporated. The cell controller will generate the necessary control signals to govern the sequential timing of the processes performed. The way in which the cell is designed to operate is described in the block diagram of ,Figure 5.16.

5.4.2 Methodology for cell controller

The components described in the preceding section represent the enabling technologies for the manufacturing cell. the success of such a system, however, will depend on its ability to operate effectively with a minimum of manual intervention, and in a manner conductive to creation of an effective business process within the operating company. This, in turn, is determined by the control structure and software system for the cell.

A hierarchical control system has been adopted, with the cell control computer having superior control, as can be seen in the block diagram ,Figure 5.16. All data for cell operation are centralised to this computer to ensure single-point updating of data and effective transfer of data to the system concerned.

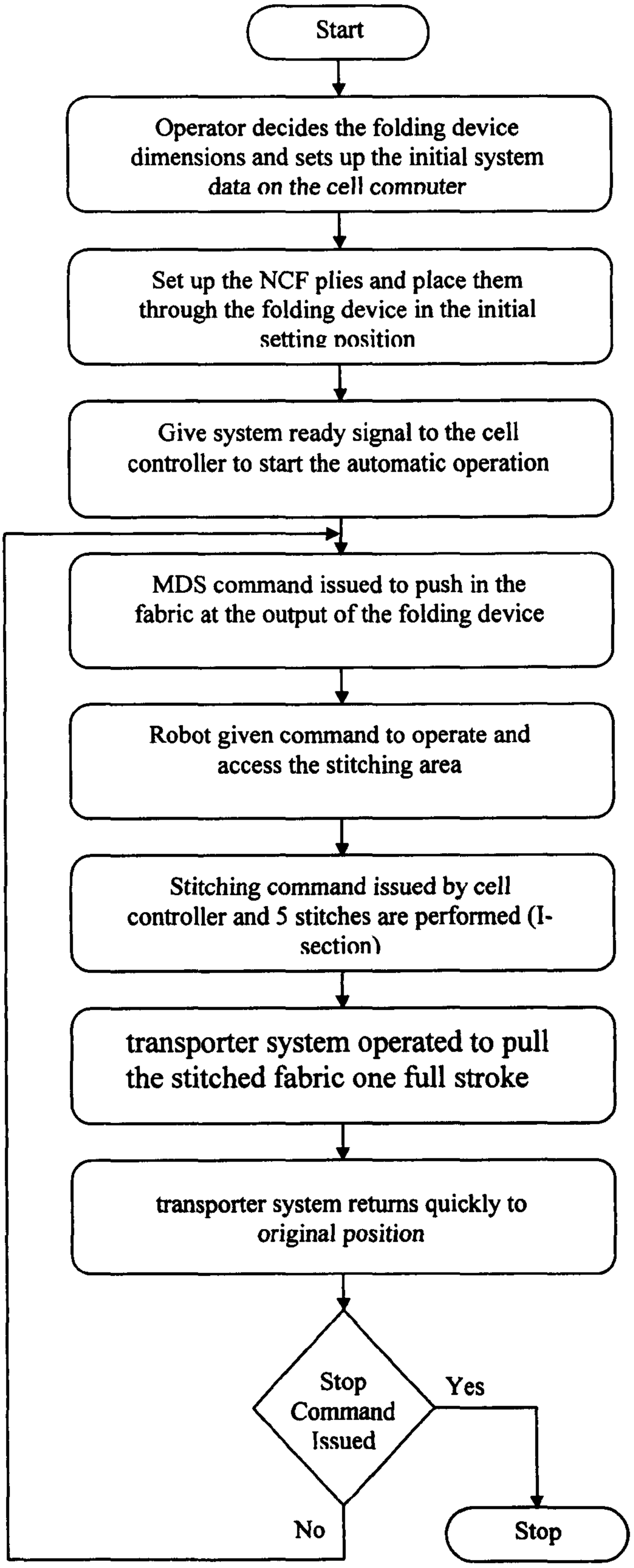

Figure5.16 Operational_block_diagram

5.4.3 Cell controller software

The cell controller software (Appendix B) was designed in a single file format for simplicity. A number of versions were written each with a different function, this was necessary to overcome the code size limitations imposed by the Borland C implementation. The format is the same for all versions however, split up as follows:

- Include files
- Constant and definitions
- Global variables
- Cutting table code
- Fanuc code
- RTD code
- Digiboard code
- Special functions
- Main routine

5.4.3.1 Cutting table

Code has been written to allow downloading of cutting data to the cutting table. There are two areas to consider: generation of the data, and operation.

5.4.3.1.1 Cutting data generation

This is carried out within the DNC program. The .dxf file containing the appropriate profile is loaded, the frame, laser and environment set up as required, and then execute option is made. Within the execute menu, there is a debug button when pressed, a filename is requested. Enter the filename with a .dnc extension, then hit go. The cutting data will be sent to the file rather than the cutting table. This is the file used by the cell program.

The sign-on and sign-of window in the frame window must be set up correctly for the cell program to operate correctly. The correct strings are:

Sign on: \RESET05

Signoff:\F1000\T1500\AX620000AY350000\DWE250\DWE1000\RESET05\ END

5.4.3.1.2 cell controller code operation

The file is loaded, and the ASCII data is transmitted to the cutting table, the handshaking being a hex 0d character returned by the cutting table each time the same character is transmitted. End of file is detected by waiting for "END" sequences. The cutting table then cuts the profile, which is polled by the cell controller.

5.4.3.2 Fanuc robot

The Fanuc communications code is divided into a number of sections: low level code for sending and receiving message packets, and then higher level function to carry out, for instance, move commands or status requests. It is strongly to use only the higher level functions in other coding.

5.4.3.2.1 Low level functions

Low level functions are simple in this case, since the protocol has been kept simple. However, one point to note is the use of bytes_to_double and double_to_bytes for conversion of double data to byte format for serial transfer. These functions implement IEEE standard definition of doubles.

5.4.3.2.2 High level function

High level functions for the Fanuc have been written specifically for operation with the robotic tacking device (RTD), hence functions are: move relative and

move absolute, get current position, and index to the next stitching point. However, given the get position and move commands, most function can be performed.

5.4.3.3 Robotic tacking device (RTD)

The RTD code was written in accordance with specifications from the manufacturer, BTTG. The communication protocol is very simple, the cell controller requesting a given function (status message, normal or final stitch) as a single byte, and the RTD responding with a single byte containing diagnostic information. Unfortunately such simplicity leads to the risk of handshaking error, but modification can only be introduced by changing RTD code which is contained in firmware.

Code of performing a tack has been written, incorporating all functions for both the RTD and the Fanuc robot, on which the RTD is mounted. Any point within the Fanuc workspace can be selected, and the orientation of the tack can be specified.

5.4.3.4 Digiboard hardware

The interface motherboard incorporated an RS-232-C socket for direct connection from the controller. The IF1 and IF2 interface cards permit up to three stepper motors to be controlled via an RS-232-C serial link.

The required information like speed, acceleration etc, is transmitted to the interfaces on the form of a series of commands. From this information the interfaces generate a ramped pulses waveform suitable for feeding directly to the clock input of a stepper drive. The controller is then free to perform other tasks while the motor is running. The interfaces used in this work are listed in detail in table 5.1.

Table 5.1 interface data

Interface No.	Interface 1	Interface 2
Type	PCB 1310.019.04	PCB 1310.045.03
Acceleration	10 K step/s^2	20 K step/s^2
Speed	100 steps per 10 ms	100 steps per 5 ms
Start/stop speed	Up to 500 step/s	Up to 500 step/s

It was not possible to use one interface, because two independent stepper motors have been used at the same time with their own different settings as speed, acceleration, number of steps, etc.

The interfaces and their inputs for axis limit switches and emergency stop switches are used as follows:

- Interface 1 is connected to the two axis limit switches and the main emergency stop of the linear track system.
- Interface 2 is connected to the main emergency stop, which acts like an entire system-stop.

5.4.3.5 Digiboard software

The software has been written for controlling the folding device, linear track and the MDS. When the program is executed the initialisation procedure on both ports will be automatically executed. If no error occurs during the initialisation (the program displays the successful initialisation procedure), both interfaces are set up properly. Then, the program and the stepper motors system are ready to receive instructions.

The program has been written to check the interface communications before entering the main menu. If the intialisation of only one or both interfaces fails, then a communication fault is assumed. In that case, it is recommended firstly, to check the communications and fix the fault. Secondly, to switch on the stepper motors system and after a delay of approximately 10-15 sec booting up the PC. The delay is very important for the automatically executed internal initialistion procedure/system-check of the interfaces.

5.5 Safety aspects

With articulated robot holding the stitch machine and laser cutting system contained in the manufacturing cell. Safety aspects are paramount. The first safety mechanism is to ensure that personnel can not enter the cell during operation. This is achieved by a physical barrier around the cell.

An emergency stop control circuit has been implemented which stops all cell systems if any emergency stop circuit element is achieved. Additionally, emergency stop is activated if communications failure occurs between the cell controller and any other element.

5.6 Conclusion

This chapter has described a prototype robotic assembly cell for composite lay-up of reinforcement structures for aerospace applications. The aim of the chapter has been to introduce new techniques, which may be used to produce the 3D component for aerospace industry.

The integration of the MDS and transporter with the folding and robotic stitching device should enable the lay-up of 3D preforms while retaining their designed shapes. The resulting product can be stored until RTM is applied. The cell is optimised for the NCF material and can be easily readjusted for other fabrics.

Additionally, the risk of error occurring between design and manufacture are minimised by the ability of the system to operate directly from CAD data file. The set up of the folding device dimensions and manipulated shape is performed on the cell computer at the startup. This should enable the system not to require major readjustments and tuning of the sizing and dimensional variations when changing from one section to the other.

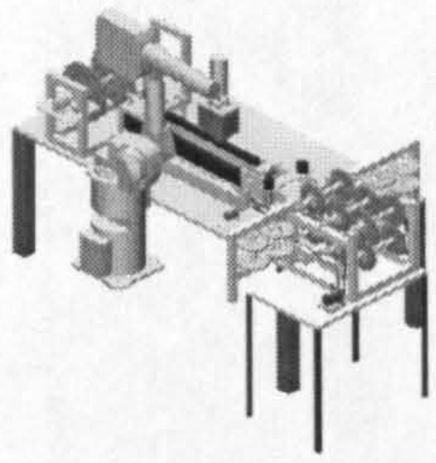

Chapter 6 Cell Optimisation

6.1 Introduction

After the cell has been developed and preliminary tested for number of operations, it was found that an appropriate modification needs to be conducted in order to achieve the optimum performance. Such modification should serve the following purposes:

6.2 Optimisation of the movements process

Stepper motors system has been used to drive all the movements in the cell. Stepper motors and their controller units offer a large variety of features for a flexible control over the designed cell, e.g. in speeds, accelerations. In addition to these features it is easy to connect limit switches and emergency stops to the system.

The most important point is that a stepper motor can provide definite steps, respectively defined distance of the laid-up material in a closed-loop circuit under the condition that the maximum torque of the motor is not exceeded or even reached.

Synchronous start and feeding velocity for all the elements; material bank, MDS, folding device and linear track system has been made through the interfaces that used to drive the stepper motors through the pc software.

After the cell had been implemented and connected to the stepper motors drive system, it was tested. This means that the principal method of the feeding process has to be verified to see if the cell is able to introduce accurate products.

Before an accurate process is achieved, care needs to be taken to ensure that certain limits are not exceeded. The process should operate within the limits specified below. As the test result has shown the limits differ in their importance for the entire process, and therefore they are listed from the most important to the less important;

6.2.1 Limits

The limits are listed below and shown in ,Table 6.1:

1. torque limit of rubber roller motor
    a. increase with gear ratio
    b. function of material properties and pressure between rollers
2. Material slip
    a. function of pressure between rollers
    b. function of acceleration and velocity
    c. function of the material to be delivered
3. Min/max material lay-up speed

    Function of entire process speed, the slowest element is the RTD. In all probability, the maximum lay-up speed of the linear track system and MDS will never be exceeded.
4. Frequency of resonance
    a. depends on moved masses, their accelerations and behaviour of oscillation.
    b. Depends on pulsating behaviour of stepper motors. Reducible by choice of suitable step rate or step-sequence- mode.

6.2.2 Accuracy

Accuracy of lay-up depends on

1. positioning of the material between rubber rollers?

2. slip behaviour
3. drive and controlling
4. position and parallelism of rollers, rotational and transitional movements.

Table 6.1 Limits, test results and consequences

LIMITS	Test results	Consequences
Torque limit	Was reached and exceeded very fast	Modified MDS has got a gear box to increase torque on rollers
Material slip	Because of the exceeded torque limit the pressure between rollers could not be increase too much.	Due to the increased torque on the rollers the pressure on rollers can be increased. Material slip can be avoided over a wide range.
Min/max speed	The slower the speed the less material slip occurs. But minimum speed let the MDS vibrate, because the stepper motors' acceleration is very jerky. Maximum speed was never tested and reached, because material slip occurred before.	Due to the increase of torque on the rollers and less material slip, the speed could be put up. But it will not reach the provided maximum value.
Frequencies of resonance	Frequencies of resonance occurred during slow speed and certain combinations of chosen parameters.	Avoid these combinations, by finding suitable alternative combinations that are more or less resonance free.

Table 6.1, has already represented the experience gained out of the preliminary tests. The required modifications to optimise the cell performance have been done. (Detailed modification in the following sections), Table6.2, shows the results of several tests with a specific setting.

The tests have been done in varying stepper motor drive settings and the pressure on the composite material between the rollers. The magnitude of the pressure is unknown; therefore the distance in mm is given. The distance is measured by measuring the displacement of the displaceable roller towards the fixed roller. The distance is set to 0 mm when no gap exists between the composite material and the two rollers. From this position on, the rollers were pressed together (distance > 0).

The tests showed that a distance less than 1mm is to be recommended and that several parameter combination of the stepper motor system has to be avoided because they caused resonance vibrations, recognisable through the increased noise.

Table 6.2 Tests results

Test	Distance (mm)	Speed rate	Acceleration rate	Start/stop speed	Final speed	Result
1	0.5	4	20	24	200	Proper feeding process, slippery while accelerating
2	0.8	4	20	24	200	Proper feeding process.
3	1.3	4	20	24	200	Step losing, motor stopped, motor torque exceeded.
4	1.3	1	20	24	100	Better performance, but motor torque is still exceeded

6.3 Optimisation of the MDS

The preliminary tests revealed that the torque limit of the motor, which drives the rubber roller, was exceeded. Consequently, the stepper motor lost steps and stopped rotation meanwhile the linear track system continued to work properly.

An automatic adjustment, Figure6.1, has been established instead of a manual one of the first prototype. It was clear that only an automatic adjustment could guarantee that the composite material is fed in a straight way over a long distance. Therefore a gearbox has been added to the MDS to provide the required transmission ratio.

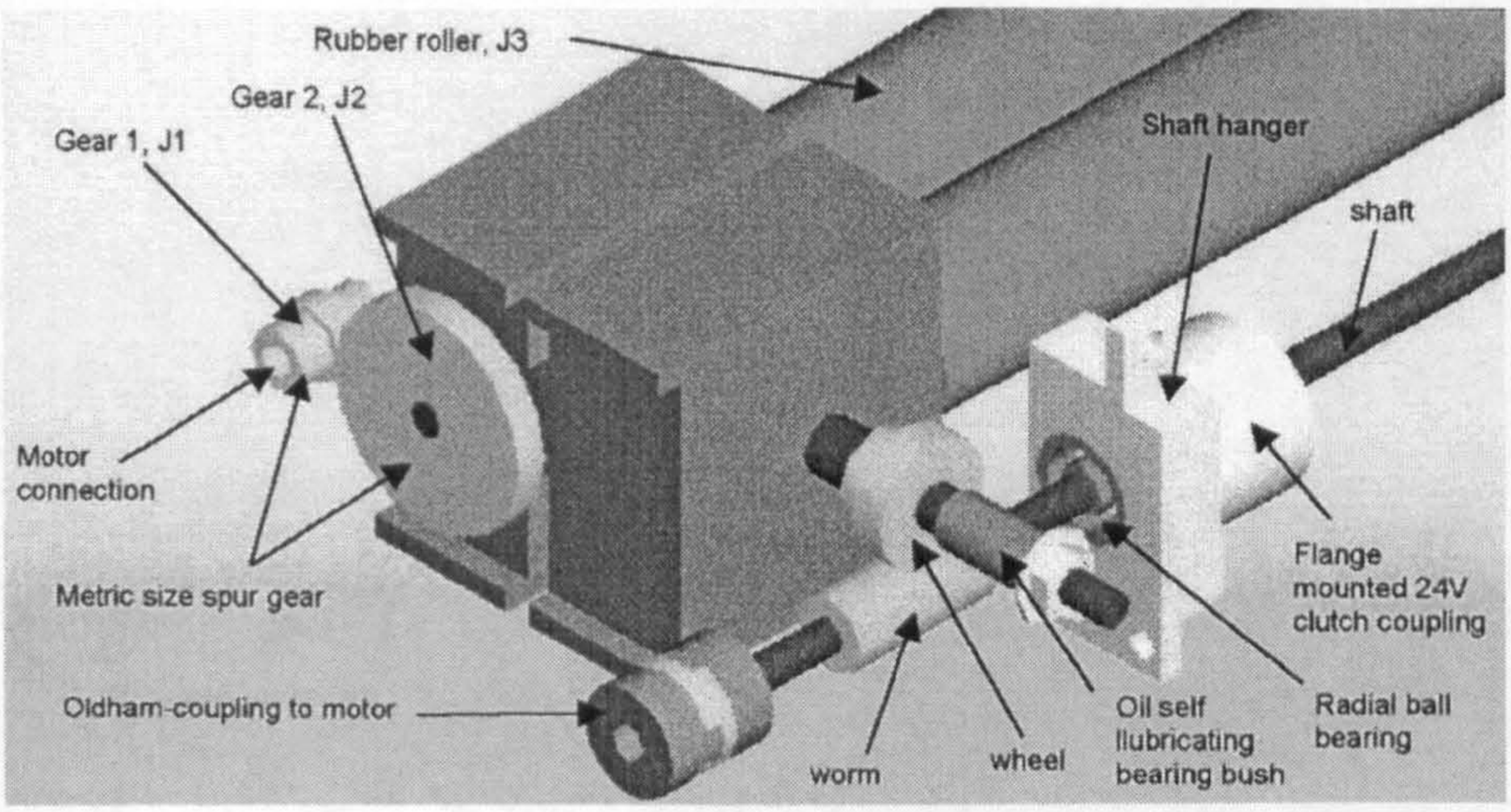

Figure 6.1 Gearbox and automatic adjustment

A pair of worm gears has been chosen to fulfil the requirements. Figure 6.2, shows the position of the worm gears and the stepper motor. Each worm is connected to a shaft. A shaft holder holds the shaft on the left side, through bearings. The stepper motor drives the left shaft via an Oldham-coupling. The other end of the shaft is coupled to an electro- magnetic clutch that connects both shafts together if the clutch is active. Two shaft holders hold, via bearings, the shaft on the right hand side..

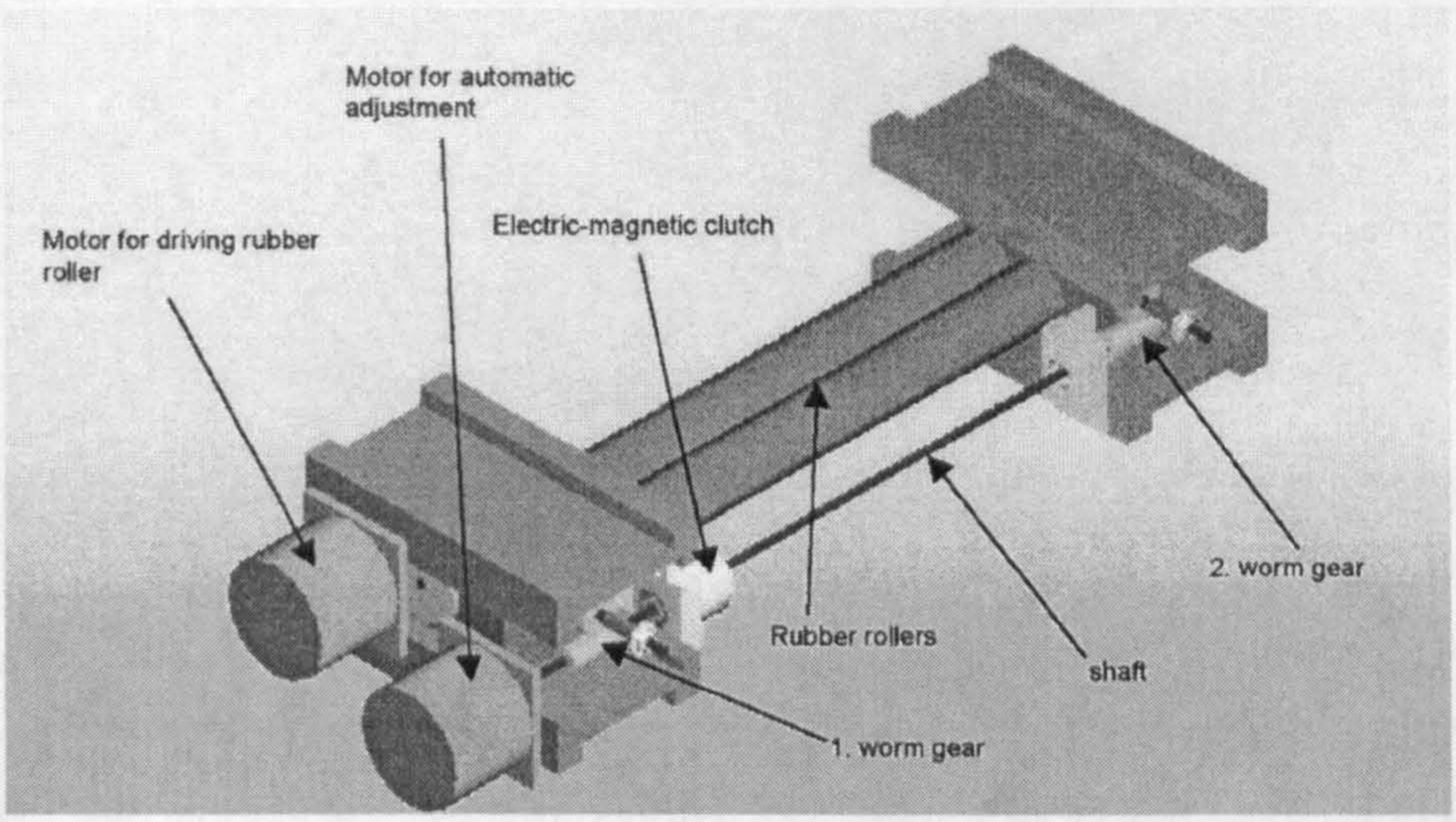

Figure 6.2 automatic adjustment

Both wheels found their places on another two shafts where originally the bolts for the manual adjustment were mounted. The two shafts are supported on one side by a self-lubricating bronze bearing and by the threads of the solid on the other side.

At the end, this modification provided a gear transmission ratio of 0.1mm displacement of displaceable solids per 400 motor-steps. The threads convert the rotation into a linear translation of the solids as shown in the following equation;

Automatic adjustment gear transmission ratio:

1. worm and wheel gear ratio

$$i_1 = \frac{\text{number of teeth in wheel}}{\text{number of starts in worm}} \quad (1)$$

Nmber of teeth in wheel = 25
Number of starts in worm = 2

$$i_1 = {}^{25}\!/_{2} = 12.5$$

2. Bolt ratio (converts rotation into linear translation)

$$s = \frac{\text{pitch}}{\text{revoltion}} \quad (2) \qquad \text{pitch} = 1.25\text{mm}, \text{s : distance}\left[\frac{\text{mm}}{\text{rev}}\right]$$

- total conversion rate: $12.5\ \text{motor}_{\text{revolution}} \equiv 1\text{shaft}_{\text{revolution}} \equiv 1.25\ \text{mm part}_{\text{displacement}}$
- $1\ \text{motor}_{\text{revolution}} \equiv \frac{1.25\ \text{mm part}_{\text{revolution}}}{12.5\ \text{motor}_{\text{revolution}}} \equiv 0.1\ \text{mm part}_{\text{displacement}}$
- $0.1\ \text{mm part}_{\text{displacement}} \equiv {}^{\text{number of steps}}\!/_{\text{rev}} \equiv 400\ \text{steps}$

6.4 Optimisation of the folding operation

The forming tool was built so that the inner surfaces matched the exact dimensions required for the finished, stitched NCF component. The critical surfaces were those shown in ,Figure 6.3.

These critical surfaces are the edges that correspond to those of reinforcement structures produced from the forming tool, and are critical to achieving the correct dimensions for reinforcement structures.

This method gave a high degree of control on the edges of the NCF lay-up, and allowed the material to be controlled when passing through the folding device.

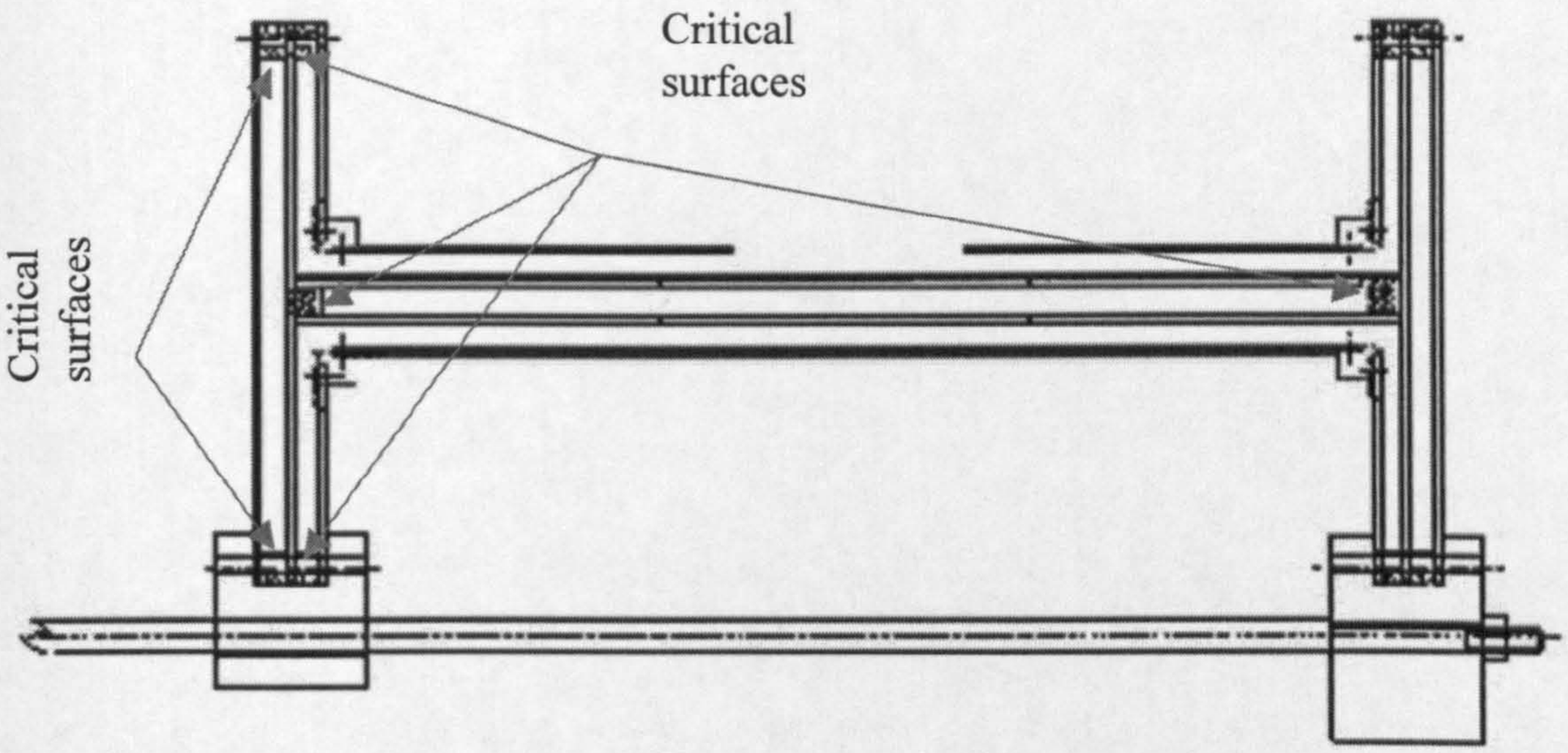

Figure 6.3 Critical Faces of the Forming tool; front view

6.5 RTD Optimisation

The first trials to use the RTD showed that the RTD causes movement in the ply being tacked. The major source of ply disturbance was the repositioning of the RTD after a stitch cycle had been completed and the sewing head moved to the next stitch site. This created up to 10 mm of ply movement, when the RTD controller is reprogrammed to switch off the motor that producing back

tension in the yarn during the step to the next stitch location, the problem is greatly reduced.

Through the implementation of various integral automated clamping devices, ply disturbance is further reduced to less than ±0.2 mm for small plies (less than 150 mm by 150 mm) but for larger plies, the effect of ply disturbance is negligible. The implementation of the integral clamping device was also found to have positive effects in reducing fibre misalignment in the area of the tack.

6.5.1 Optimisation of tacking parameters

- **orientation of the stitches**

A set of experiments were conducted to evaluate the effect of stitch orientations on the movement between two plies of the dry fabric. Samples of 450 mm long for the top ply and 400 mm for the bottom ply and 250 mm width for both used to check the movement of the top ply relative to the bottom ply under a certain force.

Two tacks were implemented per sample with different number of stitches per tack to study the effect of the number of stitches per tack on the movement between plies. At one end of the plies, 50 mm of the top ply was fixed between the two flat plates in the gripping system and a certain dragging force applied to drag the two plies for a certain distance after implementing the stitches. Difference between the edges of the other end of the two plies was determined as the movement between the plies.

Samples were produced with tacks at two different orientations to z axis stitches in the NCF. One with the stitches in the tack were perpendicular to the z axis direction stitching in the NCF; in the other stitches in the tack were running parallel to the lines of z axis stitching in the NCF. Samples of both orientations were produced with tacks consisting of between 2 and 8 stitches.

The results of the tests are given in ,Figures 6.4-6.7; Figures 6.4-6.6, are graphs showing the effect of stitch number per tack against relative ply movement. Figures 6.4-6.6, show the results when the force was applied in 0° orientation of the plies, while Figure 6.7 shows the results when the force was applied in 90° orientation and 150 mm apart.

The tests have been performed in 250, 200 and 150 mm apart between the two tacks respectively. It is clearly shown by the results obtained that the greatest stability, and hence minimal movement, is achieved when the distance is decreased to 150 mm and the stitches are running parallel with the lines of the z direction stitching in the NCF. Consequently, all further results analysis was performed on these samples.

Finally, the results ,Figure 6.6, showed that RTD was capable of performing the stitches to secure the plies together, while having the potential to allow enough inter-ply movement for the preform to match the mould geometry without wrinkling.

- **no of the stitches per tack**

From the experiments carried out ,Figures 6.4-6.6, it was found that there is a decrease in the movement between the stitched plies as the number of stitches per tack is increased. The greatest increase in ply stability for a unit stitch increase occurs when the stitch number is increased to five stitches.

This can be seen in, Figure 6.6, which shows a graph of ply movement versus stitch number per tack. The graph shows that there is an inversely proportional relationship between the number of stitches and displacement.

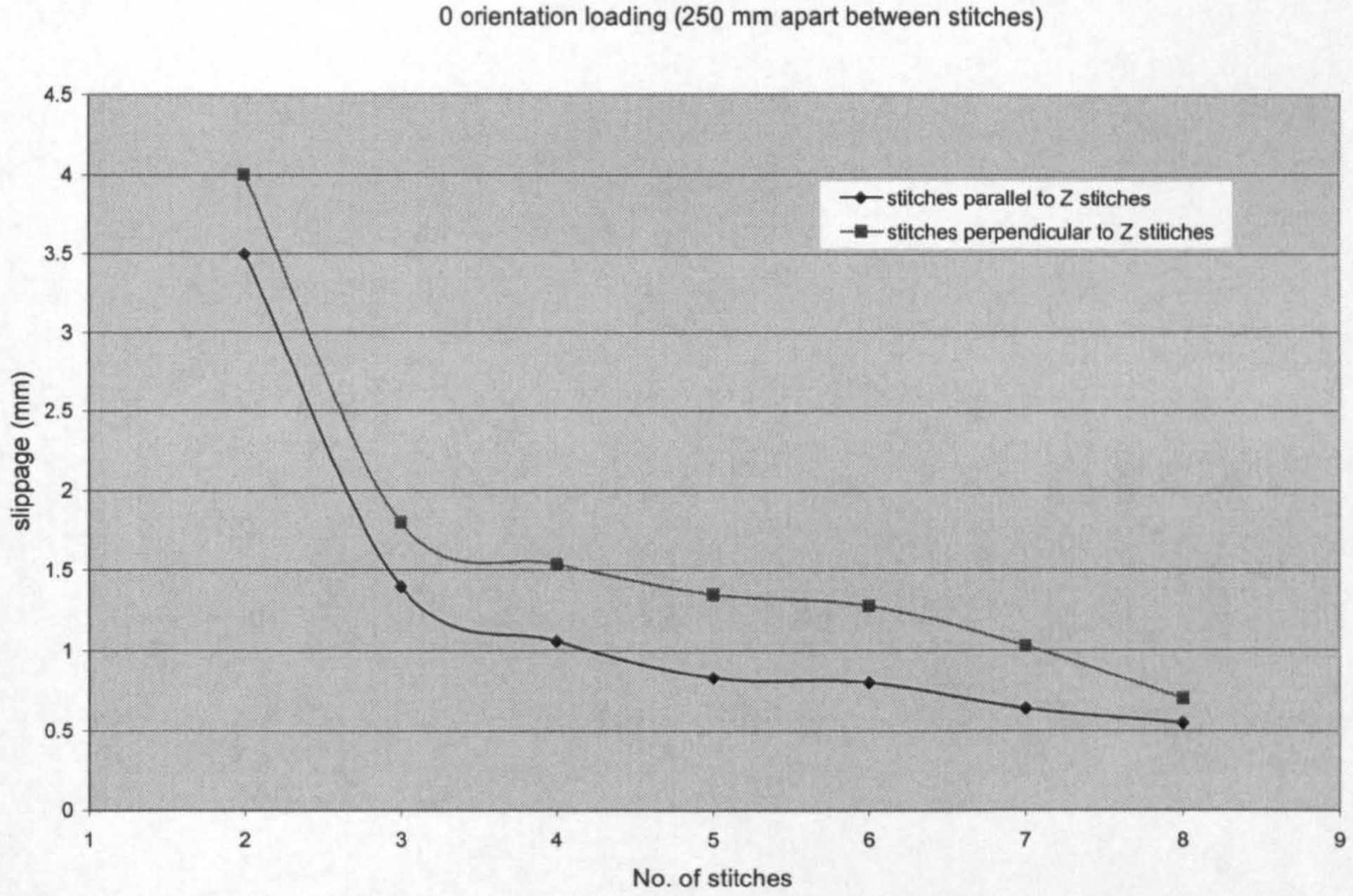

Figure 6.4 Effect of stitches orientations on the ply movement, 250 mm apart between the stitches

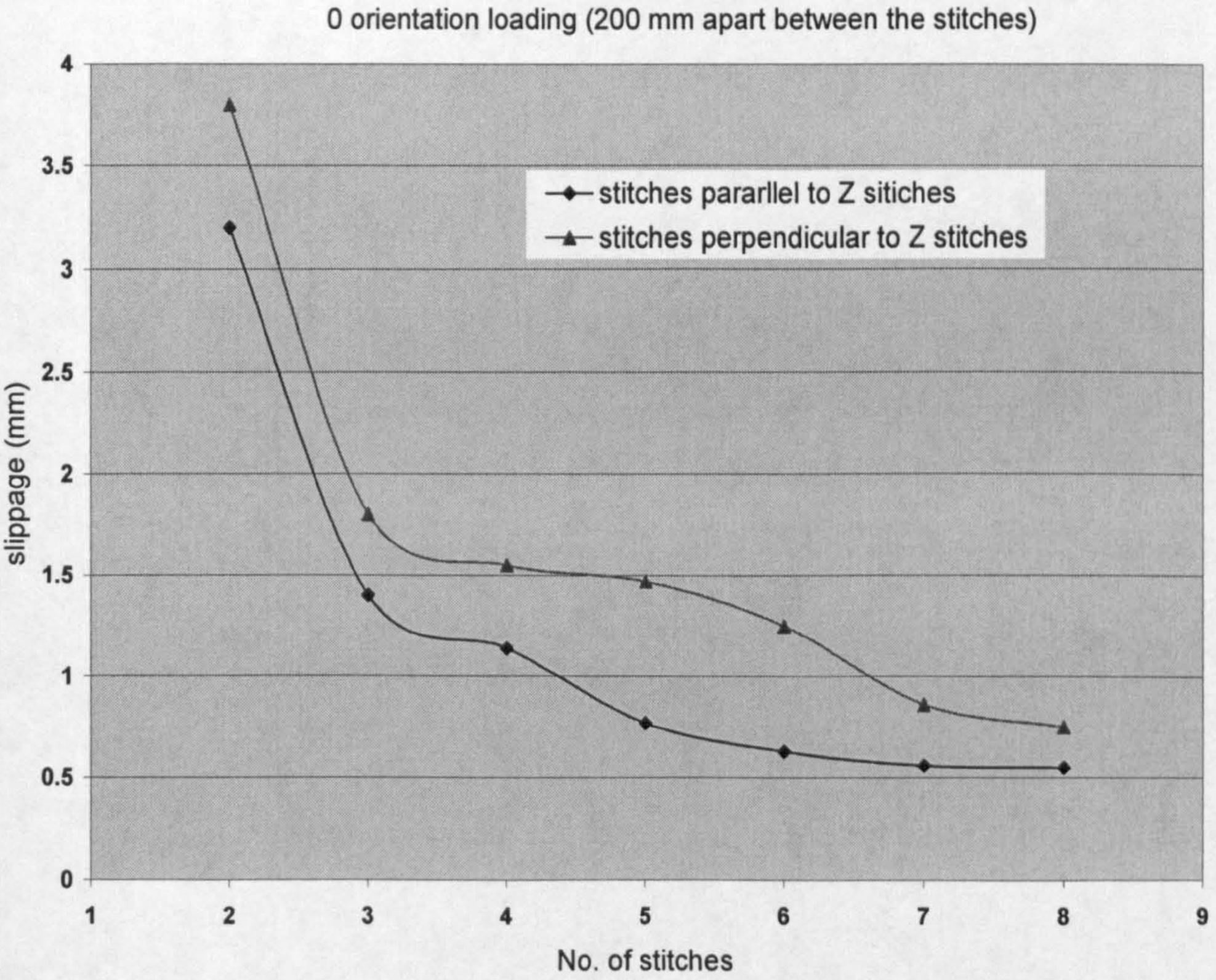

Figure 6.5 Effect of stitches orientations on the ply movement, 200 mm apart between the stitches

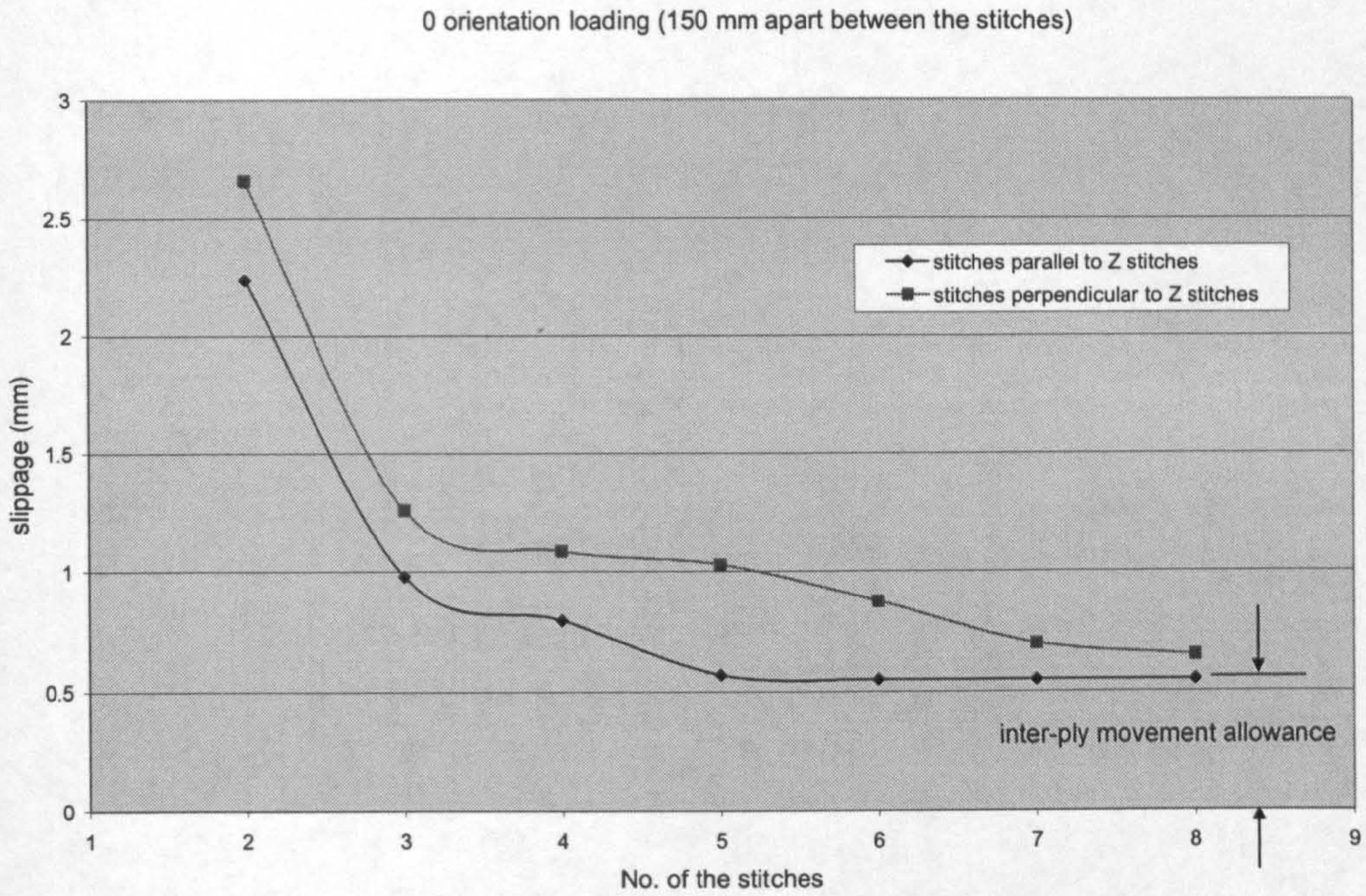

Figure 6.6 Effect of stitches orientations on the ply movement, 150 mm apart between the stitches

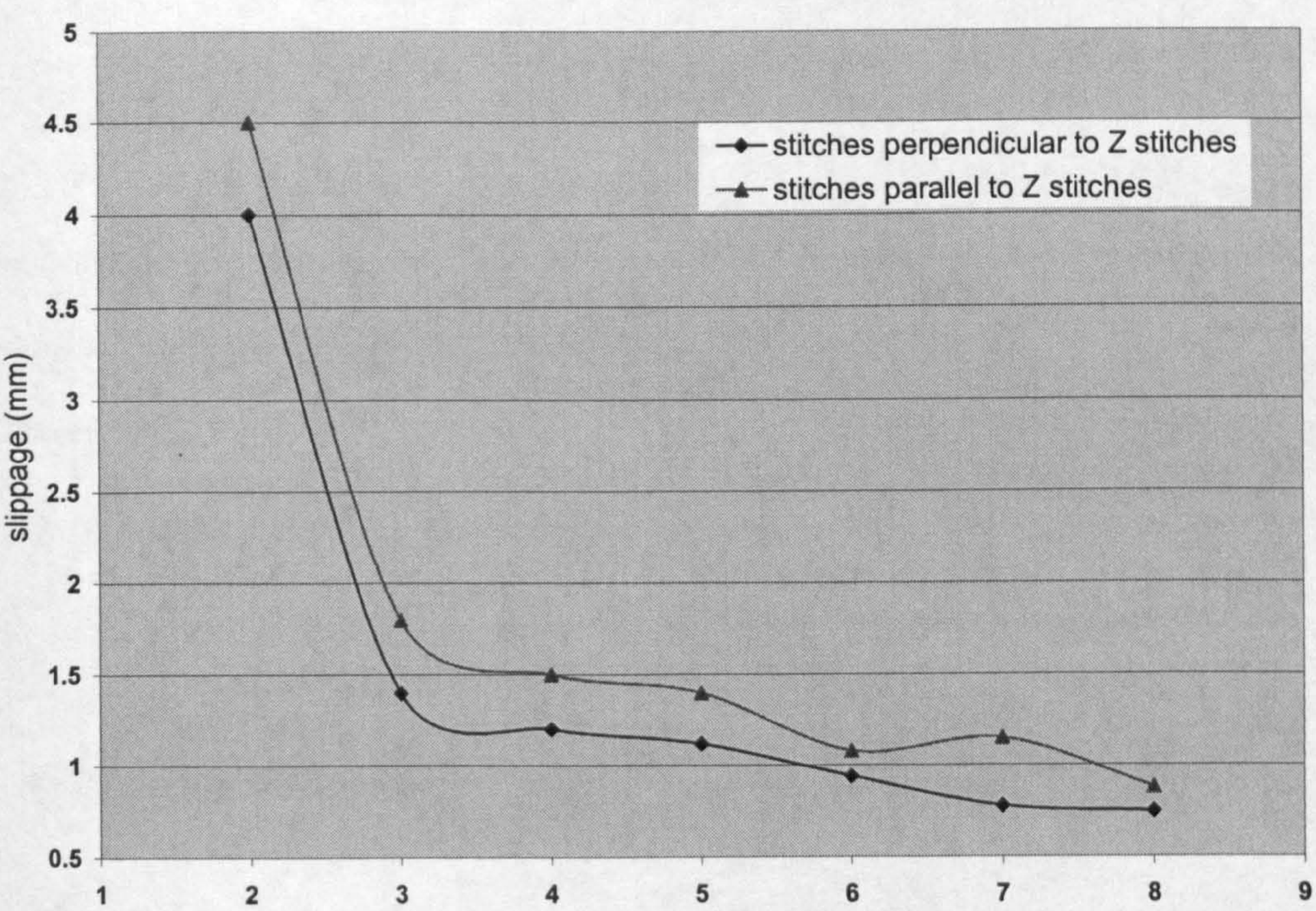

Figure 6.7 Effect of the load orientations on the ply movement, 150 mm apart between the stitches

6.6 Optimisation of the production time

Table 6.3, presents the production time for different reinforcement structures that have been produced by the manufacturing cell. Following a series of experimental work to examine the production time required for producing the reinforcement structure, it was found that an optimisation is required to minimise the processing time. The optimisation was carried out on both tacking and dragging time. The movement of the robot (which carried the tacking device) from the home position to reach the stitching area was much faster than the movement during stitching task. Therefore, it is appropriate to increase the speed of the robot to reach the stitching area from the home position, thus, minimising the time required for the entire process.

Optimisation was also carried out on the dragging time. It was possible to reduce the time taken to reach the structure (forward stroke) as the transporter is free of material. Whereas it is very difficult to reduce the time taken to drag the structure back to the collector (backward stroke).

6.7 Conclusion

Optimisation was conducted for each cell element. The testing procedure includes the optimisation of the speeds, the torque limit of rubber roller motor and the pressure between rollers. The following sections dealt with the optimisation of the stitches that join the plies through fine tuning of tacking parameters e.g. orientation and the number of the stitches.

A set of the experiments were conducted to study the inter ply movement and the results showed that the greatest increase in ply stability for a unit stitch occurs when the stitch is performed parallel to 0^{o} direction and the number of the stitches is increased to five stitches per tack.

Table 6.3 Production time for the different reinforcement structures.

Time	**Reinforcement structures**						
Feeding [f]			**I**	**T**	**J**	**C**	**Remarks**
			8 Sec				
			2F+W	F+W	1.5F+W	F+W	F refers to flange and W for web
Tacking time	Stitch [a]		2(3*5*10)+(3*5*5) sec	(3*5*10)+(3*5*5) sec	1.5(3*5*10)+(3*5*5) sec	(3*5*10)+(3*5*5) sec	5 refer to number of stitches per tack 3 refer to time to perform single stitch 10 refer to the number of tacks per flange and web/m
	Robot [b]	home position	8 sec	8 sec	8 sec	8 sec	
		stitch position	2(3*3*10)+(5*10) sec	(3*3*10)+(5*10) sec	1.5(3*3*10)+(5*10) sec	2(3*3*10)+(5*10) sec	
Gripping time [c]			(9*5) sec				9 refers to number of drags 5 refers to time per drag
Total time	f+a+b+c		11 min/m	7 min/m	9 min/m	7 min/m	

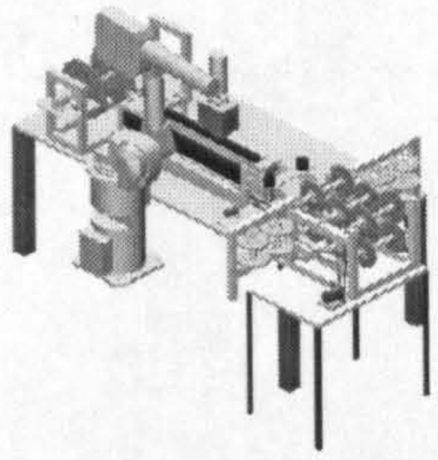

Chapter 7 Examination of the cell performance

7.1 Introduction

This chapter is concerned with the performance assessment, through statistical analysis, of the manufacturing cell. To achieve an acceptable level of confidence in the reliability of the cell performance, the significance of measurements were qualified by carrying uncertainty calculations. To examine the effects upon the cell performance of the deformation, ply and edge deviations that occur during the forming process, statistical interpretations of the results obtained from various testing parameters are described in this chapter. Furthermore, the influence of the number of the stitches which holds the plies together will be considered.

7.2 Test description

The tested samples were prepared as follows:

1. The samples, Figure 7.1and 7.2, of sizes 450mm x 250mm for **U** plies, 450mm x 130mm, for middle flat plies, and 450mm x 120 mm for side plies were cut from the raw material roller using the laser cutting table to achieve accurate dimensions for all tested samples, this eliminate the variation among all samples.
2. The topmost and bottommost plies ,Figure 7.1, which go through the upper and lower holes of the folding device to form the upper and lower **U** plies, were cut 0.8mm (thickness of the ply) shorter than the other plies. This is to account for the misalignment between the edges as a result of the plies stacking.

3. 90 x 90 mm^2 was marked, Figure 7.2, to measure the longitudinal and transverse deformation, Figure 7.1, shows the measurement of the ply and edge deviation.
4. The cut plies were pushed into the folding device through the MDS, as shown in ,Figure 7.1. Two plies were pushed into the upper hole of the folding device, the third and fourth plies through the middle hole, and the last two were pushed through the bottom hole. Four vertical plies, two from each side, were pushed through the side-ways. This operation forms the I-beam structure and it is used for all experimental work.
5. Once the sample reached the front of the folding device, various stitching were performed.
6. The gripping system gripped and dragged the material at the required pre-defined distance (200 mm) out of the folding device.

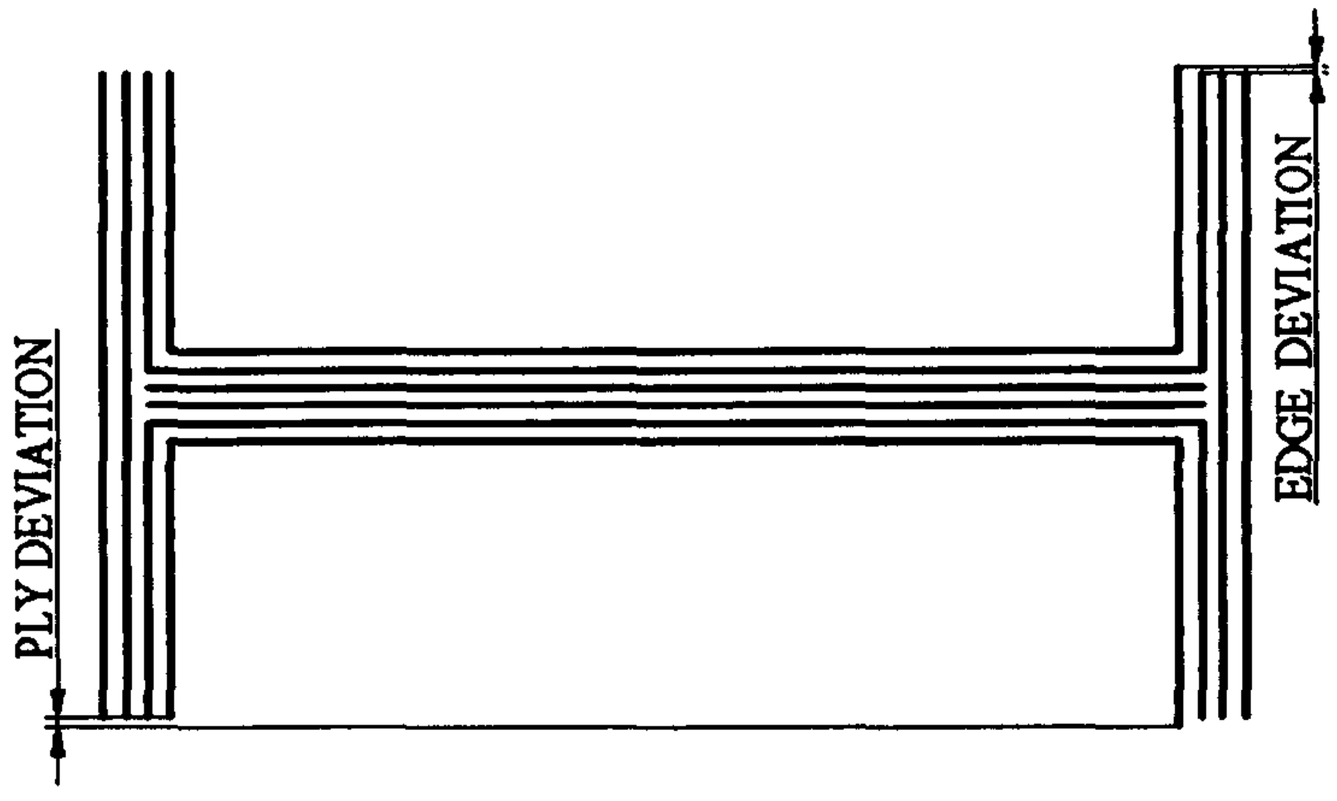

Figure 7.1 Front view of the I-beam structure showing the edge and ply deviatio

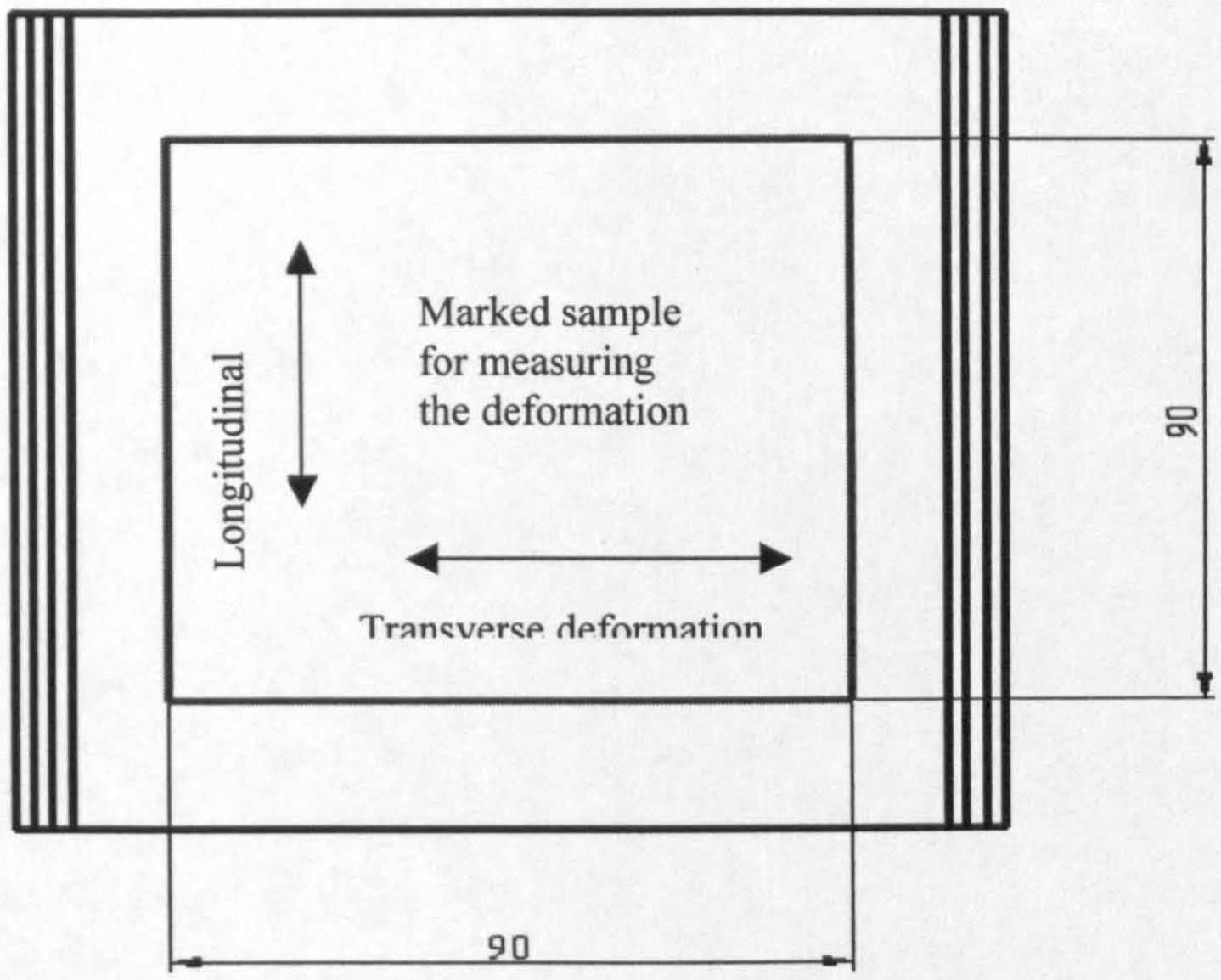

Figure 7.1 Top view of the I-beam structure showing the longitudinal and transverse deformation.

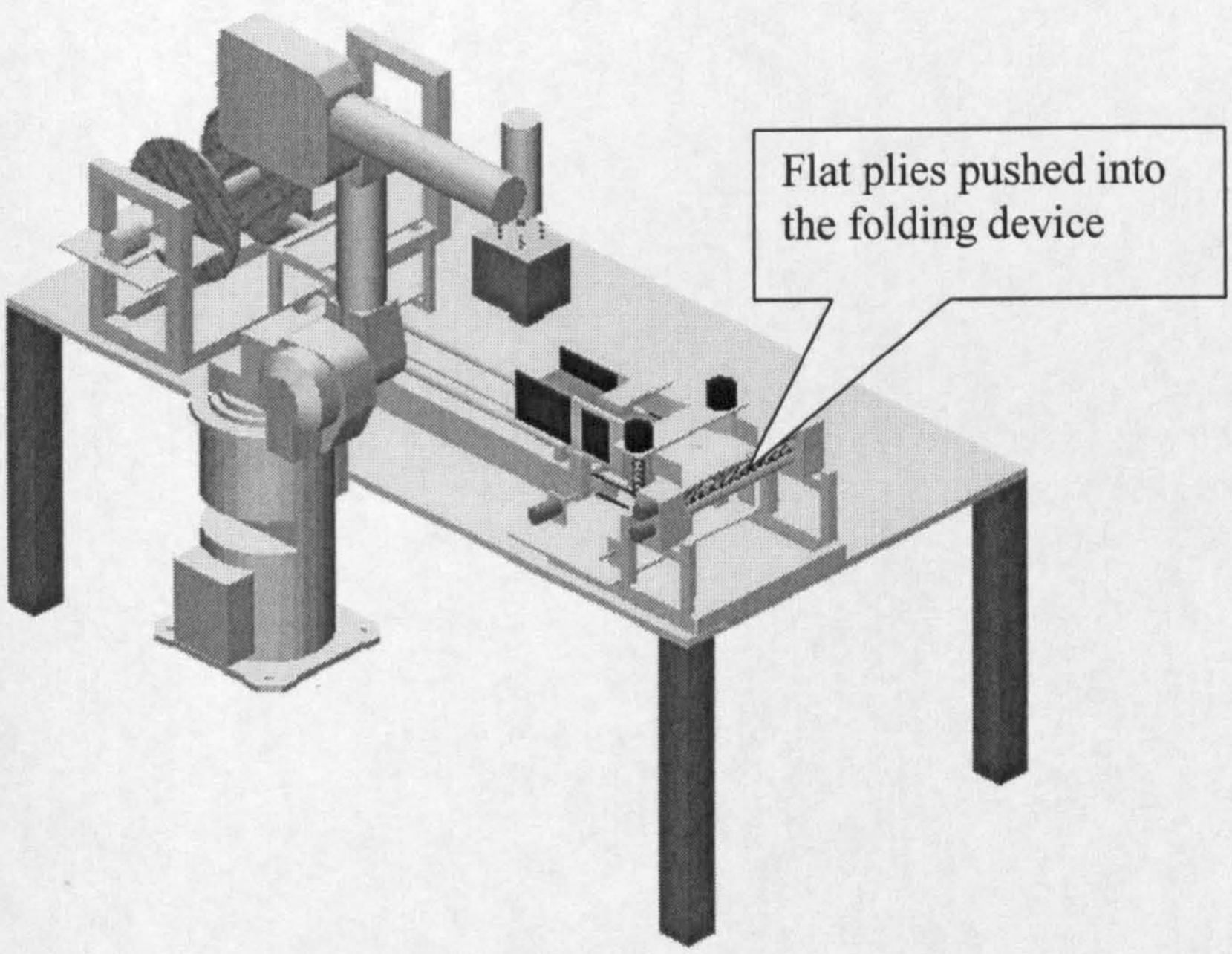

Figure 7.3 Description of the experimental procedure.

7.3 Uncertainty of measurements

Every measurement is subjected to some uncertainty. A measurement result is only complete if it is accompanied by a statement of the uncertainty in the measurement. Measurement uncertainty can come from the measuring instrument, from the item being measured, from the environment, from the operator, and from other sources. Such uncertainties can be estimated using statistical analysis of a set of measurement, and using other kinds of information about the measurement process. There are established rules (Appendix C) for calculating an overall estimate of uncertainty from these individual pieces of information. The use of good practice, such as traceable calibration, careful calculation, good record keeping, and checking, can reduce measurement uncertainties. When the uncertainty in a measurement is evaluated and stated, the fitness for purpose of the measurement can be properly judged.

7.3.1Sources of uncertainties

Many factors can undermine a measurement. Flaws in the measurement may be visible or invisible. Because real measurements are never made under perfect conditions, errors and uncertainties can come from:

- **The measuring instrument:** instruments can suffer from errors including bias, changes due to ageing, wear, or other kinds of drift, poor readability.
- **The item being measured:** This may not be stable.
- **The measurement process:** the measurement itself may be difficult to make.
- **Operator skill:** some measurements depend on the skill and judgement of the operator. One person may be better than another at the delicate work of setting up a measurement, or at reading fine detail by eye.
- **Imported uncertainties:** calibration of the instruments has an uncertainty which is then built into the uncertainty of the measurements was made.

7.3.2 Calculations of uncertainty

Bellow is a worked calculation of the uncertainty analysis of the tested samples. Following the rules of uncertainty of measurement (appendix C), the following steps have been conducted:

- Decide what calculations are needed to produce the final result.
- Carry out the measurements needed.
- Estimate the uncertainty of each input quantity that feeds into the final result.
- Calculate the result of your measurement (include any known corrections for things such as calibration).
- Find the combined standard uncertainty from all the individual aspects.
- Express the uncertainty in terms of a coverage factor, and state the level of confidence.

To help in the process of calculations, it was useful to summarise the uncertainty analysis in spreadsheet as in ,Table 7.1.

Table 7.1 calculation of uncertainty of measurement

source of uncertainty	value ±	Probability distribution	divisor	standard uncertainty
calibration uncertainty	0.02	Normal	2	0.01
resolution(size of division)	0.01	Rectangular	$\sqrt{3}$	0.005
sample not lying perfect straight	0.1	Rectangular	$\sqrt{3}$	0.05
standard uncertainty of mean of 10 readings	0.11	Normal	1	0.11
combined standard uncertainty		Assumed normal		0.13
expanded uncertainty		Assumed normal (k=2)		0.24

Table 7.1, shows the result of 10 repeated measurements of the tested samples. The result is corrected for the estimated effect of the string not lying completely straight when measured.

7.4 statistical analysis

Basic statistical descriptors of the data were obtained. This is in the form of mean, standard deviation, variance and standard error. Table 7.2 shows these statistical descriptors for each test parameter. It is important to note that for every test parameter, the measurement task was repeated 60 times. i.e. n=60.

It can be noticed from these data that the standard error is low for most parameters. Also very low standard deviation was achieved with respect to the mean throughout the measurement. Fore example for longitudinal deformation STD was 0.15.

Table 7.2 Statistical descriptors of testing parameters, n=60 for all samples.

Criteria	Statistical descriptors					
		min	max	mean	Std	Std error
deformation	Longitudinal	0.4	0.95	0.64	0.15	0.012
	Transverse	0.6	1.1	0.80	0.13	0.011
No. of stitch	3 stitches	0.96	1.85	1.37	0.24	0.03
	5 stitches	0.51	1.1	0.77	0.14	0.012
Deviation	Upper ply	0.7	1.7	1.09	0.30	0.032
	Lower ply	0.4	1.1	0.70	0.20	0.022
	Upper edges	0.52	1.28	0.81	0.22	0.023
	Lower edges	0.26	0.72	0.44	0.13	0.013

7.4.1 Longitudinal and transverse deformation

Figure 7.4 (a,b), show histogram representations of both longitudinal and transverse deformations at n= 60. It can be noticed that for longitudinal deformation most of measurement fall into range between 0.5-0.75 i.e. very close to the mean value, whereas for transverse deformation, the range was slightly higher between 0.7-0.9. Also the minimum and the maximum values for both differ as shown in table 7.2. This difference is due to the absence of the fibre at 90^0 that leads to higher transverse deformation in comparison with the presence of fibre at 0^0 in the case of longitudinal deformation.

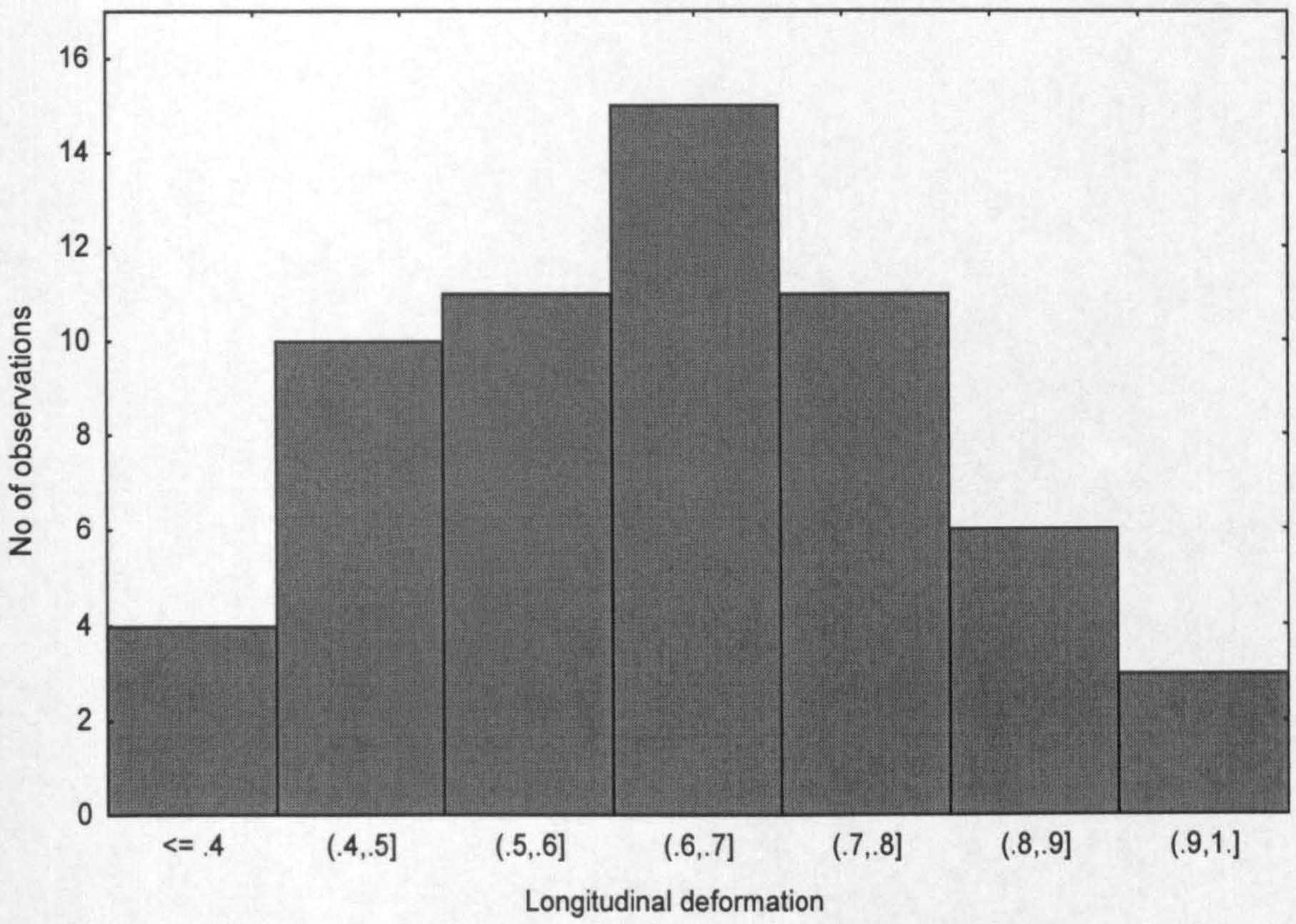

Figure 7.4a Histogram of longitudinal deformation

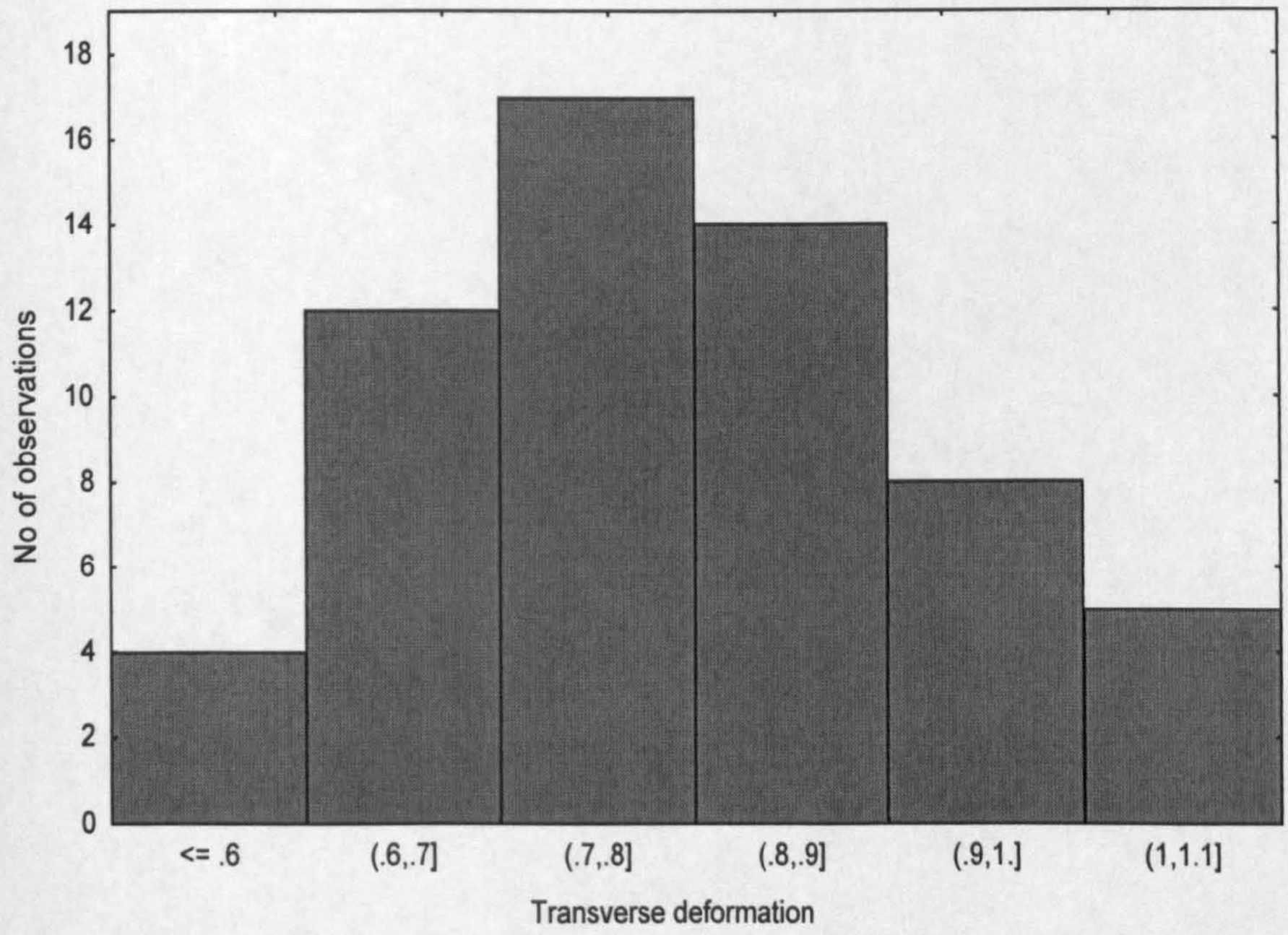

Figure 7.4b Histogram of transverse deformation

Normality testing

The previous histogram representations suggest that the data appears to be normally distributed.

In order to verify this assumption, normality tasks were conducted as follow

Histogram with normal fitting

Figure 7.5a, below shows histogram of the longitudinal deformation as shown in ,Figure 7.4a, with normal fitting curve. It appears that most of the values fall within the normal fitted curve. Similarly with the transverse deformation data as shown in ,Figure 7.5 b.

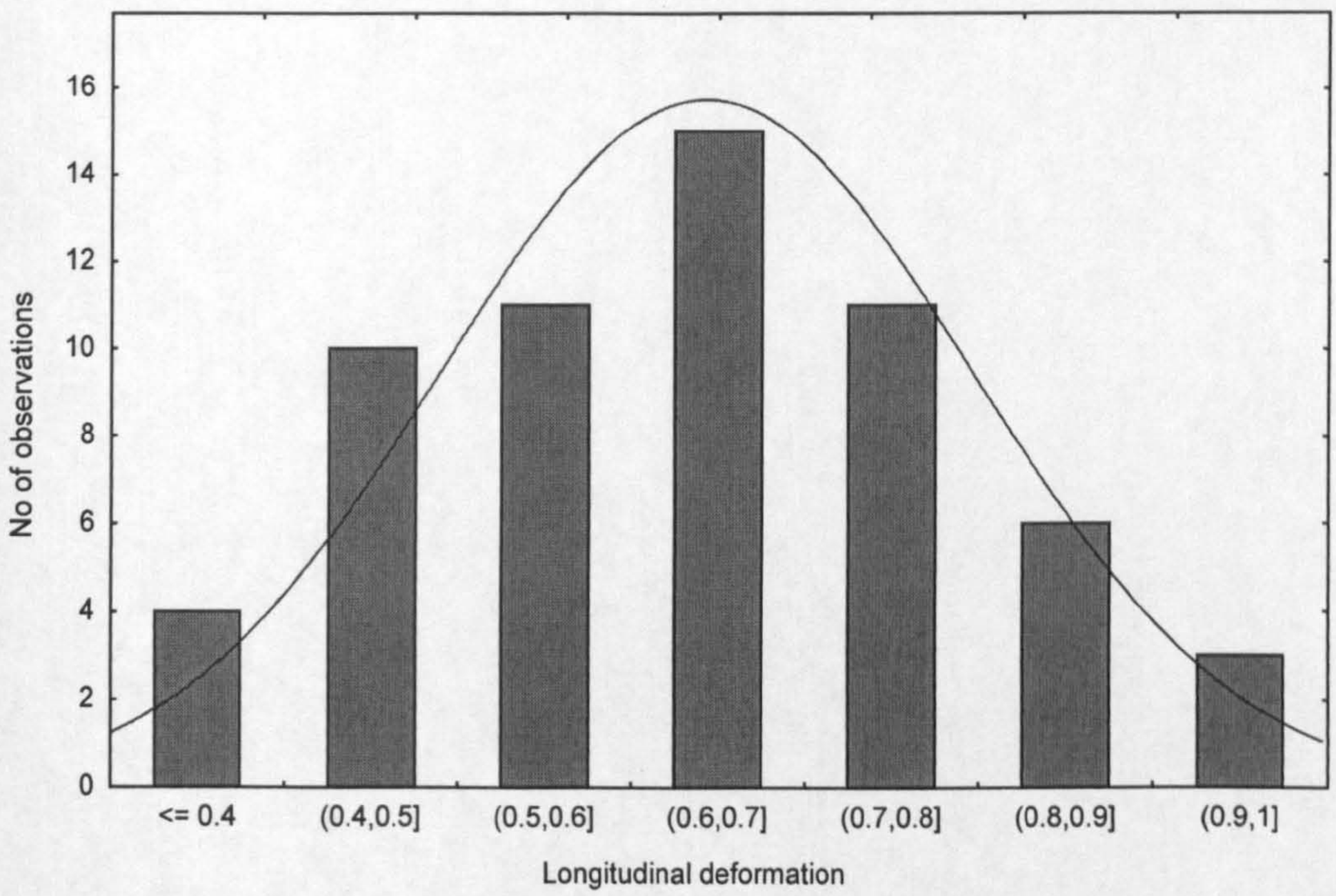

Figure 7.5a Normal fitting to histogram of longitudinal deformation data

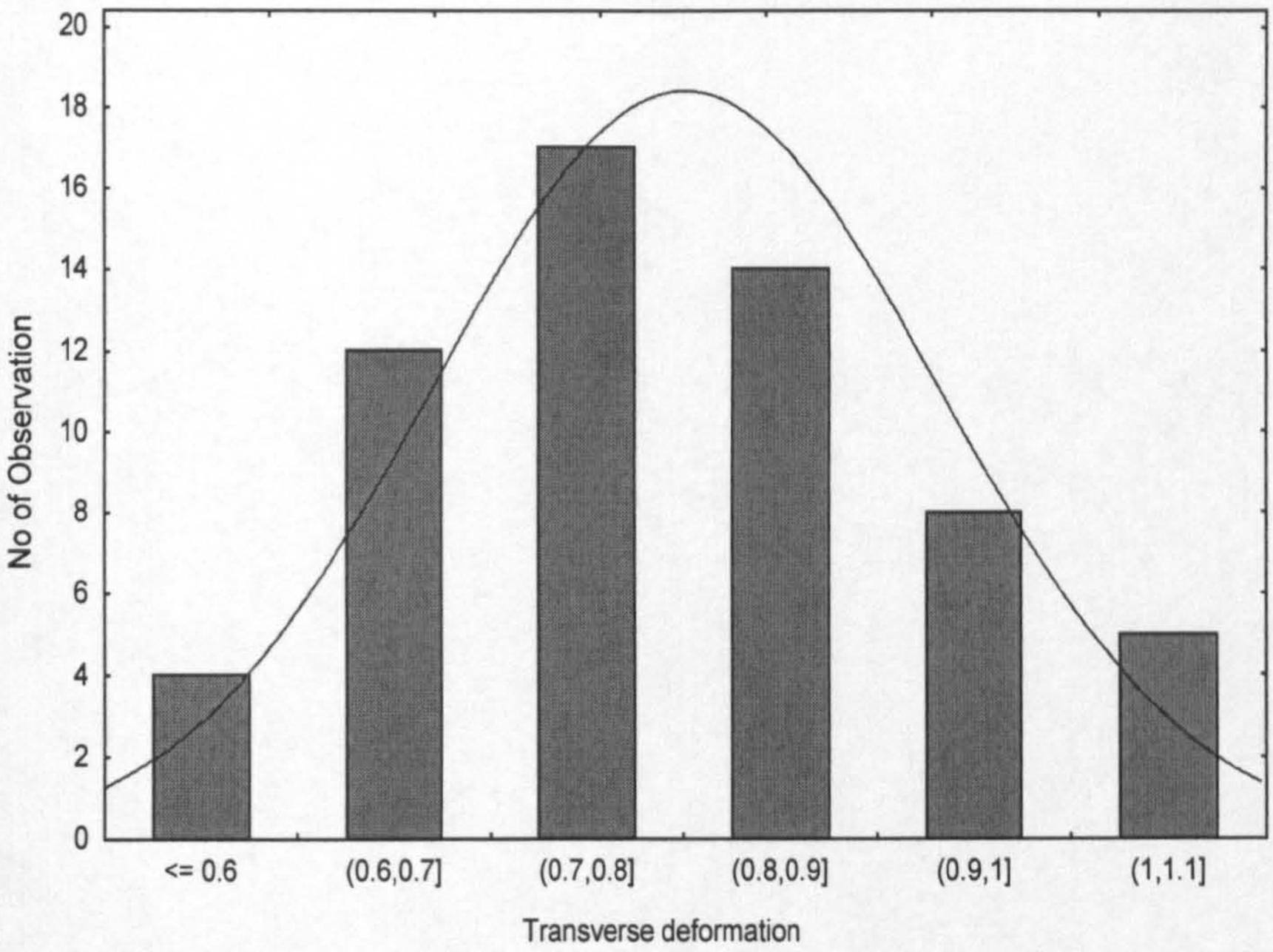

Figure 7.5b Normal fitting to histogram of transverse deformation data

Probability plot

This type of graph is used to evaluate the normality of a variable, that is, whether, and to what extent, the distribution of variable follows the normal distribution. The selected variable will be plotted in a scatter plot against the values "expected from the normal distribution" the standard normal probability plot is constructed as follows. First, the deviations from the mean (residual) are rank ordered. From these ranks the program computes z values (i.e. standardised values of the normal distribution) based on the assumption that the data come from a normal distribution. These z values are plotted on the y-axis in the plot. If the observed residuals (plotted on the x-axis) are normally distributed, then all values should fall onto a straight line. If the residual are not normally distributed, then they will be deviated from the line to form a clear pattern (e.g. an S shape) around the line.

Figure 7.6a, shows illustration of normal probability plot as described for the longitudinal deformation data. As it can be seen almost all the point fall on, or close to, the expected normal curve line. Only few points deviate from the

straight line. This support the hypothesis that the experimental data is normally distributed.

Similarly, Figure 7.6b, illustrates the plot between the expected normal against the observed transverse deformation data. However, most of the points are fall on, or close to, the expected normal curve line with a small number of point scattered around the straight line. This scattering is due to reasons explained earlier.

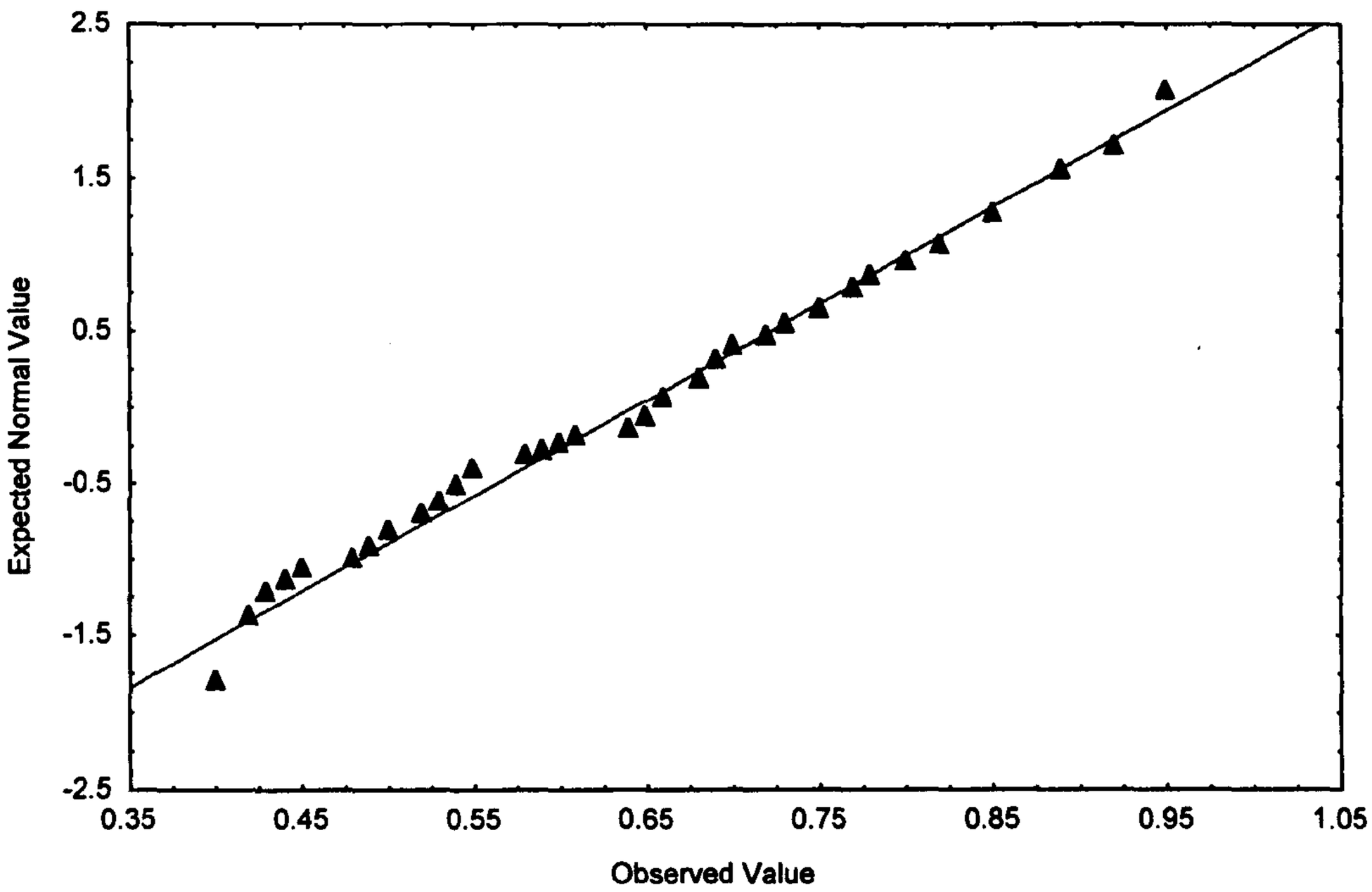

Figure 7.6a Expected normal value against observed longitudinal deformation

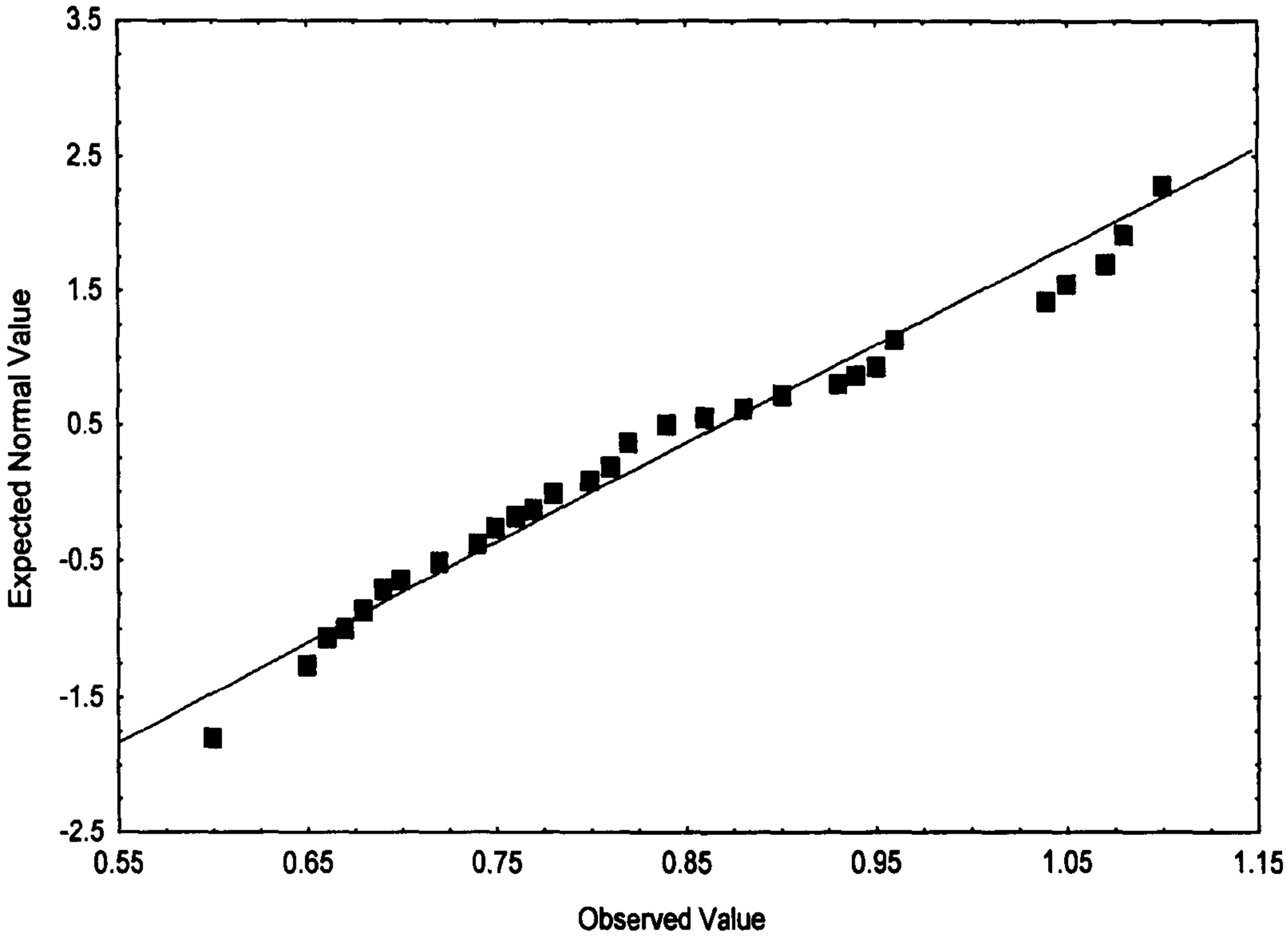

Figure 7.6b Expected normal value against observed transverse deformation

7.4.2 Number of stitches

Figure 7.7(a,b), show histogram representation of the effect of different number of stitches on the behaviour of the reinforcement structure. These show that the data from 3 stitches are concentrated in the range of 1-1.4mm whereas in the case of 5 stitches the data are concentrated in the range between 0.6-0.8mm. This histogram representation also suggests that both data are normally distributed. As the number of stitches increase, it was noticed that the deviation between the middle plies and the vertical plies decreased drastically. Further increase to the number of stitches to 7 was also done but a minimal decrease in the deviation was achieved. It was concluded that increasing the number of stitches to five would be an ideal number that can be applied to achieve the minimum distortion of the plies. Data from 7 stitches were not reported here due to insignificant practical usage. Figure 7.8 (a,b), represent histogram plot with fitting curve which appeared to be normal in both cases. However normality testing of the data was also carried out as outlined earlier and represented in ,Figure 7.9 (a, b). Both curves show

a reasonable matching between the expected normal data against the observed values. Small amount of scattering were observed in the case of 3 stitches due to the effect explained earlier.

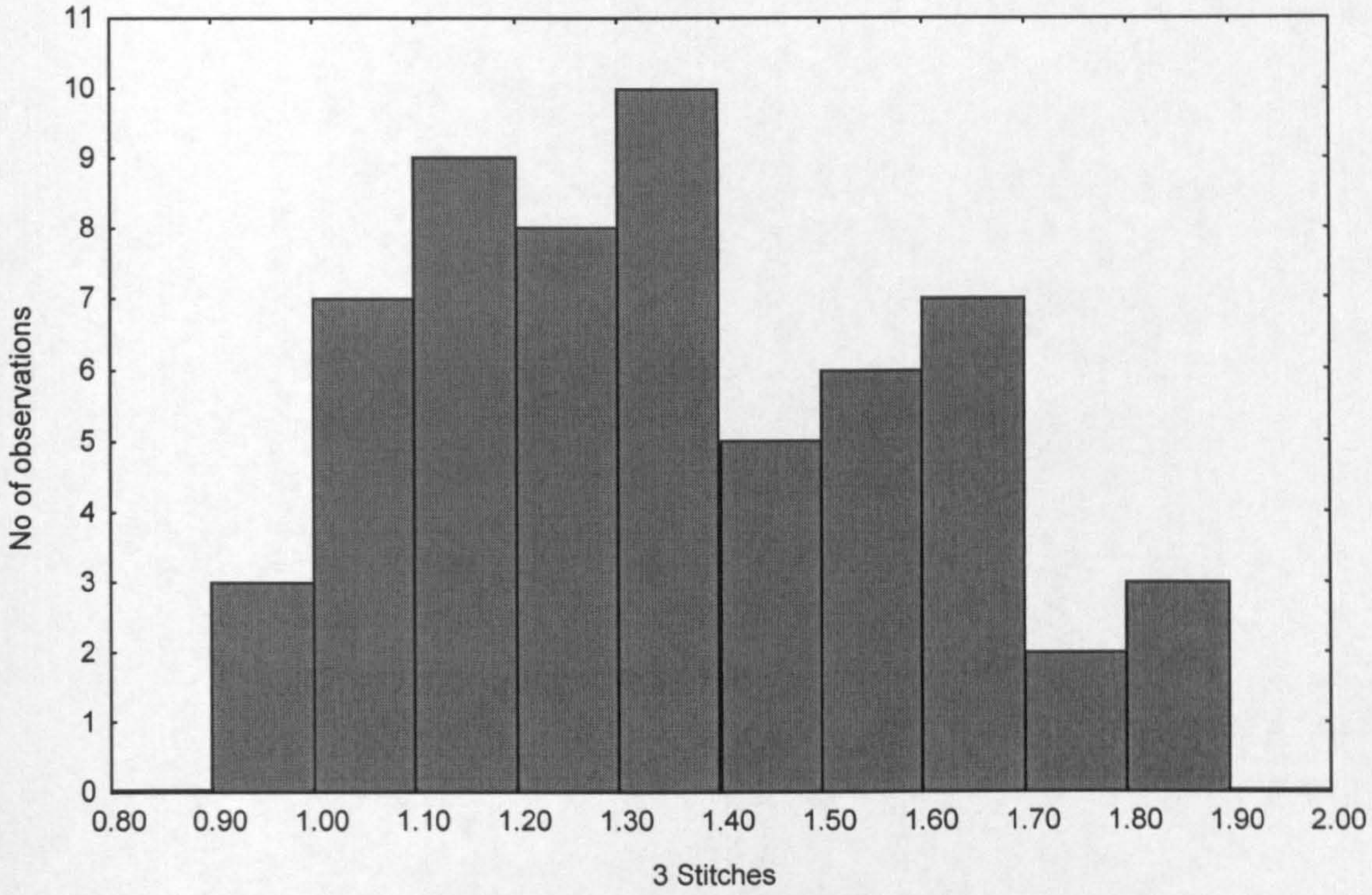

Figure 7.7a Histogram of 3 stitches deviation

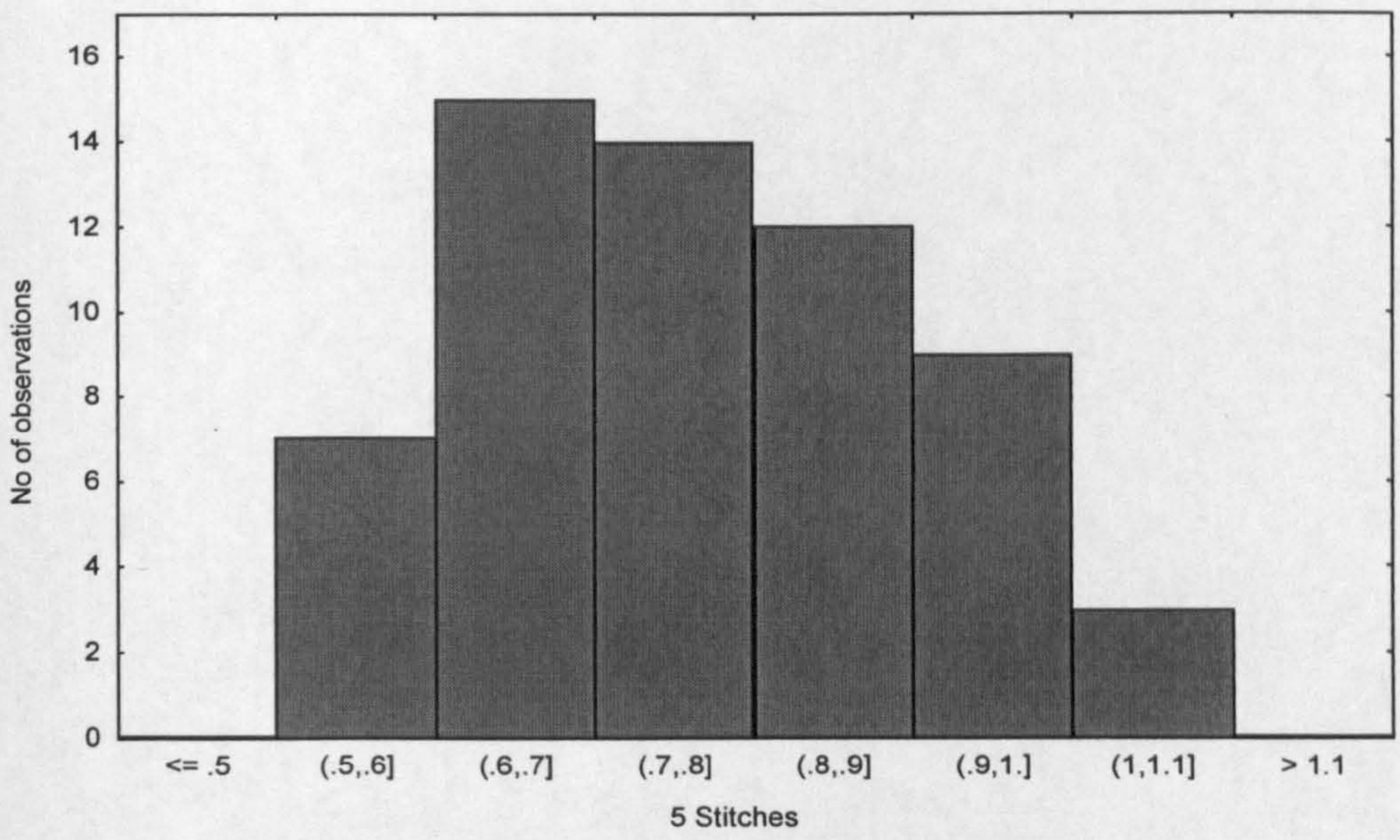

Figure 7.7b Histogram of 5 stitches deviation

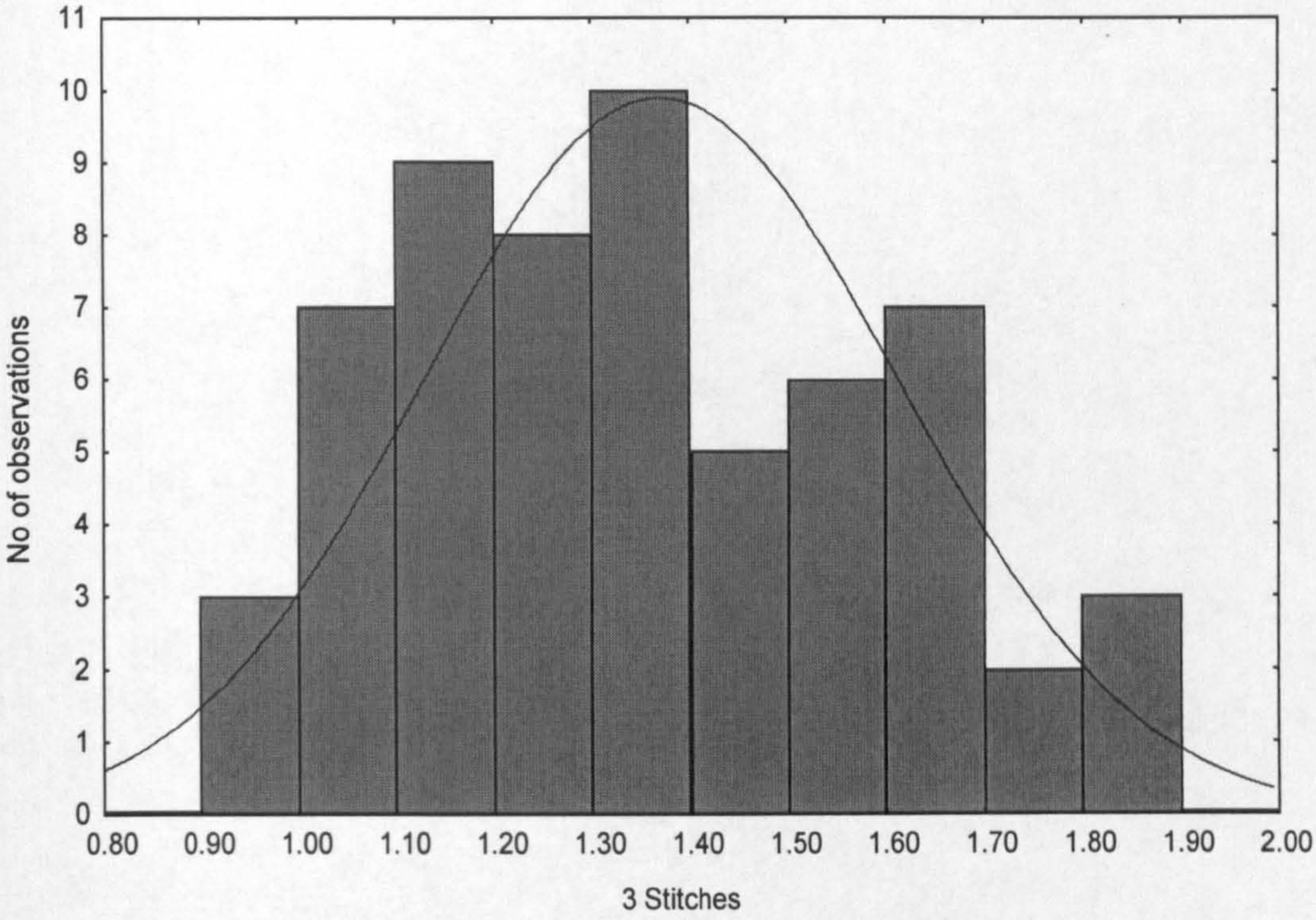

Figure 7.8a Histogram of 3 stitches deviation with normal fitting curve

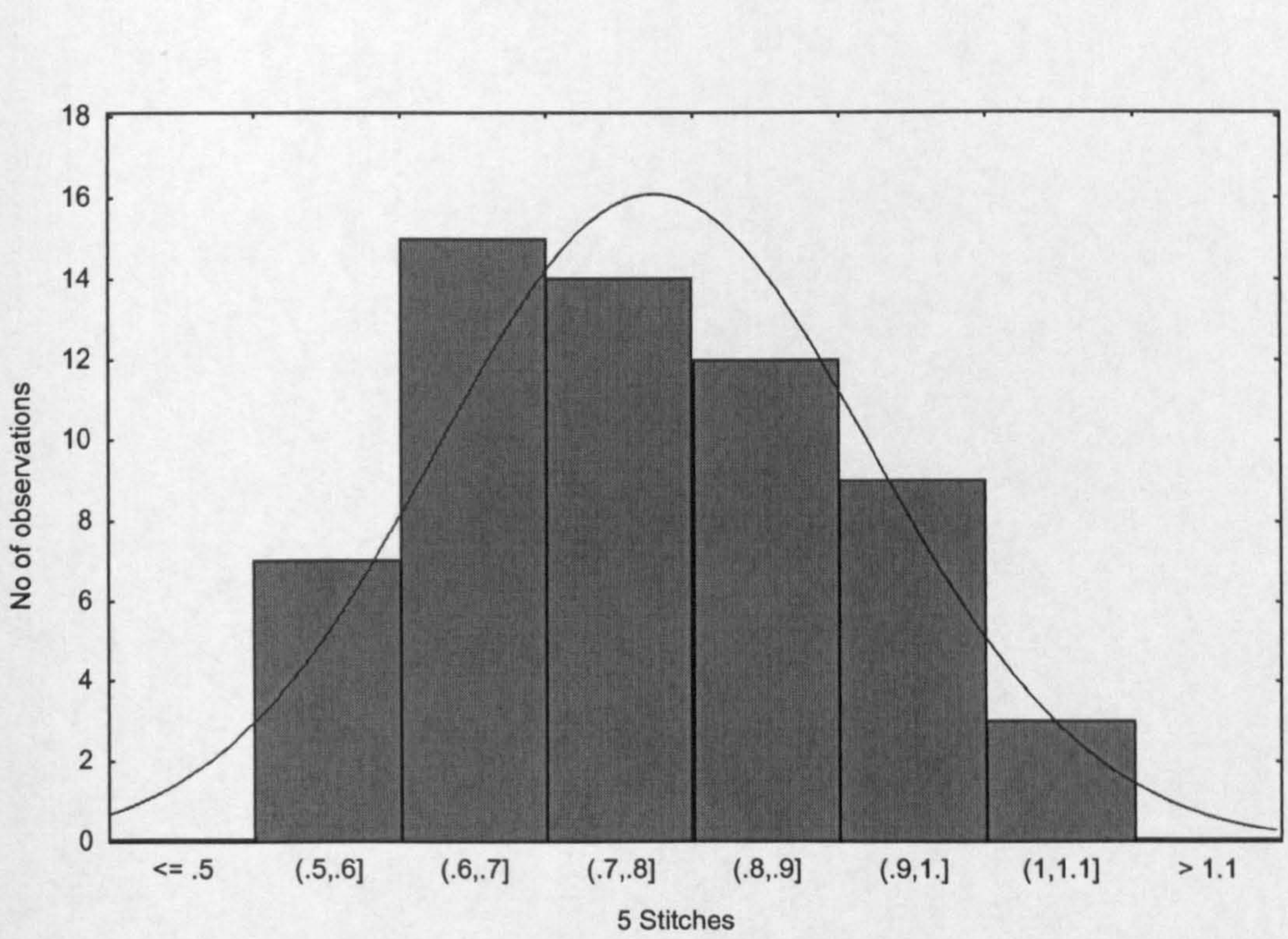

Figure 7.8b Histogram of 5 stitches deviation with normal fitting curve

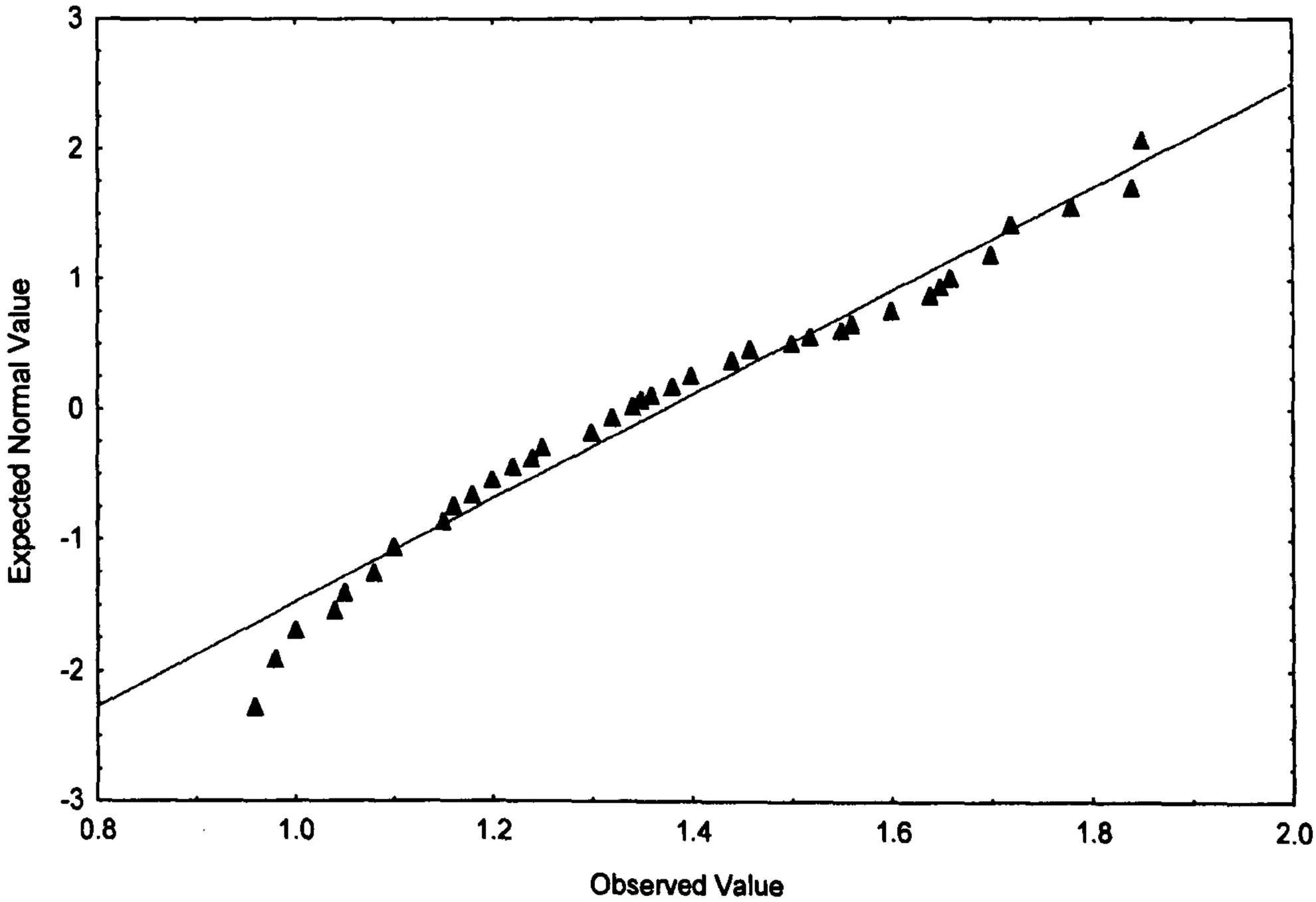

Figure 7.9a Expected normal value against observed 3 stitches

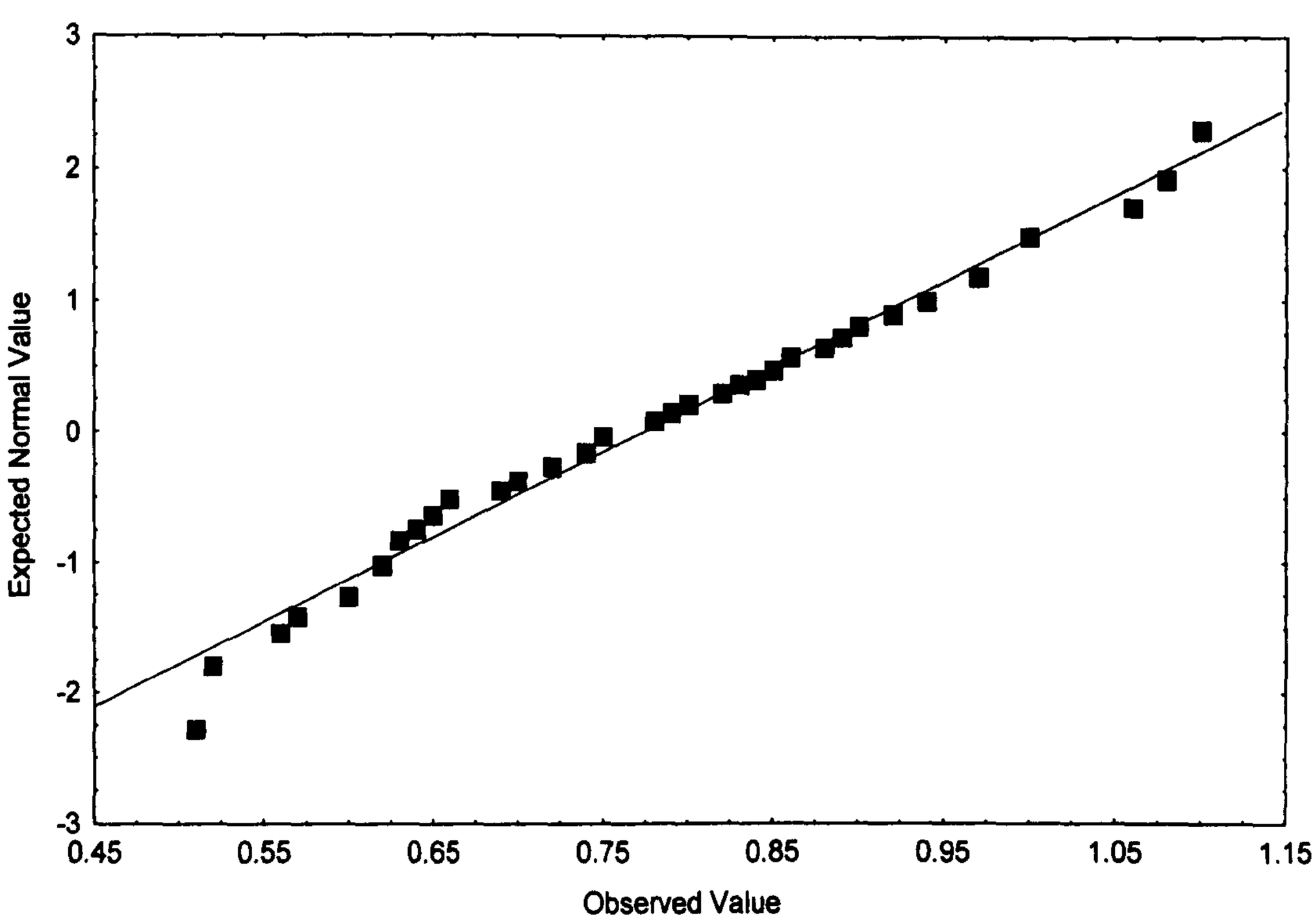

Figure 7.9b Expected normal value against observed 5 stitches

7.4.3 Ply deviation

Histogram representations of the data from both upper and lower ply deviations are shown in Figure 7.10 (a,b). It appears that the data from lower plies is more likely to be normally distributed. However, Figure 7.11 (a,b) illustrate normal curve fitting for both cases with the lower plies deviation shown to be more normally distributed than the upper plies deviation. This may be due to the nature of ply forming, as it is much easier for the material to fold downward rather than upward folding since the latter goes up against the fibre weight. Therefore the downward movement is most likely to be the cause of slighter deformation. When the data was fitted to normal distribution curves, it appears that most of the lower plies observations fell into the straight line of the expected normal against the observed value as shown in Figure 7.12a. In comparison with the upper plies observations which is also normally distributed, however there is small amount of scattering around the expected normal line, see Figure 7.12b.

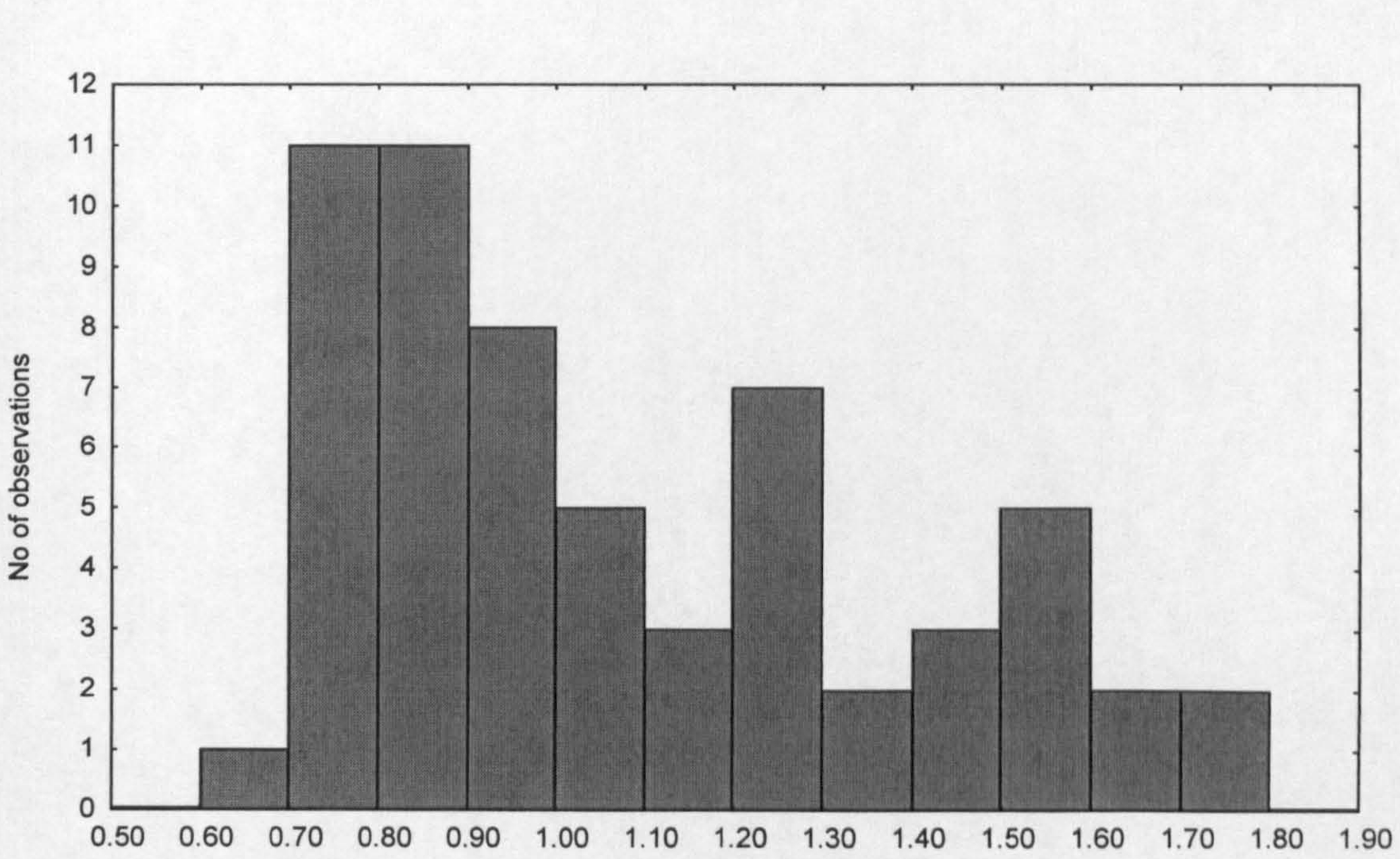

Figure 7.10a Histogram of upper plies deviation

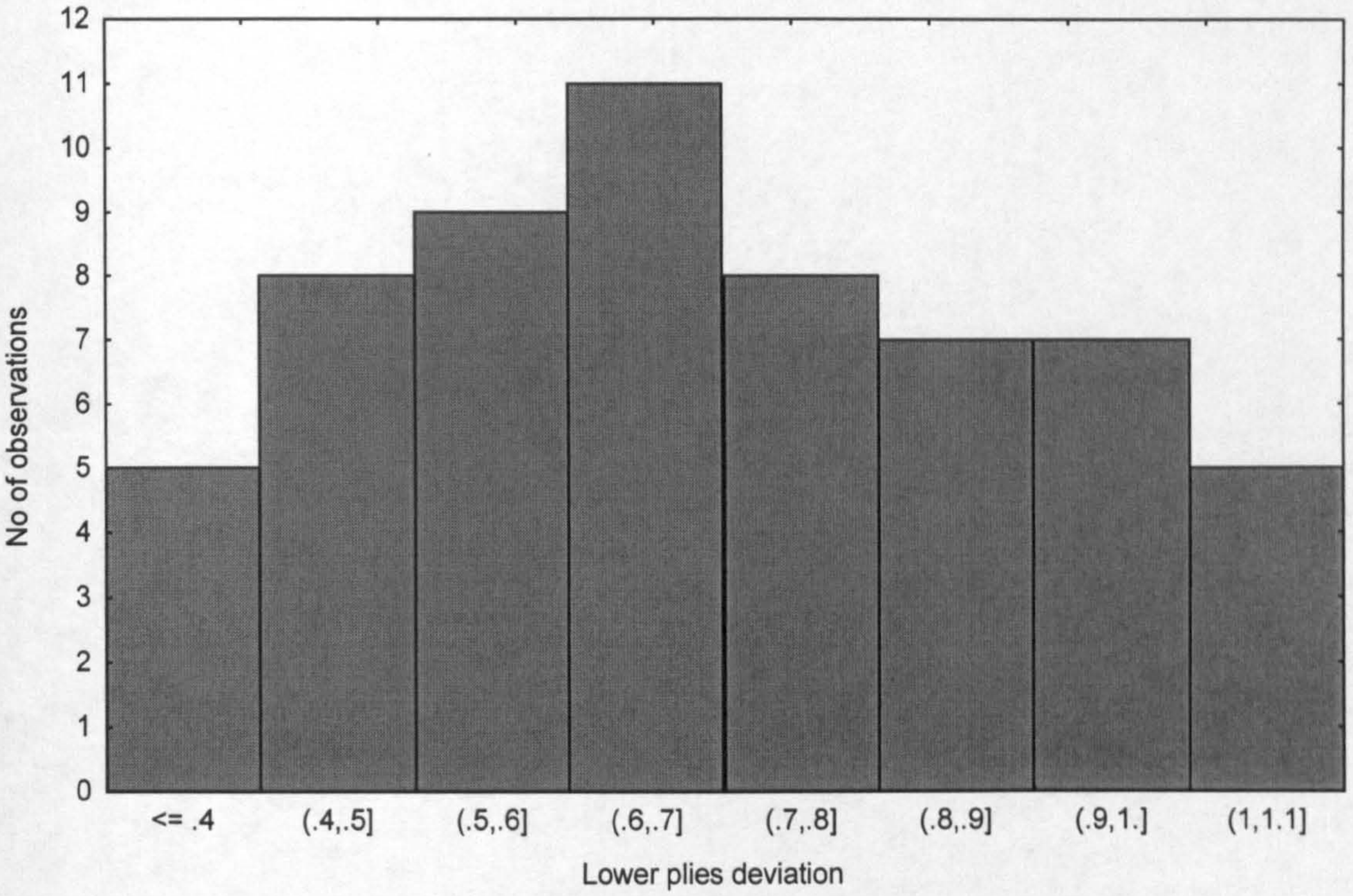

Figure 7.10b Histogram of lower plies deviation

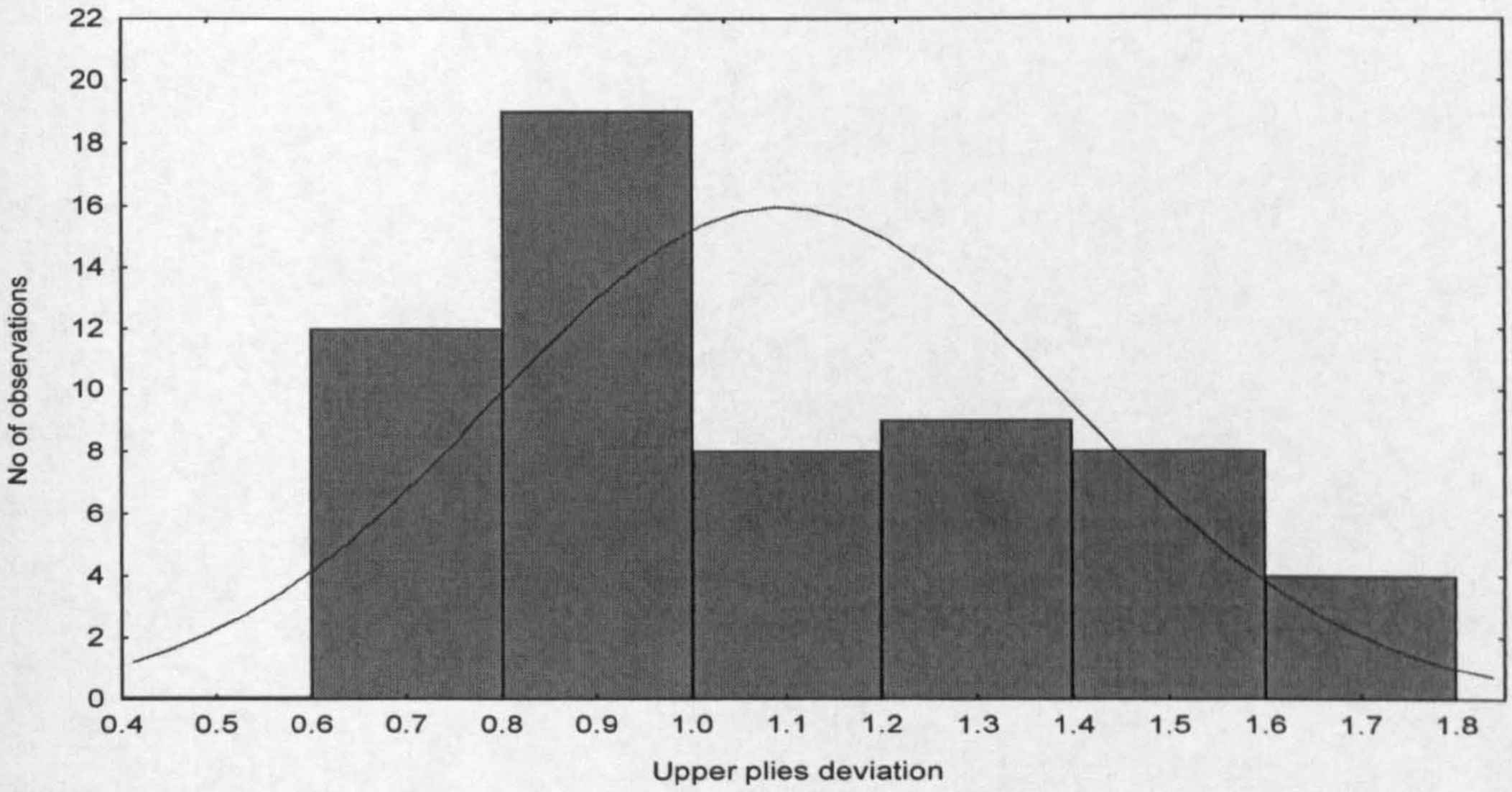

Figure 7.11a: Histogram of upper plies deviation with normal fitting curve

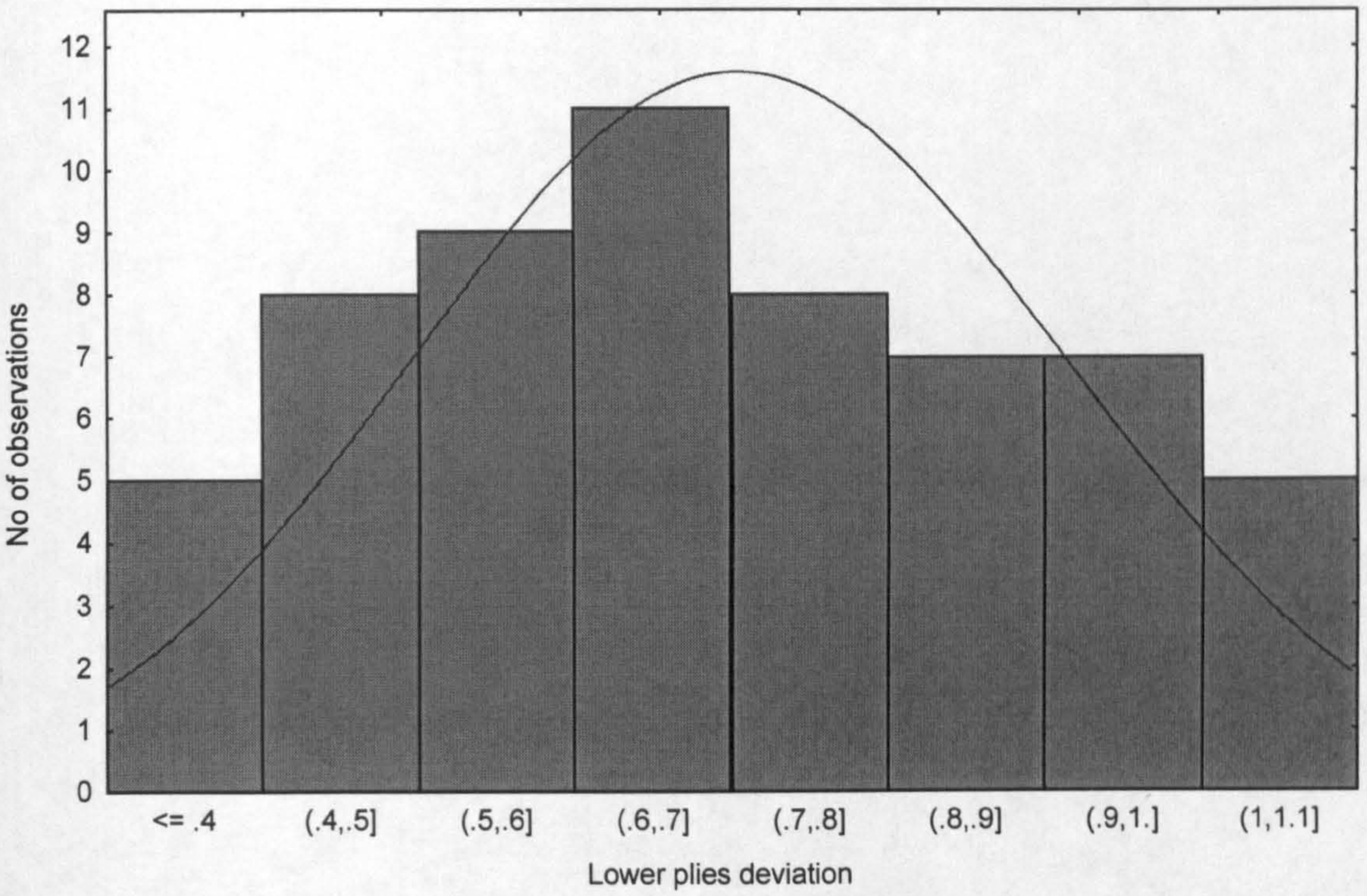

Figure 7.11b Histogram of lower plies deviation with normal fitting curve

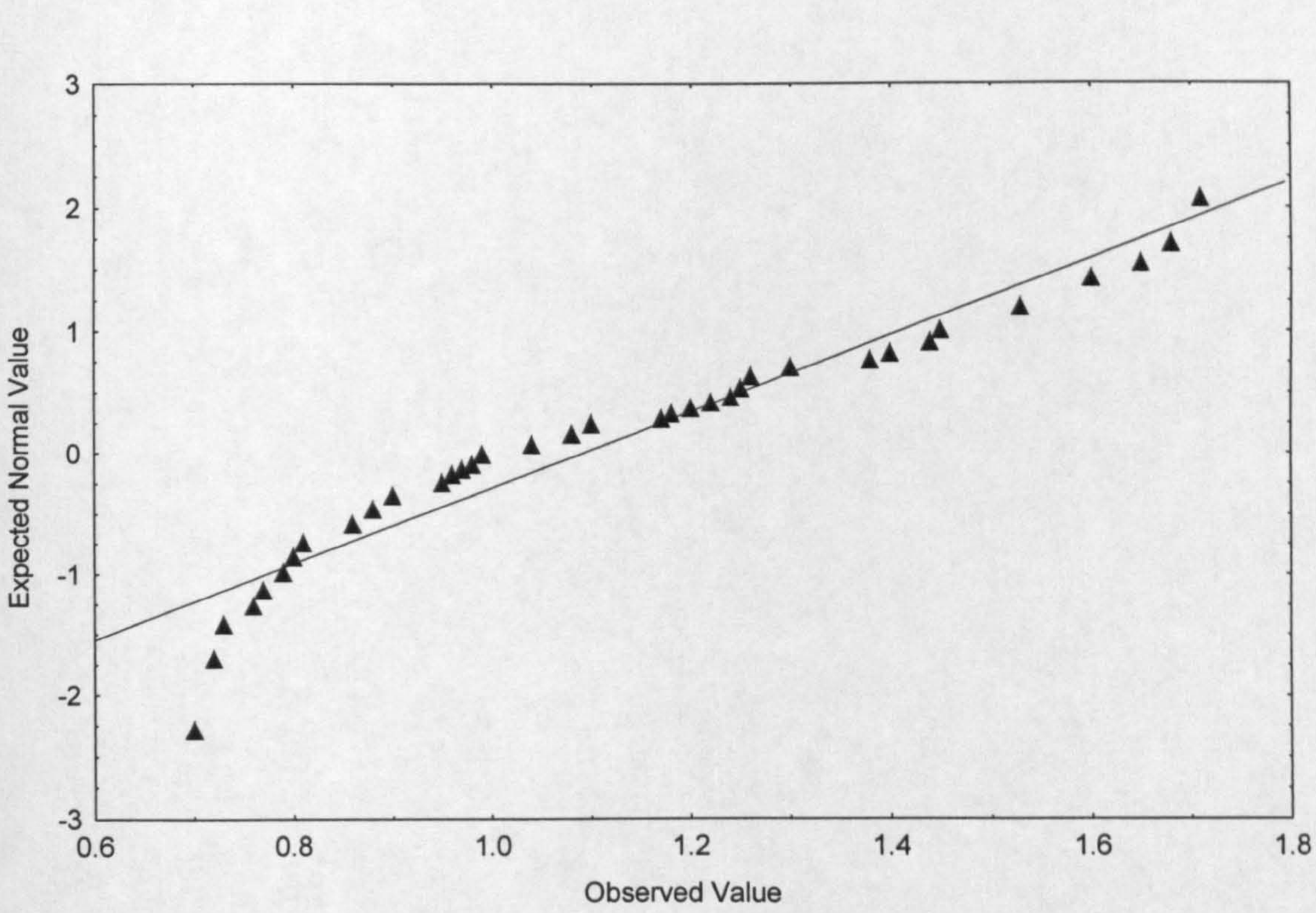

Figure 7.12a Expected normal value against observed upper plies deviation

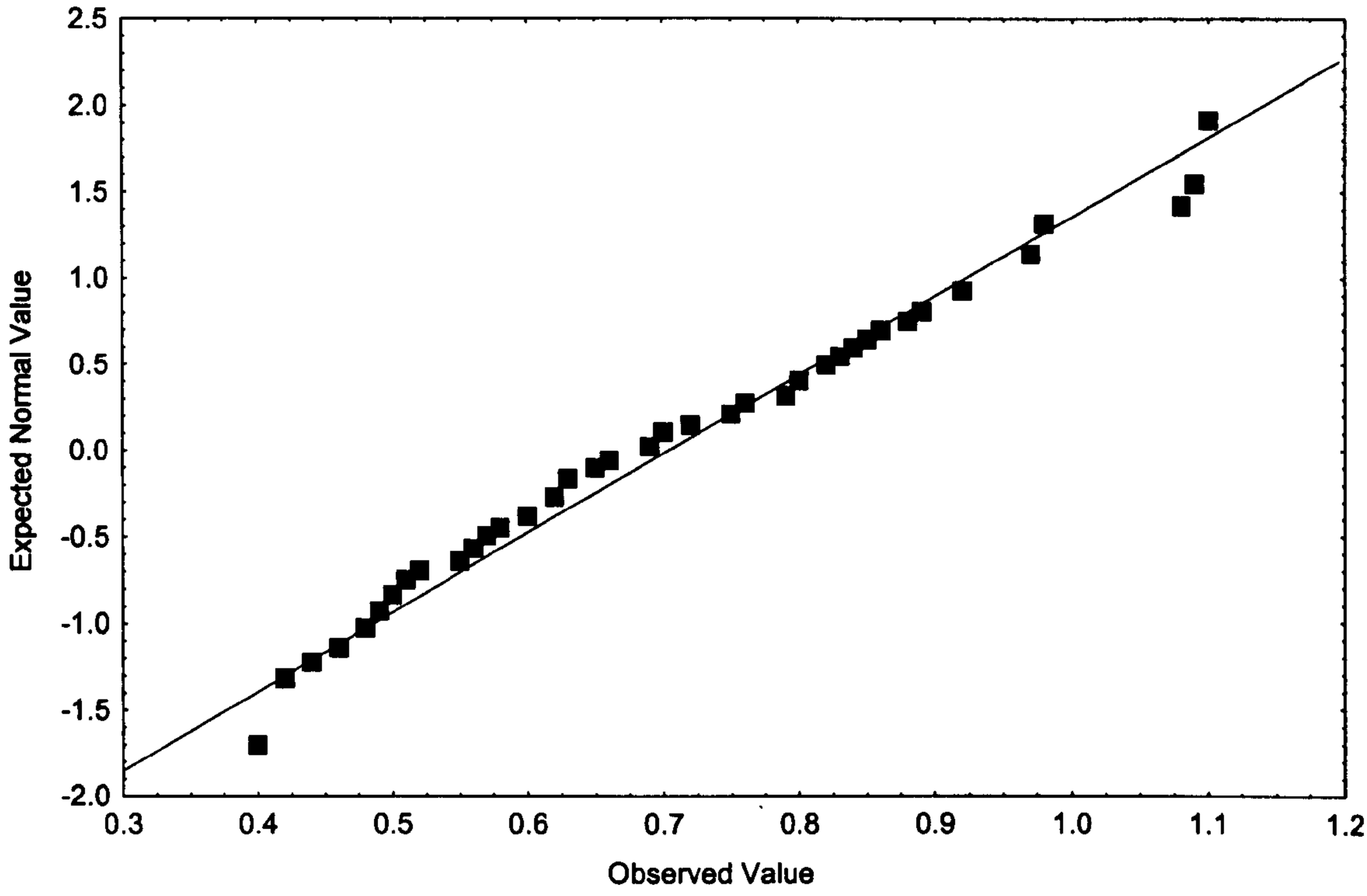

Figure 7.12b Expected normal value against observed lower plies deviation

7.4.4 Edge deviation

Figures 7.13 (a,b) and 7.14 (a,b) show Histogram and normal curve fitting representations of the data from both upper and lower edges deviation. It can be seen that the data from lower and upper edges are more likely to be normally distributed. However with the upper edges, there is a slight deviation and scattering from the normal line, as illustrated in Figure 7.15 (a,b). This may be due to the friction between the upper and lower formed plies. However, the upper ply movements, it is against the gravity. Thus causing disturbances between the plies which may lead to edge variation. In the case of the lower ply, this effect was not as high as the upper edge. This was evident as it can be seen from Figure 7.15 (a,b) where most of the points in the case of lower edge fall on the straight line. Whereas in the case of upper edge small variation and scattering has been seen.

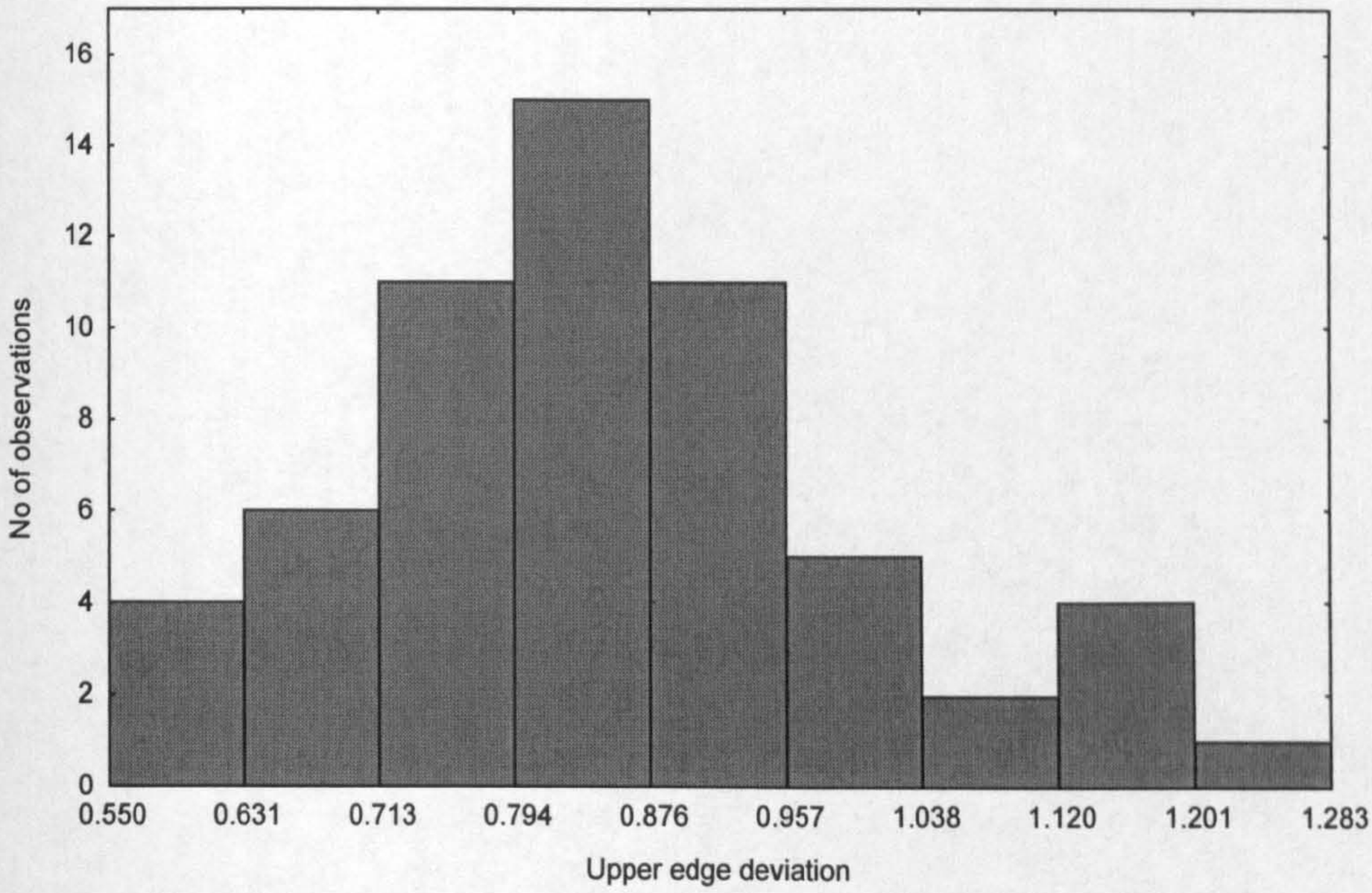

Figure 7.13a Histogram of upper edge deviation

Figure 7.13b Histogram of lower edge deviation

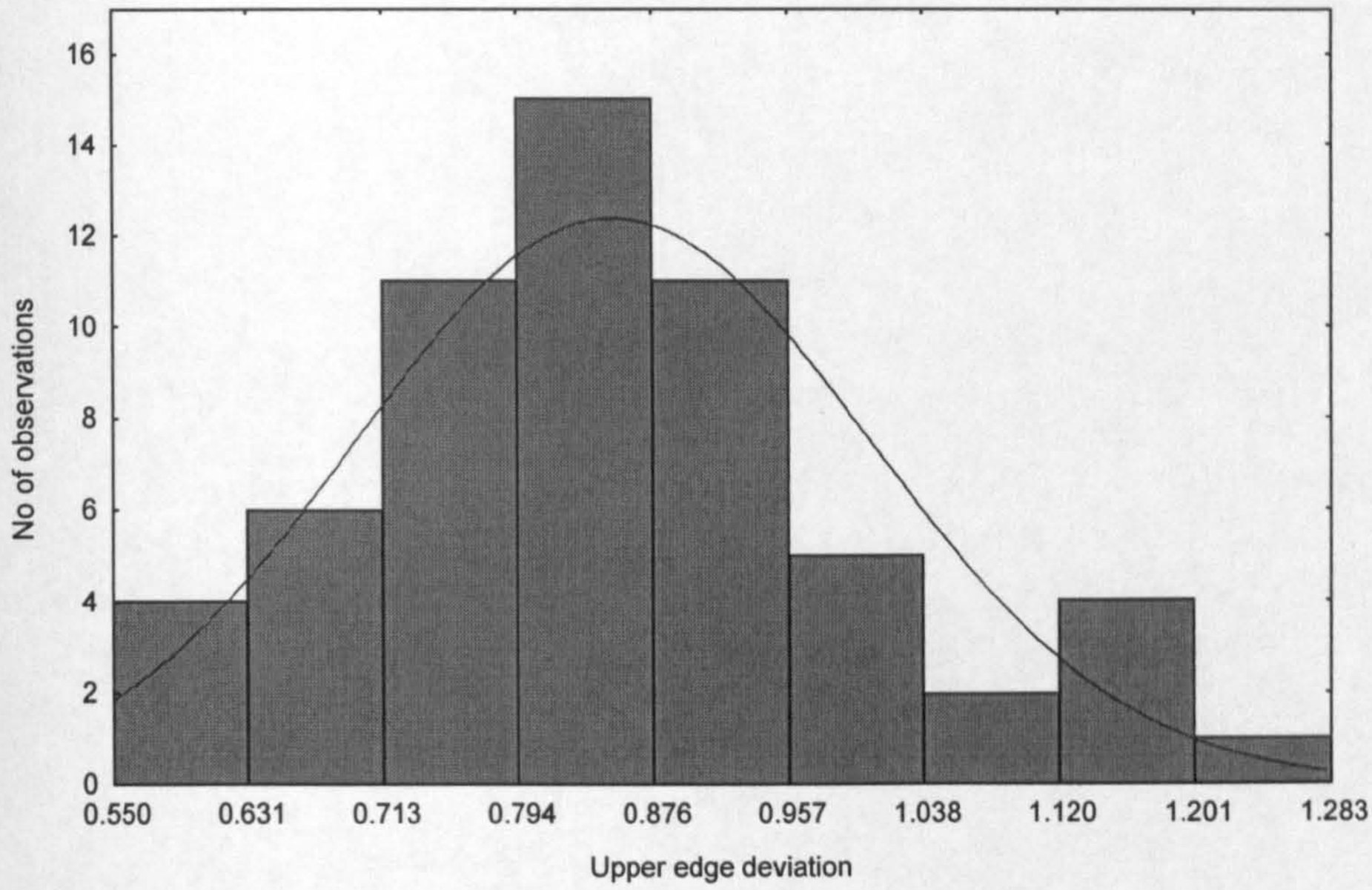

Figure 7.14a Histogram of upper edges deviation with normal fitting curve

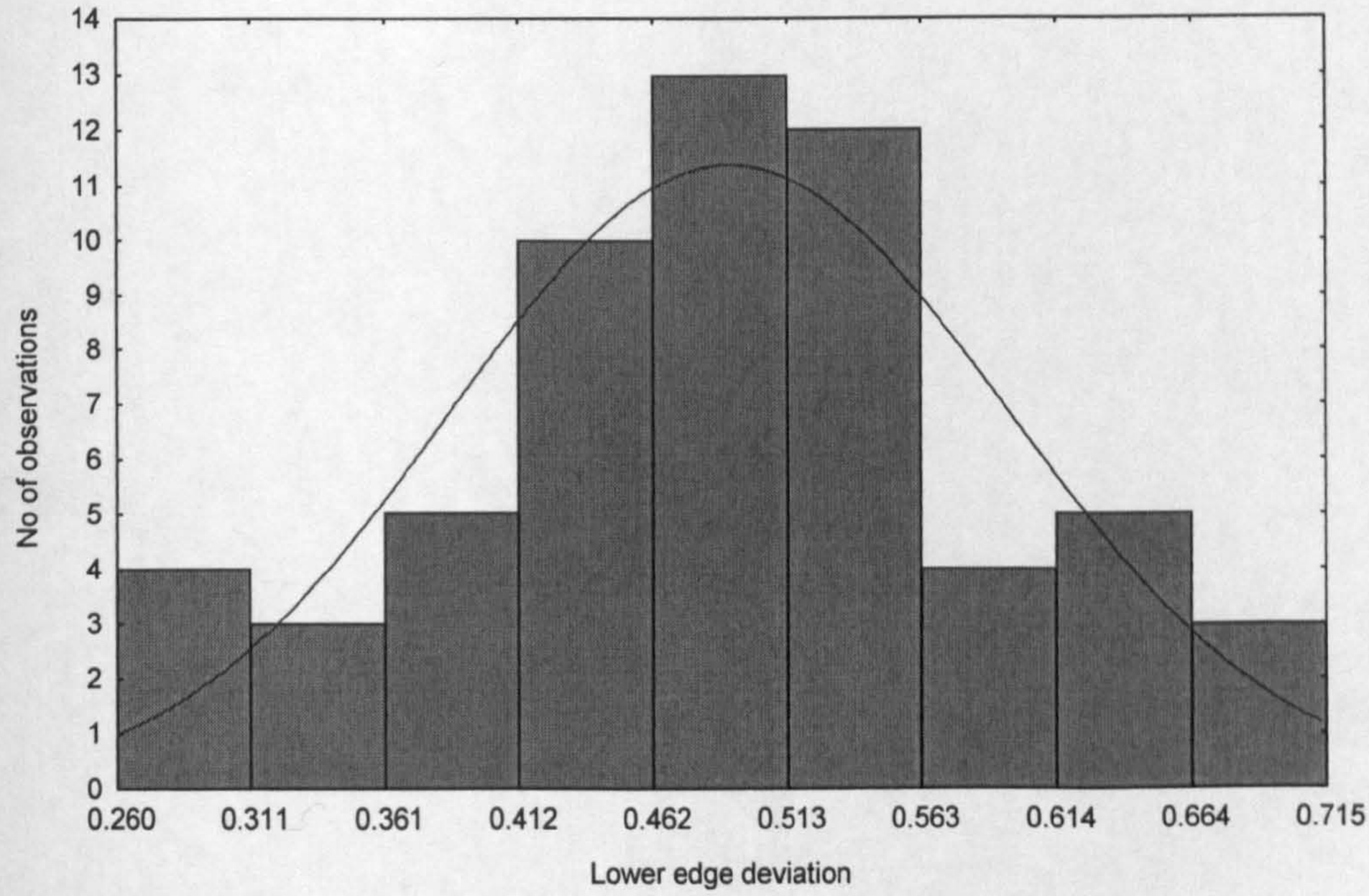

Figure 7.14b Histogram of lower edges deviation with normal fitting curve

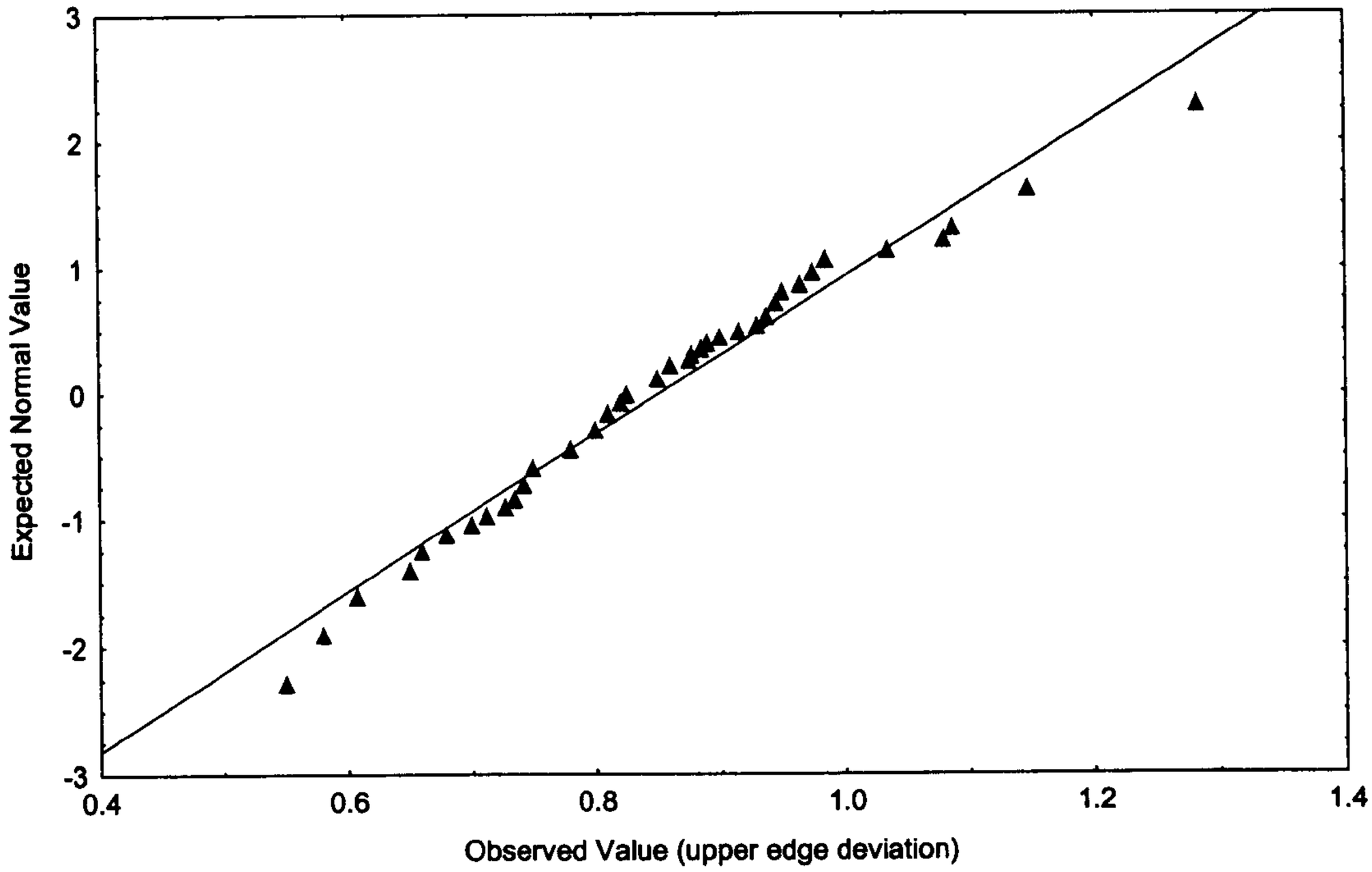

Figure 7.15a Expected normal value against observed upper edges deviation

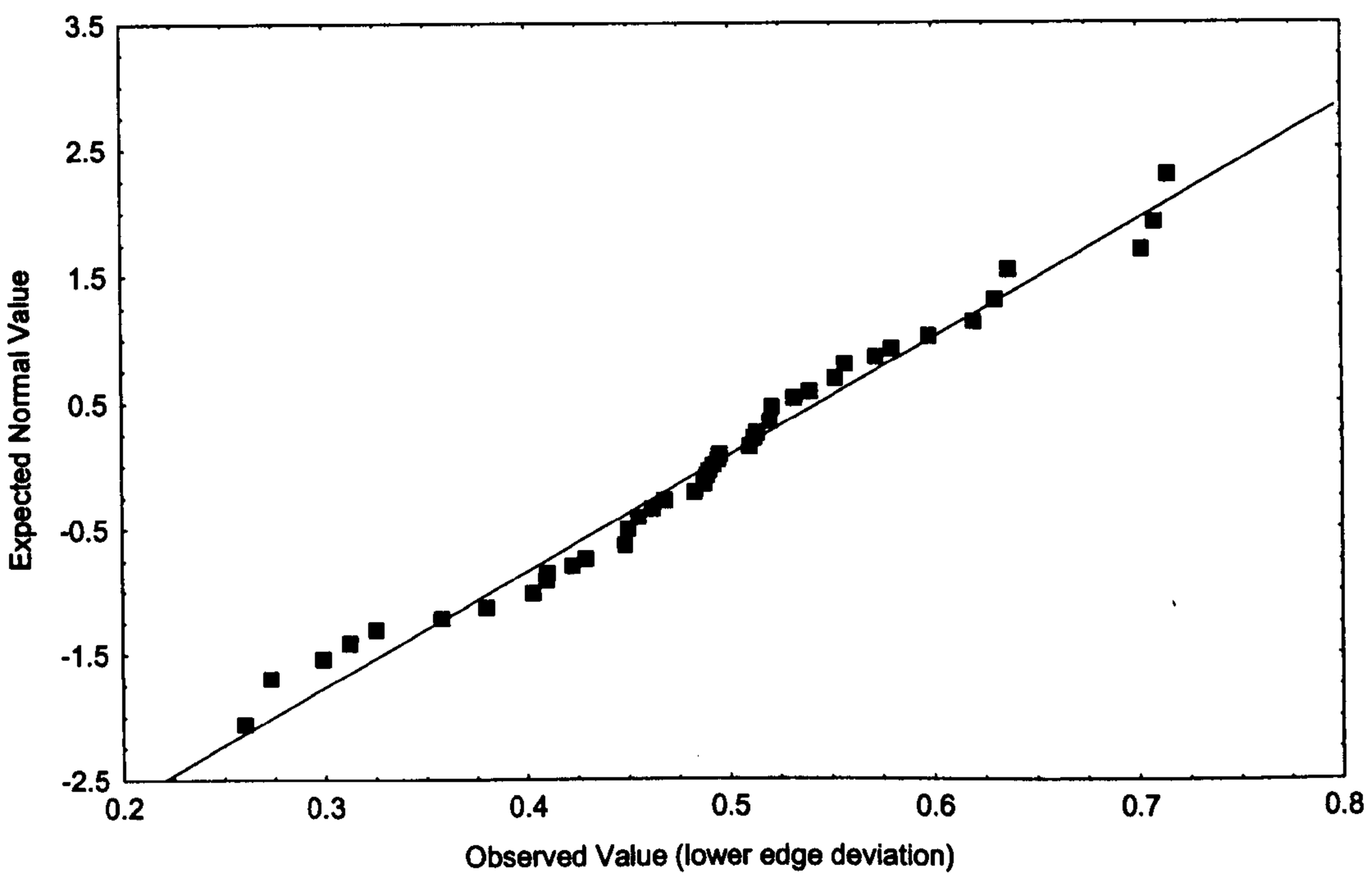

Figure 7.15b Expected normal value against observed lower edges deviation

7.5 Conclusion

The performance of the manufacturing cell has been tested for the different types of deformation, the effect of number of stitches and plies and edges deviation. Each of these tests was considered and examined carefully in order to assess the overall cell performance for its repeatability and consistency. Uncertainty task were undertaken to qualify the measurement for further statistical analysis and interpretations. It was concluded from the statistical analyses that the cell performance is very repeatable and consistent. These analyses also showed that the tested parameters followed normal distributions. This enable an operator to predict the cell performance based on the simple statistical parameters such as mean and standard deviation.

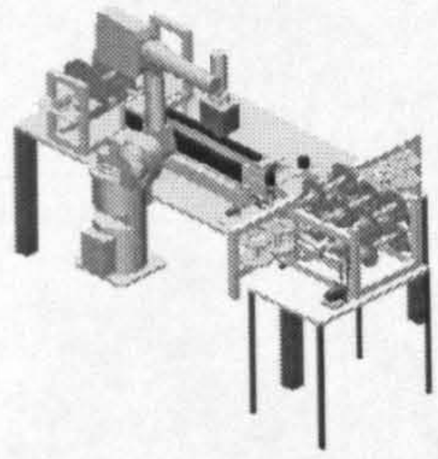

Chapter 8 Effect of stitches on the behaviour of the reinforcement structures

8.1 Introduction

A set of mechanical experiments were conducted to:

- Develop generic numerical models for predicting the behaviour of the reinforcement structures.
- Characterise the mechanical behaviour and damage tolerance of such structural component
- Study the effect of the stitches that were made during assembly on the behaviour of the whole structure.

In order to conduct a proper experimental program, prototype reinforcement structures are needed. There were, however, difficulties in producing such consolidated structures. There were the lack of proper consolidation facilities and the high cost of outsoaring the project. Instead, simpler flat specimens have been prepared to conduct a set of experiments for determining the structural characteristics of the stitched and non stitched specimens. These specimens were cut from the reinforcement structures that were formed and stitched by the fully automated cell. Compression and tension tests were conducted on the flat specimens to measure the material's mechanical properties such as stiffness and strength needed for developing the analytical models that were used for the investigation.

With the advent of high–speed computers the emphasis in engineering analysis has moved towards more versatile numerical methods. One of these is the finite element method. This approach has a distinct advantage in treating problems involving geometrically complicated systems. Furthermore,

this procedure allows the analysis of the overall behaviour of the whole structure or any local part of it. In research and development, the finite element method can be used for the prediction of the structural behaviour and for the analysis of the experimental results. This approach was judged most appropriate for the present study and was therefore adopted.

The main objective of this chapter is to explain in some details the analytical procedure employed to study the effect of the stitches, which were performed to hold the plies of the structure together, on the overall behaviour of the structure.

8.2 Test specimens and experimental program

The construction of the non crimp fabric (NCF) specimens investigated in this work is shown in ,Figure 8.1. NCF laminates were produced with an untwisted fibre bundle in a triaxial lay-up, by Hexel Company, namely Hand A and B. the lay-up, which is knitted together by a polyester yarn, has a distribution of areal weight as follows: [$\mp 45^0$ (230 g/sm) 0^0 (390 g/sm)].

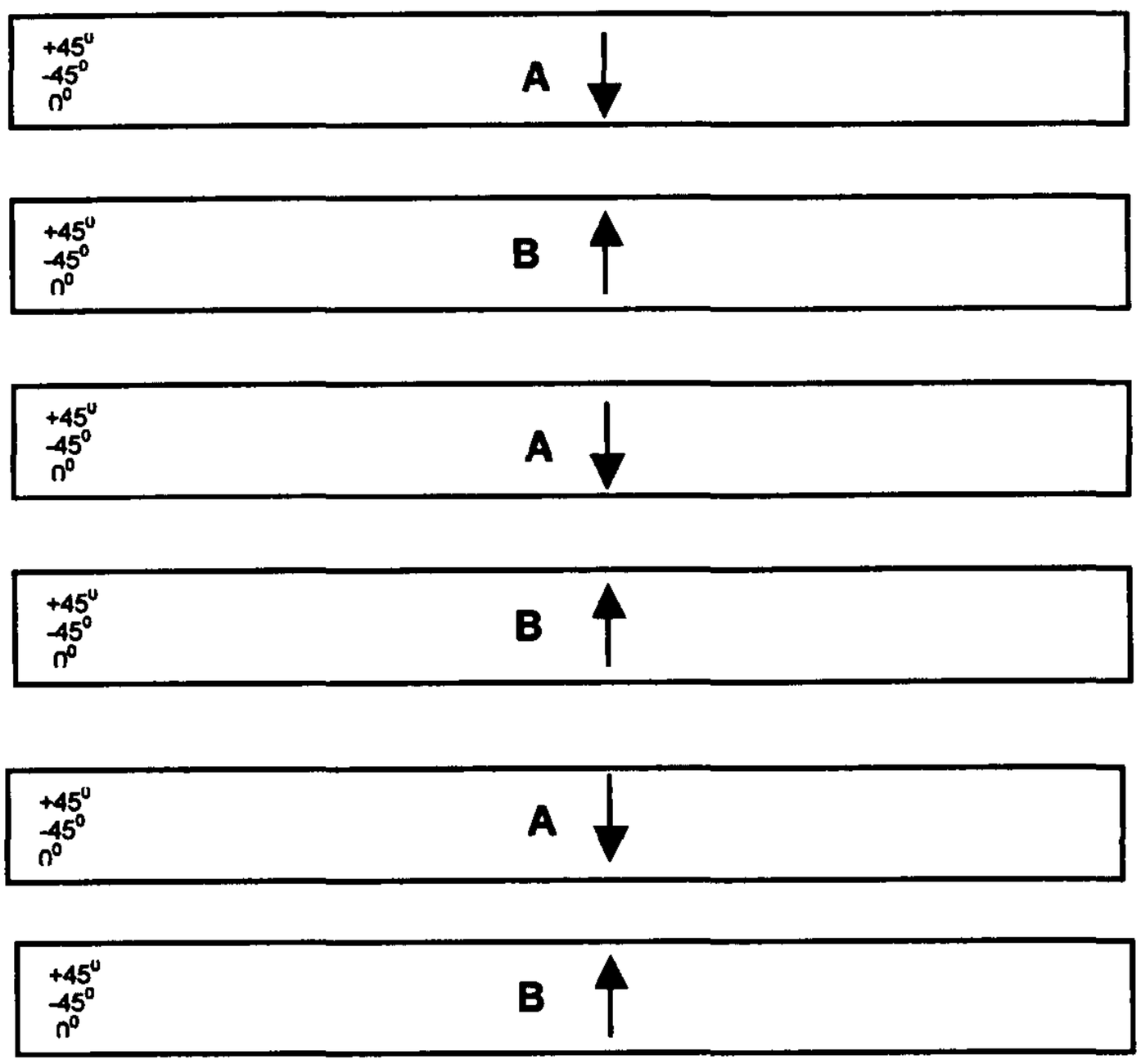

Figure 8.1 construction drawing of the NCF specimens

The specimens consist of six plies, Figure 8.1. stitched together, two of them hand A and two of them hand B, allowing symmetric laminates to be produced. The Hexel 914 epoxy resin system was used in the resin transfer moulding (RTM) to fabricate the composite test specimens. The resin is infused in to the preform under vacuum and pressure with minimum viscosity of 30 cps at a temperature 160^0 C. The achieved volume fraction from this process was 58%.

All the specimens were routinely screened non-destructively by ultrasonic C-scanning after manufacture to ascertain the quality of the product. Any defective material was rejected.

The test specimens used in this investigation are shown in ,Figure 8.2. Stitched and non stitched specimens have been cut from the consolidated

panels for tests in tension and compression with a diamond cutter, in both 0^0 and 90^0 fibre orientations. All ends tabbing material was aluminium with square ends.

All basic mechanical tests were conducted on instron 8501. 10 specimens were tested for each material per orientation. Full stress- strain curves have been obtained by strain gauges samples on a single surface, this allowed the determination of moduli in tension and compression, and by using cross gauges, the Poisson's ratios were measured. All tests have been carried out at room temperature, 20^0 C.

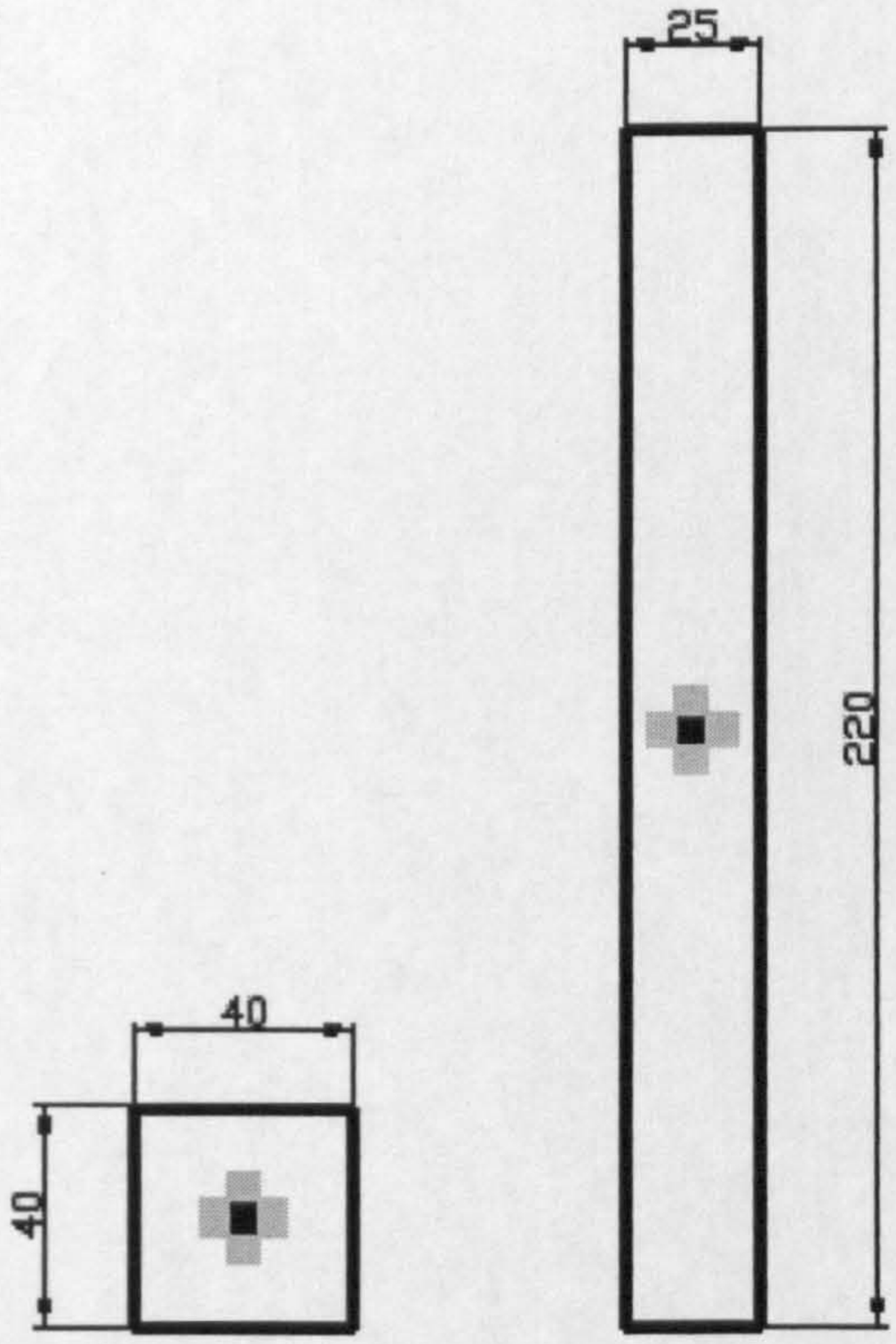

Figure 8.2 specimens geometry for determination of tensile and compression properties of composite material

8.3 Results and Discussion

9.3.1 Tension properties

The average tension strength for the stitched and non stitched specimens is shown in ,Figure 8.3. Test results are shown for 0^0 and 90^0 orientations. A significant difference was noted when the specimens were loaded in the 90^0 direction as shown in ,Figure 8.4. The measured strength of the non stitched specimens, tested in 0^0 direction, reached the failure point on average 580 MPa, whereas it was 150 MPa for the 90^0 direction specimens. The absence of the fibre reinforcement in 90^0 direction reflects the drop of the mechanical properties for both stitched and non stitched specimens.

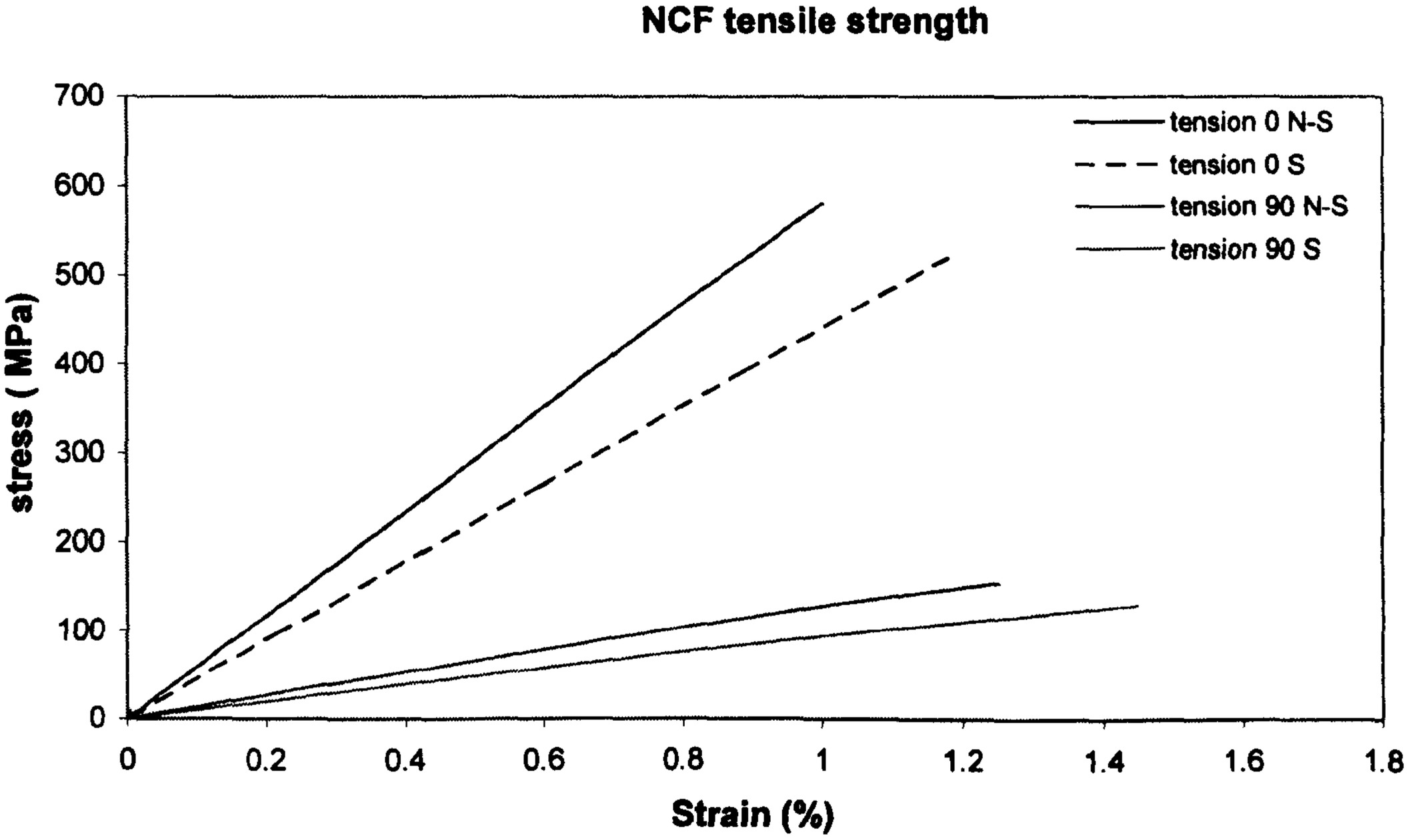

Figure 8.3 Tension stress strain response for stitched and non stitched specimens in 0^0 & 90^0 orientations

Thus, the tested results have shown that the tensile strength of the stitched samples was 12% lower than the non stitched samples in the same 0^0 orientation, and 18% lower in the case of 90^0 direction samples.

These strength reductions may be caused by fibre misalignment; damage to the carbon fibre tows, local stress concentration due to resin pocket around the stitched area may occur during the deformation as shown in ,Figure 8.5.This clearly appeared in the fracture origin which initiated in the stitched area as shown in ,Figure 8.6.

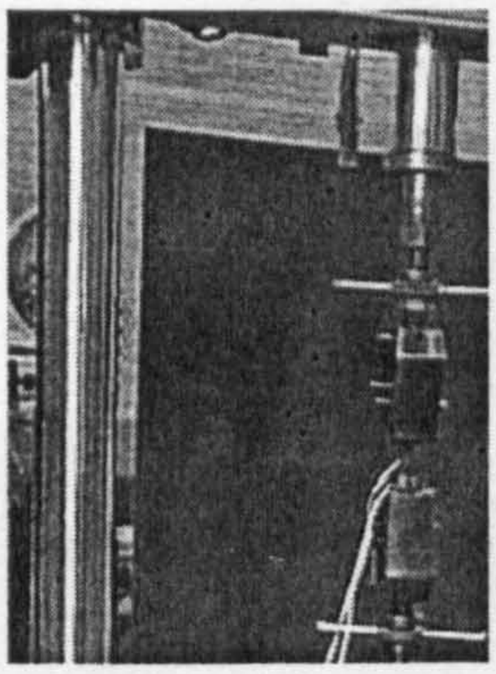

loto of the tension specimen with strain gauge
conducted with instron machine

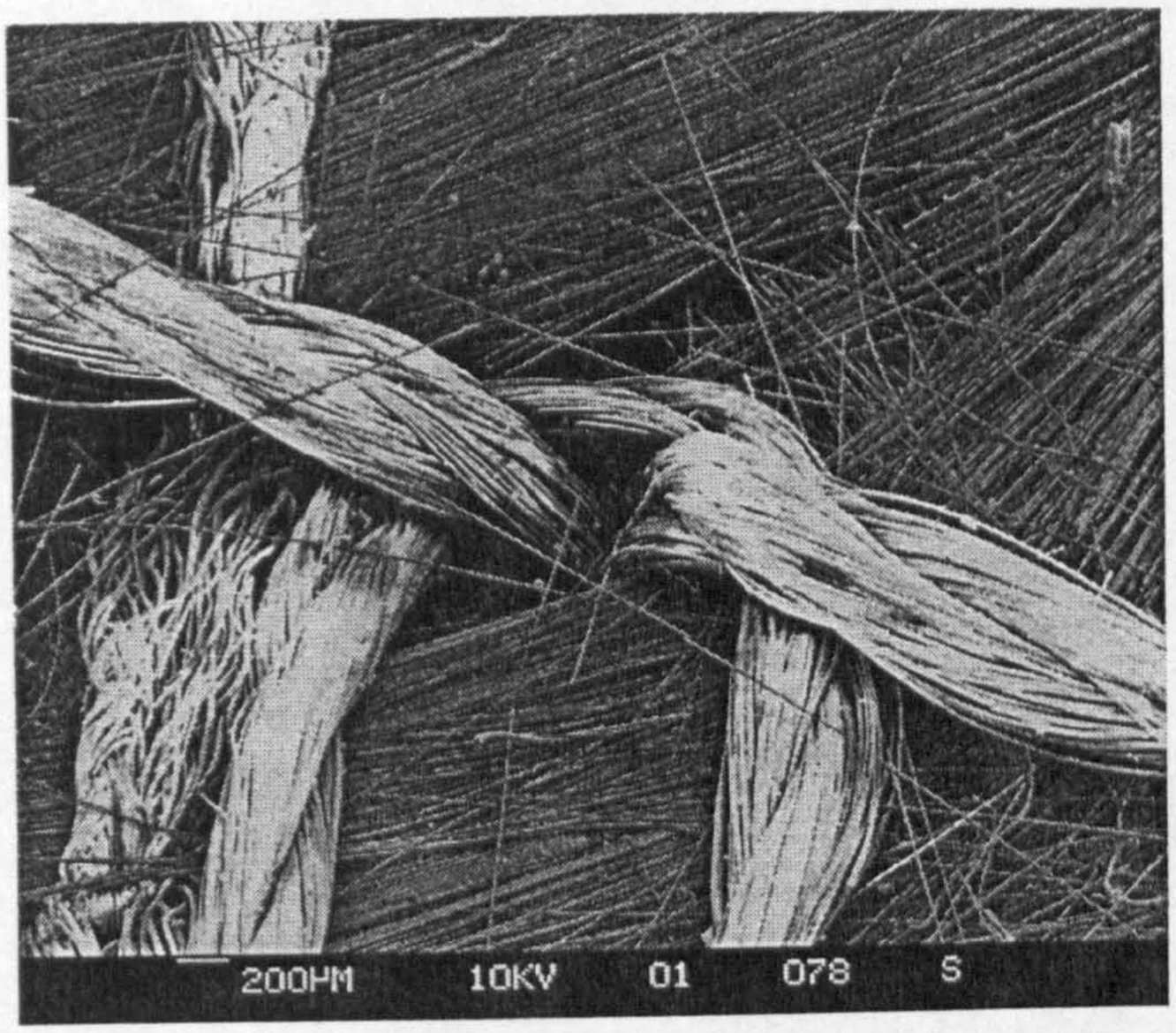

Figure 8.5 scanning electron microscopic (SEM) fractograph of the stitch through the reinforcement structure

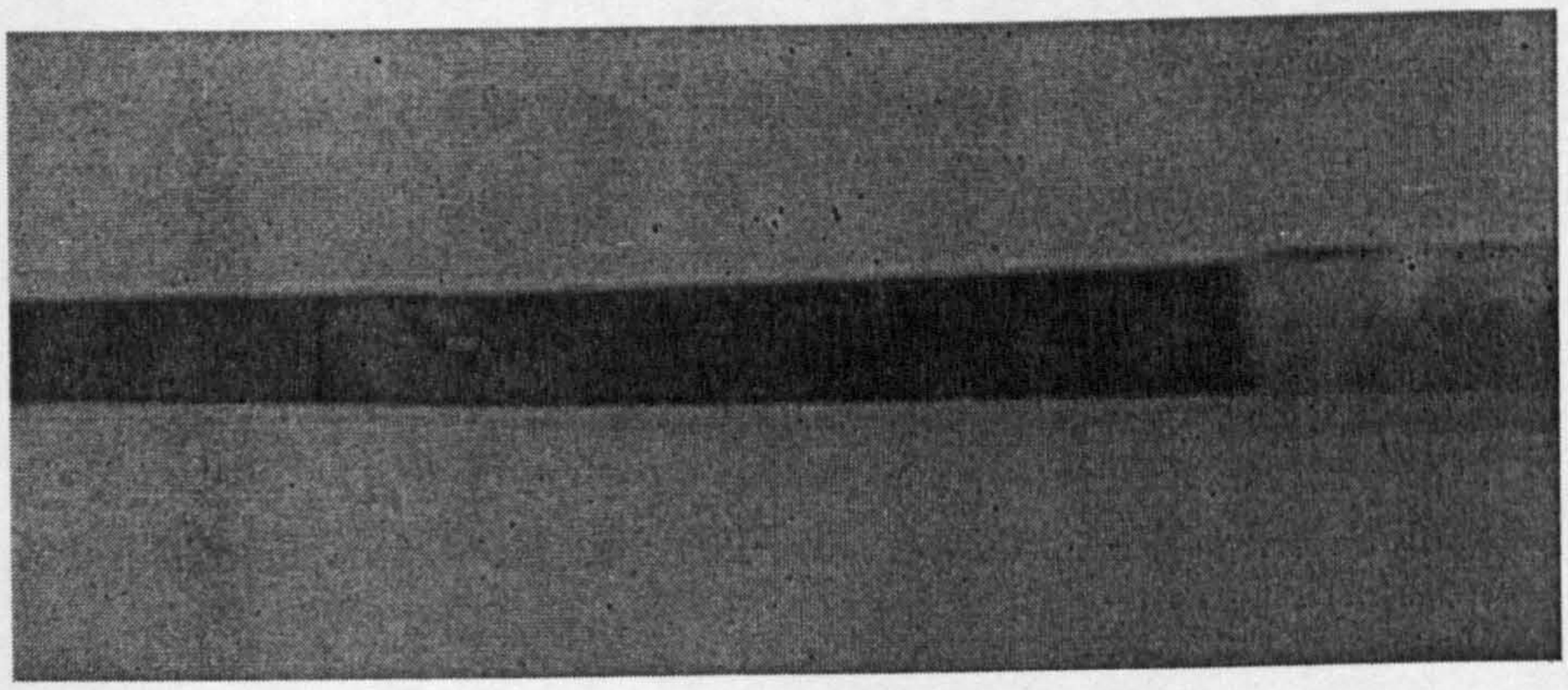

Figure 8.6 Fracture of the stitched specimen

The average tensile moduli for the stitched and non stitched specimens are shown in ,Figure 8.7. The modulus of the stitched specimens in 0^0 was 13% lower than that of the non stitched specimens. And 24% lower in 90^0 specimens. These variations can be attributed to the fibre volume fraction variations due to the stitches.

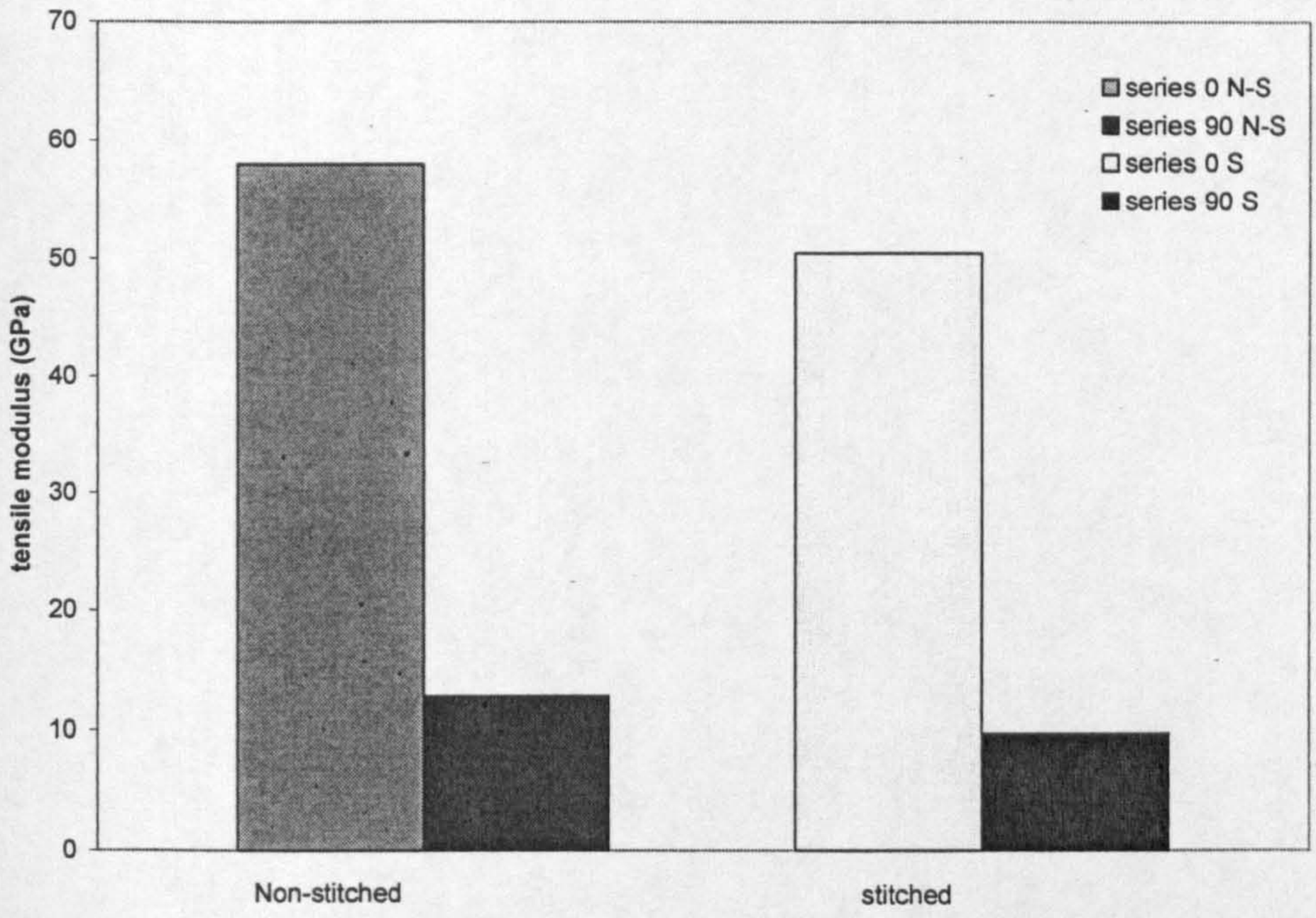

Figure 8.7 Tensile modulus of the stitched and non stitched specimens in 0^0 and 90^0 orientations

Using a cross strain gauging arrangement allowed for a reasonably accurate measurement of the Poison's ratios for both stitched and non stitched specimens as shown in ,Figure 8.8. The poison's ratio for the non stitched specimens was higher than that of the stitched specimens in both 0^0 and 90^0 directions.

8.3.2 Compression properties

The specimens have been loaded at right angle to the 0^0 orientation ,Figure 8.8. The results indicate that the stitched plies exhibited a 14% lower

strength than the non stitched plies. This reduction may be attributed to fibre damage, gaps between the fibre tows.

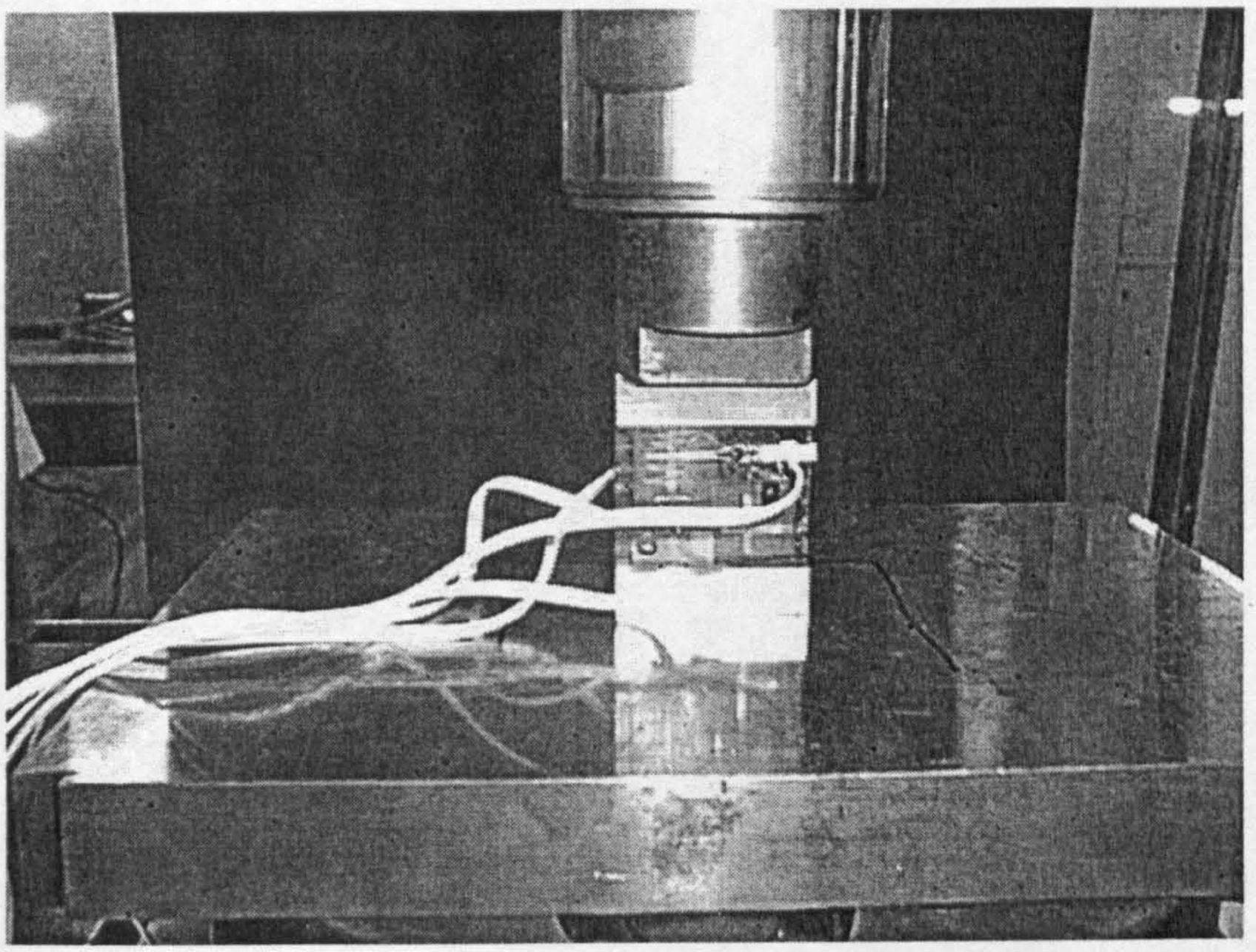

Figure 8.8 photo of the compression specimen loaded at a right angle to the 0^0 orientation

The failure of the specimens was very complex and dependent upon a number of factors as the failure may occur through shear deformation, or buckling depending on the stiffness of the specimens i.e. if the laminate stiffness is low then failure may be due to buckling and if the laminate is stiff with a high shear modulus, then the failure will be attributed to shear deformation).

The average compression strengths of the stitched specimens compared with the strength of the non stitched specimens in both 0^0 and 90^0 orientations are shown in ,Figure 8.9. The results show that the average compression strength for the stitched specimens is about 11% lower than the strength for the non stitch specimens in the 0^0 orientation.

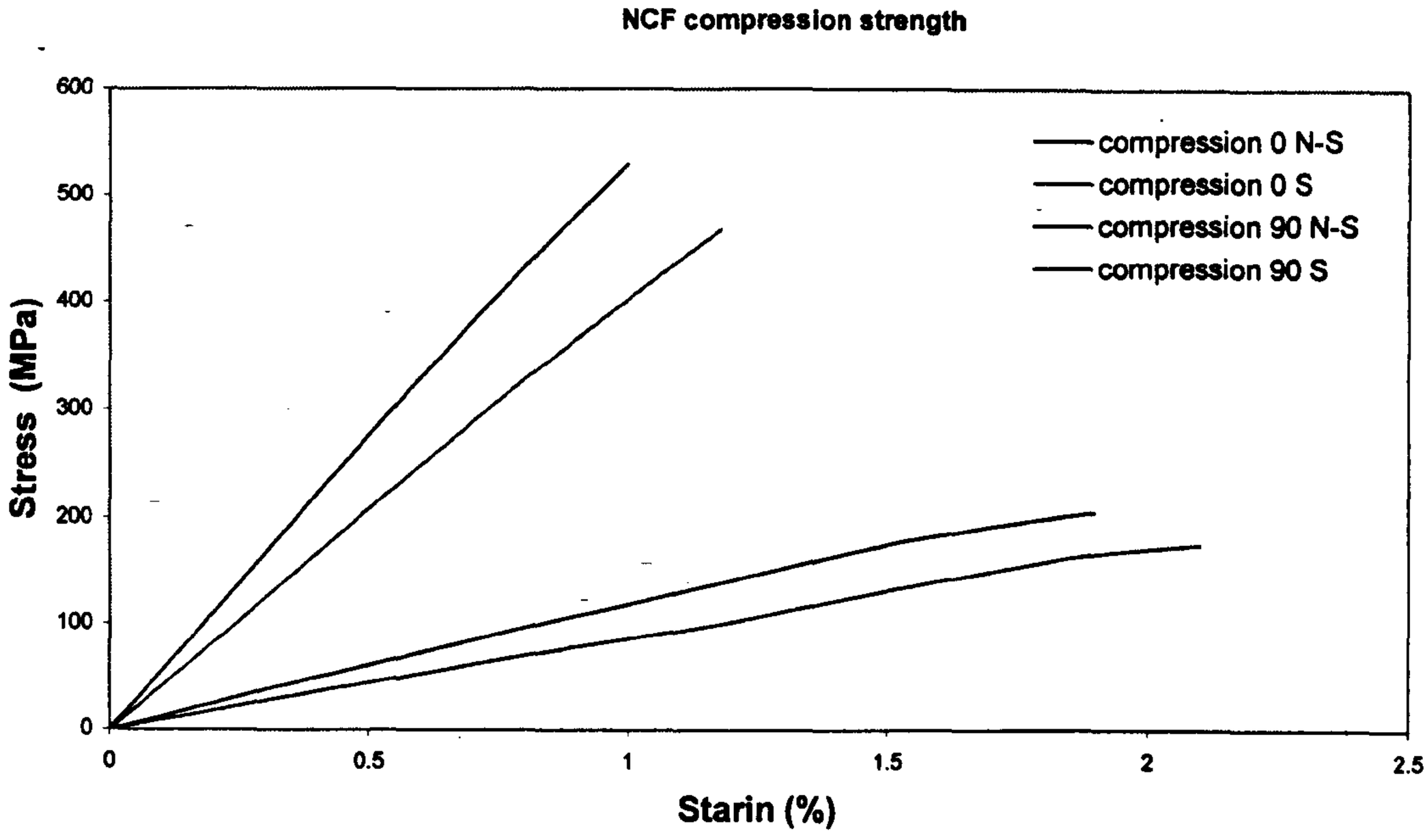

Figure 8.9 Compression stress strain response for stitched and non stitched specimens in 0^0 & 90^0 orientations

The measured compression strength of the specimens, tested in 0^0 direction, reached the failure point on average 520 MPa, whereas it was 200 MPa for the 90^0 direction specimens.

Average compression modulus for the stitched specimens has been compared with the non stitched specimens in ,Figure 8.10. The average modulus for the stitched sample in the 0^0 directionhas has been found to be 13% lower than that of the non stitched specimens. in the 90^0 direction, however, the average modulus for the stitched specimens was 18% lower than that of the stitched specimens. The stitches used to assemble the reinforcement structures could have reduced the volume fraction in the stitched areas and around them, and this may be the reason for the reduction in the modulus for the stitched specimens.

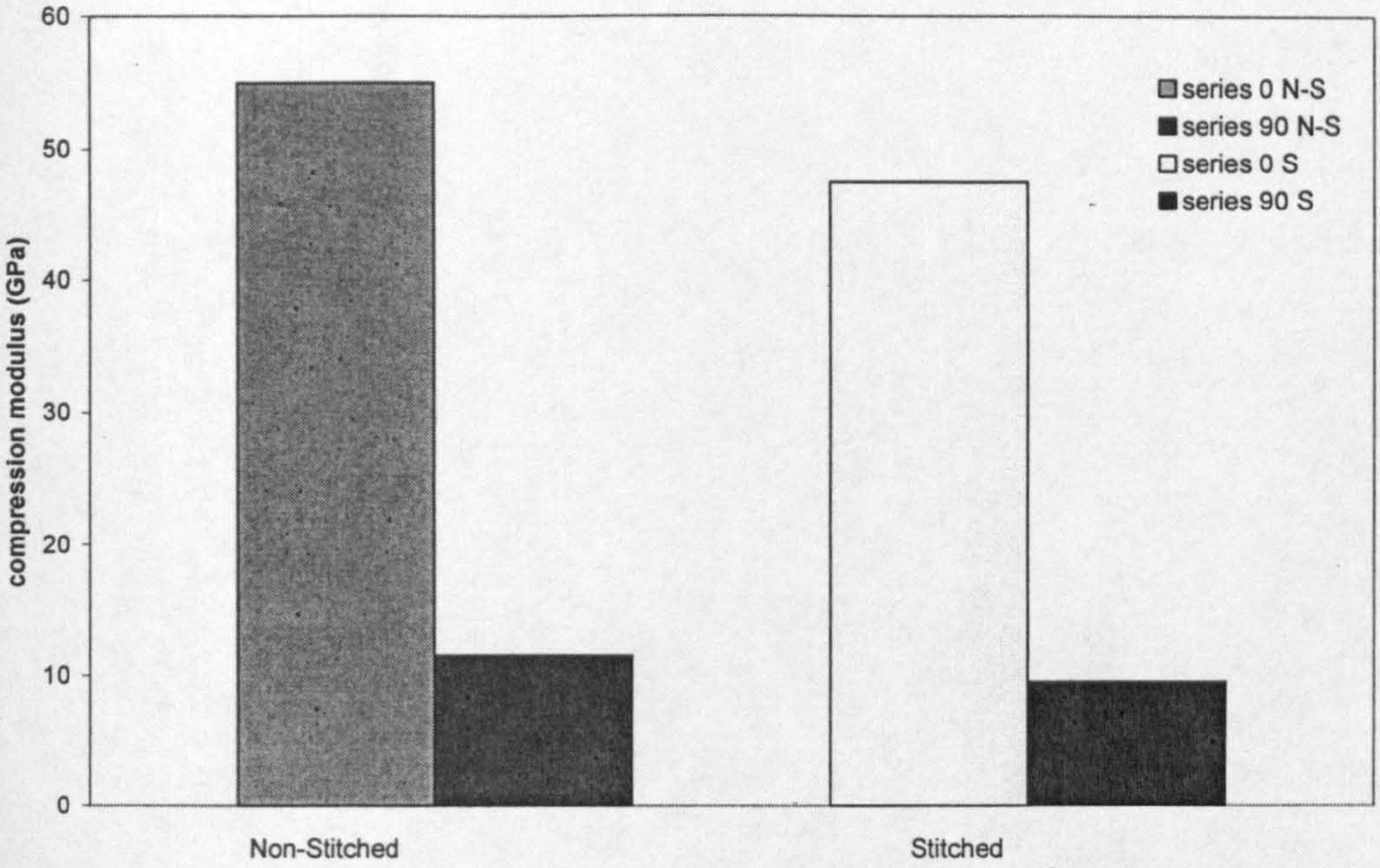

Figure 8.10 Compression modulus of the stitched and non stitched specimens in 0^0 and 90^0 orientations

8.4 Finite Element Analysis (FEA)

8.4.1 Aim of the analytical study

- To develop analytical models for predicting the behaviour of the reinforcement structure (I, T, J, C) with different geometries; and
- To study the effect of the stitching characteristics on the overall behaviour of the structural components (consolidated parts).

8.4.2 What is Finite Element Analysis?

Finite Element Analysis (FEA) is a computer-based numerical technique for calculating the strength and behaviour of engineering structures. It can be used to calculate deflection, stress, vibration, buckling behaviour and many other phenomena. It can be used to analyse either small or large-scale deflection under loading or applied displacement. It can analyse elastic deformation, or "permanently bent out of shape" plastic deformation. The

computer is required because of the astronomical number of calculations needed to analyze a large structure. The power and low cost of modern computers has made Finite Element Analysis available to many disciplines and companies.

In the finite element method, a structure is broken down into many small simple blocks or elements. The behaviour of an individual element can be described with a relatively simple set of equations. Just as the set of elements would be joined together to build the whole structure, the equations describing the behaviours of the individual elements are joined into an extremely large set of equations that describe the behaviour of the whole structure. The computer can solve this large set of simultaneous equations. From the solution, the computer extracts the behaviour of the individual elements. From this, it can get the stress and deflection of all the parts of the structure. The stresses will be compared to allowed values of stress for the materials to be used, to see if the structure is strong enough.

The FE method was first developed for use in the aerospace and nuclear industries where the safety of structures is critical. Today, the growth in usage of the method is directly attributable to the rapid advances in computer technology in recent years. As a result, commercial finite element packages exist that are capable of solving the most sophisticated problems, not just in structural analysis, but for a wide range of phenomena. FEA has been used in high volume production & manufacturing industries for many years and it is now used routinely to solve problems in structural strength design, fluid flows & fluid-structure interaction, thermal analysis, acoustics, shock & vibrations, crash simulations, electrical analyses, dynamic problems, electromagnetic evaluations, metal forming etc.

Finite Element Analysis makes it possible to evaluate a detailed and complex structure, in a computer, during the planning of the structure. The demonstration in the computer of the adequate strength of the structure and

the possibility of improving the design during planning can justify the cost of this analysis work. FEA has also been known to increase the rating of structures that were significantly over designed and built many decades ago.

In the absence of Finite Element Analysis (or other numerical analysis), development of structures must be based on hand calculations only. For complex structures, the simplifying assumptions required to make any calculations possible can lead to a conservative and heavy design. A considerable factor of ignorance can remain as to whether the structure will be adequate for all design loads. Significant changes in designs involve risk. Designs will require prototypes to be built and field tested. The field tests may involve expensive strain gauging to evaluate strength and deformation.

With Finite Element Analysis, the weight of a design can be minimized, and there can be a reduction in the number of prototypes built. Field testing will be used to establish loading on structures, which can be used to do future design improvements via Finite Element Analysis.

8.4.3 Modelling and Analysis procedures

The ANSYS finite element package was used to investigate the problem. The ANSYS program is one of the most popular and most powerful Computer-Aided Engineering tools which specialises in producing finite element analysis solutions for Structural, Thermal, Vibration, Electro-Magnetic, Fluid Flow and Impact simulation problems.

It was employed here to simulate the experiments in order to obtain the material characteristics for the general models and to investigate the effect of the stitches on the behaviour of those models. hence, the analytical study has been divided into two main parts:

I. Modelling of the samples specimens, simulation of the compression and tension tests described earlier in the

experimental section and predicting stitched and non stitched material data.

II. Modelling typical I-beam with and without stitches and analysing the effect of the stitches, their number and pattern on the behaviour and strength of the beams.

In both parts the FE procedure adopted consisted of the following steps:

- Setting the type of analysis to be used; i e, structural.
- Creating the geometrical models, the dimensions of which are according to those of the samples, used the tension and compression tests for part(i) and those of a typical prototype I-beam for part (ii).
- Defining the element type to use for modelling the specimens. Shell element 63 has been used in this study. It has bending and membrane capabilities and both in-plan and normal loads can be applied to it **[Ansys 5.7 manual]**.
- Assigning material properties. These have been obtained from the experiments carried out on the simple rectangular compression and tension specimens. the orthotropic feature of the material used has been taken into account by assigning appropriate value in the three different directions.
- Generating the FE meshes for the stitched and non stitched cases.
- Applying boundary conditions: fixed at one end and loaded at the other for case (i) and simply supported in the case of bending or one end fixed and the other free in case of torsion for case (ii).
- Applying loads: pure tensile and compression axial loads for case (i) and bending and torsional forces for case (ii). In all cases the load (or loads) increased by increments until the failure stress is reached at a location of the specimen.

- Solution: selecting the solver algorithm and executing the solution phase and obtained the results.
- Post-processing the results and analysing the output data.

8.4.4 Compression and tension tests modelling and calibration

,Figure 8.11& 8.12 show typical FE models used for simulating the tension tests. The same procedure has been followed to simulate the compression tests.

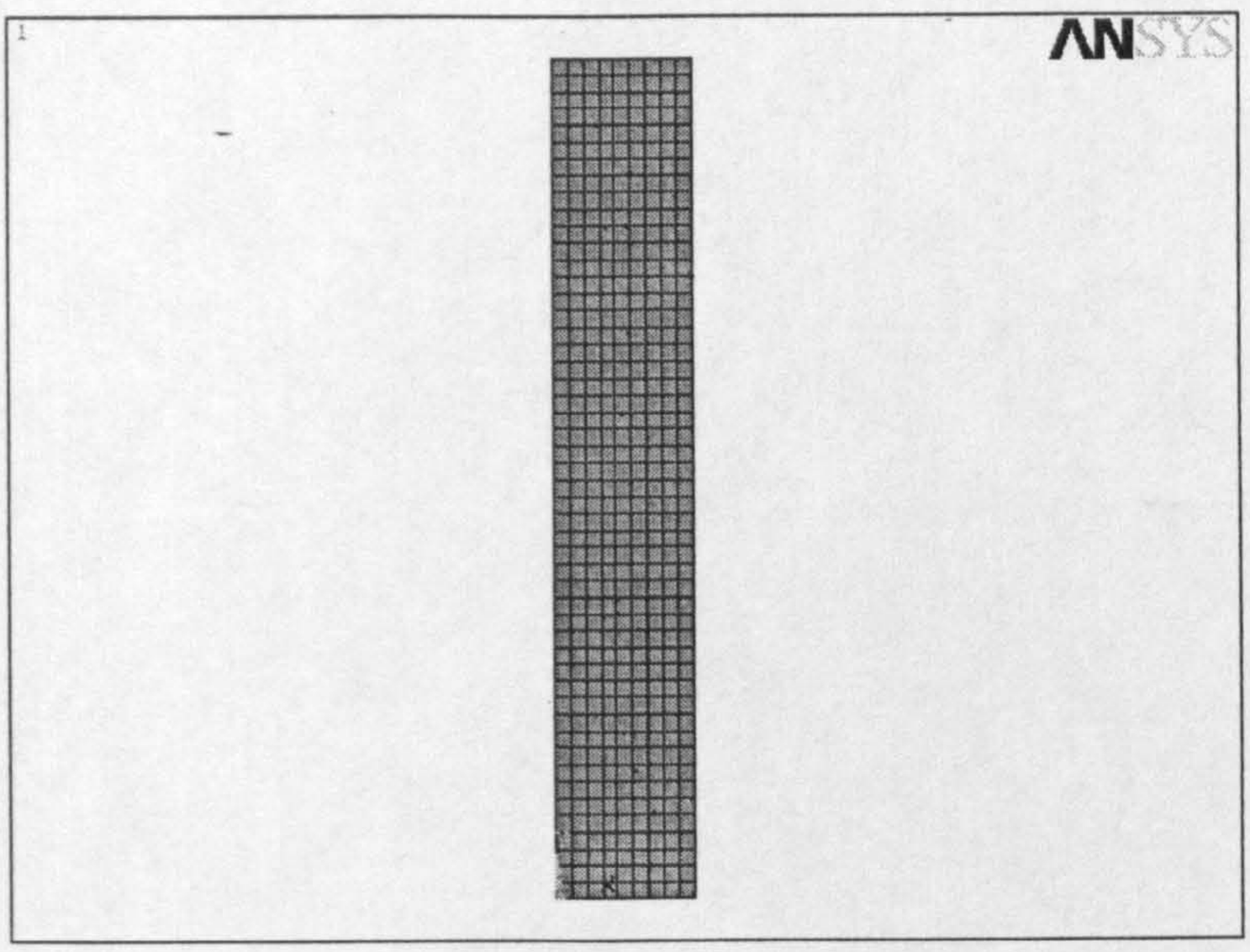

Figure 8.11 Finite element meshes for non stitched specimen

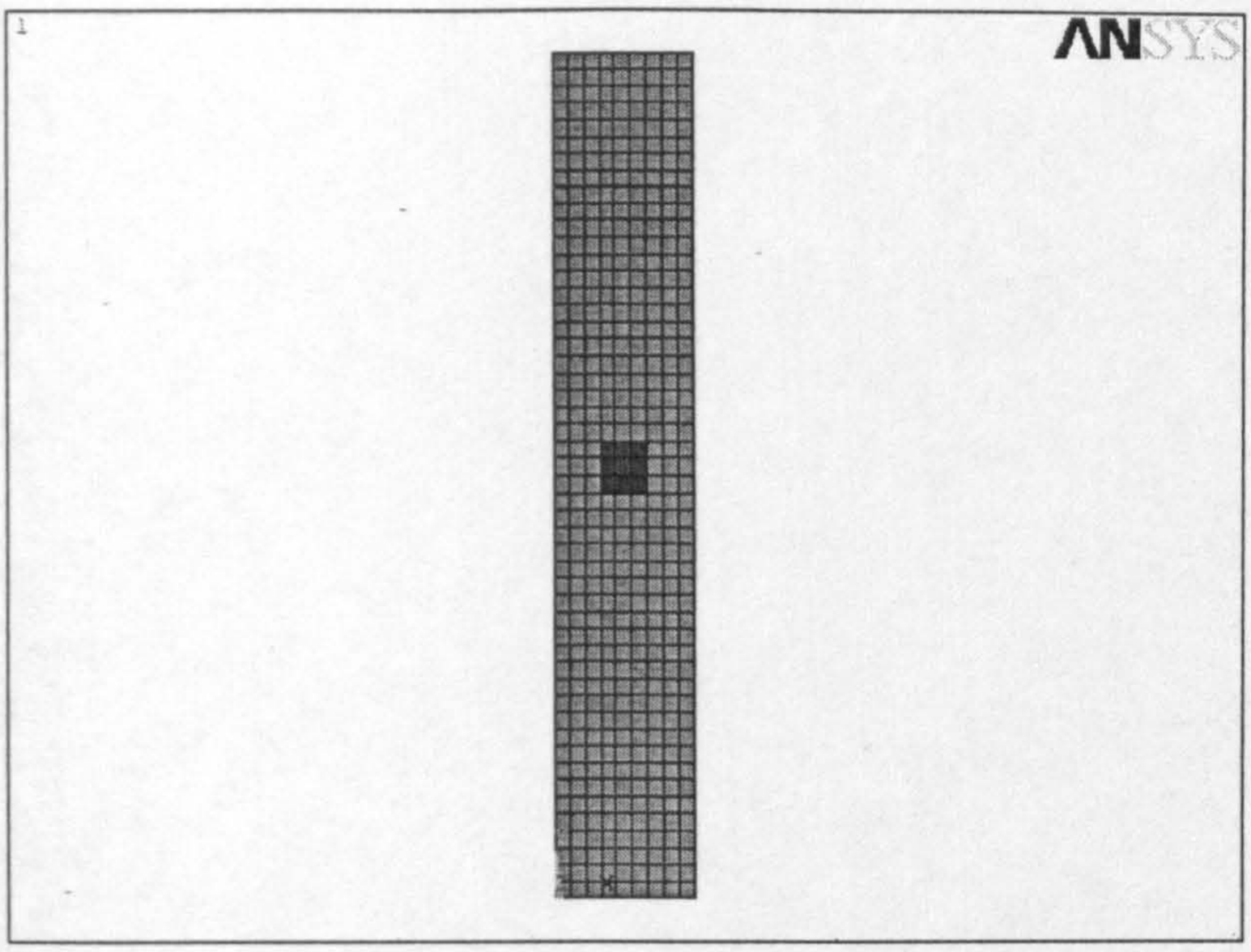

Figure 8.12 Finite element mesh for stitched specimen

In order to check the accuracy of the material properties obtained by the FE analysis of the compression and tension specimens, the models have been validated by comparing the FE results with the corresponding experimental data. Both the FE elastic modulii and the stress failure results were compared against those obtained by the experiments.

Figure 8.13 to 8.16, show the axial stress distribution at failure level for both the tension and compression tests in the 90° and 0° material directions. In the case of non stitched specimens, the stress distribution was uniform and was, therefore, not presented.

As can be seen for both cases, the specimens experienced higher concentration of stress at locations adjacent to the stitched areas. For each case the material properties that were applied for FEA summarised blow each Figure.

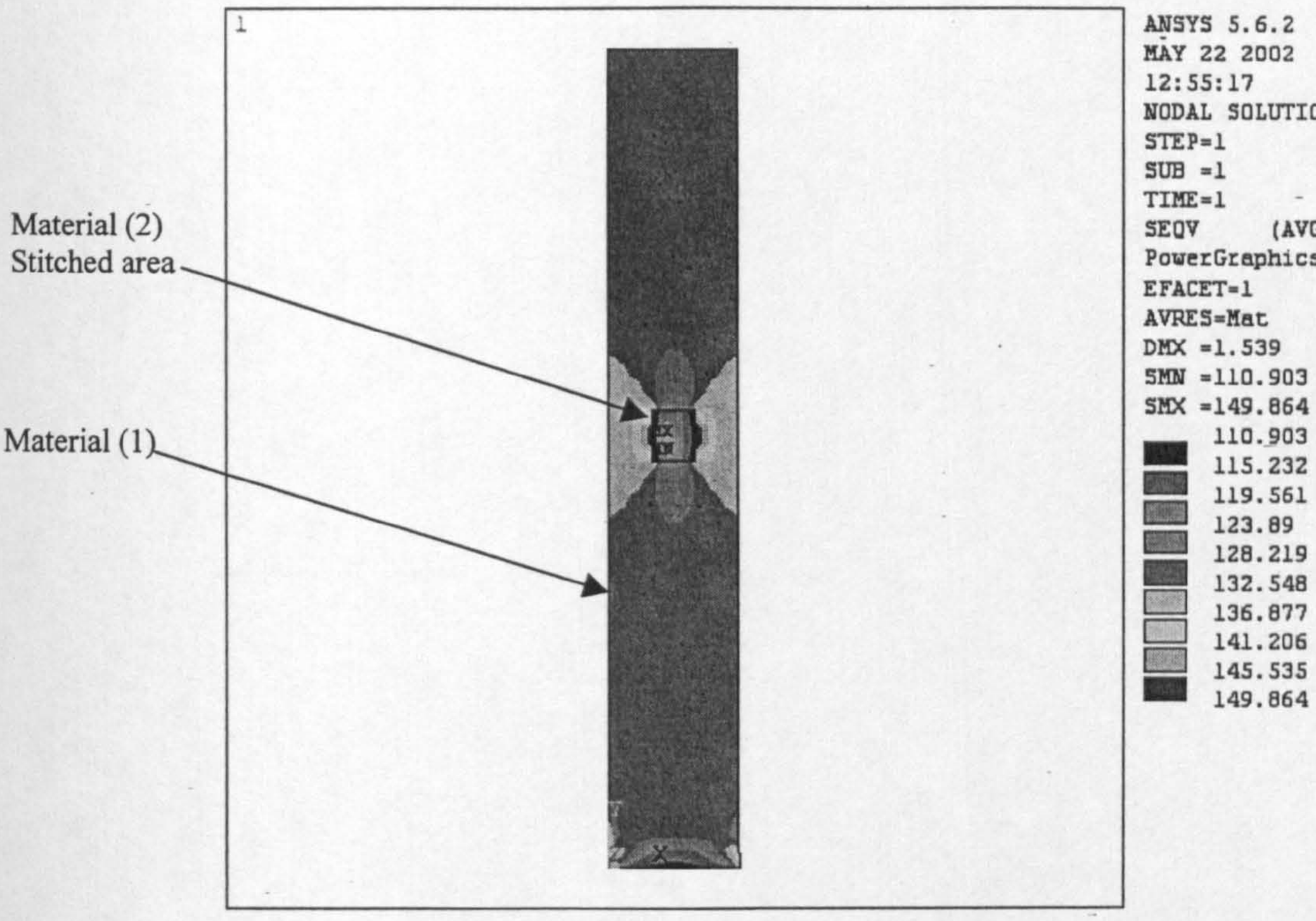

Figure 8.13 Stress distribution of stitched ncf 90^0 specimen (MPa)

Load:

Failure load P = 124 MPa

Material (1) properties for FEA:

1-elastic modulus

$E_x = 58000$ MPa
$E_y = 12800$ MPa
$E_z = 12800$ MPa

2-shear modulus

$G_x = G_y = G_z = 4500$ MPa

3-poisson's ratios

NUXY = 0.7
NUXZ = 0.3
NUYZ = 0.3

Material (2) properties for FEA:

1-elastic modulus

$E_x = 50500$ MPa
$E_y = 9700$ MPa
$E_z = 9700$ MPa

2-shear modulus

$G_x = G_y = G_z = 4000$ MPa

3-poisson's ratios

NUXY = 0.59
NUXZ = 0.24
NUYZ = 0.24

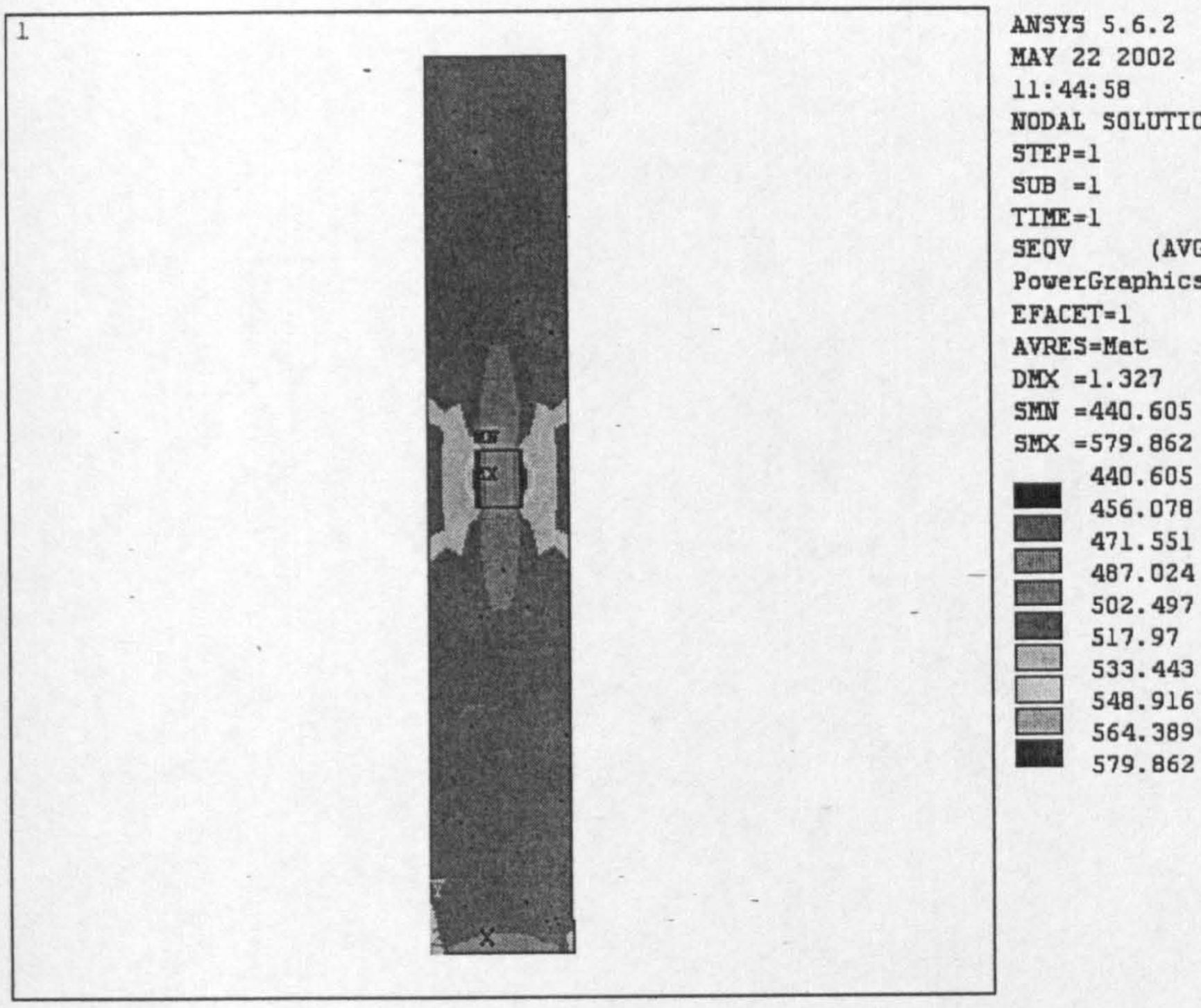

Figure 8.14 Stress distribution of stitched ncf 0^0 specimen (MPa)

Load:

Failure load P = 510 MPa

Material (1) properties for FEA:

1-elastic modulus

E_x = 58000 MPa
E_y = 12800 MPa
E_z = 12800 MPa

2-shear modulus

$G_x = G_y = G_z$ = 4500 MPa

3-poisson's ratios

NUXY = 0.7
NUXZ = 0.3
NUYZ = 0.3

Material (2) properties for FEA:

1-elastic modulus

E_x = 9500 MPa
E_y = 44000 MPa
E_z = 9500 MPa

2-shear modulus

$G_x = G_y = G_z$ = 4000 MPa

3-poisson's ratios

NUXY = 0.7
NUXZ = 0.3
NUYZ = 0.3

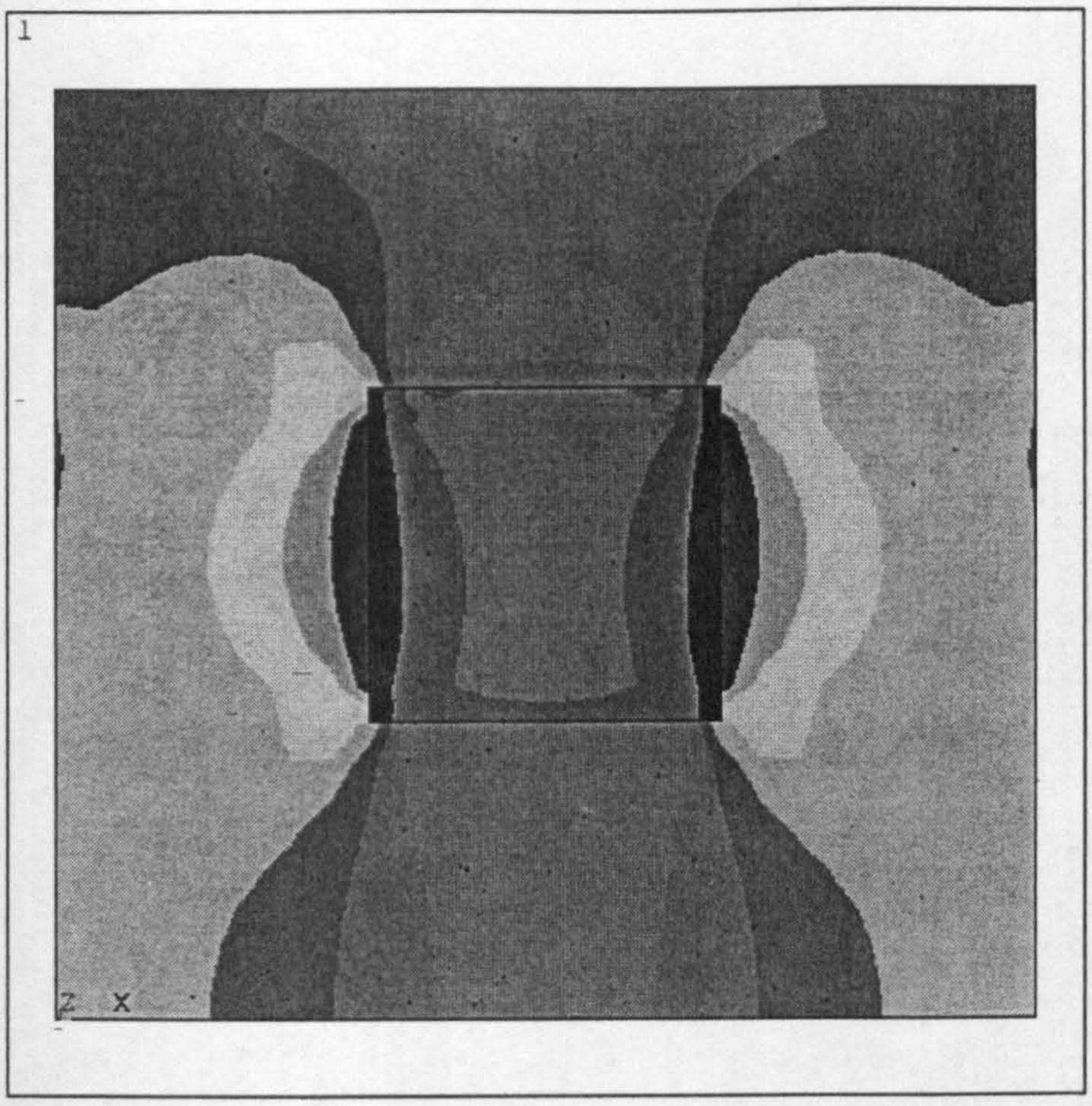

Figure 8.15 Stress distribution of stitched ncf 90^0 specimen (MPa)

Load:

Failure load P = 174 MPa

Material (1) properties for FEA:

1-elastic modulus

E_x = 58000 MPa
E_y = 12800 MPa
E_z = 12800 MPa

2-shear modulus

$G_x = G_y = G_z$ = 4500 MPa

3-poisson's ratios

NUXY = 0.7
NUXZ = 0.3
NUYZ = 0.3

Material (2) properties for FEA:

1-elastic modulus

E_x = 44000 MPa
E_y = 9500 MPa
E_z = 9500 MPa

2-shear modulus

$G_x = G_y = G_z$ = 4000 MPa

3-poisson's ratios

NUXY = 0.59
NUXZ = 0.24
NUYZ = 0.24

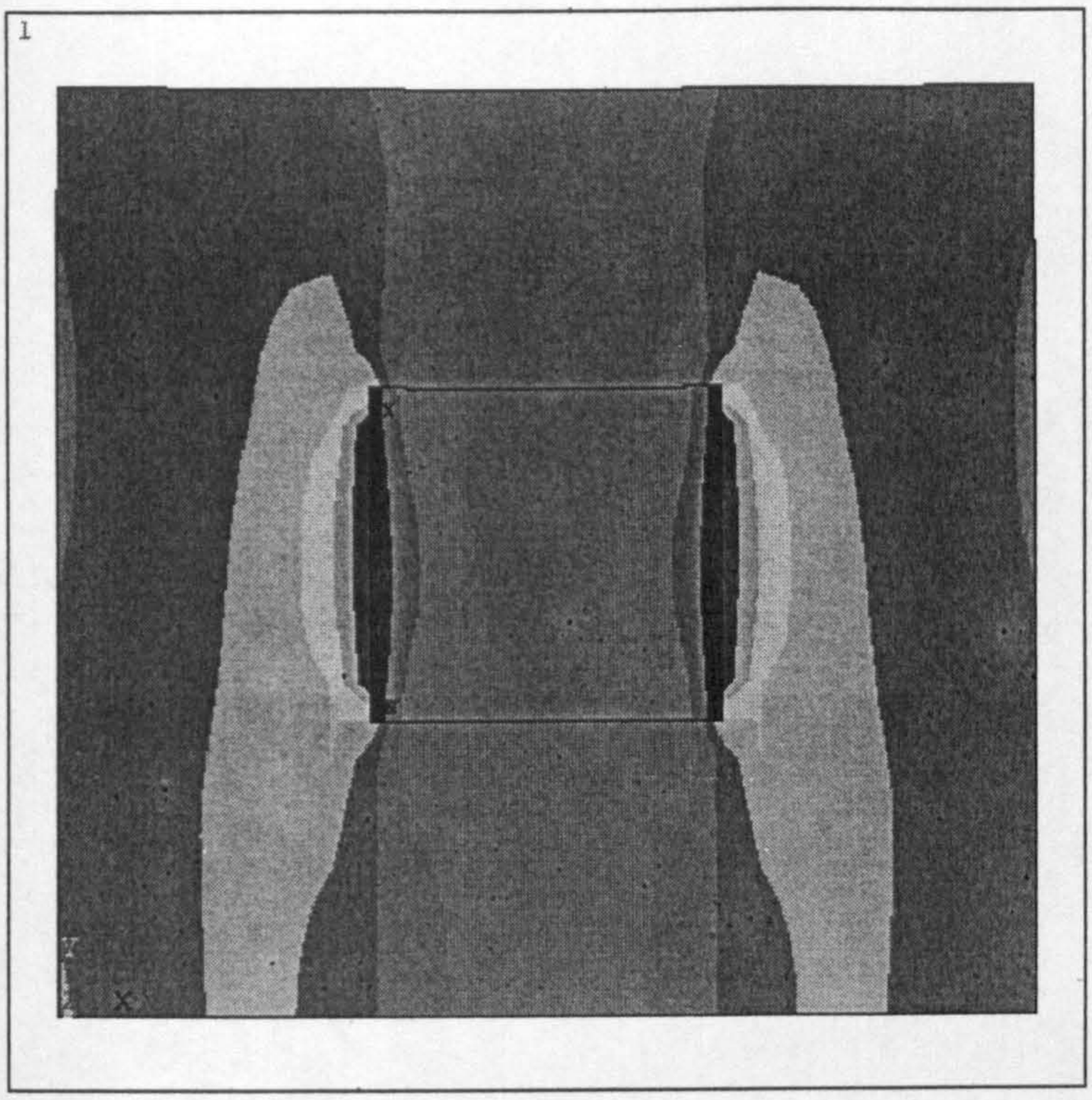

Figure 8.16 Stress distribution of stitched ncf 0^0 specimen (MPa

Load:

Failure load P = 460 MPa

Material (1) properties for FEA:

1-elastic modulus

$E_x = 12800$ MPa
$E_y = 58000$ MPa
$E_z = 12800$ MPa

2-shear modulus

$G_x = G_y = G_z = 4500$ MPa

3-poisson's ratios

NUXY = 0.3
NUXZ = 0.7
NUYZ = 0.3

Material (2) properties for FEA:

1-elastic modulus

$E_x = 9500$ MPa
$E_y = 44000$ MPa
$E_z = 9500$ MPa

2-shear modulus

$G_x = G_y = G_z = 4000$ MPa

3-poisson's ratios

NUXY = 0.24
NUXZ = 0.59
NUYZ = 0.24

8.4.5 Parametric study

After the successful validation of the FEA compression and tension test models against the experimental data, a parametric study was conducted. The aim of the parametric study was to investigate the influence of stitches, an important manufacturing parameter, and their number and pattern on the overall behaviour of the reinforcement structures and its failure level.

The study was conducted on a typical I- beam section with and without stitched with following main parameters being varied:

a. By editing the positions of the taking device in the robot program can easily change the stitched positions. Three patterns of the stitches as shown ,Figures 8.17 t o 8.19, have been considered.
b. Loading conditions: three different types of loads were applied on a simply supported I-beam model: a vertical bending uniform load applied along the top flange of the I-beam ,Figure 8.20, two concentrated loads on the top flange of the I-beam applied over the stitched position as shown in ,Figure 8.21. and a torsional load applied at one end of the I-beam, the other end being fixed Figure 8.22

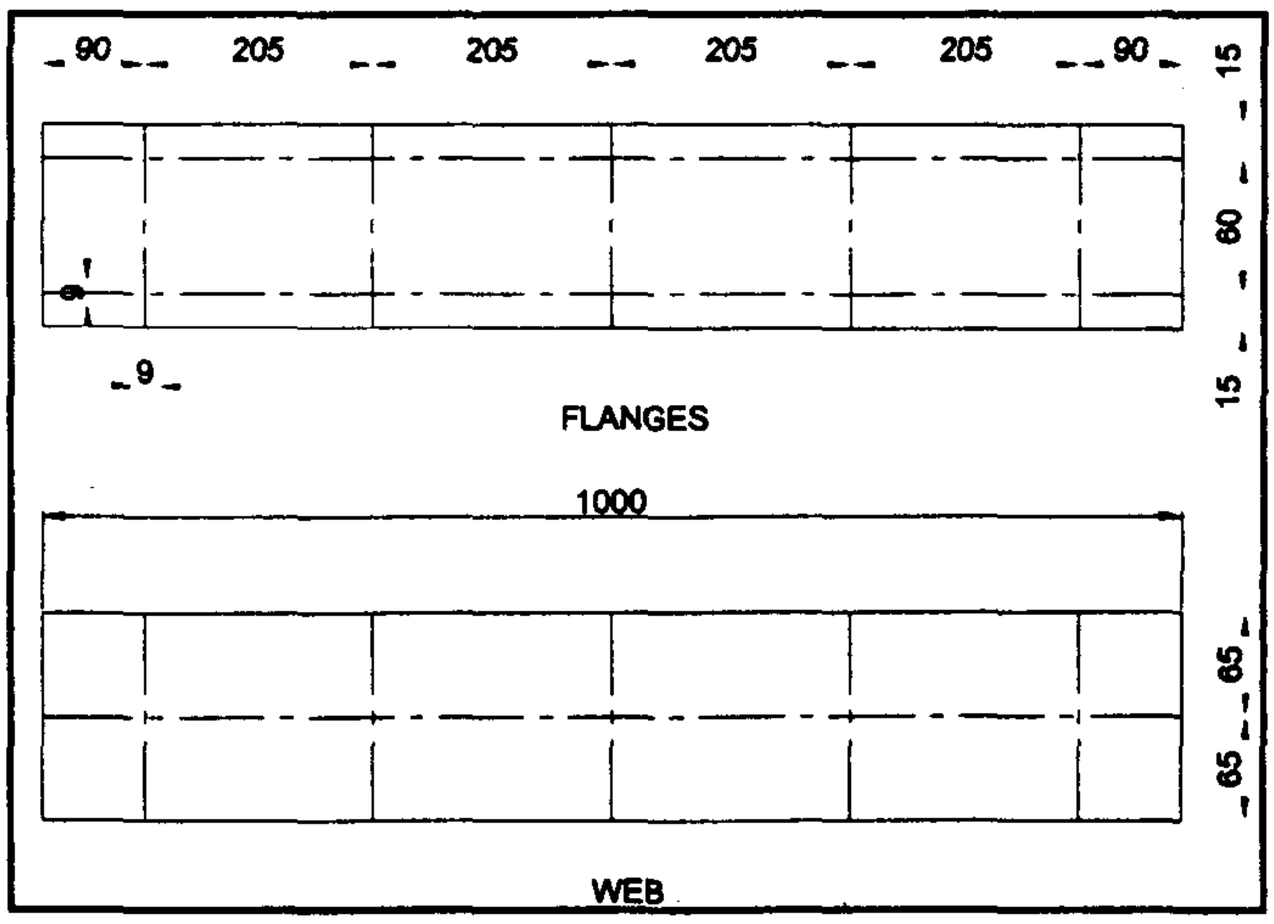

Figure 8.17 position of the stitches pattern (1) basic pattern

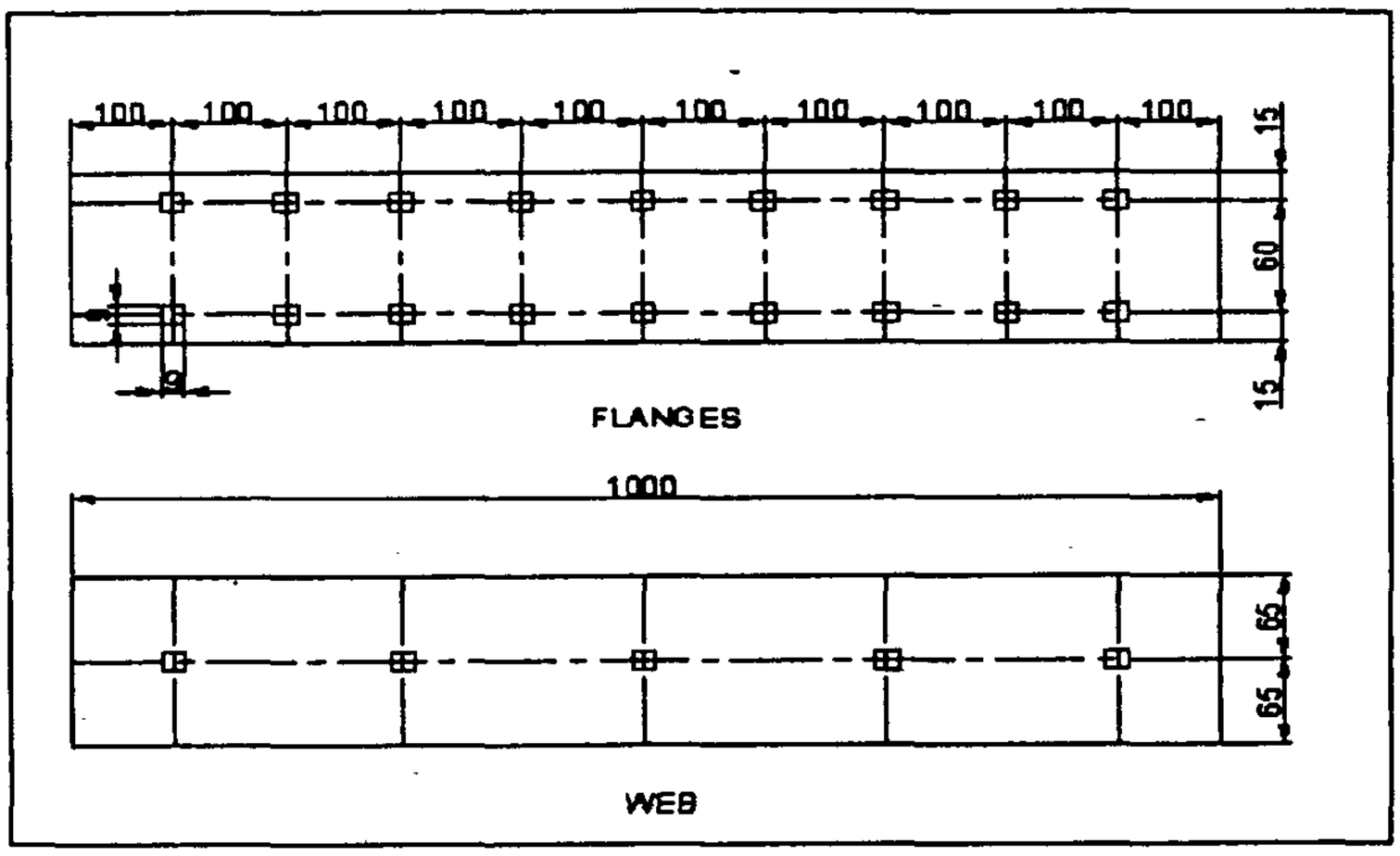

Figure 8.18 position of the stitches pattern (2) double number of stitches

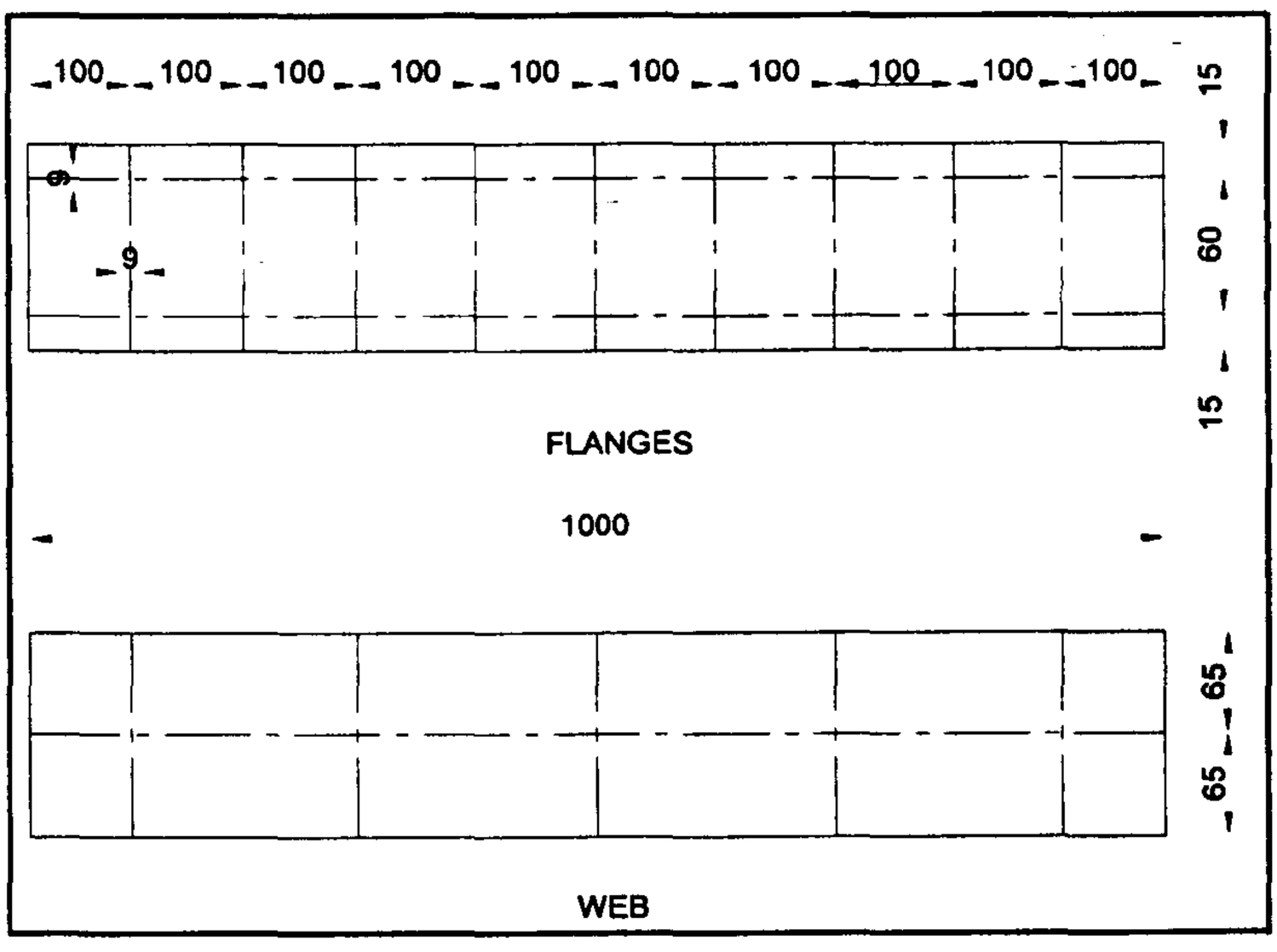

Figure 8.19 position of the stitches pattern (3) zigzag pattern

FE models of the I-beam have been developed by adopting the same procedures that has been described in section 9.4.3:

After the creation of the models for the stitched and non stitched prototype I-beams as shown in ,Figure 8.20 to 8.22 using shell 63, material properties obtained experimentally have been assigned to the corresponding stitched and non stitched parts of the I-beams. Then, appropriate boundary

conditions and loads are applied on the models, the solution phase is executed and the results were obtained and analysed.

It should be noted here that a linear static analysis has been used in which the load is increased until the beam reaches the failure level of the material (stitched and non stitched) at its weakest location. In each stitched I-beam case, the failure level and position is recorded and compared with the corresponding case of the non stitched I-beam.

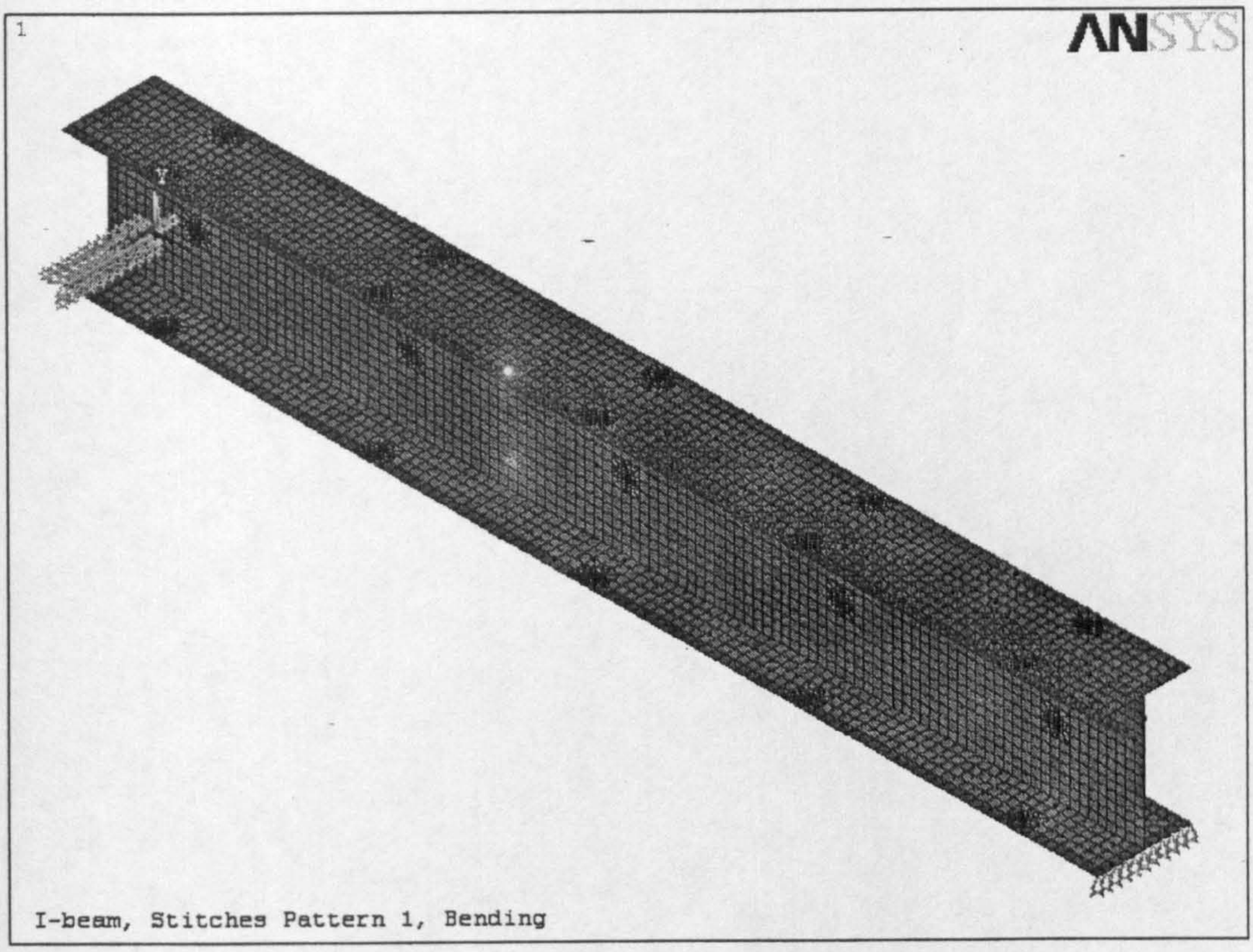

Figure 8.20 Uniform load applied to stitched I Beam

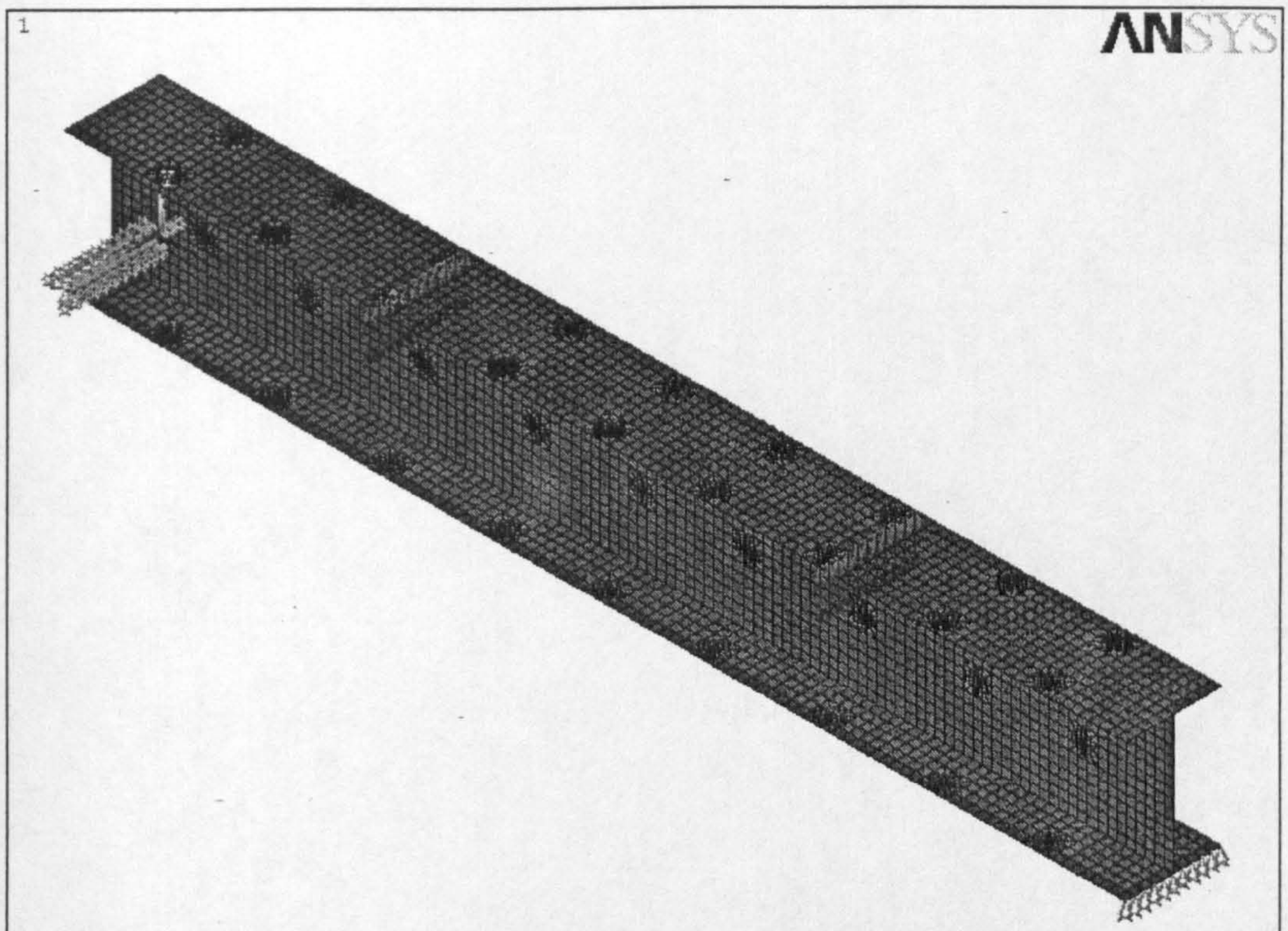

Figure 8.21 Concentrated load applied to stitched I Beam

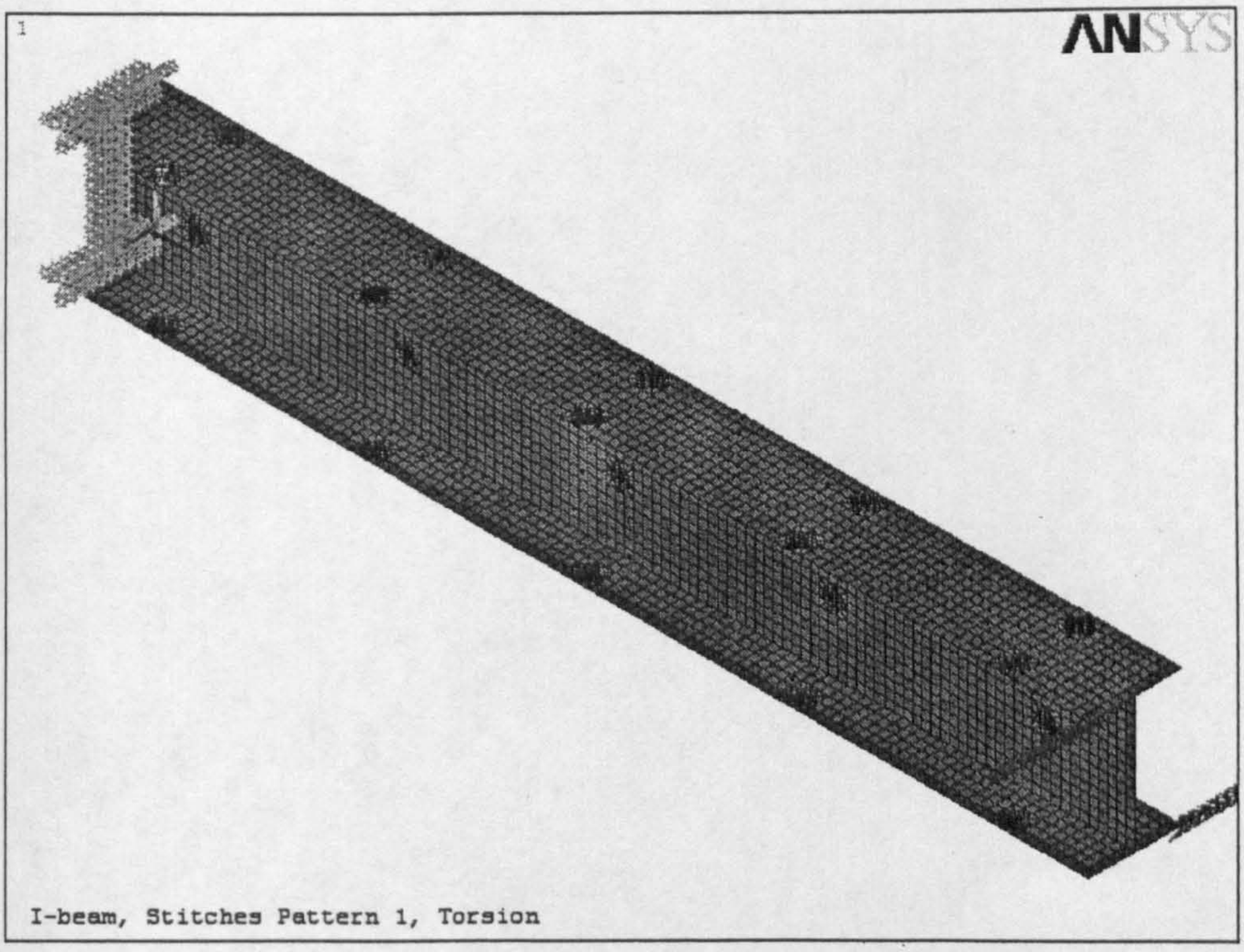

Figure 8.22 Torsion load applied to stitched I Beam

8.4.6 Presentation of results

The compression and tension tests described earlier showed that the material used behaves almost linearly until sudden failure. This justifies the use of a linear analysis in the numerical investigation. It is believed, therefore that such an analysis would predict the failure level of the beam models with a reasonable accuracy.

This is good enough for the present analysis qualitative parametric study. Furthermore, the I-beam has been selected for the study as it is fairly good representation of other typical structures (T,C,J). The range of loading conditions adopted here also comprises all types of loads that such structures would be subjected to in practice (mainly bending -uniform distributed or concentrated- and torsion).

The failure level used in the analysis of the 3D I-beams were the same corresponding levels obtained from the uniaxial compression and tension tests. This is perfectly justified by the stress histories presented in this section which show that under the loads considered here, the beam web and flanges behave virtually in a uniaxial manner (the stresses are always very close to the von Mises stresses, i.e. the transverse stresses are closed to zero.

Figures 8.23 to 8.25, show the equivalent von Mises stress distribution for the non stitched beam cases at the failure level under a bending line load, two concentrated bending loads and a torsional load respectively. The failure area for each case is as shown in the corresponding Figure. The most highly stressed element is picked up from that area, its stress history is plotted and its failure load is determined based on the failure stress level.

Figures 8.26 to 8.28, show the equivalent von Mises, transverse and longitudinal stress histories of the most stressed elements for the non

stitched beam under uniformly distributed load, concentrated load and torsional load respectively. These are used to extract the failure loads as shown in ,Figure 8.26a.

The stitched I-beam models (stitches patterns 1,2,3) have been subjected to the same loading cases as the non stitched beam. The stress distribution plots for these cases are shown in ,Figures 8.29 to 8.37, and the corresponding stress histories are presented in ,Figures 8.40 to 8.46. The failure load for each case is determined in the same way as described earlier.

The typical results presented in these Figures indicate that in the case of the line load and concentrated load cases for all the three stitches patterns, the maximum stress moved to stitched area positions. In the case of the torsional load, however, there was no difference from the behaviour observed with the non stitched beam.

The results of the parametric study for all the cases considered are presented in tables 8.1to 8.5. These show the stitch positions and the type of load applied, and give the failure load obtained by the analysis for selected elements within the failure area of the beam.

Table 8.6 gives a summary of the absolute maximum failure loads for both the non stitched {NS} beams and the stitched {S} beams. This corresponds to the (zig-zag) stitched pattern 3. Comparison between the {NS} and the {S} cases show that stitches reduce the failure load by 5% under the uniform bending and by 8% under concentrated loads bending. The stitches, however, do not have any effect under torsional loading.

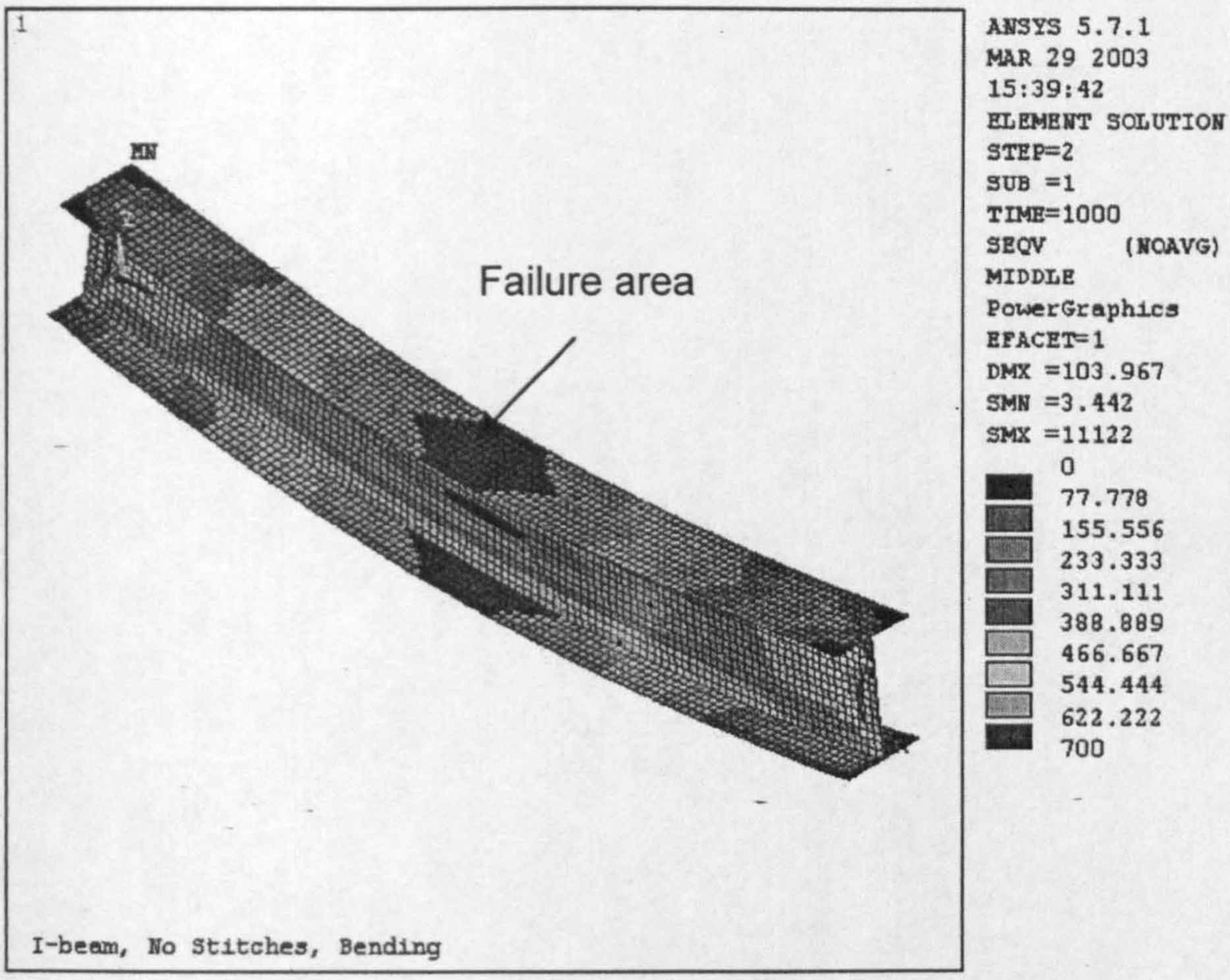

Figure 8.23 I Beam non stitched subjected to uniform load

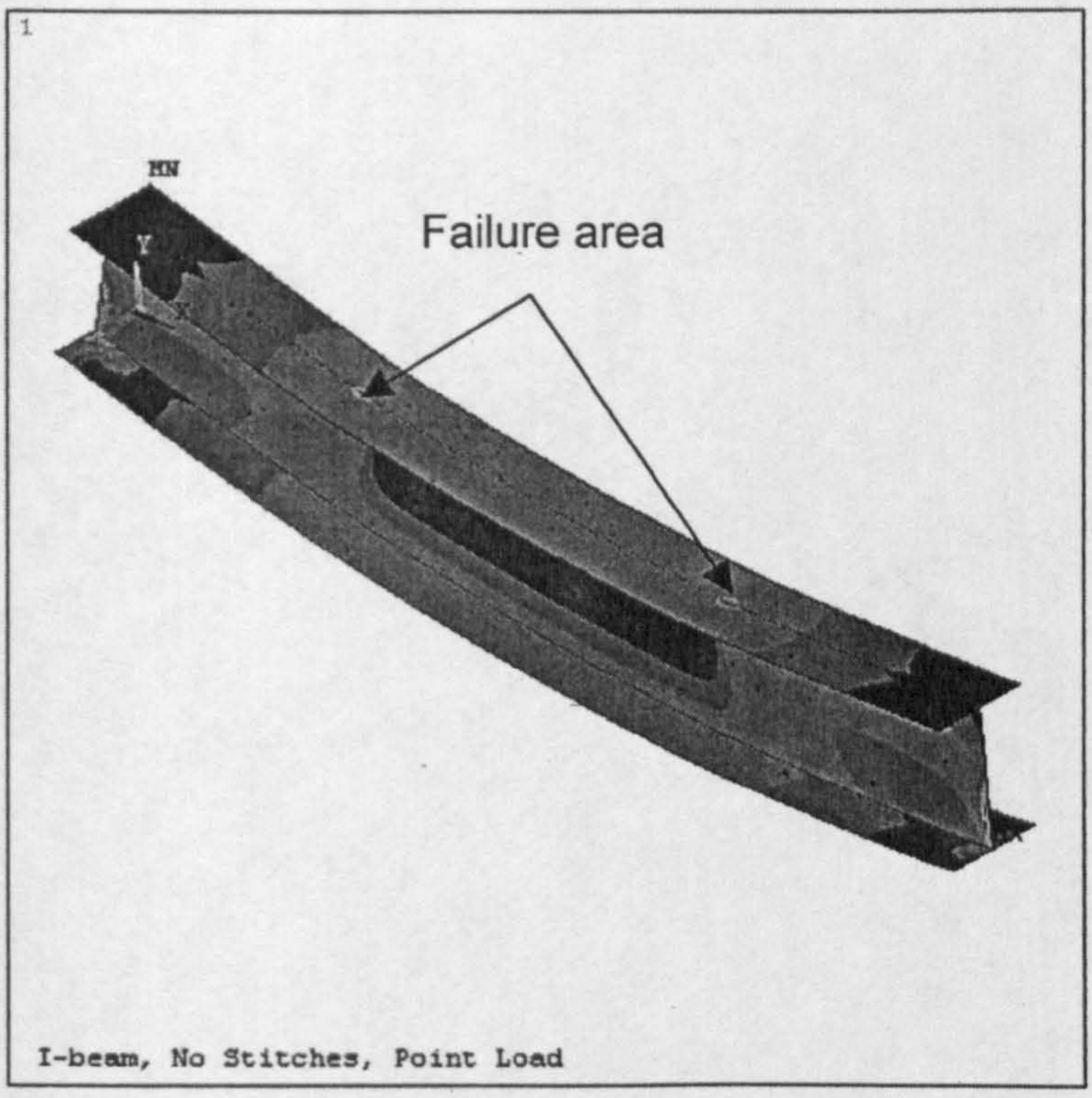

Figure 8.24 I Beam non stitched subjected to concentrated load

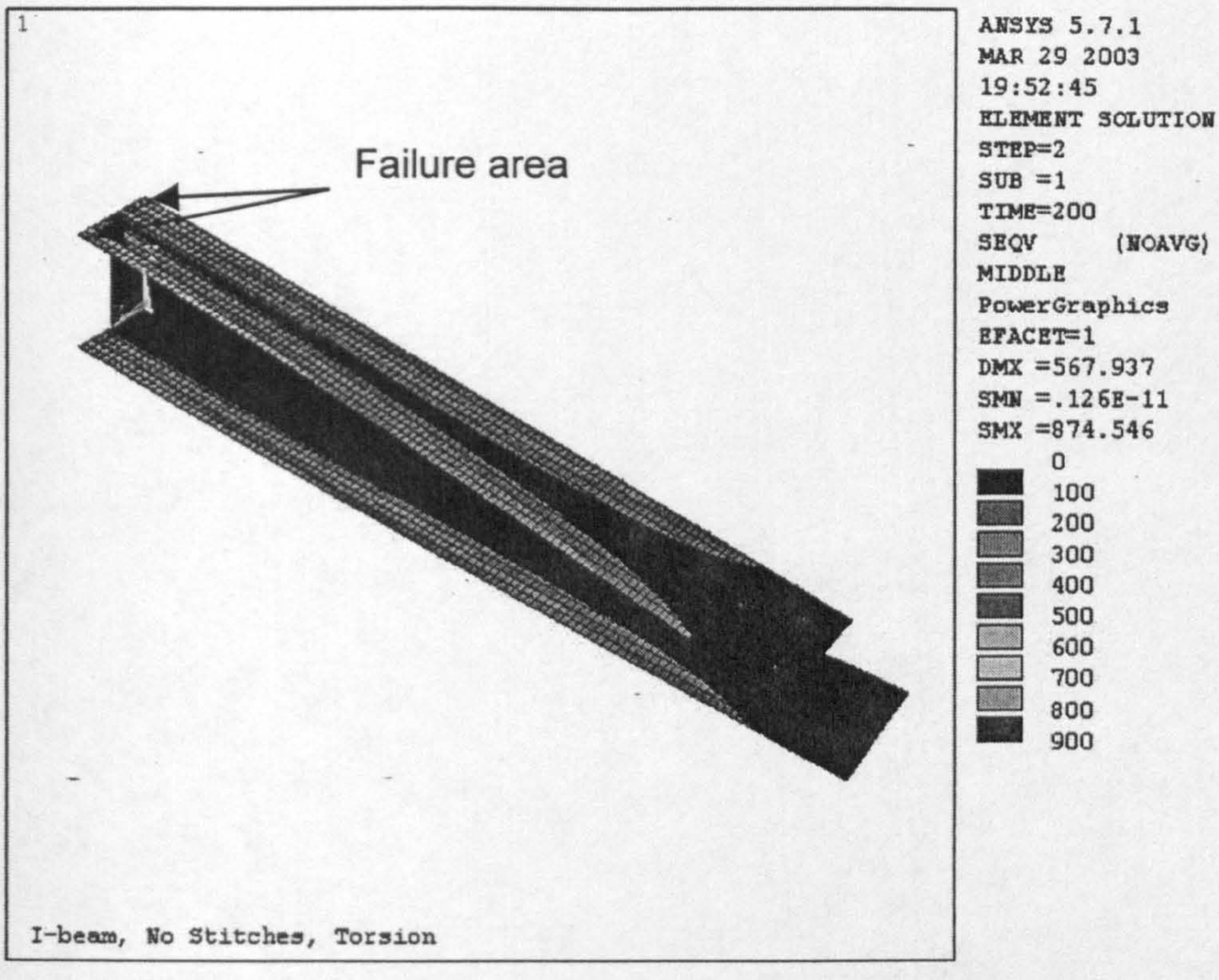

Figure 8.25 I Beam non stitched subjected to torsional load

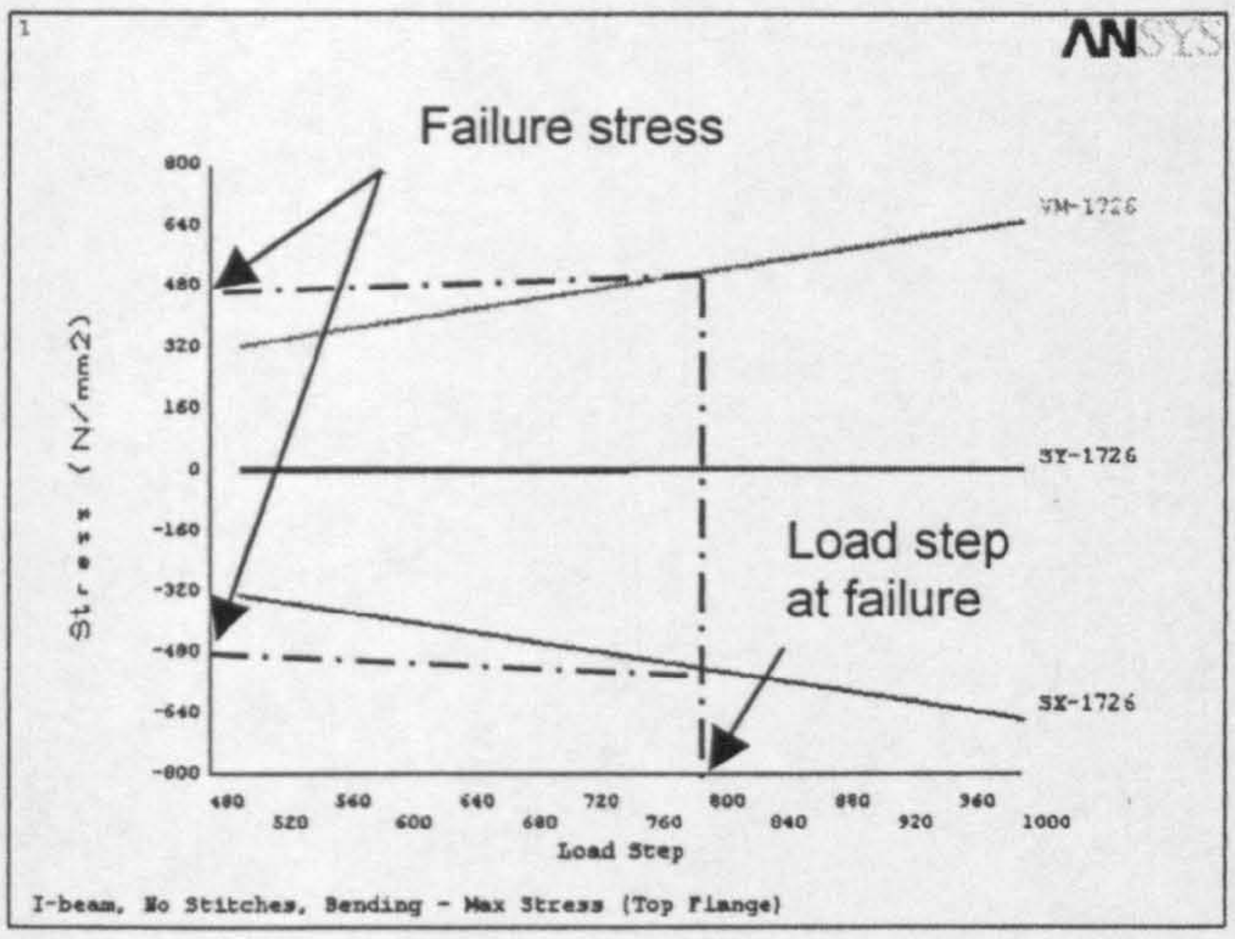

Figure 8.26a top flange non stitch (NS) element under max stress (uniform load)

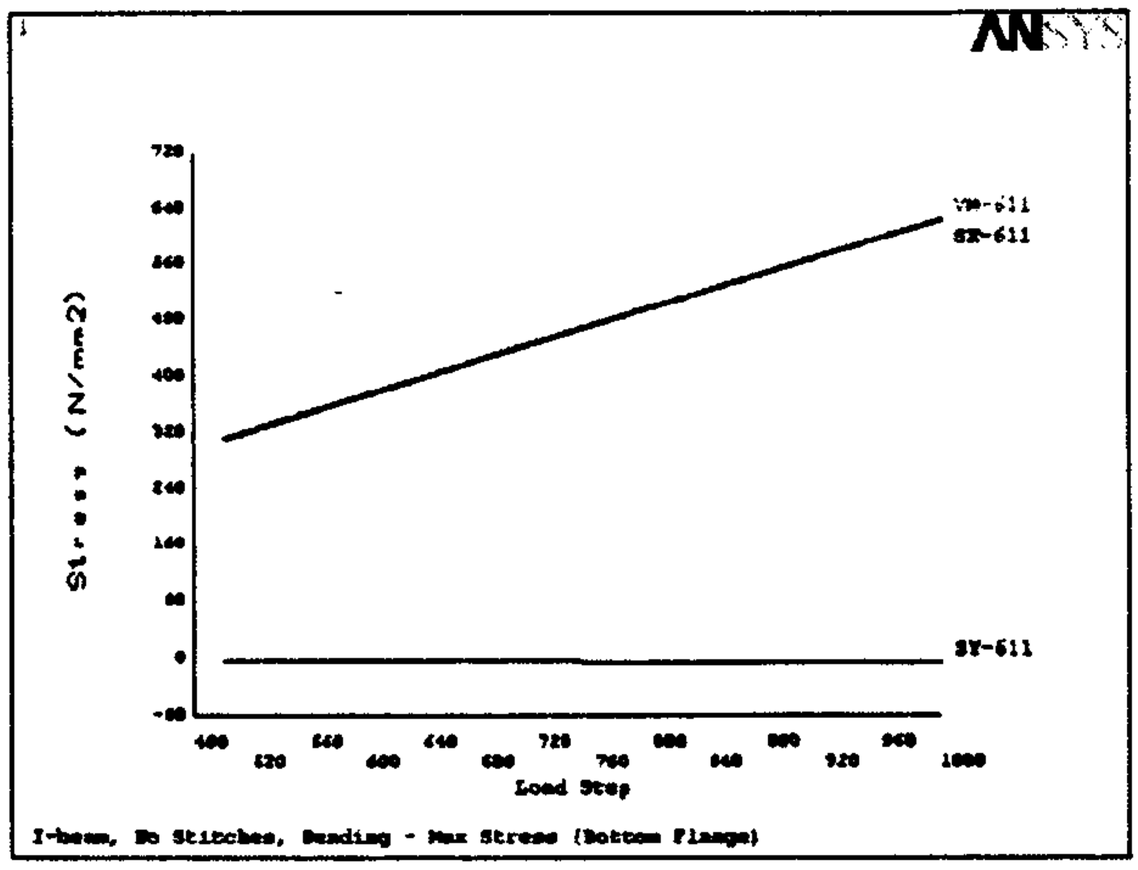

Figure 8.26b bottom flange NS element under max stress (uniform load)

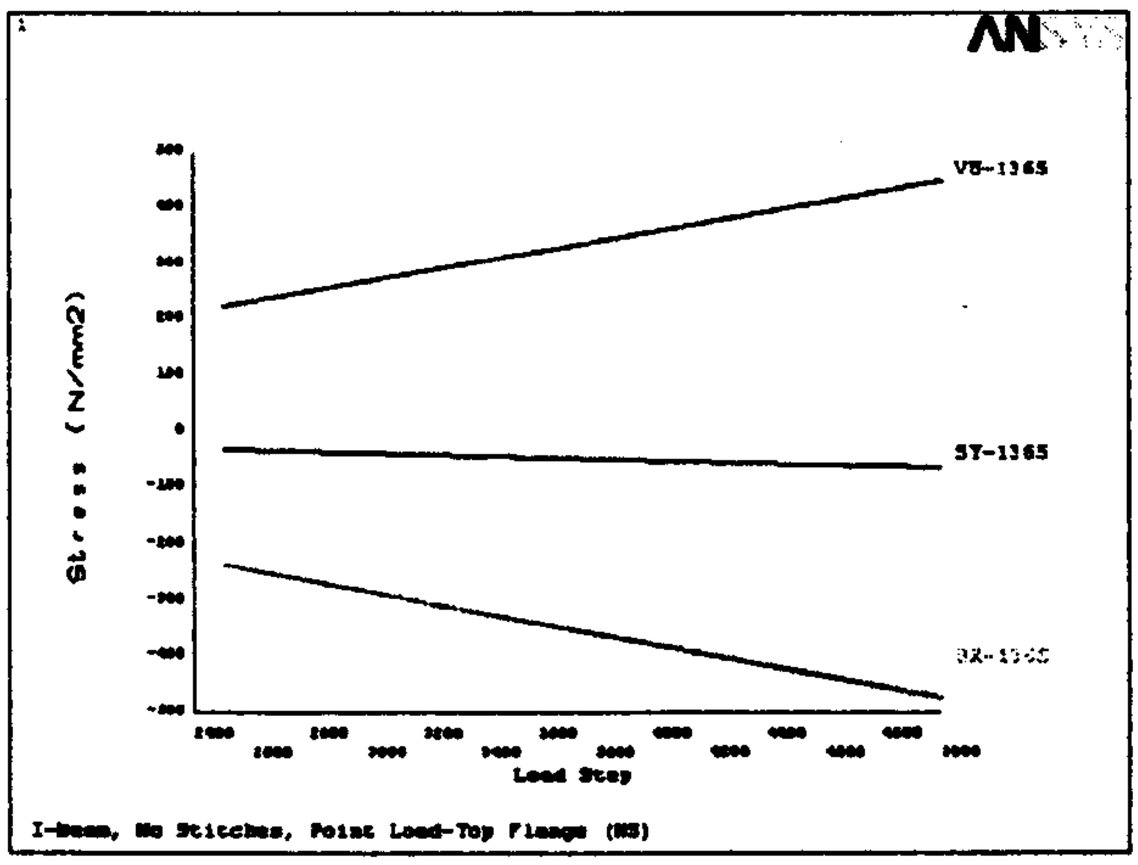

Figure 8.27a Top flange NS element under max stress (concentrated load)

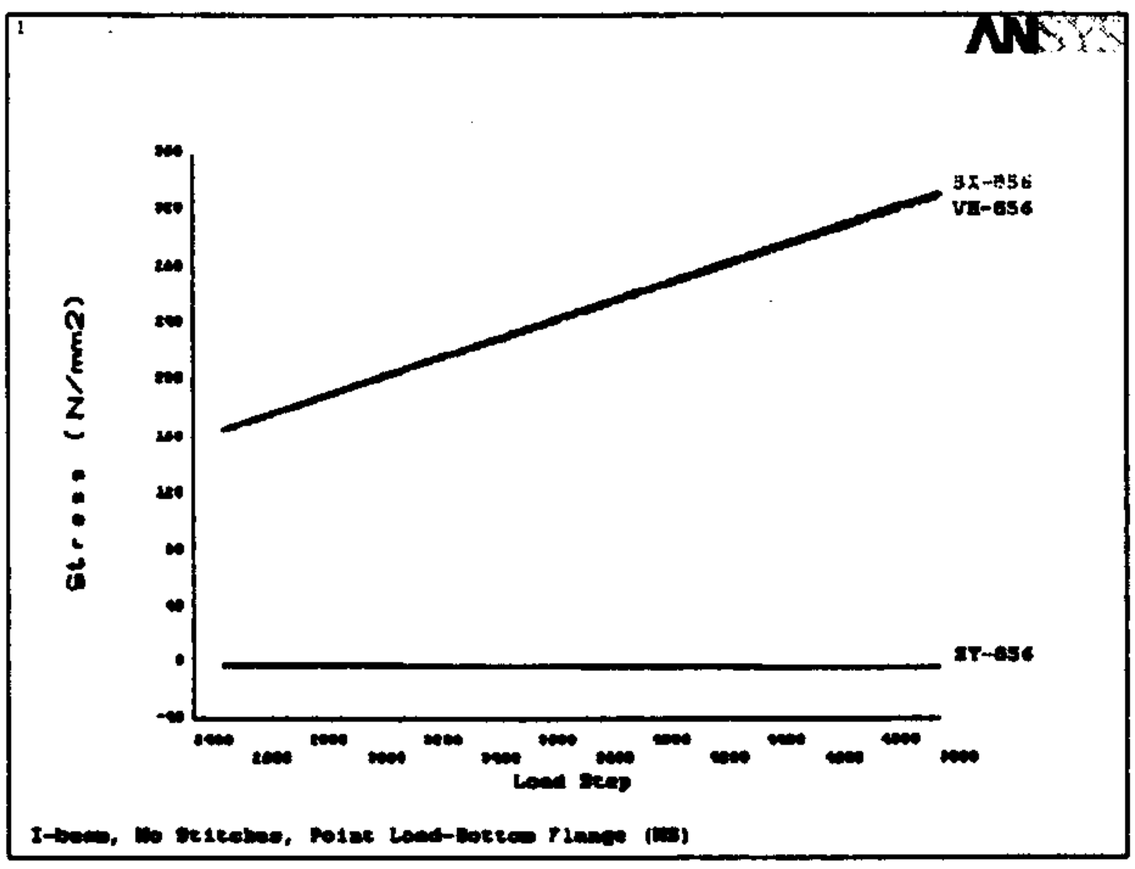

Figure 8.27b bottom flange NS element under max stress (concentrated load)

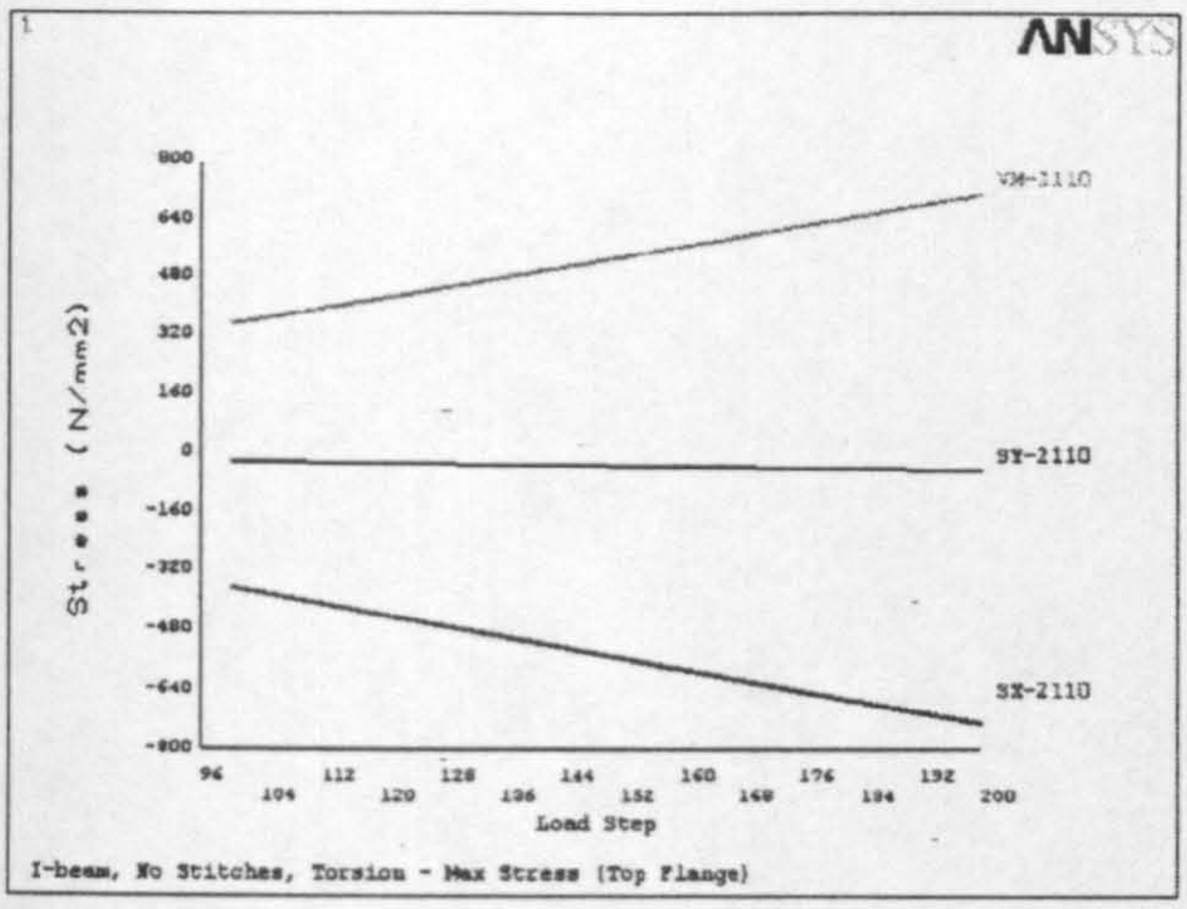

Figure 8.28 top flange NS element under max stress (torsion)

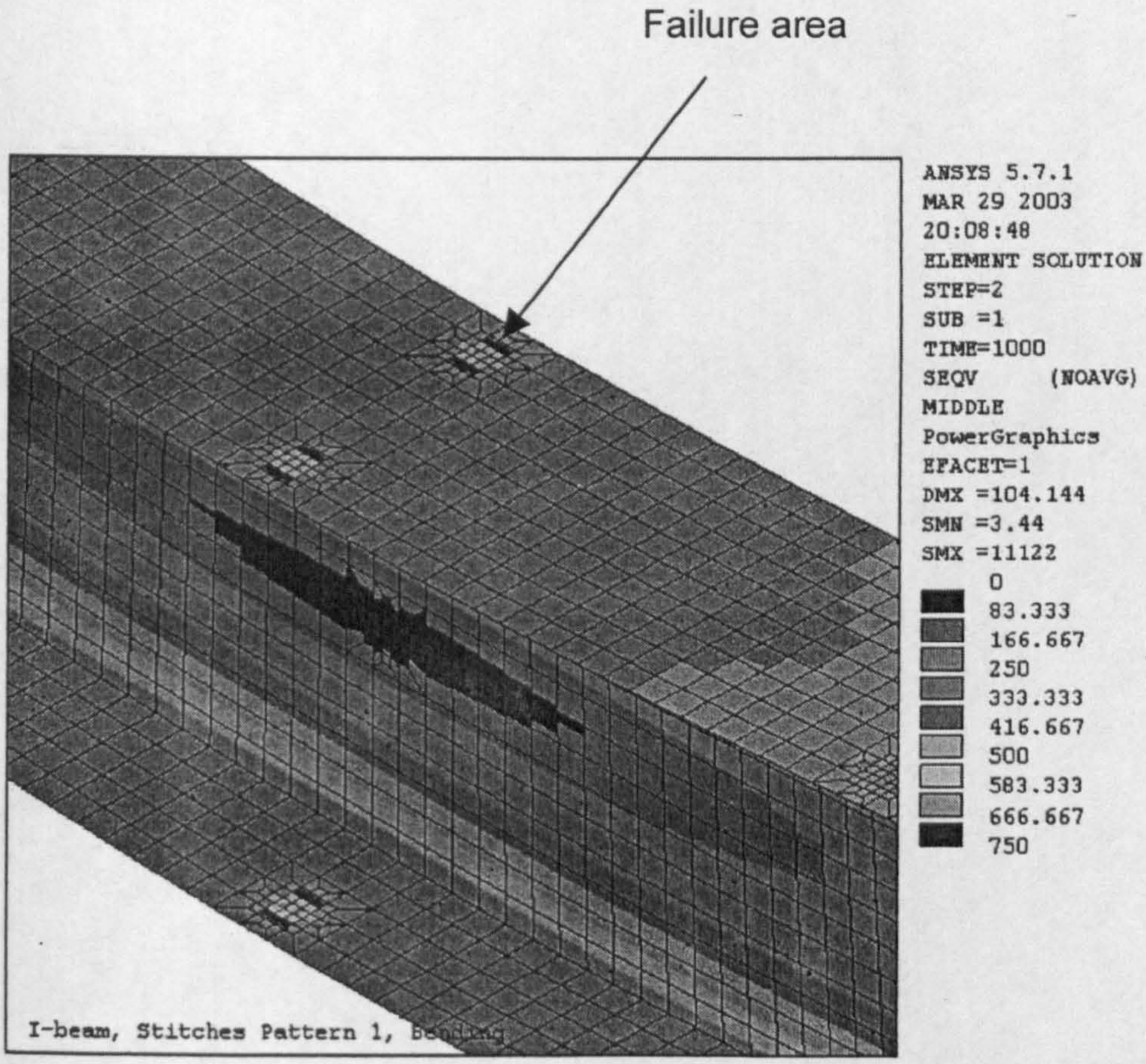

Figure 8.29 I beam S pattern 1 subjected to uniform load

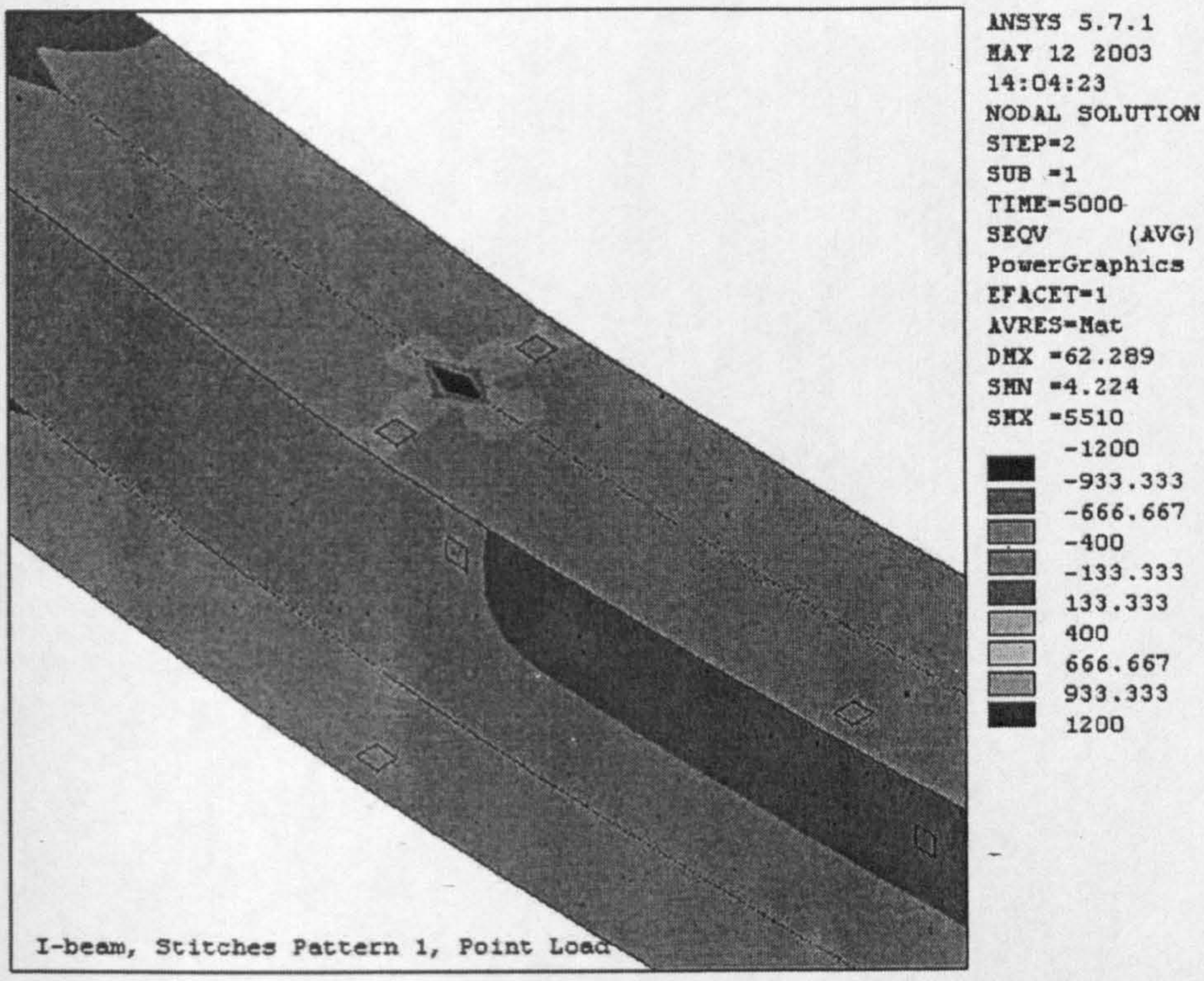

Figure 8.30 I beam S pattern 1 subjected to concentrated load

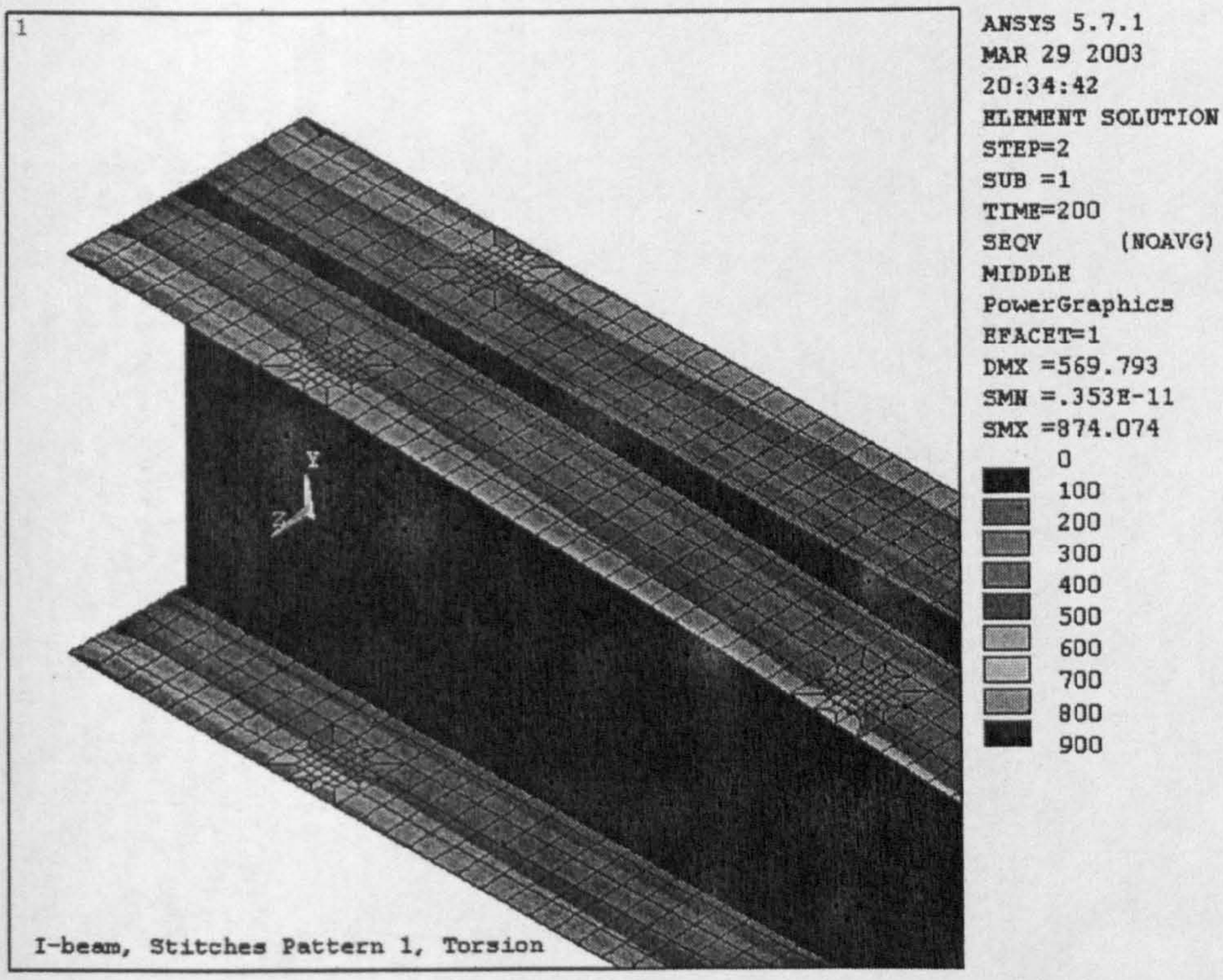

Figure 8.31 I beam S pattern 1 subjected to torsion

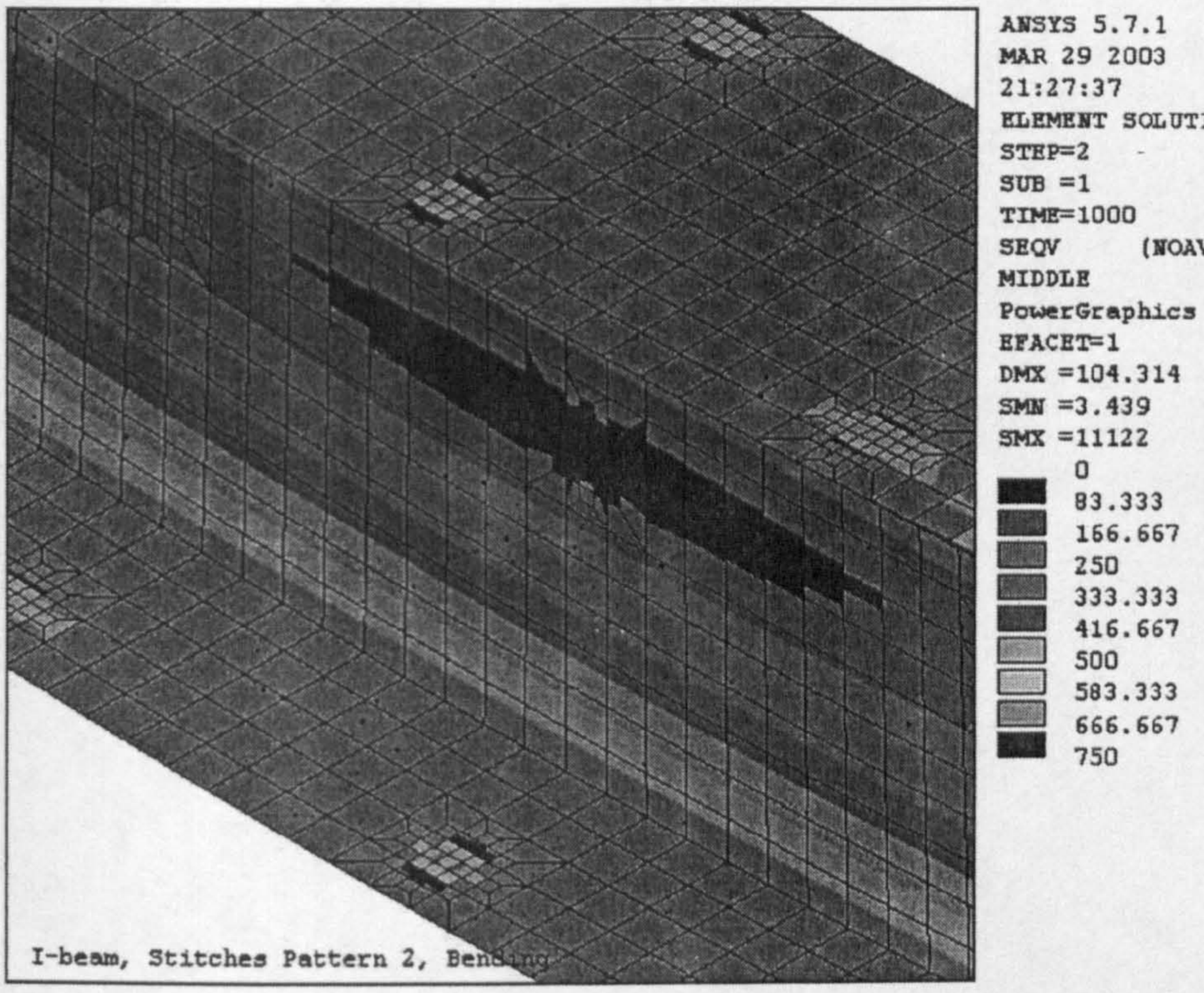

Figure 8.32 I beam S pattern 2 subjected to uniform load

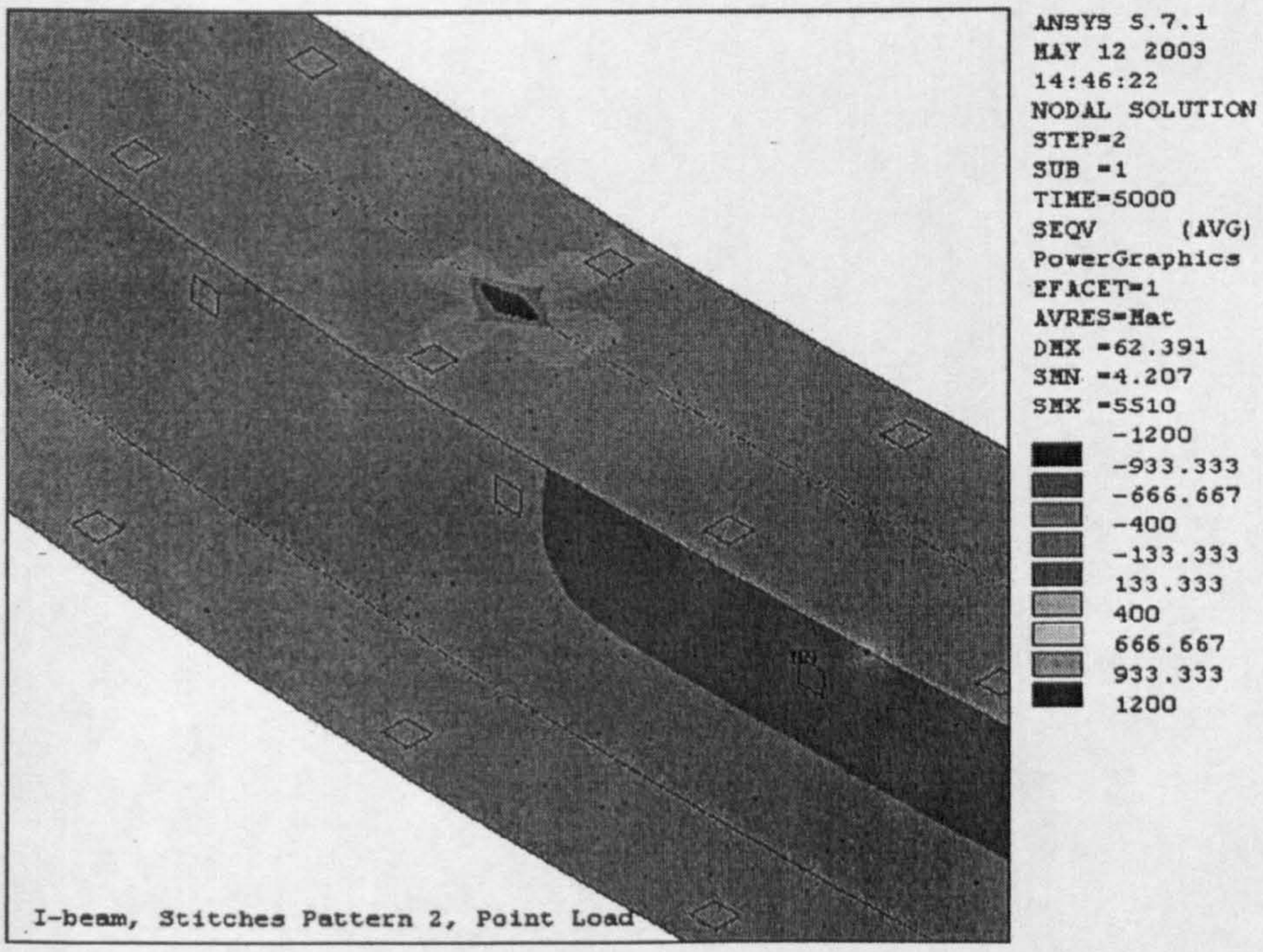

Figure 8.33 I beam S pattern 2 subjected to uniform load

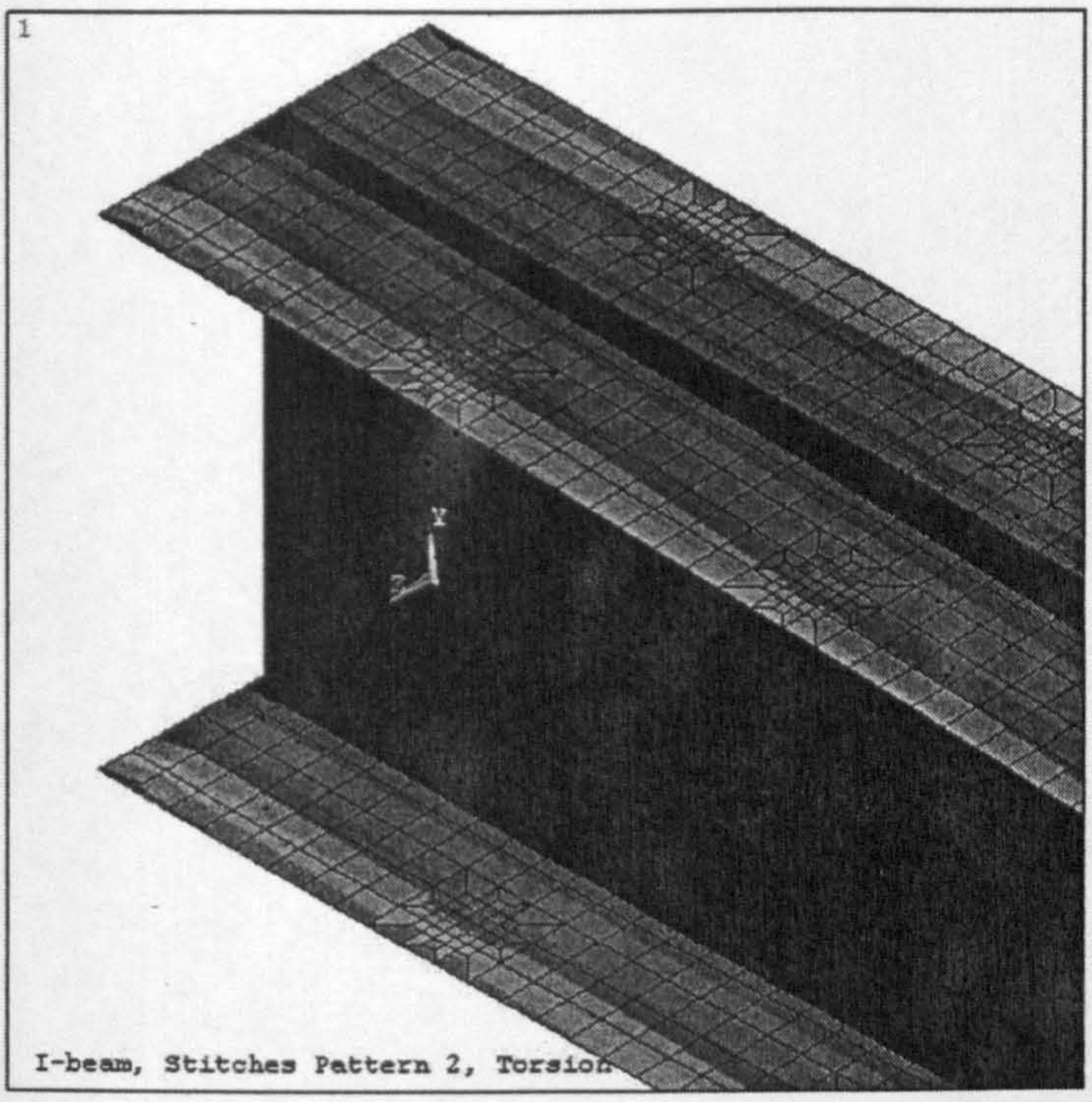

Figure 8.34 I beam S pattern 2 subjected to torsion

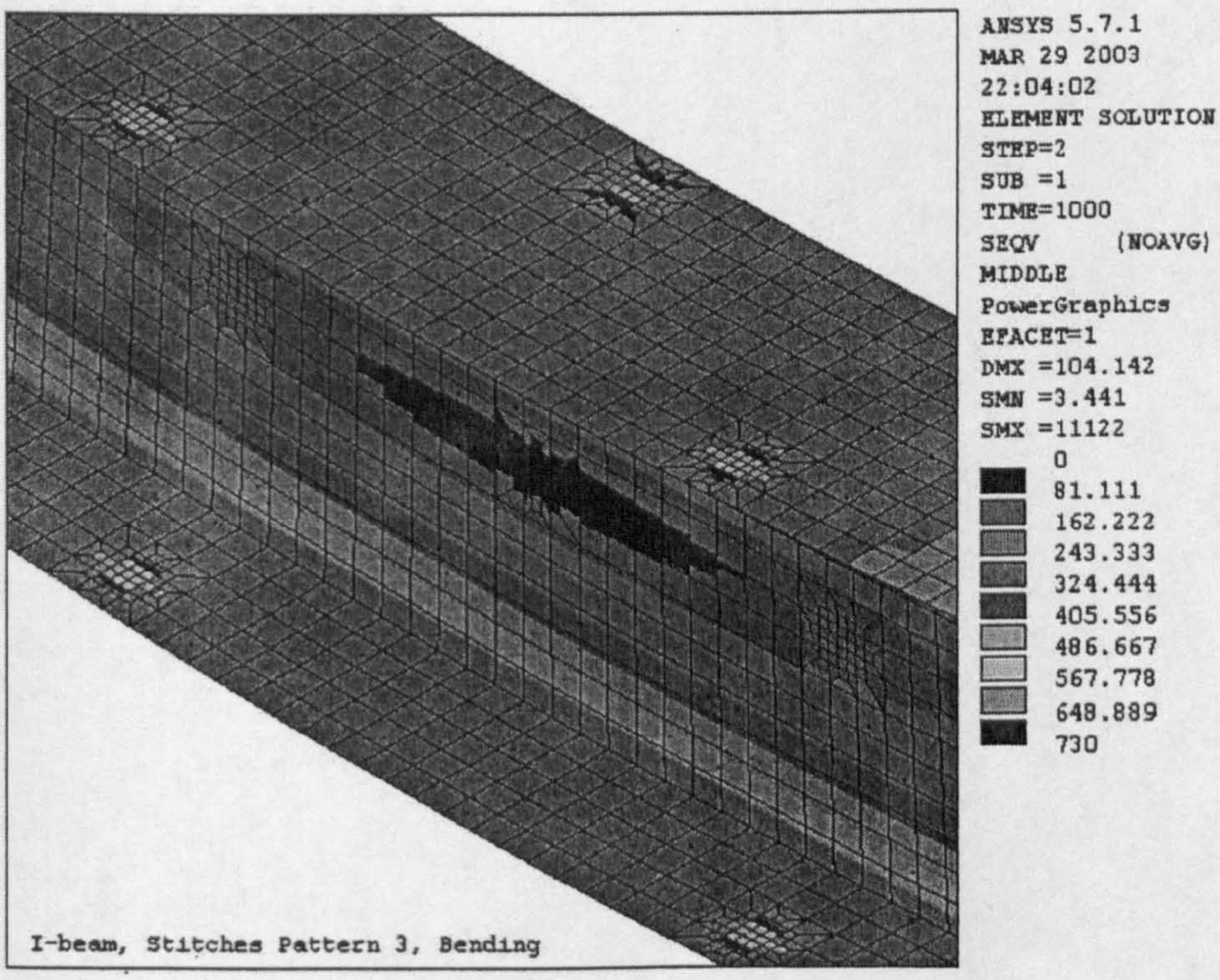

Figure 8.35 I beam S pattern 3 subjected to uniform load

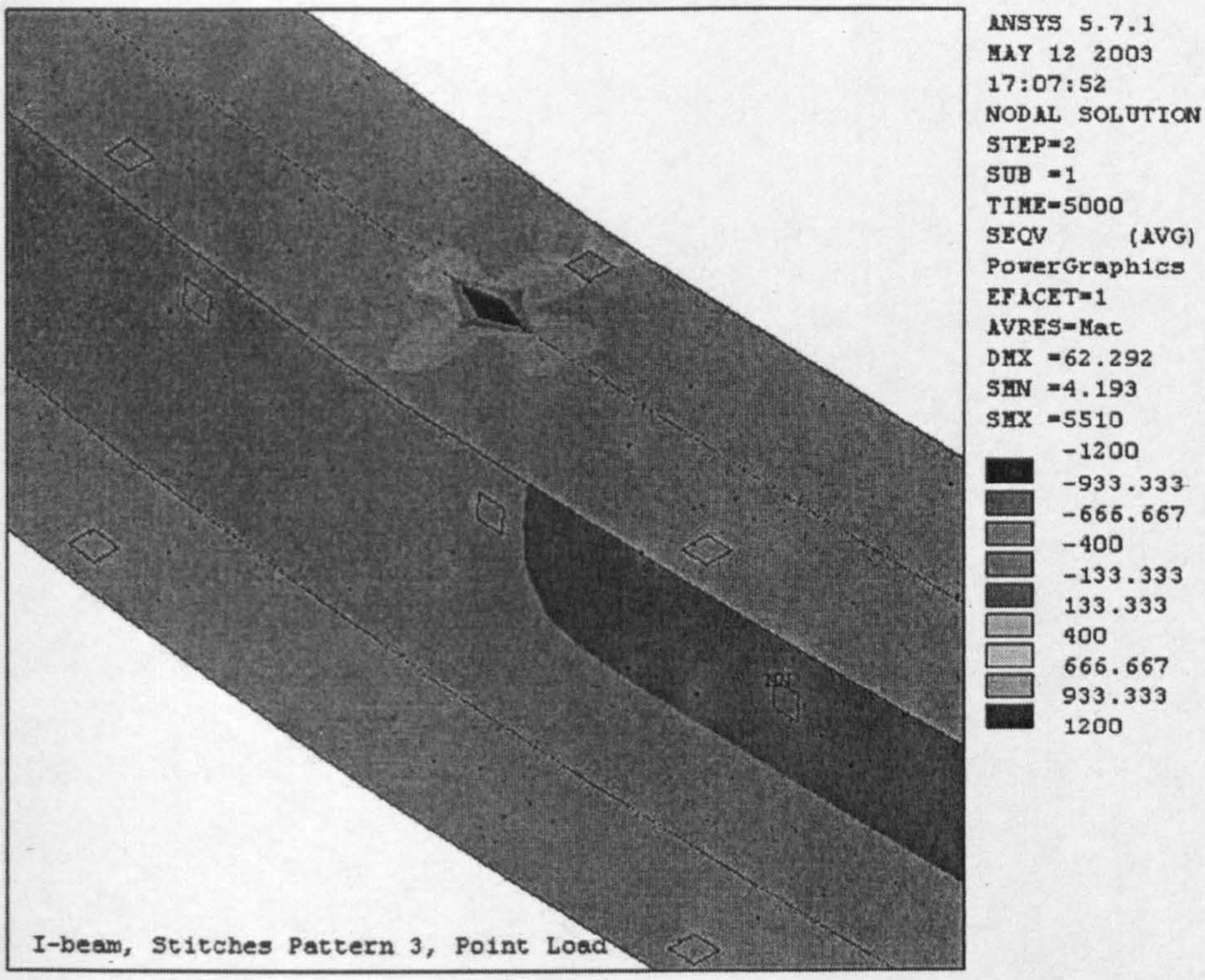

Figure 8.36 I beam S pattern 3 subjected to concentrated load

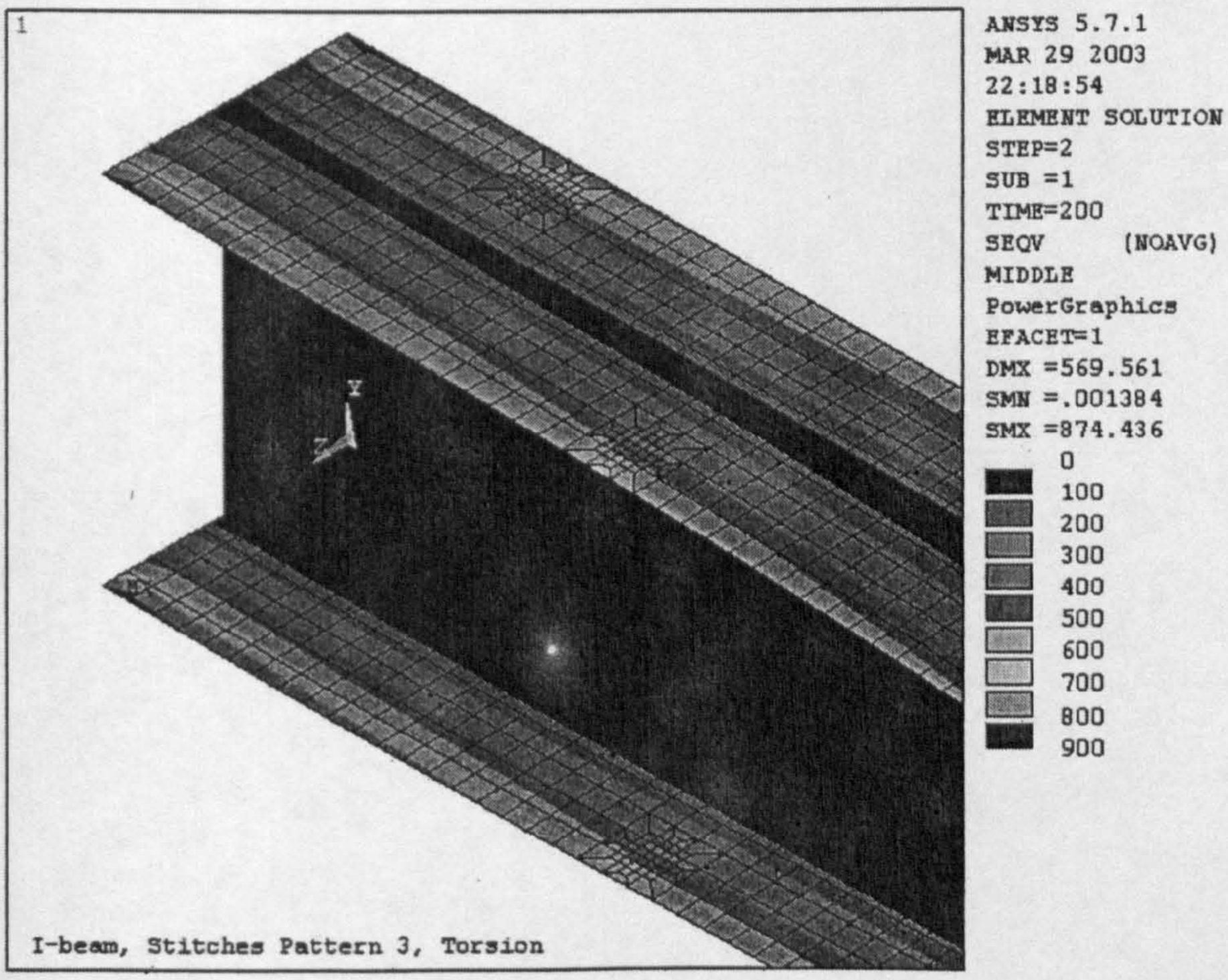

Figure 8.37 I beam S pattern 3 subjected to torsion

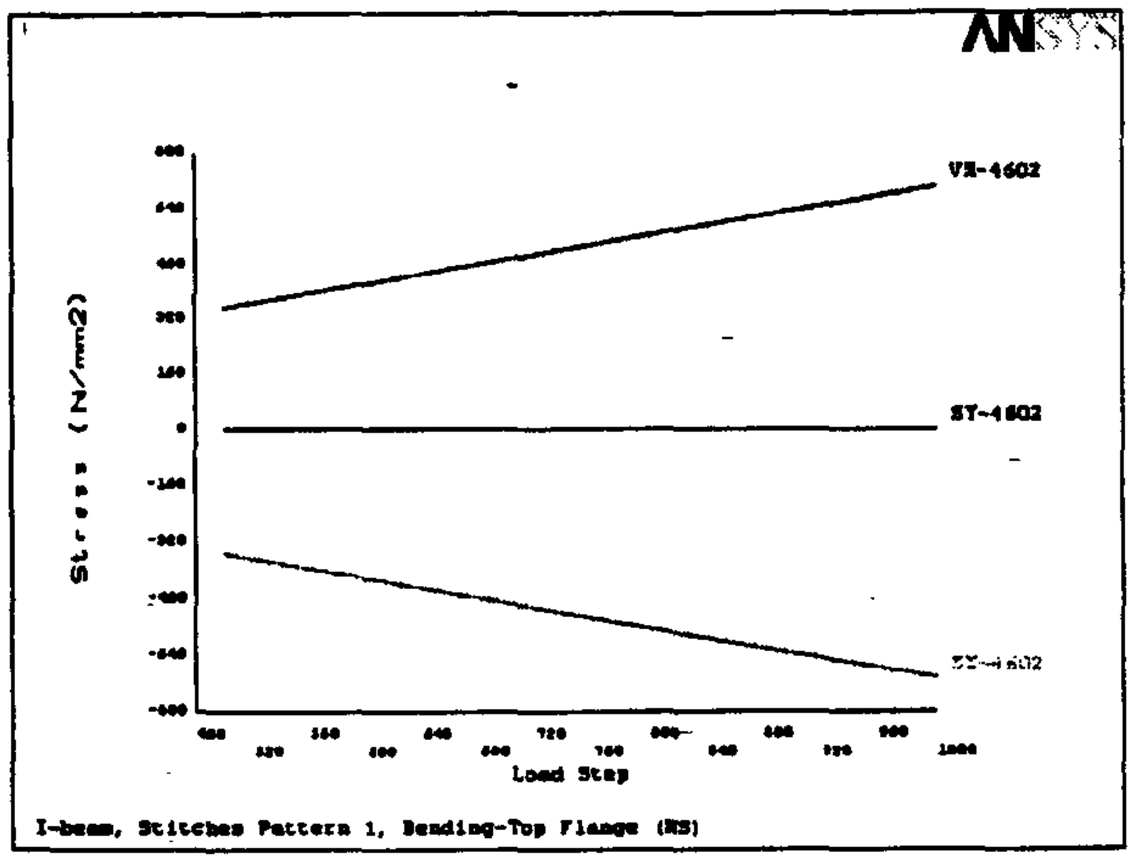

Figure 8.38a top flange S patten 1 element under max stress (uniform load)

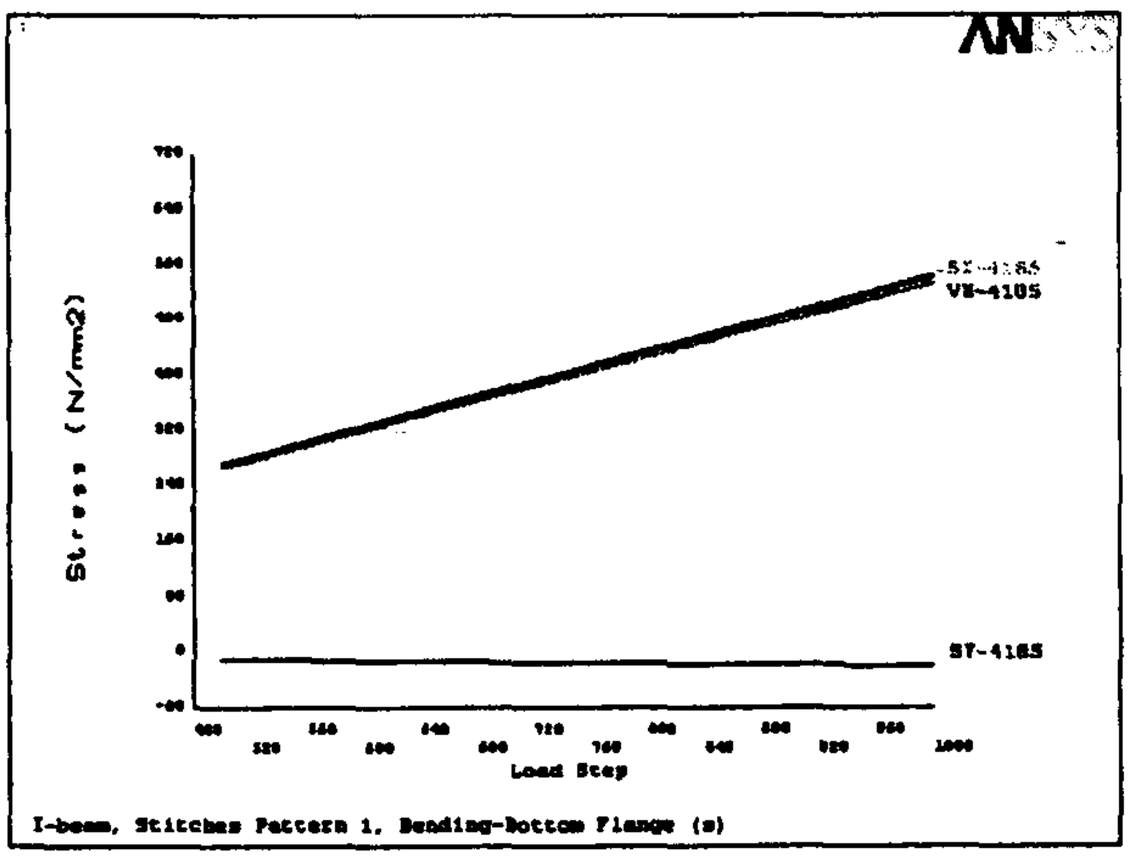

Figure 8.38b bottom flange S pattern 1 element under max stress uniform load)

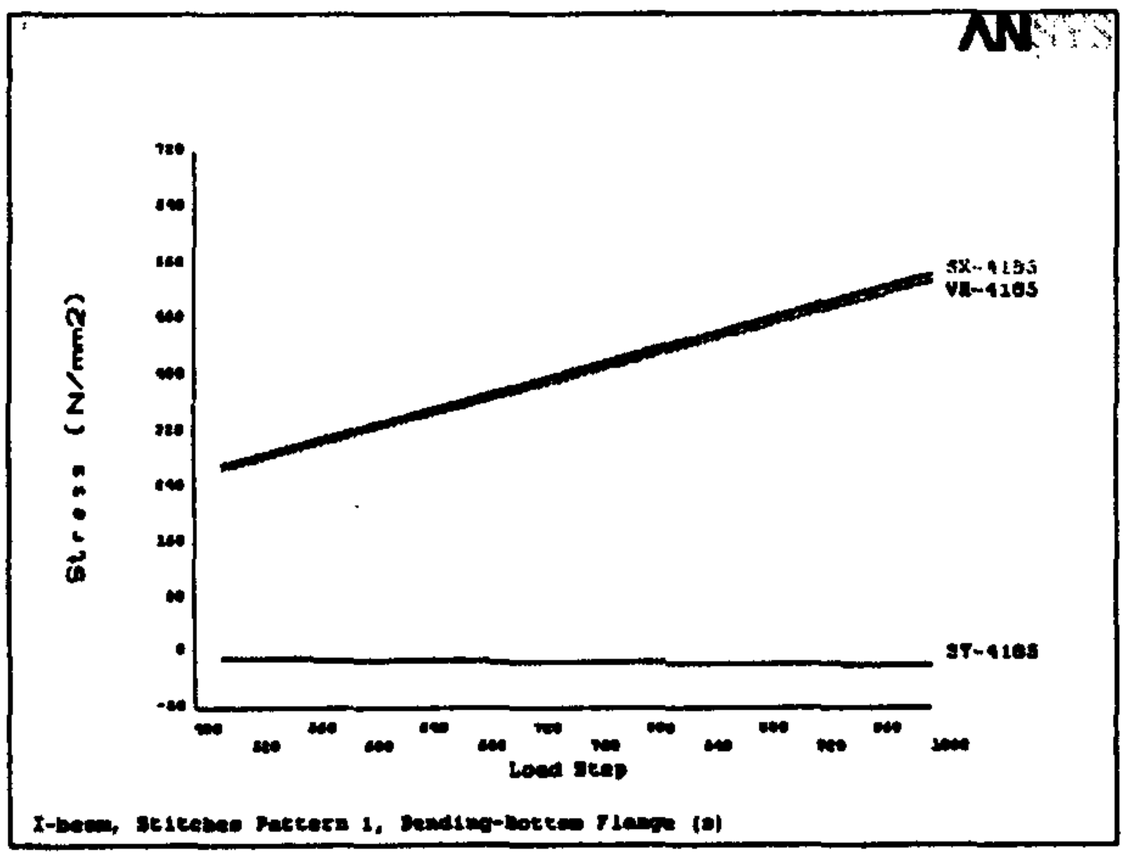

Figure 8.39a Top flange S pattern 2 element under max stress (uniform load)

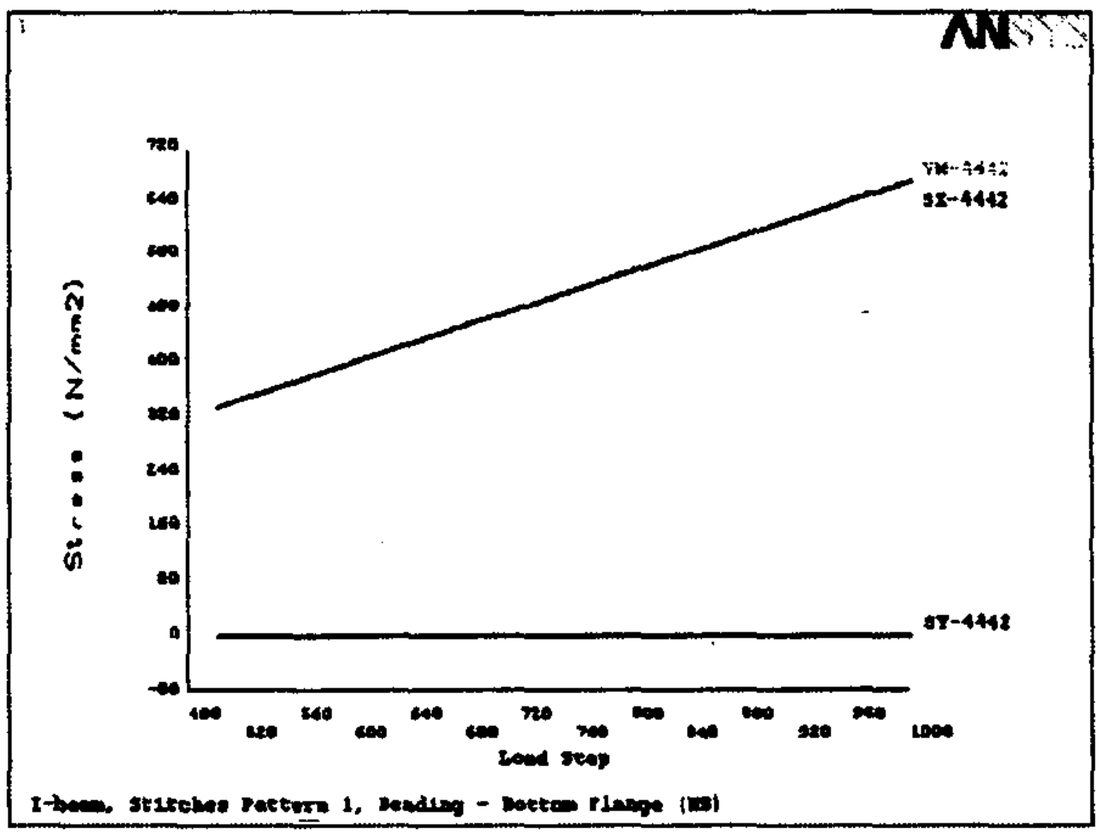

Figure 8.39b bottom flange S pattern 2 element under max stress(uniform load)

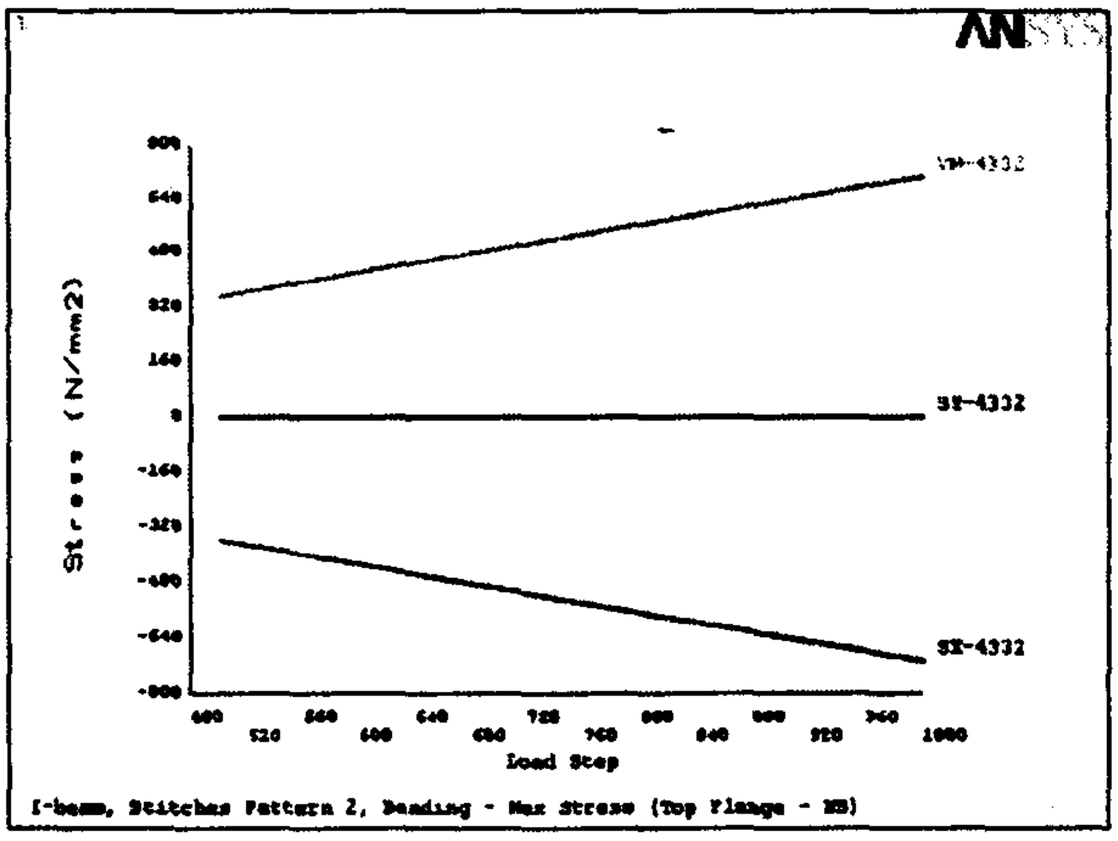

Figure 8.40a top flange S pattern 3 element under max stress (uniform load)

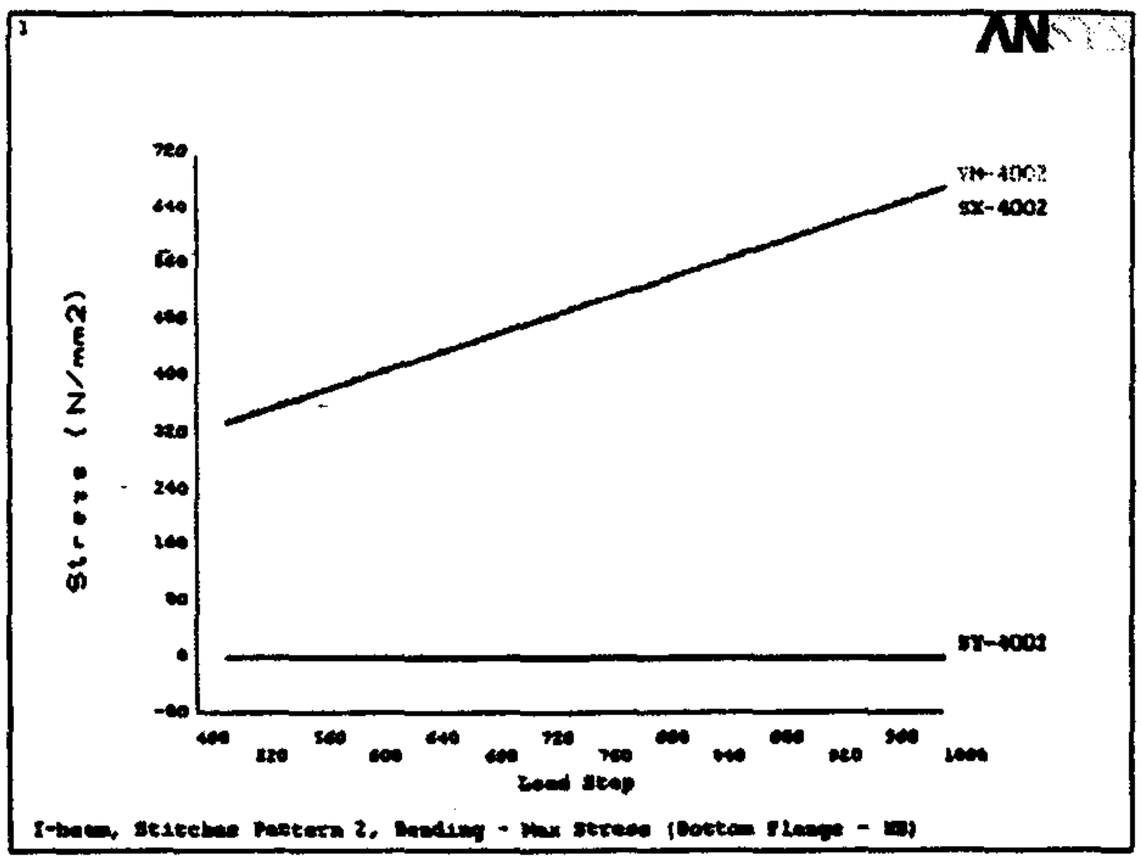

Figure 8.40b bottom flange S pattern 3 element under max stress (uniform load

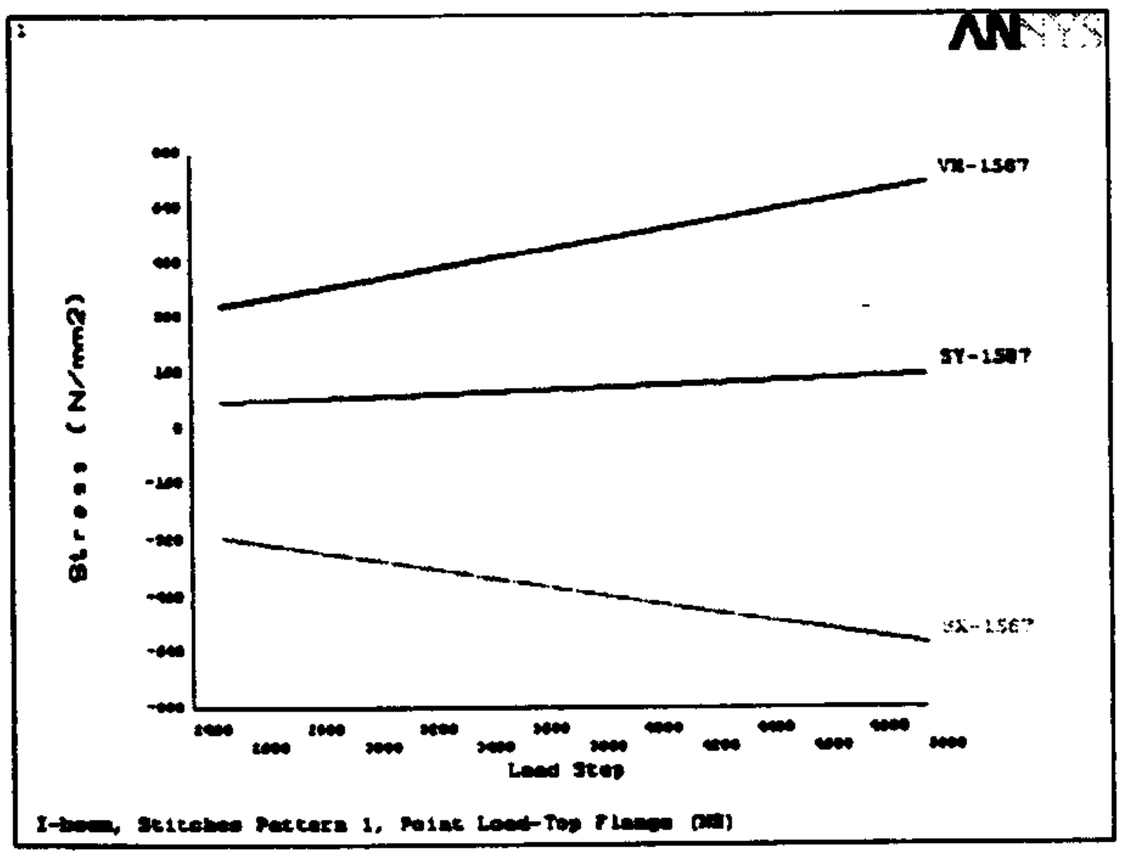

Figure 8.41a top flange S pattern 1 element under max stress(concentrated load)

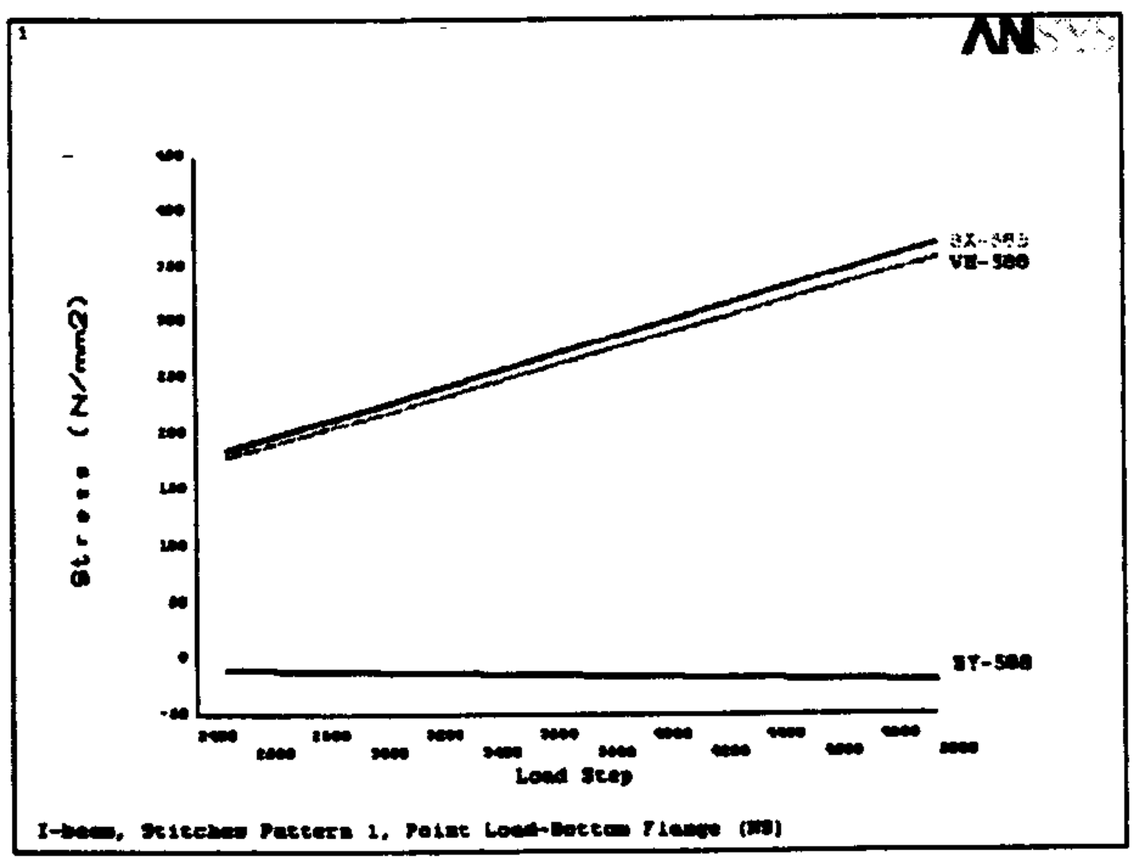

Figure 8.41b bottom flange S pattern 1 element under max stress (concentrated load)

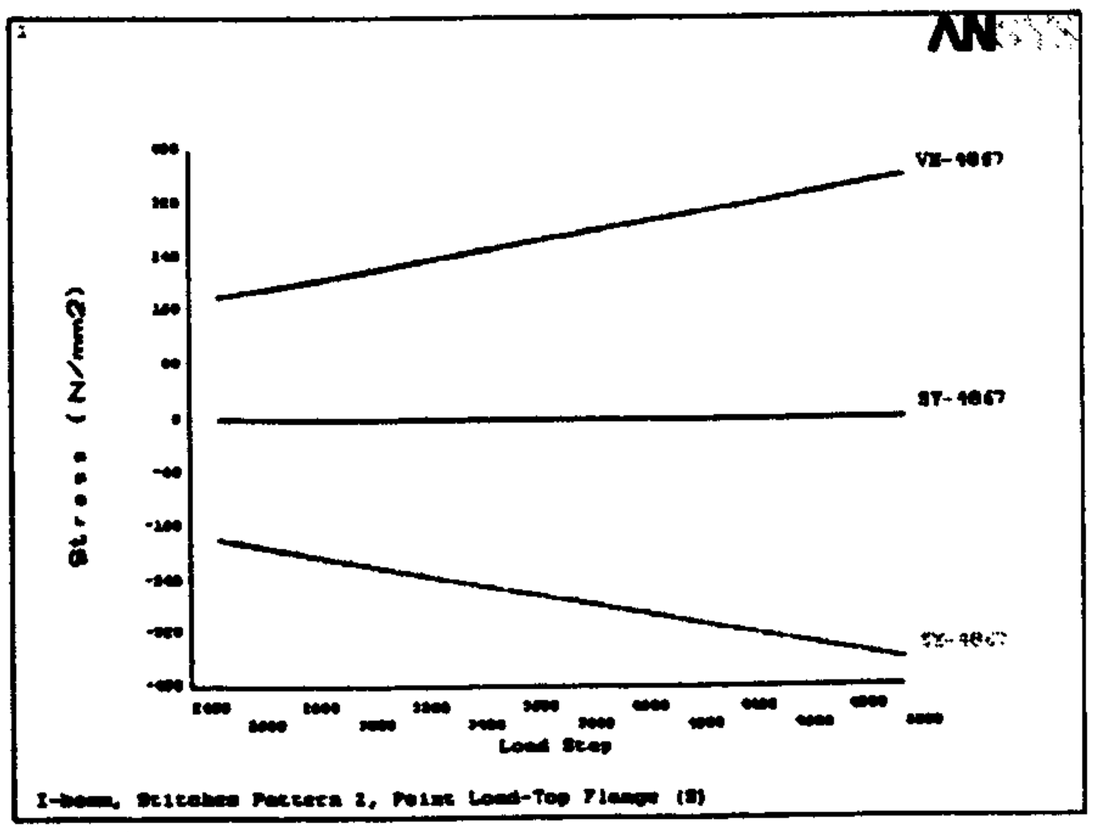

Figure 8.42a top flange S pattern 2 element under max stress (concentrated load

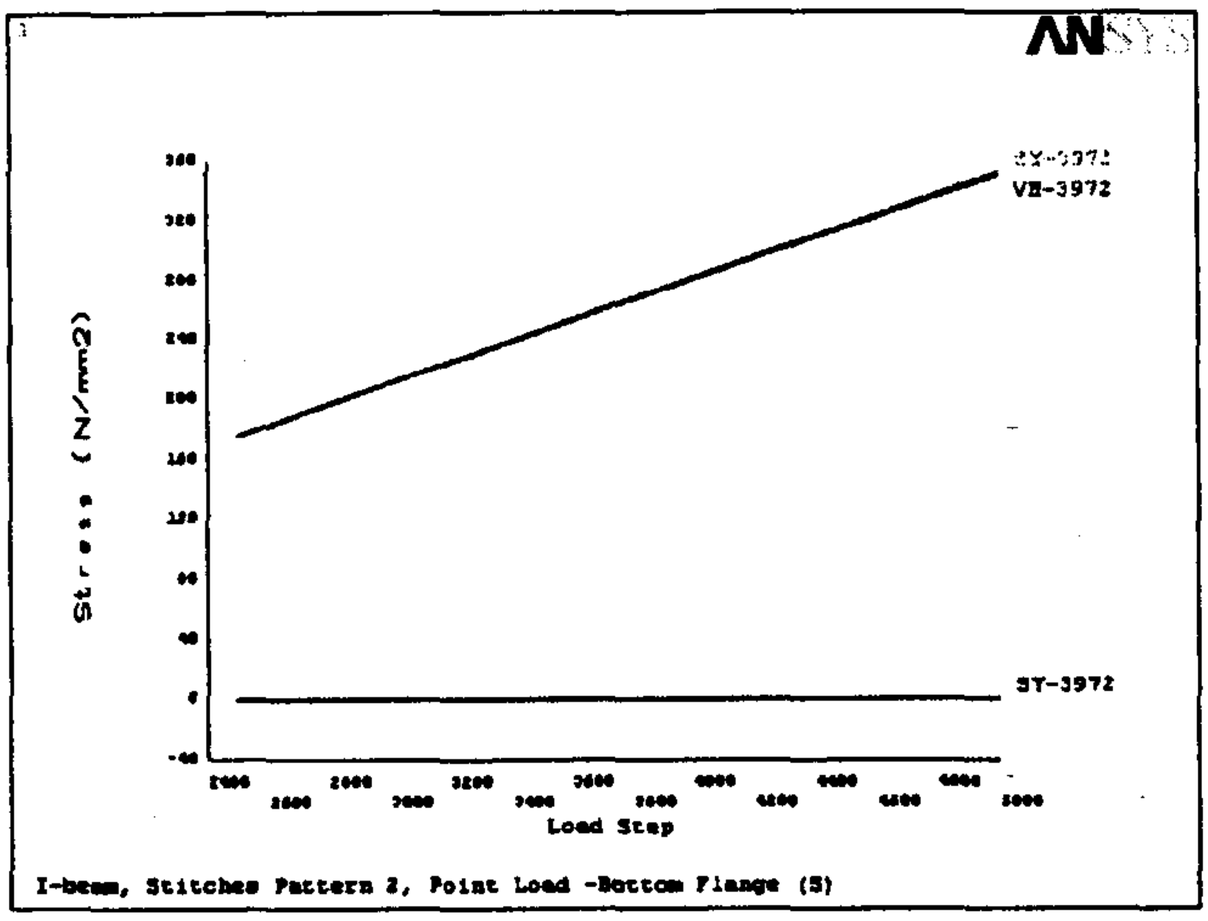

Figure 8.42b bottom flange S pattern 2 element under max stress (concentrated load)

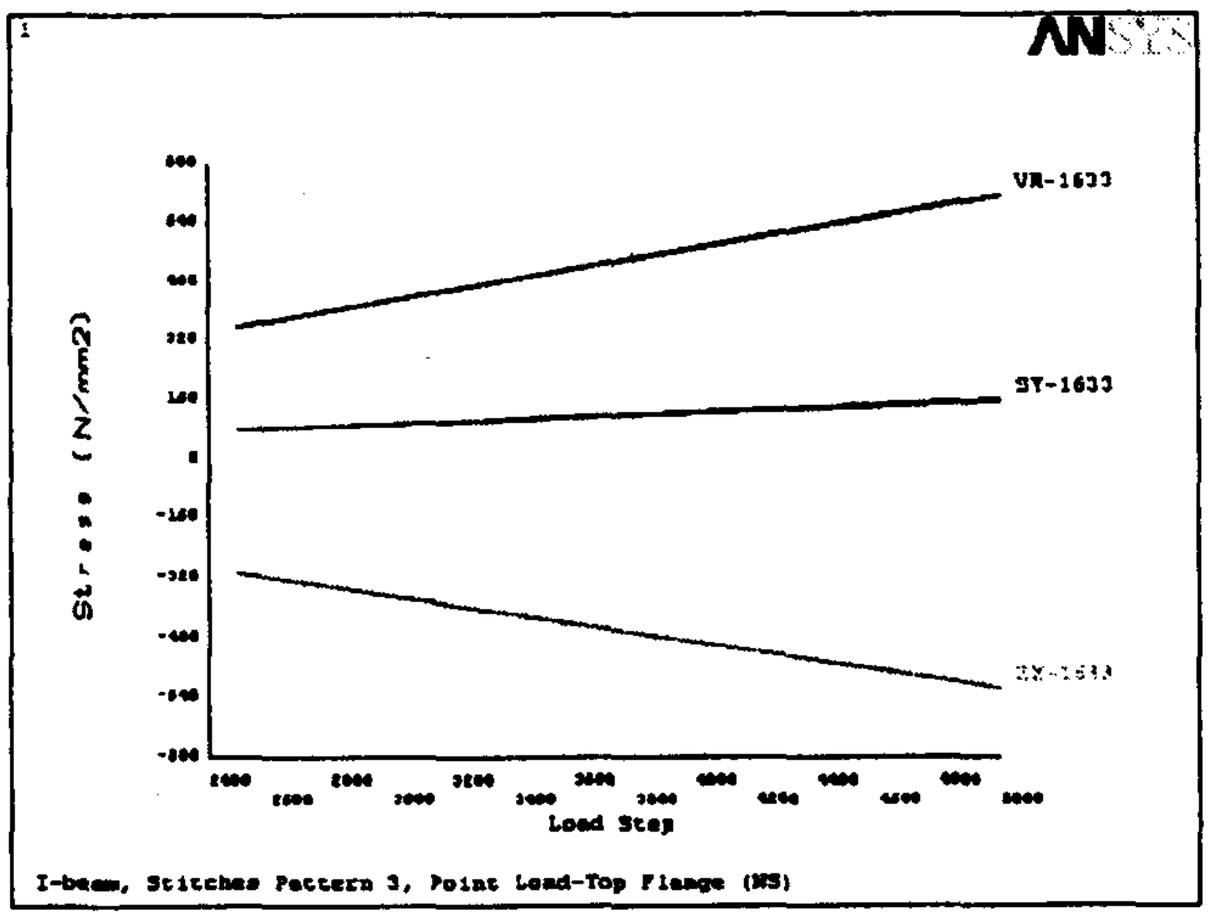

Figure 8.43a top flange S pattern 3 element under max stress (concentrated load

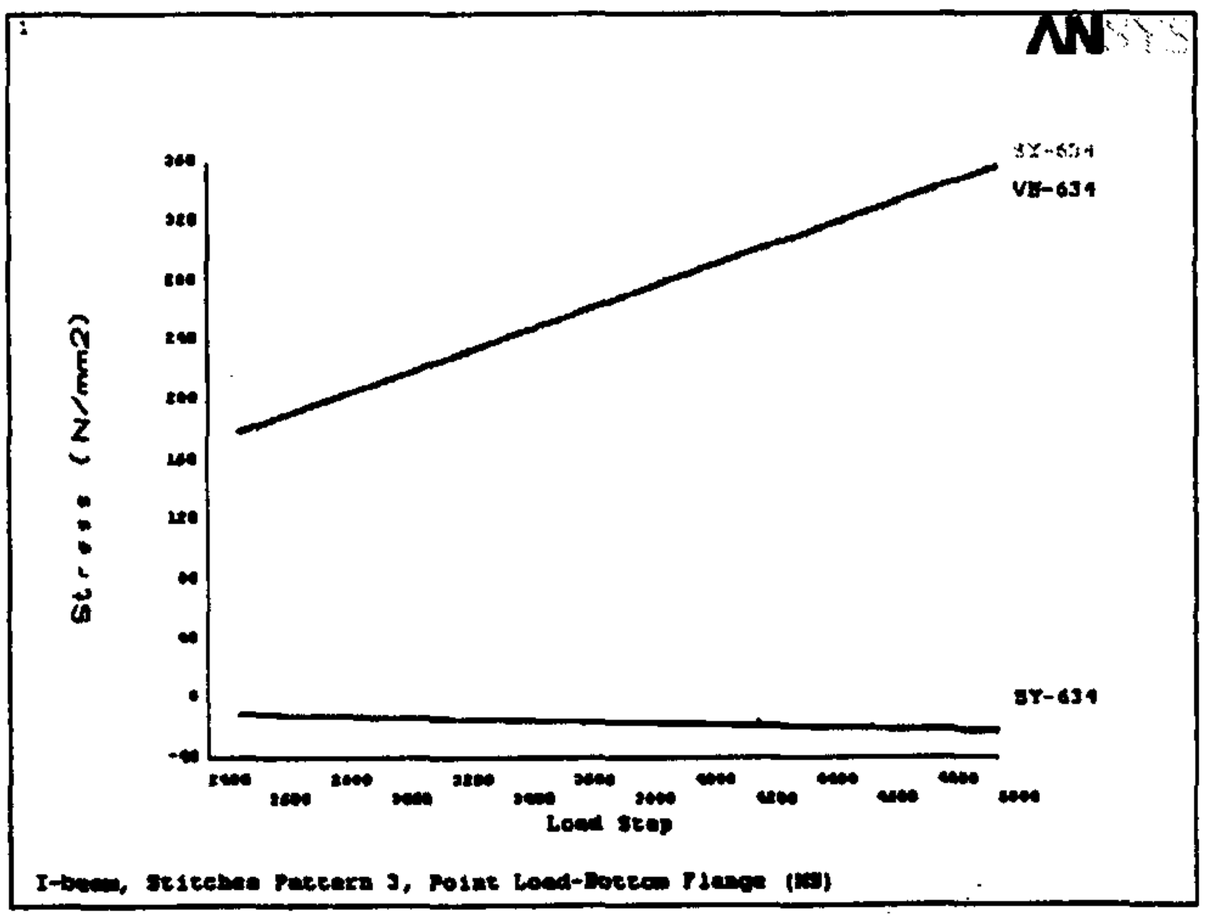

Figure 8.43b bottom flange S pattern 3 element under max stress (concentrated load

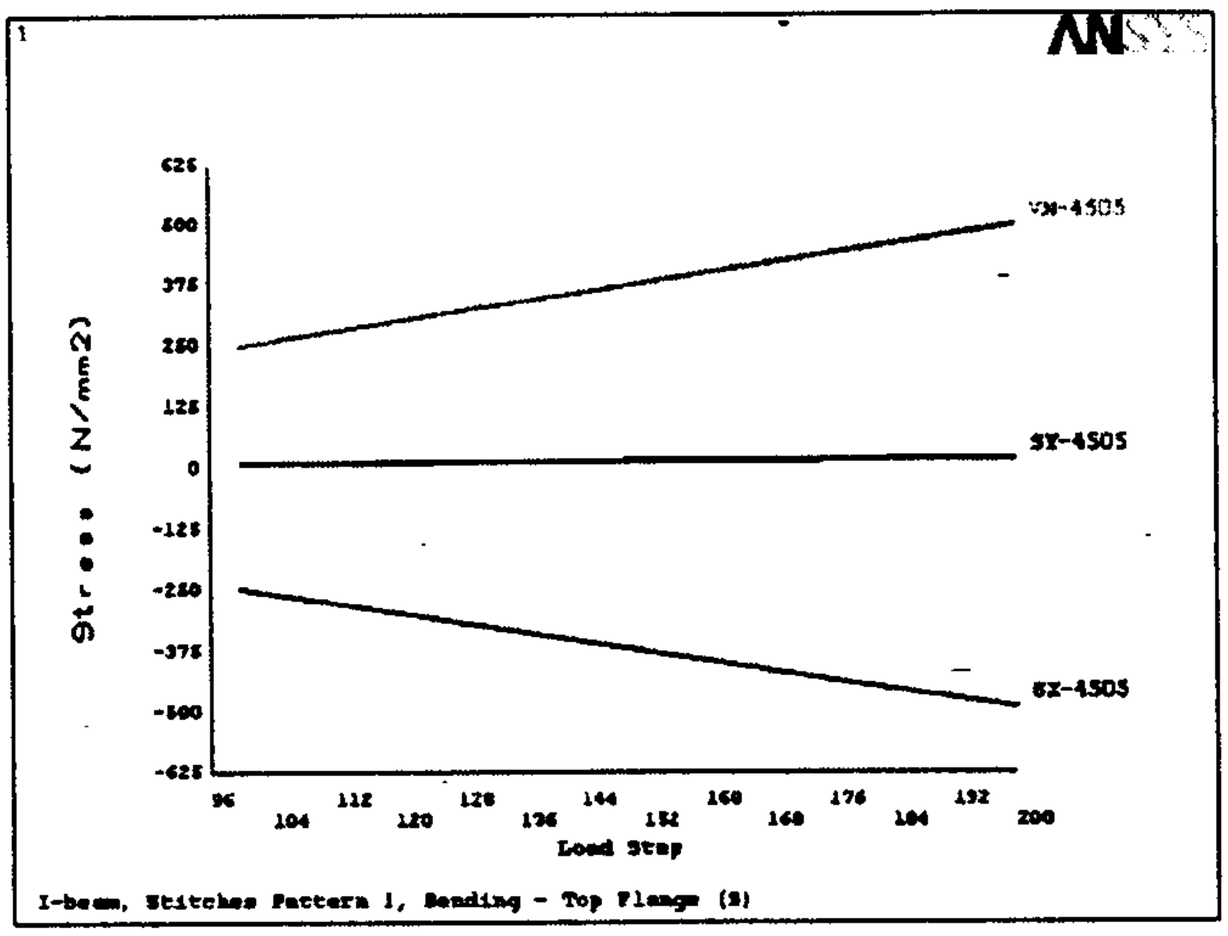

Figure 8.44a top flange S pattern 1 element under max stress (torsion)

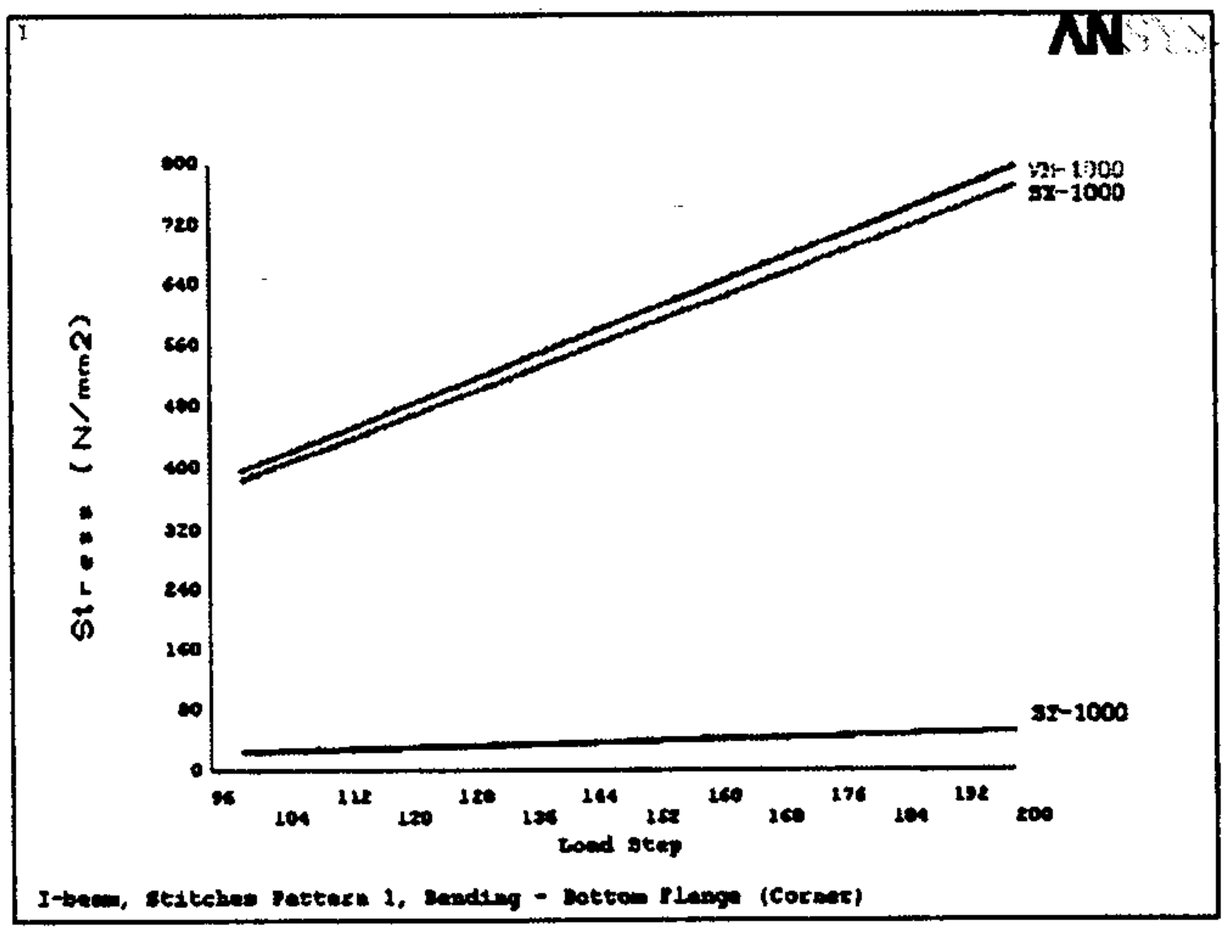

Figure 8.44b bottom flange S pattern 1 element under max stress (torsion)

Table 8.1 failure load for I-beam subjected to uniform and torsional load

Element No.	Element type	critical element Position	Load Type	Failure Load (N/mm)
Pattern 1 200 mm apart between the stitches				
NS-B-611	NS	Bottom Flange	uniform	206.67
NS-B-1726	NS	Top Flange	uniform	177.06
NS-T-1000	NS	Bottom Flange	Torsion	32.40
NS-T-2110	NS	Top Flange	Torsion	35.31
S-B-1-4185	[S]	Bottom Flange	uniform	212.8
S-B-1-4202	S	Bottom Flange	uniform	193.01
S-B-1-4585	[S]	Top Flange	uniform	178.70
S-B-1-4602	S	Top Flange	uniform	164.20
S-T-1-2110	NS-C	Top Flange	Torsion	31.70
S-T-1-1000	NS-C	Bottom Flange	Torsion	32.44
S-T-1-4105	[S]	Bottom Flange	Torsion	44.57
S-T-1-4122	S	Bottom Flange	Torsion	36.91
S-T-1-4505	[S]	Top Flange	Torsion	40.98
S-T-1-4522	S	Top Flange	Torsion	34.55
Pattern 2 100 mm apart between the stitch				
S-B-2-4442	S	Bottom Flange	uniform	193.18
S-B-2-5162	S	Top Flange	uniform	164.21
S-T-2-2110	NS-C	Top Flange	Torsion	31.68
S-T-2-1000	NS-C	Bottom Flange	Torsion	32.42
Pattern 3 Zigzag line stitch				
S-B-3-4002	S	Bottom Flange	uniform	192.49
S-B-3-4332	S	Top Flange	uniform	163.78
S-T-3-2110	NS-C	Top Flange	Torsion	31.70
S-T-3-1000	NS-C	Bottom Flange	Torsion	32.40
S-T-3-3892	S	Bottom Flange	Torsion	37.01
S-T-3-4252	S	Top Flange	Torsion	38.59

Table 8.2 Failure load for non stitched I-beam subjected to concentrated load

Non-Stitch-I-Beam				
Element No.	Element type	critical element Position	Load Type	Failure Load (N/mm)
NS-PL-1365	NS	Top Flange	concentrated	121.96
NS-PL-1411	NS	Top Flange	concentrated	121.61
NS-PL-1920	NS	Top Flange	concentrated	121.96
NS-PL-1966	NS	Top Flange	concentrated	121.61
NS-PL-255	NS	Bottom Flange	concentrated	196.62
NS-PL-301	NS	Bottom Flange	concentrated	195.86
NS-PL-810	NS	Bottom Flange	concentrated	196.62
NS-PL-856	NS	Bottom Flange	concentrated	195.86

Table 8.3 Failure load for stitched pattern 1 under concentrated load

Pattern 1 200 mm apart between the stitches(Point Load)				
Element No.	Element type	critical element Position	Load Type	Failure Load (N/mm)
S-PL-1-4332	S	Top Flange	concentrated	130.52
S-PL-1-4347	[S]	Top Flange	concentrated	139.95
S-PL-1-4345	[S]	Top Flange	concentrated	132.43
S-PL-1-4362	S	Top Flange	concentrated	116.31
S-PL-1-4532	S	Top Flange	concentrated	116.31
S-PL-1-4547	[S]	Top Flange	concentrated	132.43
S-PL-1-4545	[S]	Top Flange	concentrated	139.95
S-PL-1-4562	S	Top Flange	concentrated	130.52
S-PL-1-4412	S	Top Flange	concentrated	130.08
S-PL-1-4427	[S]	Top Flange	concentrated	139.49
S-PL-1-4425	[S]	Top Flange	concentrated	132
S-PL-1-4442	S	Top Flange	concentrated	115.97
S-PL-1-4612	S	Top Flange	concentrated	115.97
S-PL-1-4627	[S]	Top Flange	concentrated	132
S-PL-1-4625	[S]	Top Flange	concentrated	139.49
S-PL-1-4642	S	Top Flange	concentrated	130.08
S-PL-1-4162	S	Bottom Flange	concentrated	183.79
S-PL-1-4145	[S]	Bottom Flange	concentrated	201.91
S-PL-1-4147	[S]	Bottom Flange	concentrated	200.82
S-PL-1-4132	S	Bottom Flange	concentrated	181.60
S-PL-1-3962	S	Bottom Flange	concentrated	181.60
S-PL-1-3945	[S]	Bottom Flange	concentrated	200.82
S-PL-1-3947	[S]	Bottom Flange	concentrated	201.91
S-PL-1-3932	S	Bottom Flange	concentrated	183.79
S-PL-1-4242	S	Bottom Flange	concentrated	183
S-PL-1-4225	[S]	Bottom Flange	concentrated	201.10
S-PL-1-4227	[S]	Bottom Flange	concentrated	200
S-PL-1-4212	S	Bottom Flange	concentrated	180.89
S-PL-1-4042	S	Bottom Flange	concentrated	180.89
S-PL-1-4025	[S]	Bottom Flange	concentrated	200
S-PL-1-4027	[S]	Bottom Flange	concentrated	201.10
S-PL-1-4012	S	Bottom Flange	concentrated	183

Table 8.4 Failure load for stitched pattern 2 under concentrated load

Pattern 2 100 mm apart between the stitches(concentrated load)				
Element No.	Element type	Stitch Position-	Load Type	Failure Load (N/mm)
S-PL-1-4692	S	Top Flange	concentrated	130.58
S-PL-1-4707	[S]	Top Flange	concentrated	140
S-PL-1-4705	[S]	Top Flange	concentrated	132.47
S-PL-1-4722	S	Top Flange	concentrated	116.34
S-PL-1-5052	S	Top Flange	concentrated	116.34
S-PL-1-5067	[S]	Top Flange	concentrated	132,47
S-PL-1-5065	[S]	Top Flange	concentrated	140
S-PL-1-5082	S	Top Flange	concentrated	130.58
S-PL-1-4852	S	Top Flange	concentrated	130.14
S-PL-1-4867	[S]	Top Flange	concentrated	139.55
S-PL-1-4865	[S]	Top Flange	concentrated	132
S-PL-1-4882	S	Top Flange	concentrated	116
S-PL-1-5212	S	Top Flange	concentrated	116
S-PL-1-5227	[S]	Top Flange	concentrated	132
S-PL-1-5225	[S]	Top Flange	concentrated	139.55
S-PL-1-5242	S	Top Flange	concentrated	130.14
S-PL-1-4362	S	Bottom Flange	concentrated	183.90
S-PL-1-4345	[S]	Bottom Flange	concentrated	202
S-PL-1-4347	[S]	Bottom Flange	concentrated	202.91
S-PL-1-4332	S	Bottom Flange	concentrated	181.67
S-PL-1-4002	S	Bottom Flange	concentrated	181.67
S-PL-1-3985	[S]	Bottom Flange	concentrated	202.91
S-PL-1-3987	[S]	Bottom Flange	concentrated	202
S-PL-1-3972	S	Bottom Flange	concentrated	183.90
S-PL-1-4522	S	Bottom Flange	concentrated	183.17
S-PL-1-4505	[S]	Bottom Flange	concentrated	201.22
S-PL-1-4507	[S]	Bottom Flange	concentrated	202.12
S-PL-1-4492	S	Bottom Flange	concentrated	180.95
S-PL-1-4162	S	Bottom Flange	concentrated	180.95
S-PL-1-4145	[S]	Bottom Flange	concentrated	202.12
S-PL-1-4147	[S]	Bottom Flange	concentrated	201.22
S-PL-1-4132	S	Bottom Flange	concentrated	183.17

Table 8.5 Failure load for stitched pattern 3 under concentrated load

Pattern 3 Zigzag line (Point Load)				
Element No.	Element type	critical element Position	Load Type	Failure Load (N/mm)
S-PL-1-4292	S	Top Flange	Concentrated	130.15
S-PL-1-4307	[S]	Top Flange	Concentrated	139.64
S-PL-1-4305	[S]	Top Flange	Concentrated	132.23
S-PL-1-4322	S	Top Flange	Concentrated	116.18
S-PL-1-4372	S	Top Flange	Concentrated	129.72
S-PL-1-4387	[S]	Top Flange	Concentrated	139.18
S-PL-1-4385	[S]	Top Flange	Concentrated	131.82
S-PL-1-4402	S	Top Flange	Concentrated	115.83
S-PL-1-3962	S	Bottom Flange	Concentrated	181.42
S-PL-1-3945	[S]	Bottom Flange	Concentrated	200.54
S-PL-1-3947	[S]	Bottom Flange	Concentrated	201.47
S-PL-1-3932	S	Bottom Flange	Concentrated	183.28
S-PL-1-4042	S	Bottom Flange	Concentrated	180.71
S-PL-1-4025	[S]	Bottom Flange	Concentrated	199.75
S-PL-1-4027	[S]	Bottom Flange	Concentrated	200.67
S-PL-1-4012	S	Bottom Flange	Concentrated	182.55

Table 8.6 summary: comparison of Max failure loads between stitched and non stitched beam cases

Element No	Load type	Element type	Critical element position	Failure Load N/mm	percentage difference %
NS-B-1726	uniform	NS	Top Flange	177	7.5
S-B-3-4332		S	Top Flange	164	
NS-B-611	uniform	NS	Bottom Flange	207	6.7
S-B-3-4002		S	Bottom Flange	192	
NS-PL-1966	concentrated	NS	Top Flange	122	4.8
S-PL-3-4402		S	Top Flange	116	
NS-PL-301	concentrated	NS	Bottom Flange	196	7.7
S-PL-3-4042		S	Bottom Flange	181	
NS-T-1000	Torsion	NS	Bottom Flange	32.40	0
S-T-3-1000	Torsion	S	Bottom Flange	32.40	

8.5 Conclusion

A Finite Element Analysis was conducted to investigate the stitches and their patterns on the strength of typical I-beams model of the reinforcement structures.

In order to determine the properties of the material used, simple compression and tension tests have been carries out. To this end, simple stitched and non stitched specimens have been cut from the consolidated panels using a diamond cutter and tested in both the 0° and 90° fibre orientations. ten specimens have been loaded for each material per orientation and the average material properties (elastic modulus, Poisson's ratio and failure stress) determined for each case.

Simple uniaxial FE models have then been developed using the material properties that were determined experimentally. Those models were

successfully validated against the test data and used as a basis from which the main models were generated.

These latter FE models were employed to conduct a series of analyses on typical I-beams with a variation of stitch patterns and loading conditions. the investigation has shown that the stitches would reduce the strength of the beam by 8% at the most.

Hence, it can be concluded that the stitching operation adopted in the proposed manufacturing process has reduced the load carrying capacity, or behaviour, of the structural beams made of a dry carbon fibre composite by 8%.

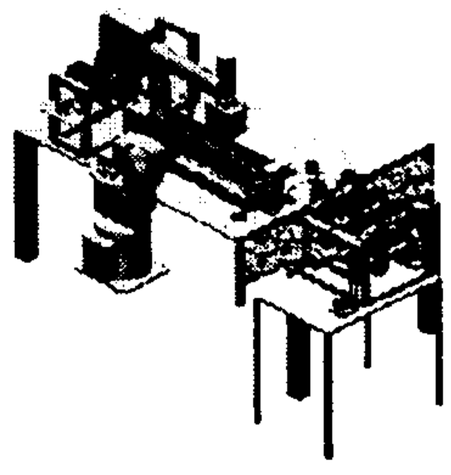

Chapter 9 Conclusions and further work

9.1 Summary of Findings

9.1.1 Review of the literature

A literature survey has been conducted to provide brief account of composite material, their properties and their importance in the aerospace industry. It was concluded that composite materials have excellent structural properties, and where their application is correctly selected a much-improved product from the fatigue, corrosion and weight aspect is achieved. The survey also highlighted the importance of advanced composite materials in terms of their application in aerostructures mainly due to their weight reduction potential that cannot be achieved with metals. Thus adequate industrialised fabrication techniques have to be developed to allow complex part manufacture at low cost .

9.1.2 Joining and manipulation technique

Various means of attachments have been discussed in details. This included the use of blind stitching to join the composite structures. This method has been adopted and developed as a robotic tacking device (RTD), which has been integrated in the automated cell to form a series of stitches to join the composite plies, A number of manipulation and control techniques were also discussed. It was concluded that previous techniques have various limitations. However, a novel method so-called '*all in one forming tool*' was proposed to allow the tool to introduce the pr-defined shapes of structural components (I,J,C and T) with varied dimensions in one single shot.

9.1.3 Modelling and simulation of manufacturing cell

A complete manufacturing cell has been developed and proposed for use in automatic manufacture of the aerospace component. Constituent components of the cell have been modelled and arranged as in the real world, and subsequently stored in an individual data file. Simulation has been carried out for modelled entities in the work environment with different paths. The required tracks were created considering the communication between the individual systems. The cycle time of the process was determined from the simulation studies. The right sequences for the cell elements were created and the required area for the automated cell was calculated.

9.1.4 The manufacturing cell

A prototype robotic assembly cell for composite lay-up has been designed and implemented and assembled for manufacturing aerospace composite structures. The cell comprises:

- Automated cutting table, to cut the required ply shapes from a roll of appropriate material using laser cutter.
- Material bank with a set of pulleys connected to stepper motor through single reduction gearbox for material storage.
- Novel folding device for performing ply folding.
- Material delivery system (MDS), to automatically grab the dry fabric perform from a material roll, feed and lay it up accurately through the folding device.
- Transporter, for delivering the material safely to the final device of the serial line, has been implemented to grab and drag the material to the final stage.
- Collector, to store and introduce the structure when the perform is loaded into the mould.

Automated means have been provided for adjustments in physical dimensions to accommodate the range of structural shapes (I,C,T,J) studied in this thesis.

9.1.5 Cell controller and operation

A cell controller has been designed to control all the cell movements and generate data files for each component, robot control, tacking device, folding device and MDS. The cell controller will generate the necessary control signals to govern the sequential timing of the processes performed.

9.1.6 Optimisation of cell movement

Cell optimisation was performed to overcome the limitation of initial design. As a result of the preliminary tests it was recognised that the torque limit of the motor, which drives the rubber roller, was exceeded. An automatic adjustment device was developed to replace the manual one presented in the first prototype. It was evident that only an automatic adjustment could guarantee that the composite material is fed in a straight way over a long distance.

9.1.7 Optimisation of RTD

Initial trials showed that the RTD causes movement in the ply being tacked. The problem was overcome by reprogramming the controller to switch off the motor that produces back tension in the yarn during the step to the next stitch location.

9.1.8 Optimisation of inter-ply movement

A set of the experiments have been conducted to study the inter ply movement. The results showed that the greatest improvement in joined plies stability occurs when the number of the stitches was increased to five stitches per tack and the stitches were performed parallel to the 0^{o} direction.

9.1.9 Cell performance

The performance of the manufacturing cell has been tested for the different types of deformation, the effect of number of stitches, and plies and edge deviation. Statistical analysis and interpretations, including uncertainty tasks, were performed for all measurements undertaken. It was concluded from the statistical analysis that the cell performance is very repeatable and consistent. These analyses also showed that the tested parameters followed normal distributions. This technique enables an operator to predict the cell performance based on the simple statistical parameters such as mean and standard deviation.

9.1.10 Practical and numerical studies on the reinforcement structure

A set of mechanical experiments were conducted to characterise the mechanical behaviour and damage tolerance of the reinforcement structures. These experimentations were also aimed at studying the effects of the assembly stitches on the behaviour of the whole structure. The mechanical properties were used in FEA to study the behaviour of such structural component. Since the consolidation of the whole structure is rather complex and outside the scope of this thesis, the FEA analysis was particularly useful for parametric study of different geometric parts.

9.2 Contribution to knowledge

9.2.1 New manufacturing methodology for introducing aerospace component

A new manufacturing methodology, termed shape inclusive lay-up has been developed which, enables preforms for 3D components to be produced and stored flat, introducing the shape only when the preform is loaded into the mould. Components with varying degrees of complexity can be manufactured

using this methodology. This methodology enables flat storage of perform, furthermore preforms have infinite shelf life (since dry-fibre materials are used). Other advantages also includes reduction in manufacturing costs and time. Also the resulting parts integration drastically reduce the number of moulding cycles and eliminate the need for bonding.

9.2.2 Design Novel flexible folding device

A novel device has been designed, implemented and incorporated with the manufacturing cell. The mechanism is very flexible in producing a range of aerospace reinforcement structures. The novel concept relies on gradually folding the ply with a device similar to that used in extrusion processes. This technique reduces any stresses on the material and results in minimum damage to the fibre. Moreover, the process in this form is considered to be easily applicable to any number of plies. One of the main advantages of the folding system is that it can be used to produce different shapes of reinforced structures (I, J, C and T sections) as shown Chapter 6. Moreover, variable width mechanisms have been developed to enable automated adjustment of structural dimensions.

9.2.3 Integration of fully automated manufacturing cell

In relation to producing large aircraft components with a limited working area, a fixed manufacturing cell (fixed robot and tables) is unable to provide adequate improvement of the manufacturing cell. The MDS, and the transporter with the folding and the robotic stitching device were integrated to enable the lay-up of 3D preforms while retains their designed shapes. The resulting product can be stored until RTM is applied. The cell is optimised for the NCF material and can be easily readjusted for other materials.

9.2.4 Generic analysis study

A generic numerical analysis study for predicting the behaviour of such structural component has been developed to study the effect of the assembly stitches on the structures.

Flat samples were used to generate experimental data on material properties. FE model of the flat sample was developed and successfully validated against the experimental data. These were then used to develop the main models for (I,C,T,J) structures for further analysis. The FE analysis proved that the stitching operation, which was developed in this thesis for manufacturing process has reduced the load carrying capacity of the reinforcement structures by 8%.

9.3 Further work

In the course of doing this research, the following ideas have occurred which may be worth further research and development:

- It is realised in order to enhance the performance of the cell, the need for new mechanism to hold the RTD must be considered. The new proposed mechanism,Figure 9.1, suggested the use of three tacking devices as a way of replacement of the robot. This due to the fact that of complication involve of using robot, furthermore the high cost of using both robot and the required controller. The proposed system should be fully integrated with the folding device which minimise the space and cost of operation and the time.

- It is recommended that the further work should focus on the development of a more experimental work to produce a series of consolidation reinforcement structures, to be used in a more complicated finite element model to predict the characteristics of the

structures around the stitched areas. It is proposed that the finite element model employed in the present study be used as a basis for such development.

- This thesis has, in the main, covered the assembly of preforms from dry fabrics. In practice, there is a requirement for adding insertions to structural joints to prevent ply distortion during consolidation. Further work is needed to develop automated or semi automated means of adding insertion into structural joints.

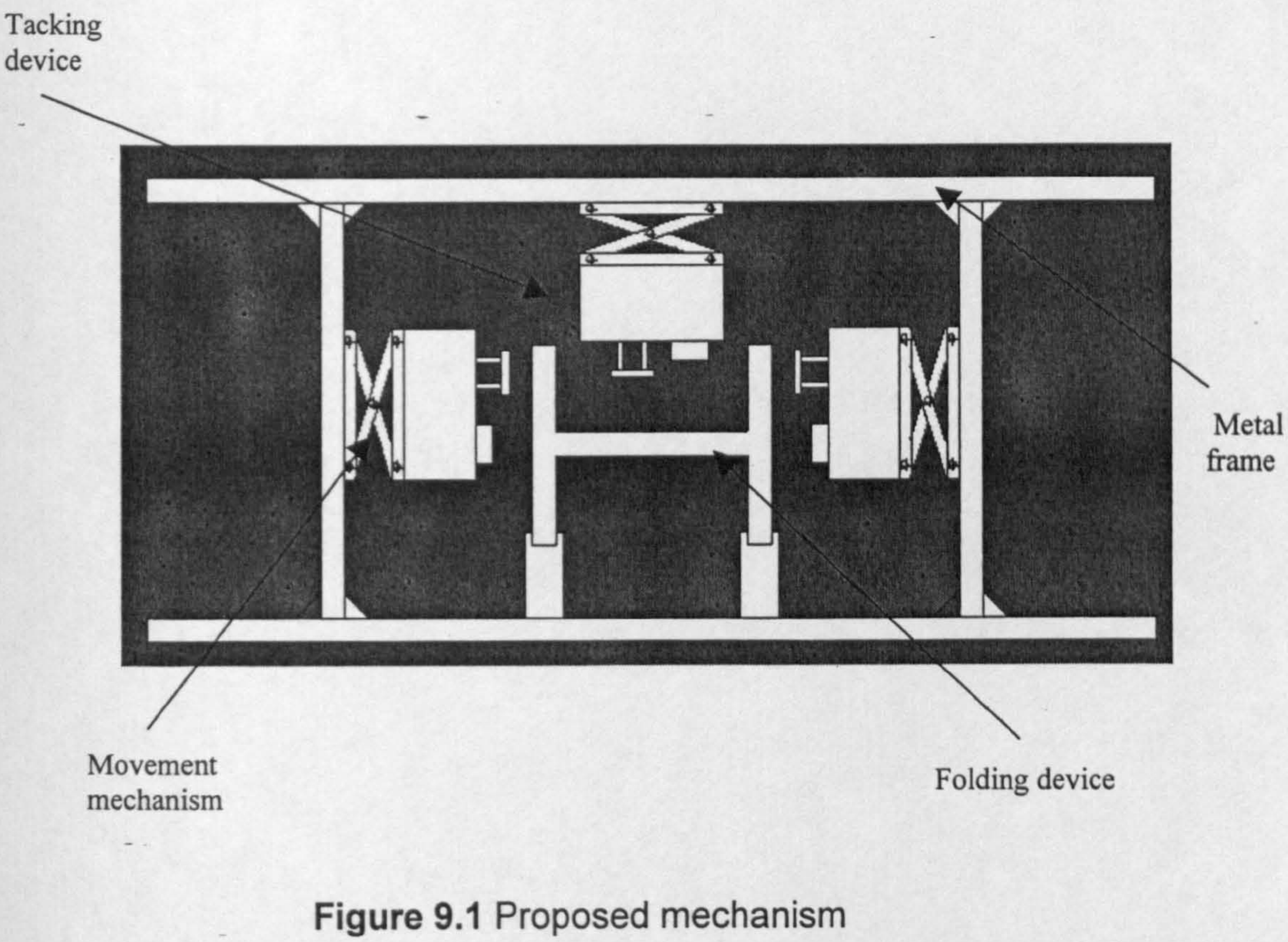

Figure 9.1 Proposed mechanism

References

Agarwol B. D. and Broutman L. J. 1980, Analysis and Performance of Fibre Composites. John Wiley & Sibs,.

Altin N, 2002, GmbH Technology That Forms: Stitching in Time and Space Marketing and Sales Literature, Collected at SAMPE, USA.

Anderson T C and Holzwarth R C , 1998, Design and Manufacture of a Low-Cost Composite-Bonded Wing Collection of Technical Papers - AiAA/ASME/ASCE/AHS/ASC Structures, Structural Dynamics and Materials Conference, Vol. 3, pp 2199-2209.

Andrew M, Graham B, and Rob B, 1999, Innovative Materials and Manufacturing Porcesses for the Cost Effective Manufacture of Composite Airframe Structures International SAMPE Symposium and Exhibition (Proceedings), Vol. 44 (II), pp 2255-2267.

Andrew R, 1996 Mills Manufacturing Technology Development for Aerospace Composite Structures The Aeronautical Journal, Vol.100, No. 1000, pp 539-545.

Arnold, M. R, 1986, Carbon Brakes-Their Development and Service History. World Aerospace Profile, Arthur, ed., Sterling Publ. Ltd. London, pp. 237-239.

Arthur V ,1994, Preliminary Design of an Advanced Technology Composite Wing for a Transport Aircraft 53rd Annual International Conference on Mass Properties Engineering of the Society of Allied Weight Engineers, SAWE Paper No. 2235, Category No. 27.

Bersuch L, Benson R, Owens S, 1998, Affordable Composite Structure for Next Generation Fighters International SAMPE Symposium and Exhibition (Proceedings), Vol. 43, No. 1, pp 56-65.

Bibo G A, Hogg P J, and Kemp M,1997, Mechanical Characterisation of Glass and Carbon-Fibre-Reinforced Composites Made With Non-Crimp Fabrics Composite Science and Technology, 57, pp 1221-1241.

Bibo G A, Hogg P J, Backhouse R and Mills A, 1998, Carbon-Fibre Non-Crimp Fabric Laminates for Cost-Effective Damage-Tolerant Structures Composites Science and Technology, 58, pp 129-143.

Bickerton S and Advani S G, 1997, Experimental investigation and flow visualization of the resin-transfer mould-filling process in a non-planar geometry, Composites Science and Technology 57, pp 23-33.

Brayden, T. H, 1989, Effect of cure cycle parameters on 350 ^{o}F cocured epoxy honeycomb core panels, 34th international SAMPE Symposium, 861.

Buckingham R O, Newell G C, 1996, Automating the Manufacture of Composite Broadgoods Composites - Part A: Applied Science and Manufacturing, Vol. 27, No. 3, pp 191-200.

Chen J., Crisfield M., Kinlock A.J,.Busso E.P, Mathews F.L and Qiu Y.,2000, predicting progressive delamination of composite material specimens via interface elements, mechanics of composite materials and structures, volume 6, pp 301-317.

Chestney J A, 2000, The Use of Electrostatic Force in Automated Manufacture of Composite RTM Preforms MPhil Thesis, Department of Manufacturing and Engineering Systems, Brunel University,

Chestney J A, Moore S J and Sarhadi M,1995, A Methodology for Preforming Three Dimensional Aerospace Components Advanced Composite Letters, Woodhead Publishing, Vol. 4, No. 5, pp137-141.

Chestney J. A. Sarhadi, M. 1996, control and integration techniques in a fully automated manufacturing cell for carbon composites, IEE Proc.-Control theory appl., Vol. 143,No. 2.

Cochran R, Matson C, Thoman S, and Wong D, 1997, Advanced Composite Processes for Aerospace Applications International SAMPE Symposium and Exhibition (Proceedings), Vol. 42, No. 1, pp 635-640.

Corso L M, Popelka D A and Nixon M W, 2000,Design , Analysis, and Test of a Composite Tailored Tiltrotor Wing Journal of the American Helicopter Society, Vol. 45, No. 3, pp 207-215,

Curiskis J I, Bannister M K, and Herszberg I,1997, Manufacture and Analysis of Textile Preforms for Advanced Composite Materials World Conference of the Textile Institute, Proceedings, Vol. 2, pp 280-281.

David j S, Richard F and B,1998, Developing Time Estimating Models for Advanced Composite Manufacturing Processes Aircraft Engineering and Aerospace Technology, Vol. 70, No. 6, pp 445-450.

Dewing, A., Sarhadi, M., Mitchell, T. A. and Eastham, J., 1999, Robotic tacking of high-quality composite preforms, Proc Instn Mech Engrs, Vol. 213,

Dexter H B and Gregory H H,1996, Mechanical Properties and Damage Tolerance of Multiaxial Warp-Knit Composite Composites Science and Technology, 56, pp 367-380.

Dexter H B,1996, Innovative Textile Reinforced Composite Materials for Aircraft Structures 28th International SAMPE Teechnical Conference, Vol 28, pp 404-416.

Didier L, 1997, Recent Advances in Smart Composite Structures in Aerospatiale Proceedings of the US-Japan Workshop on Smart Materials and Structures, pp 273-279.

Edie, D.D,1990 Pitch and Mesophase Fibres, Carbon Fibres, Filaments and Composites, Kluwer Academic Publ., pp. 647-655.

Elaldi F, Lee S, and Scott R F,1995, Manufacture of Composite Panels with J-Shape Stiffeners Materials and Manufacturing Processes, Vol. 10, No. 1, pp 27-36.

El-Amin H, 1981, In Resin Transfer Moulding: Tooling is the key to Success, Plast. Technol.,Vol 27(No.12), Nov, pp97-99.

Ford T, 1998, Continuing Wing Production Aircraft Engineering and Aerospace Technology, Vol. 70, No. 1, pp 9-14.

Fracchia, C. A., Castro, J. and Tucke, C. L., 1995, A finite element/control volume simulation of Resin Transfer Moulding filling, In proc. American society for composites 4th ann. Tech.Conf.

Glaessgen E H, Raju I S, Poe CC, 1999, Delamination and Stitch Failure in Stitched Composite Joints Collection of Techncial Papers - AIAA/ASME/ASCE/AHS/ASC Structures, Structural Dynamics and Materials Conference, Vol. 1, pp 486-507.

Green J E, 2000, The Future of Defense and Aerospace Research: A View From the Front The Aeronautical Journal, Vol 104, No. 1031, pp 39-46.

Harris H., Schinske R, Kruger N, and Swanson, B, 1991, Multiaxial stitched preform reinforcements for RTM fabrication, International SAMP symposium and exhibition, San Diego, California, pp15-18.

Hashim Z., 1983, Analysis of composite materials-a survey, journal of applied mechanics. Vol.50, pp 481-505.

Hickman, G, T., & Williams, D. J., 1988, 3-D knitted preforms for structural reaction injection moulding (S.R.I.M.). How to apply advanced composites technology, ASM international™ , pp. 367-370.

Holzwarth R C , 1998, Structural Cost and Weight Reduction Potential of More Unitized Aircraft Structures Collection of Technical Papers - AiAA/ASME/ASCE/AHS/ASC Structures, Structural Dynamics and Materials Conference, Vol. 3, pp 2218-2227.

Hull D. and Clyde T.W, 1996, an introduction to composite materials, Cambridge solid state science series, Cambridge university press, ISBN: 0 52138 855 1.

Iyer C, 1985, Textiles and composites, 92 Conference proceedings, Tamper, Finland, 138, 1992.

Johnson C F, Chavka N G, and. Houston D. Q,1986, Resin Transfer Moulding of automotive structures, paper 12-A, in proceedings of the 41st SPI annual conference, Society of the Plastics Industry.

Jordan T M, 2003, MPhil Thesis, Brunel university.

Joseph R. deCillis, Carla D. Caputo, 1998, Affordable approaches to the production of complex aerospace composite components via Resin Transfer Moulding, 43rd International SAMPE symposium May 31-Jun4.

Kageyama M and Yoshida S, 2000, Development of XF-2 Fighter Structures (Cocured Composite Wings) Collection of Technical Papers - AIAA/ASME/ASCE/AHS Structures, Structural Dynamics and Materials Conference, Vol. 1, No. 1, pp 301-305.

Karal M and Thrash P, CAD Software and Laser Projection Bring Textile-Industry Technology to Boeings AircraftManufacturing Process Availabel
http://www.nasatech.com/NEWS/rtb.boeing 0125.html.

Karkanas P L, Partridge I K and Attwood D, 1996 Modelling the Cure of a Commercial Epoxy Resin for Resin Transfer Moulding Polymer International, Vol. 41, No. 2, pp183-191.

Ko, frak K., and Kutz, John, 1988, Multiaxial warp-knit for advanced composites, How to apply advanced composites technology, ASM international™ , pp. 377-384.

Ko, frak K., Pastore, C.M., Yang, J. M., and Chou T.W, 1986, structure and properties of multi-directional warp knit fabric reinforced composites, Composites 86,Recent advances in Japan and the United States, Proceeding-Japan-U.S. CCM-III, Tokyo, pp21-28.

Kolax M W, (Deutshce Airbus GmbH, Hamburg, Ger.) Composite Wing Results of Deutsche Airbus Technology Program International SAMPE Symposium and Exhibition, Vol. 37, 1992,

Lee D. E and Hahn H,1995, Applications of Virtual Manufacturing in Composite Airframe Structure_Assembly Proceedings of the American Society for Composites Tenth Technical Conference, pp 32-40.

Li P and Chen X ,1998, Development and Application of Resin Transfer Moulding (RTM) to Aviation Industry Cailiao Gongcheng/Journal of Materials Engineering, No. 1, pp46-48.

Liu B, Bickerton S, and Advani S, 1996 Modelling and Simulation of Resin Transfer Moulding (RTM - Gate Control, Venting and Dry Spot Prediction Composites - Part A: Applied Science and Manufacturing, Vol. 27, No. 2, pp 135-141.

Loos A. C, Macrae J D, Hood D, Kranbuehl D E, and Dexter H B, 1996, Resin Film Infusion (RFI) Process Simulation of Complex Shaped Composite Structures Collection of Technical Papers - AIAA/ASME/ASCE/AHS Structures, Structural Dynamics and Materials Conference, Vol. 3, pp1828-1839.

Loos A. C. and MacRae J D, 1996, Process Simulation Model for the Manufacture of a Blade-Stiffened Panel bu the Resin Film Infusion Process Composites Science and Technology, Vol. 56, No. 3, pp 273-289.

Lubin G. 1982, Handbook of composites, Van Nostrand Reinhold.

Martin, C. J., Putnam, J. W., Seferis, J. C., and Turner, M. J, , 1997, Effect of impregnation conditions on prepreg properties and honeycomb core crush, Polymer Composites.,Vol. 18, No.90.

Martin, C. J., Seferis, J. C. and Wilhelm, M. A., 1996, frictional resistance of thermoset prepregs and its influence on honeycomb composite processing, Composites part A, 27, 943-951.

Mathews F.L., Davies G.A.O., Hitchings D., and Soutis C.,2000, Finite element modelling of composite materials and structures, woodhead Publishing, Cambridge,ISBN 1 85573 422 2.

Mathews F.L., Rawlings R D,1994, Composite materials, engineering and science, Publishing, Chapman and Hall, ISBN 0412 55960 9.

Michaels N. E., Laven J., and Bauer J, RTM-The Right Choice for the 80's, section 15-B, proceedings of the 37th annual conference, Society of the Plastics Industry, 1982, pp 1-16.

Mills A, 200, Automation of Carbon Fibre Preform Manufacturee for Affordable Aerospace Applications Composites - Part A: Applied Science and Manufacturing, Vol. 32, No. 7, pp 955-962.

Mitchell L, Herszberg I, Paton R, and Scott M L , 1993, Design and Manufacture of a Blade-Stiffened Composite Panel Made From a Stitched Preform National Conference Publication - Institute of Engineers, Australia, Vol. 1, No. 93, Pt. 6, pp 115-119.

Mitchell T.A., Chestney, J. A., Sarhadi M, ,1994, a prototype assembly cell for lay-up of carbon composite preforms, robotics & computer integrated manufacturing, Vol. 11,pp335-343

Murman E M, Walton M and Rebentisch E, 2000, Challenges in the Better, Faster, Cheaper Era of Aeronaurical Design, Engineering and Manufacturing The Aeronaurical Journal, Vol. 104, No. 1040, pp 481-489.

Peel C J, 1996, Advances in Materials for Aerospace The Aeronautical Journal, Vol 100, No. 1000, pp 487-506.

Philiip Steggall 1999, Devevloping Multiaxial Non-Crimp Renforcements for the Cost Effective Solution International SAMPE Technical Conference, Vol. 31, pp 341-354,

Pipes R.B. and Pagano N.J., 1970, international stresses in composite laminates under uniform axial extension. Journal of composite material, volume 4, Issue 4, pp 538-549.

Potter K D, 1999, Early history of the Resin Transfer Moulding Process for Aerospace Applications Composites - Part A: Applied Science and Manufacturing, Vol. 30, No. 5, pp 619-621.

Qi B, raju J, Kruckenburg T and Stanning R, A Resin Film Infusion Process for Manufacture of Advanced Composite Structures Composite Structures, Journal of reinforced plastics and Composites, Vol. 21, No. 3, pp255-276, 2002.

Raz S, Mishal N, 1990, innovative technologies in industrial textiles, textile institute conference, Manchester, 5-6 February.

Reavely R , 1998, Design Considerations for RTM Fabricated Components International SAMPE Symposium and Exhibition (Proceedings), Vol. 43, No. 2, pp2031-2042.

Reddy J.N, 1996, a review of refined theories of laminated composite plates, applied mechanics reviews, volume 53, pp 155-199.

Reddy J.N., 1989, On refined computational models of composite laminates, international journal for numerical methods in engineering, Volume 27,pp 361-382.

Renn, D. J., Tulleau, T., Seferis, J. C., Curran, R. N. and Ahn, K. J., 1995, Composite honeycomb core crush in relation to internal pressyre measurement, Journal of advanced materials., 27,31-40.

Ric A, 1998, Damage tolerance evaluation of composite honeycomb structures, 43rd international SAMPE Symposium, May 31-June4,

Ridell, J.C, 1987, Use of composite materials in aerospace applications, proceedings of the BWEA-DEn workshop, E7SU-N-109.

Ridgard C,1997, Affordable Production of Composite Parts Using Low Temperature Curing Prepregs International SAMPE Symposium and Exhibition (Proceedings), Vol. 42, No. 1, pp147-161.

Sarhadi M and Zhang Z, 1999,Materials Modelling and Laser Inspection for the 3D Lay-up of Dry Fiber Composite Preforms Journal of Manufacturing Science and Engineering, Vol 121, No. 3, pp 466-473.

Sarhadi M and Zhang Z,1996, Integrated CAD/CAM System for Automated Composite Manufacture Journal of Materials Processing Technology, Vol 61, No 1-2, pp 104-109.

Sarhadi M, Mitchell T A and Chestney J A, 1994, A Prototype Assembly Cell for Lay-up of Carbon Composite Preforms Robotics and Computer Integrated Manufacturing, Vol 11, No. 4, pp335-343.

Sayers D.R. and Howard R. D, 1985, the potential for mass production with Resin Transfer Moulding using new methacrylate based resins, section 18-B, proceedings of the 40th annual conference, Society of the Plastics Industry, pp 1-5.

Schumacher A and W Becker 1998, Optimised Lay-ups of Composite Laminates for Aircraft Structural Design Proceedings of the International Conference on Computer Methods in Composite Materials, CADCOMP, pp 13-23.

Shaurt M. J., 1989, ailures of compression-loaded multidirictional composite laminates. AIAAJ, 27, pp. 1274-1279.

Shaurt M. J., Short-wavelength buckling and shear failures for compression-loaded composite laminates. NASA TM-87640,

Smichumacher A., and Becker, W, 1998, Optimized lay-ups of composite laminates for airframe structural design, computer methods in composite materials, CADCOMP, pp. 13-23.

Smith F C,1999, Current Status of Resin Infusion as an Enabling Technology for Toughened Aerospace Structures Materials Technology, Vol. 14, No. 2, pp 71-77.

Smith P.A.and Boniface L., 1998, Glass NCF. A comparison of transverse cracking phenomena in (0/90)s and (90/0)s CFRP laminates, applied composite materials, volume 5, pp 11-23.

Smith P.A.and Ogin S.L., 2000 characterisation and modelling of matrix cracking in a (0/90)2s GFRP Laminate loaded in flexture, proceedings Royal society London A, 456, pp 2755-2770.

Swanstrom F M and awkeT H, 2000, Design for Manufacture and Assembly: A Case Study in Cost Reduction for Composite Wing Tip Structures SAMPE Journal, Vol. 36, No. 3, pp 9-16.

Tewfic T and Sarhadi M, 2000, A fully automated manufacturing cell for laying up carbon composite preforms *Systems Engineering Conference*, Brunel University 16-17 September.

Tewfic T, Sarhadi. M and Bahai, H, 2002, Modelling and simulation of a flexible manufacturing cell for aerospace composite structures, *COMADEM International*, Birmingham, 2-4 September, pp419-428.

Tewfic T. and Sarhadi M, 2001, Integration of a robotic cell for the lay-up of large composite performs, *Proceeding of MCPL*, Vol. 2, pp 579-584.

Tewfic T. and Sarhadi, M, 2000, Novel folding device for manufacturing aerospace composite structures, *Proceeding of SPIE* Vol. 4192,pp 212-221.

Tewfic T., Sarhadi M. and H. Bahai, 2002, Investigations of an Automated Cell for Manufacturing Aerospace Composite Structures, *Proceeding of Sampe*,pp140-150.

Thompson B, Patton R, Bennett G, 1994, Composite Preform Sewing System and Stitched Composite Test Results Annual Conference: American Society for Engineering Education, Vol. 2, pp2700-2707,.

Thuis H G S J and Biemans C,1997, Design, Fabrication and Testing of a Composite Bracket for Aerospace, Applications Composite Structures, Vol. 38, No. 1-4, pp 91-98.

Thuis H G SJ,1999, Development of a Composite Cargo Door for an Aircraft Composite Structures, Applications Composite Structures ,Vol. 47, No. 1, pp 813-819.

Tibbetts G.G, 1990, Grown Carbon Fibres, Filaments and Composites, Kluwer Academic Publ., pp 79-94.

Tomblin J S, Tauriello J D, and Doyle S P, 2000, A Composite Material Qualification Method the Results in Cost, Time and Risk Reduction International SAMPE Technical Conference, Vol. 32, pp498-512.

Torsten W and Gordon B, 1997, Carbon-carbon Composites: A Summary of Recent Developments and Applications Materials and Design, Vol. 18, No. 1, pp11-15.

Uchida H, Yamamoto T, and Takashima H, 2001, Development of Low-Cost, Damage-Resistant Composites using RFI Processing, SAMPE Journal, Vol. 37, No. 6, pp16-20.

Voller V.R. and Peng, S., 1995, An algorithm for analysis of polymer filling of moulds. Polym Engng Sci., 35, pp1758-1765.

Wicox K and Sarhadi, M, 1994, investigation into the heat flow characteristics in automated assembly of dry preform. proceeding of Aerotech Seminar 32 on manufacturing options, Birmingham.

Wilks C E and Crosky A,1996, Fabrication of Fibre Reinforced Plastics using Resin Transfer Moulding Materials Forum, Vol. 20, pp207-218.

Wilson S, Wolfgang W, Derek S, and Stephen A, , 1998, Sparc' 5 Axis, '3D' Woven, Low Crimp Preforms 43rd International SAMPE Symposium, Vol 43, pp 1330-1344.

Young, W. B., han, K.,Fong, L.H. and Lee, L.J., 1991, Flow simulation in moulds with preplaced fibre mats. Polym.Comp.,12, ,91-403.

Zienkiewicz O.C.and Taylor R.L., 2000, finite element method, Volume 1, McGraw Hill book,(UK) co, London, ISBN 0 7506 5049 4.

Appendix A Listing of simulation programming

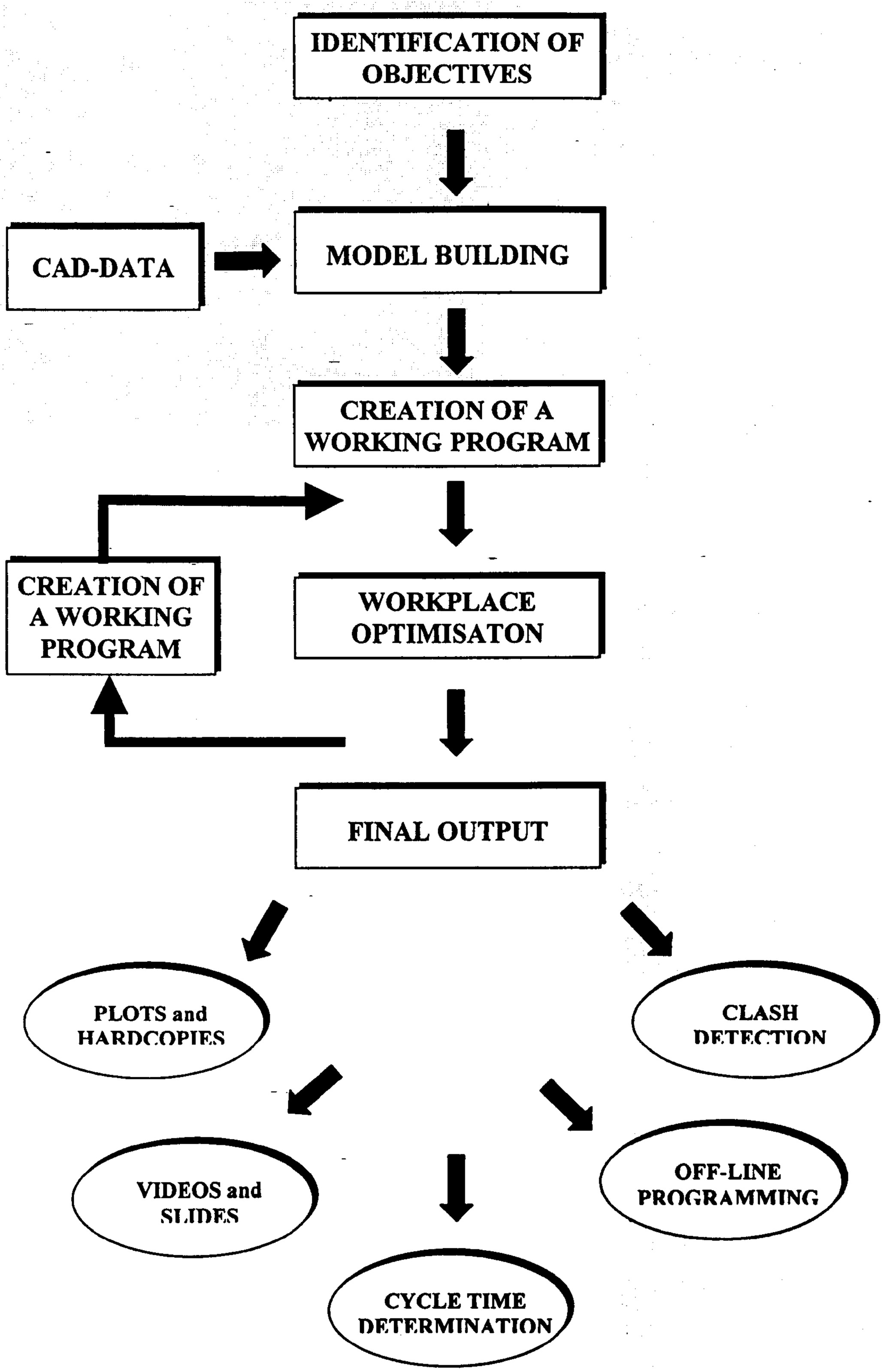

Figure A.1 Simulation stages

A.1 Robot modelling

The modelling of a robot may be divided into three separate stages. In the beginning it is necessary to generate sufficient and accurate information about the particular robot. This information should include dimensioned drawing of every single entity, type, location and orientation of every joint, joint constraint (minimum and maximum values), maximum acceleration and velocities of every joints. If it possible this data should be obtained from the supplier to guarantee accuracy, otherwise the performance the performance characteristics will not match those of the real robot.

The second stage includes the definition of the geometrical properties. The required data input can only be using the textural input method, besides of this it is necessary to enter the number of robot joints, their relative position, joint type and maximum and minimum constraints. It should be noticed that the location of each joint refers to the previous defined joint.

The tool attachment point (TAP) forms the end of the joint arrangement. This would normally be a central point at the end of the robot arm where a tool will be mounted. There are two different types of joints available in the Grasp 2000. The revolute joint allows rotation about a defined axis, and the prismatic joint is able to preform in a translated way.

A.2 Tracks

Tracks are the programs in the Grasp 2000, which defines how a robot or entity should perform movements within a Grasp 2000. The tracks can be created edited and replayed and they are made of a sequence of instructions, called steps. These steps are usually unnamed, but if desired every step may get an individual name. This option is sometimes quite useful especially when working with a few particular commands. A track is not associated with a particular robot or entity. This offers the possibility to test various robots for a specific manufacturing task.

Position steps in tracks is stored relative to named objects, therefore by careful programming, a work cell layout can be altered and the track will still perform the programmed task, thus alternative cell layout may be quickly and easily evaluated without need for reprogramming.

In the Grasp 2000 it is possible to drive/control several robots simultaneously, each of them performing a different track. Usually main program is used as the foreground track and all other required tracks are defined as background tracks. The background are also able to communicate with other background or foreground tracks via signals, furthermore it is possible to switch on as many background tracks as required at the same time.

In addition background facilities allows existing robot or object programs to be active while a new one is created. In this way all activity will be displayed as new steps and added to the current track. It is therefore possible to avoid problems of synchronisation within the cell while programming.

Creating tracks may be done using the TRACK menu. Although the general procedure for creating tracks will depend on the model type, a common way for creating a track can be described as follows:

In the beginning it is necessary to plan an overall strategy for the simulation process and all the required tracks should be identified. Then it has to find out if interaction and communication occurs between the single tracks and if necessary global variables have to be defined.

In the next stage the single tracks may be created step by step. Therefore the structure of individual tracks has to be defined, local variables should be detected and defined, and each position step has to be determined/set. If required the "unknown position" option can be used. All these considerations lead to a track in textural source file format. After all the

tracks are defined they can be read into the Grasp 2000 and modified interactively if necessary.

In the final stage the communication and interaction between the foreground and background tracks have to be checked and required optimisations may be carried out.

Once the track has been created, it can be played back. Firstly the track has to be initialised, because if the track has just been created, the current step will be the final position. To override this state the INTIALISE command has to be used.

The Grasp 2000 also offers the opportunity to display the performed track. To receive such a trace the "Creat_Trajectory" command has to be used and a trace has to be defined for the required entity, TCP or robot joint. After that the trajectory has to be activated in the "Track_Setup" menu.

A.3 Process

Once a track has been programmed, it may be transferred into process. A process is a track on a continuous time base. In contrast to a track it does not contain any steps or paths, which can be altered or optimised it only contains information which describes how the joints of a robot or entity move as a function of time.

A process is stored absolutely, and positions are not calculated each time when the process is replayed, this feature allows to replay processes faster than the tracks. For that reason if changes in the work cell has been done a process has to be recreated. It is only contained one version of all the playbacks, which are available in a track, whereas a track is programmed using high level facilities and many alternative ways of execution may be carried out/performed.

Creating a process is quite simple. After choosing the required foreground track and using the DUMP_PROCESS command the system prompts the user to enter a name for the process. Additionally, a sequence of queries has to be answered with [YES] or [NO] afterwards the steps are calculated using the joint velocities and accelerations specified in the path definition.

Processes are replayed in the ANIMATION menu using the RUN command, thereby the process to be replayed has to be the current process and information such as target time and refreshing interval have to be entered into a data form. Processes are mainly used for collision detection and fast replay of programs. Individual processes may be combined and all replayed at the same time. A process is only a special part of a track.

A.4 Hidden line removal and plot creation

All the models in the Grasp 2000 are created in wire frame mode, but especially when a lot of models are arranged in the working area it is sometimes difficult to assign lines to the owning models. The HIDDEN_LINE command suppress the covered lines and helps to clarify the display view. These plots can be stored within the program and redisplayed. It is also possible to replay tracks in hidden lines removal mode and store them in a process. In addition the Grasp 2000 also provide solid shading of models, thereby several light sources may be defined and easily modified within the work cell. Like in hidden lines mode it is also possible to store display view and full tracks can be replayed and stored in a process.

Producing plots in the Grasp 2000, the PLOT command has to be used. It is not possible to alter the current arrangement of the models within the plot menu, so all configurations have to be made before. Plots with removed hidden lines have to be created in the Hidden Line mode first of all and then the PLOT command has to be entered to produce the picture. After the PLOT command is entered the Grasp 2000 prompts for the required plot file

format in which the plot file should be output. There are two formats available, the Grasp 2000 format (GRDATA) and the DXF-format.

A.5 Clash detection

Crashes of robots with the environment are the worst situation, which can occur in a robot application. The robots not only harmfully affect humans but also they might end up with defects in the drive system, leading to lack of accuracy, which cannot be repaired.

Task simulations of robot applications in the Grasp 2000 offer the possibility to avoid such hazards in advance. Sometimes it is quite difficult and time consuming to recognise on the display if objects have collide in the space or not. To overcome these problems the Grasp 2000 contains facilities to detect clashes between objects in the workplace. There are two different types of clash detection available in the Grasp 2000.

The "Static_Clash_Detection" offers the ability to carry out collision checks at a particular instant of time. The system asks for the names of the two models, which should be checked and for a minimum clearing distance between these objects in millimeters. If the selected objects are within this defined distance then entities will flash and an appropriate message appears on the screen.

On the other hand the "On_Line_Clashdetection" checks for clashes while objects are being moved in the workplace. This kind of detection is quite useful for checks for collisions while creating a program, or to examine a finished program for unrecognised clashes. In contrast to the static clash detection, where only a single configuration is verified, the whole application is inspected for possible crashes.

A.6 Calibration

Calibration is a very important step before using the off-line programming features of the Grasp 2000. It ensures that the position and orientations of the modeled work cell match the positions and orientations of the reality.
The calibration of a model is carried out in two separate steps. In the beginning features have to be specified. In the model a set of features such as vertices, edges, faces has to be defined. These definitions are used to calibrate the positions of the modeled objects in the real work area.

In the second stage the defined feature of the modeled environment have to be adjusted accordingly to the measured data of reality. Thereby the reality has to be measured and enter this data into the Grasp 2000. The Grasp 2000 compares the entered data with the modeled work cell and if required it moves the modeled objects to positions which best fits all the measured data for the specified features. The Grasp 2000 optimise the modeled work cell to produce an accurate picture of the reality.
The calibration command is an essential aid to enable practical off-line programming.

A.7 Off-line programming with the Grasp 2000

After the simulation work has done as required and calibrated, the off-line programming option of the Grasp 2000 can be used to generate a neutral format “Grdata” file using the “Postprocess” command. This “Gradata” file, written in a high level textural programming language, may then be post processed for the target robot controller.

Appendix B Cell Controller Codes

```
/*************************************************************************** */
/*                                                                          * */
/* Program to stitch single tacks (uses COM1 for RTD and COM2 for Fanuc)    * */
/*                                                                          * */
/*************************************************************************** */

/*************************************************************************** */
/*                                                                          * */
/* Header files and definitions begin here                                  * */
/*                                                                          * */
/*************************************************************************** */

#include <stdio.h>
#include <string.h>
#include <stdlib.h>
#include <stddef.h>
#include <signal.h>
#include <conio.h>
#include <math.h>
#include <bios.h>
#include <dos.h>
#include <new.h>
#include <fcntl.h>
#include <errno.h>
#include <io.h>
#include <sys\stat.h>
#include <iostream.h>
#include <fstream.h>
#include <process.h>
#include "c:\tarik\cellfile.h"

// fix to ensure floating point is loaded
// see Borland C++ DOS reference, page 29

#pragma extref _floatconvert

// A little Syntax Sugar

typedef unsigned char byte;
typedef unsigned char* bptr;
typedef unsigned short word;

// General Defs

const return_key = 13;
const double ROOT_2 = 1.414213562;
const double PI = 3.141592654;
#define TRUE 1
#define FALSE 0

// Ply Thickness in Fanuc Coords for Tacking

const tack_thickness = 1.3; // Fanuc units

// Fanuc Defs

const FANUC_DEL    = 25;
const RAD_TO_DEG   = 57.29578;
```

```
#define MREL            50
#define POS             51
#define FEOT            52
#define FENQ            53
#define FACK            54
// #define ANGL            55
#define DOWN            56
#define NEXT            57
// #define LASER_DEL   50
const HT_PER_TACK  = 4.5; // height between stitches in mm, was 6
const ST_PER_TACK  = 5;   // number of stitches per tack
const SP_PER_TACK  = 3.0; // distance between stitches in tack in mm
int st_per_tack = ST_PER_TACK;
double ht_per_tack = HT_PER_TACK, sp_per_tack = SP_PER_TACK;
int RTD_fault;
#define Max_no_of_tacks 50
const st_base = 136.0;

struct fanuc_cal {
        double x;
        double y;
};

// Stitch Defs

const status_report  = '0';
const local_sensor   = '1';
const normal_stitch  = '2';
const finish_stitch  = '3';
const R_flag         = 0x01;
const S_flag         = 0x02;
const U_flag         = 0x04;
const Y_flag         = 0x08;
const Z_flag         = 0x10;
const failed_to_home = FALSE;
const stitch_aborted = FALSE;
const needle_fault   = FALSE;
const yarn_fault     = FALSE;
const head_in_air    = FALSE;
const head_on_deck   = Z_flag;

void read_layup_calibration_file(struct layup_mapping *);
void map_lt_to_robot_double(struct layup_mapping, double, double, double *, double *);

/*************************************************************************** */
/*                                                                          * */
/* BIOS Code begins here                                                    * */
/*                                                                          * */
/*************************************************************************** */

byte com1_read(void)
{
        byte data;
        int status;
        status = bioscom(2, 0, 0);
        data = (status & 0xff); // 8 lsbs are data
        if ((status & 0xff00) != 0) {
                printf("read comms error!\n");
                getch();
        }
```

```
        return data;
}

byte com1_status(void)
{
        int status;

        status = bioscom(3, 0, 0);
        return (status & 0xff00);
}

void com1_write(byte data)
{
        int status;

        status = bioscom(1, data, 0);
        if ((status & 0x00) != 0) {
                printf("write comms error!\n");
                getch();
        }
}

void init_com1(int verbose)
{
        int status;

        // set up COM1
        status = bioscom(0, 0xe7, 0);
        if (((status & 0x00) != 0) && verbose) {
                gotoxy (5,20); printf("Initialisation Error!");
        }
}

byte com2_read(void)
{
        byte data;
        int status;

        status = bioscom(2, 0, 1);
        data = (status & 0xff); // 8 lsbs are data
        if ((status & 0x00) != 0) {
                printf("read comms error!\n");
                getch();
        }
        return data;
}

void com2_write(byte data)
{
  int status;

  status = bioscom(1, data, 1);
  if ((status & 0x00) != 0) {
    printf("write comms error!\n");
    getch();
  }
}

void init_com2(int verbose)
{
```

```
  int status;

  // set up COM1
  status = bioscom(0, 0xe7, 1);
  if (((status & 0x00) != 0) && verbose) {
    gotoxy (5,20); printf("Initialisation Error!");
  }
}

/*****************************************************************************/
/*                                                                           */
/* Fanuc and RTD Code begins here                                            */
/*                                                                           */
/*****************************************************************************/

//
// Code to control the Fanuc directly
//

void fanuc_write(byte c)
{
  delay(100);
  com2_write(c);
}

byte fanuc_read(void)
{
  return com2_read();
}

double int_to_real(long x)
{
  double val = 0.0;
  double val1 = 0.0;

        val = pow(2.0, (((x & 0x7f800000) >> 23) - 0x7f));
        val1 = (((double)(x & 0x7fffff) / 0x800000) * val);
        val += val1;
        if (x & 0x80000000) val = (0 - val);
        return val;
}

double read_real(void)
{
  long long_int = 0;
  long array[4] = {0, 0, 0, 0};

  for (register i = 3; i > -1; i--) array[i] = fanuc_read();
  long_int = (array[3] << 24) + (array[2] << 16) + (array[1] << 8) + array[0];
  return int_to_real(long_int);
}

void real_to_int(double val, long array[])
{
  double tmp = 0.0;
  int power, sign;
  long fract;

  if ((fabs(val) > 1.175494E-38) || (fabs(val) < 3.4028236E+38) || (val == 0)) {
    for (register i = 128; ((pow(2.0, i) > fabs(val)) && (i > -127)); i--);
```

```
    power = i;                          // power is the power of 2
    tmp = pow(2.0, (double)power);
    fract = (double)((((fabs(val) - tmp)/tmp) * 0x7fffff) + 0.5);  // fract is the fractional part
    if (val < 0) sign = 1; else sign = 0;          // get sign
    array[3] = ((sign << 7) | (((power + 127) & 0xfe) >> 1));
    array[2] = (((power + 127) & 0x01) << 7) + ((fract & 0x7f0000) >> 16);
    array[1] = ((fract & 0xff00) >> 8);
    array[0] = (fract & 0xff);
  }
  else {
    gotoxy(5,13);
    printf("\aReal value out of range!");
    }
}

void send_real(double val)
{
  long array[4] = {0, 0, 0, 0};

        real_to_int(val, array);
  for (register i = 3; i > -1; i--) fanuc_write(array[i]);
}

void get_pos(struct fanuc_pos *the_pos) // NB all thetas in DEGREES
{
  double array[4];

  gotoxy(5,11); printf("                    "); // y was 13
  gotoxy(5,11); printf("Getting Position...      ");
  fanuc_write(POS);
  while (fanuc_read() != FACK);
  delay(100);
  fanuc_write(FACK);
  for (register i = 0; i < 4; i++) {
    array[i] = read_real();
    delay(50);
    if (i < 3) fanuc_write(FACK);
  }
  fanuc_write(FACK);
  the_pos->x = array[0];
  the_pos->y = array[1];
  the_pos->z = array[2];
  the_pos->theta = array[3];
  for (i = 0; i < 4; i++) {
    gotoxy(5, (14+i));
    printf("%d is %lf", i, array[i]);
  }
  gotoxy(5,11); printf("                    ");
}

void move_rel(struct fanuc_pos vector) // NB all thetas in DEGREES
{
  gotoxy(5,11); printf("                    "); // y was 13
  gotoxy(5,11); printf("Move Relative...      ");
  fanuc_write(MREL);
  while (fanuc_read() != FACK);
  delay(100);
  gotoxy(5,14); printf("x is %lf", vector.x);
  gotoxy(5,15); printf("y is %lf", vector.y);
  gotoxy(5,16); printf("z is %lf", vector.z);
```

```
  gotoxy(5,17); printf("t is %lf", vector.theta);
  send_real(vector.x);
  send_real(vector.y);
  send_real(vector.z);
  send_real(vector.theta);
  while (fanuc_read() != FACK);
  gotoxy(5,11); printf("                    ");
  gotoxy(5,11); printf("Movement completed."); // y was 13
}

void move_abs(struct fanuc_pos to_point) // NB all thetas in DEGREES
{
  struct fanuc_pos from_point, vector;

  gotoxy(5,13); printf("                    ");
  gotoxy(5,11); printf("Move Absolute...    ");
  get_pos(&from_point);
  vector.x = to_point.x - from_point.x;
  vector.y = to_point.y - from_point.y;
  vector.z = to_point.z - from_point.z;
  vector.theta = to_point.theta - from_point.theta;
  gotoxy(5,11); printf("                    ");
  move_rel(vector);
}

void index(double x, double y, double ht)
{
  gotoxy(5,11); printf("                    "); // y was 13
  gotoxy(5,11); printf("Indexing to next point...");
  fanuc_write(NEXT);
  while (fanuc_read() != FACK);
  delay(100);
  send_real(x);
  send_real(y);
  send_real(ht);
  gotoxy(5,11); printf("Sent the data...     ");
  while (fanuc_read() != FACK);
  gotoxy(5,11); printf("                    ");
  gotoxy(5,11); printf("Movement completed."); // y was 13
}

void move_down(void)
{
  gotoxy(5,11); printf("                    "); // y was 13
  gotoxy(5,11); printf("Moving Down a bit...  ");
  fanuc_write(DOWN);
  while (fanuc_read() != FACK);
  gotoxy(5,11); printf("Movement completed.   ");
}

void fanuc_quit(void)
{
  fanuc_write(FEOT);
  while (fanuc_read() != FACK);
}

//
// Re-write of Rubbishy stitch head code
//
```

```
inline byte write_read_status(byte stitch_type)
{
  int input_val = 0, more_data=0;

  gotoxy(46,3); printf("%d   ", com1_status());
  while (com1_status() & 0x100) {
    gotoxy(46,3); printf("\a%d   ", com1_read());
    getch();
  }
  com1_write(stitch_type); // Write stitch type
  do {
    input_val = com1_read();   // Receive Status
    more_data = (com1_status() & 0x100);
  } while (more_data);
  gotoxy(46,3); printf("%d   ", input_val);
  return input_val;
}

void lower_head(void)
{
  gotoxy(20,20); printf("Lowering head to deck");
  while ((write_read_status(status_report) & Z_flag) == head_in_air) {
    gotoxy(20,20); printf("Going Down down down ");
    move_down();
    delay(100);
  }
  delay(100);
  write_read_status(local_sensor); // !!! addition to try to maintain sequencing
  gotoxy(20,20); printf("                    ");
}

int check_for_stitch_fault(byte stitch_flags)
{
/*  if ((stitch_flags & S_flag) == stitch_aborted) {
    gotoxy(35, 11); printf("\aStitch Fault");
    return TRUE;
  } else return FALSE;
*/ return FALSE;
}

int check_for_machine_fault(byte stitch_flags)
{
/*        int fault = FALSE;

  if ((stitch_flags & R_flag) == failed_to_home) {
    gotoxy(35, 7); printf("Failed To Home");
    fault = TRUE;
  }
        if ((stitch_flags & U_flag) == needle_fault) {
  gotoxy(35, 8); printf("Needle Fault");
  fault = TRUE;
}
        if ((stitch_flags & Y_flag) == yarn_fault) {
  gotoxy(35, 9); printf("Yarn Fault");
  fault = TRUE;
}
if (fault) {
  gotoxy(35, 5); printf("\aMachine Fault:");
  gotoxy(35,11); printf("RESET RTD CONTROLLER");
}
```

Appendix C Statistical analysis data

C.1 Evaluation and expression of measurement uncertainty

- The objective of measurement is to determine the value of the measurand that is the value of the particular quantity to be measured.
- In general, the result of a measurement is only an approximation or estimate of the value of the measurand and thus is complete only when accompanied by a statement of the uncertainty of that estimation, Figure C-1.
- Traditionally, an error in the measurement result is viewed as having two components, namely, a random component and systematic component. Random error arises from variations in repeated measurements. And a systematic error arises from the imperfect correction of systematic effects.
- The uncertainty of the result of a measurement generally consists of several components which may be grouped into two types according to the method used to estimate their numerical values:

  Type A - those which are evaluated by the statistical methods, Type B – those which are evaluated by other means.

  There is no always a simple corresponding between the classification of uncertainty components into categories A and B and the commonly used classification of uncertainty components as "random" and "systematic". The nature of an uncertainty component is conditioned by the use made of the corresponding quality, that is, how that quantity appears in the mathematical model that describes the measurement process.

C.1.1 Type A evaluation of standard uncertainty

Type A evaluation of standard uncertainty is based on any valid statistical method in analysis of series of observations. Components of type A evaluation of standard uncertainty arising from random effect. The Gaussian or Normal law of error forms the basis of the analytical study of random effects. In most cases, the best available estimate of the expected value of a quantity q that varies randomly, is the arithmetic mean $\overline{q}$. Figure C-2, illustrate the flowchart for evaluation uncertainty of measurement of type A.

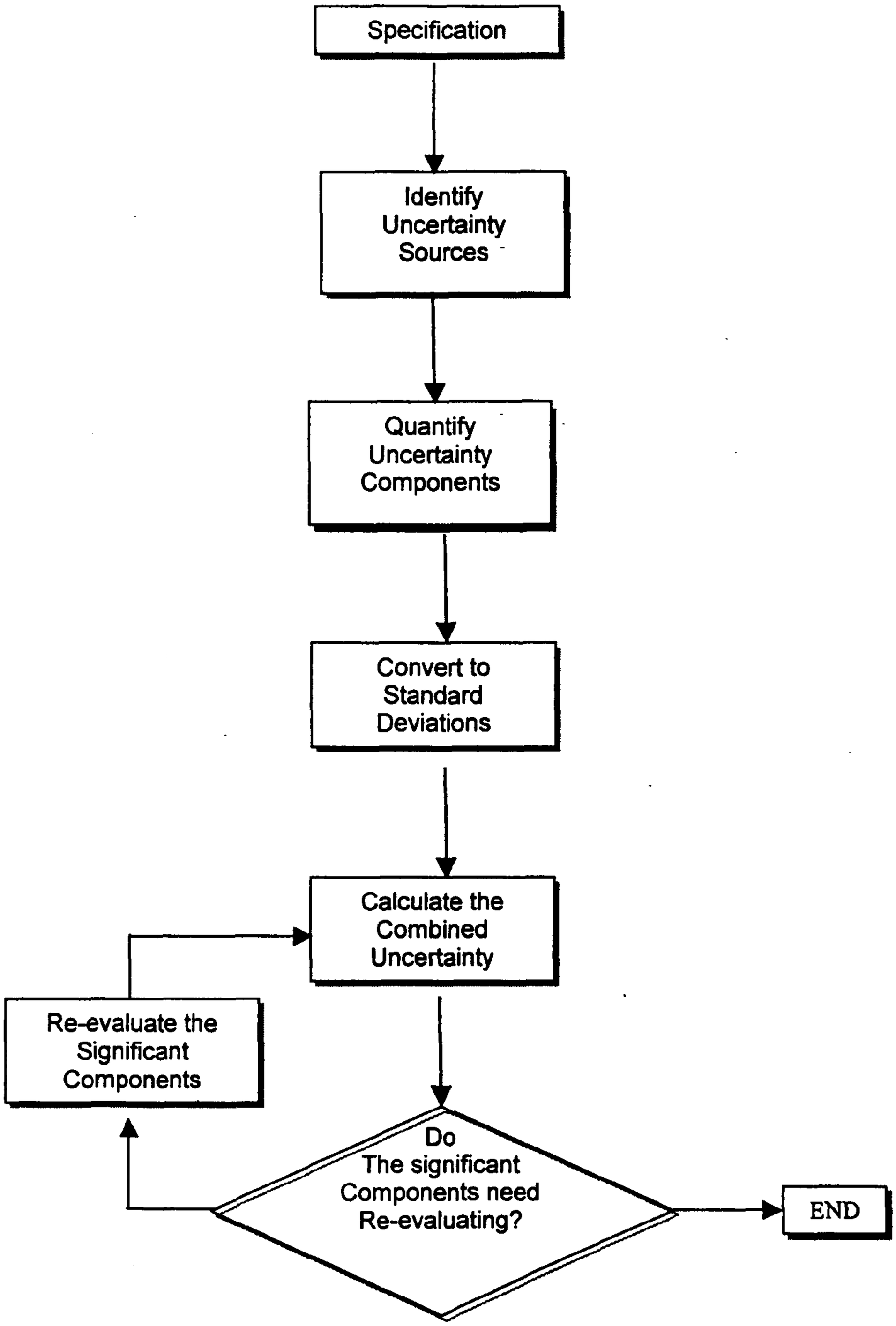

Figure C.1 Uncertainty estimation process flow chart

C.1.2 Type B evaluation of standard uncertainty

Type B evaluation of standard uncertainty ,Figure C.3. is obtained by means other than the statistical analysis of a series of observations. it is usually based on scientific judgement using all relevant information available, which may include:

- instruments manufacture's specification
- data provided in calibration and other reports and
- uncertainties assigned to reference data taken from data book.

C.2 Combining standard uncertainties

Individual standard uncertainties calculated by type A or type B evaluations can be combined validly by 'summation in quadrature'. The result of this is called the *combined standard uncertainty* u_c.

Summation in quadrature is simplest where the result of a measurement is reached by addition or subtraction. The more complicated cases can also applied for the multiplication and division of measurements as well as for other functions.

C.3 Coverage factor k

Having scaled the components of uncertainty consistently, to find the combined standard uncertainty, it may then want to re-scale the result. The combined standard uncertainty may be thought of as equivalent to 'one standard deviation'. But it may wish to have an overall uncertainty stated at another level of confidence, e.g. 95 percent. This re-scaling can be done using a *coverage factor, k.* multiplying the *combined standard uncertainty* u_c,by a *coverage factor* gives a result which is called the *expanded uncertainty*, usually shows by the symbol *U*, i.e.

$$U = k\, u_c$$

A particular value of coverage factor gives a particular confidence level for the expanded uncertainty.

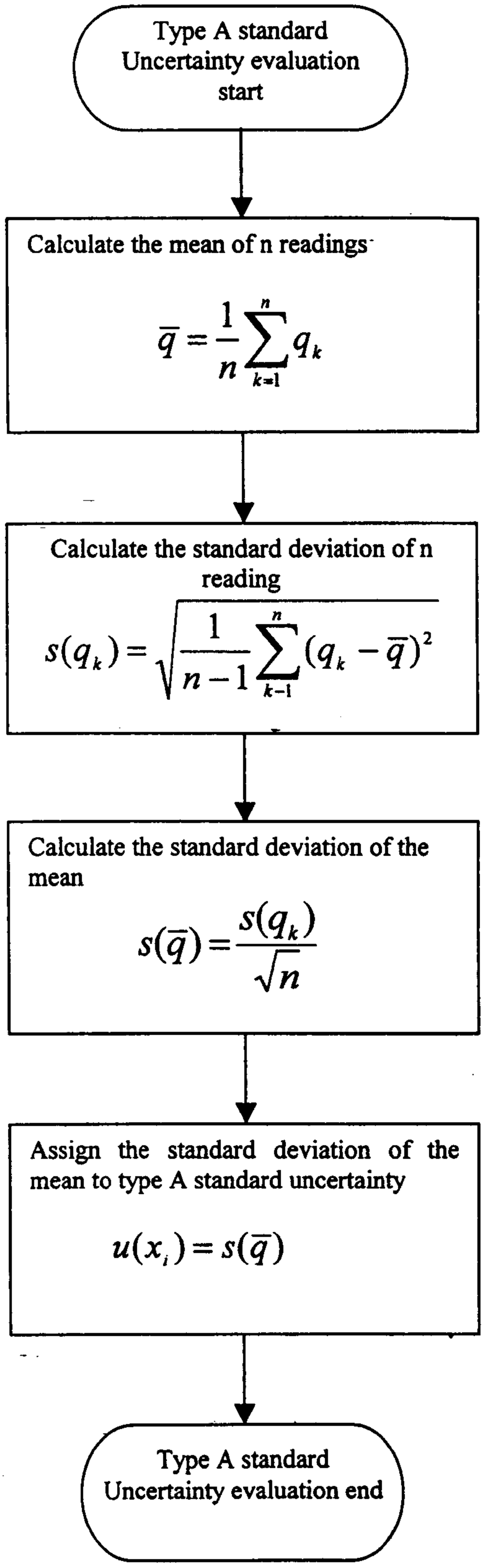

Figure C-2 Flow chart for evaluating uncertainty type A

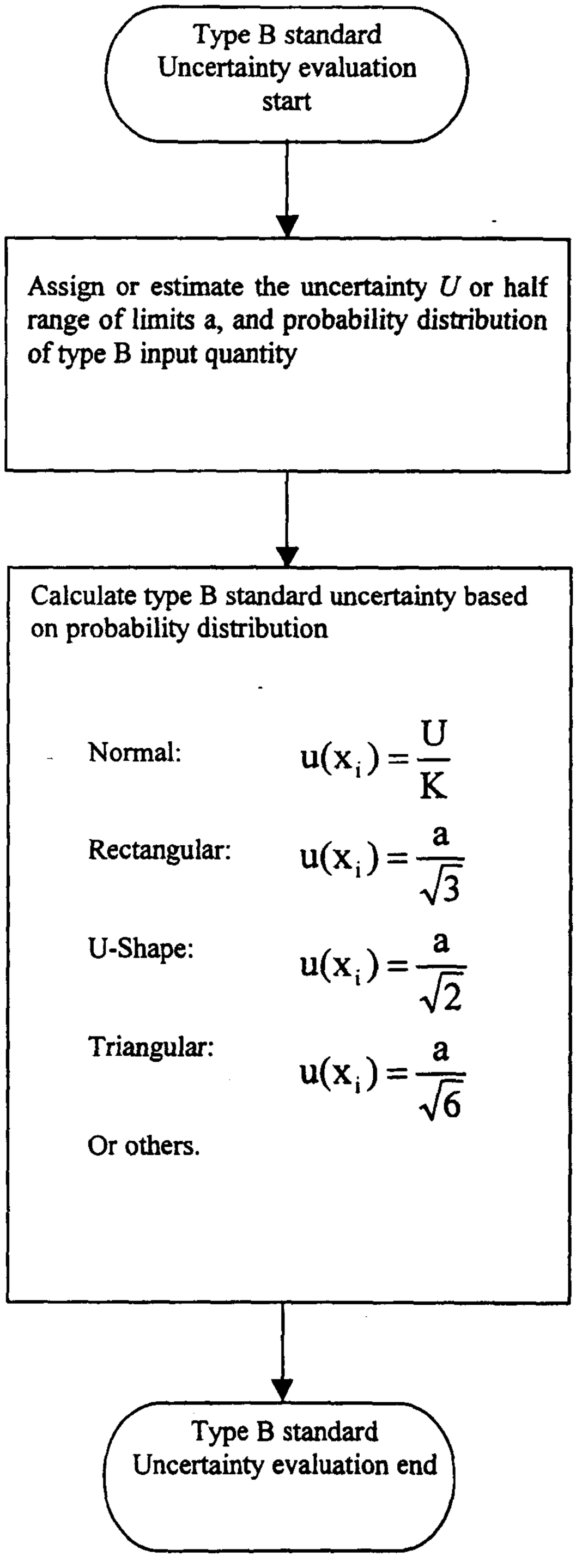

Figure C.3 evaluating uncertainty type B flow chart

Table C.1. Examined parameters for cell performance

Longitudinal deformation	Trans_ deformation	Difference In edge position		Upp_mid_ ply	Lower_mid_ ply	Upp.edges dev	Lowrer edges dev
0.53	0.66	3 stitches	5 stitches	0.95	0.6	0.71	0.39
0.45	0.72	1.05	0.6	0.81	0.52	0.61	0.34
0.4	0.65	1.6	0.52	0.72	0.4	0.54	0.26
0.61	0.68	1.08	0.46	1.08	0.69	0.81	0.45
0.95	1.04	1.22	0.7	1.71	1.1	1.28	0.72
0.55	0.72	1.85	1.09	0.99	0.63	0.74	0.41
0.44	0.65	1.15	0.63	0.79	0.42	0.59	0.27
0.58	0.68	1.44	0.51	1.04	0.66	0.78	0.43
0.65	0.74	1.18	0.66	1.17	0.75	0.88	0.49
0.77	0.9	1.3	0.74	1.38	0.88	1.04	0.57
0.68	0.76	1.52	0.88	1.22	0.72	0.92	0.47
0.45	0.66	1.36	0.78	0.81	0.4	0.61	0.26
0.8	1.1	1.2	0.52	1.44	0.92	1.08	0.60
0.5	0.78	1.6	0.92	0.9	0.4	0.68	0.26
0.66	0.74	1.5	0.58	1.2	0.76	0.90	0.49
0.69	0.78	1.32	0.7	1.24	0.79	0.93	0.51
0.7	0.82	1.38	0.78	1.26	0.8	0.95	0.52
0.48	0.65	1.4	0.8	0.86	0.45	0.65	0.29
0.41	0.82	1.2	0.55	0.73	0.41	0.55	0.27
0.4	0.94	1.3	0.46	0.72	0.46	0.54	0.30
0.59	0.95	1.2	0.46	1.1	0.7	0.83	0.46

Longitudinal deformation	Trans_ deformation	Difference In edge position		Upp_mid_ ply	Lower_mid_ ply	Upp.edges dev	Lowrer edges dev
0.49	0.86	1.18	0.62	0.88	0.56	0.66	0.36
0.45	0.68	1.1	0.56	0.81	0.46	0.61	0.30
0.5	0.77	1.35	0.52	0.9	0.57	0.68	0.37
0.53	0.66	1	0.57	0.95	0.6	0.71	0.39
0.89	1.05	1.06	0.6	1.6	1.1	1.20	0.72
0.85	0.96	1.78	1.09	1.53	0.97	1.15	0.63
0.58	0.65	1.7	0.97	1.08	0.69	0.81	0.45
0.54	0.82	1.16	0.66	0.98	0.62	0.74	0.40
0.42	0.69	1.08	0.62	0.76	0.42	0.57	0.27
0.44	0.96	1.24	0.48	0.8	0.5	0.60	0.33
0.48	0.81	1.55	0.51	0.86	0.55	0.65	0.36
0.92	1.08	1.65	0.55	1.68	1.08	1.26	0.70
0.85	0.96	1.84	1.06	1.53	0.97	1.15	0.63
0.66	0.75	1.7	0.97	1.18	0.75	0.89	0.49
0.52	0.65	1.32	0.75	0.96	0.62	0.72	0.40
0.48	0.72	1.04	0.55	0.86	0.48	0.65	0.31
0.72	0.81	0.96	0.56	1.3	0.83	0.98	0.54
0.49	0.68	1.44	0.83	0.88	0.56	0.66	0.36
0.95	1.07	0.98	0.57	1.71	1.09	1.28	0.71
0.4	0.67	1.85	1.1	0.72	0.4	0.54	0.26
0.5	0.65	1.46	0.46	0.9	0.58	0.68	0.38
0.42	0.88	1	0.52	0.76	0.48	0.57	0.31
0.78	0.88	1.72	0.48	1.4	0.89	1.05	0.58
0.69	0.78	1.56	0.89	1.25	0.8	0.94	0.52
0.8	0.9	1.38	0.79	1.44	0.92	1.08	0.60

Longitudinal deformation	Trans_ deformation		Difference In edge position	Upp_ply dev	Lower_ply dev	Upp.edges dev	Lowrer edges dev
0.54	0.8	1.6	0.92	0.97	0.62	0.73	0.40
0.43	0.69	1.08	0.62	0.77	0.49	0.58	0.32
0.85	0.96	1.24	0.46	1.53	0.97	1.15	0.63
0.6	0.68	1.7	0.97	1.08	0.69	0.81	0.45
0.42	0.77	1.2	0.69	0.79	0.5	0.59	0.33
0.55	0.82	1.66	0.48	0.99	0.65	0.74	0.42
0.66	0.75	1.1	0.63	1.25	1.1	0.94	0.72
0.4	0.66	1.32	0.75	0.7	0.44	0.53	0.29
0.85	0.96	1.15	0.46	1.53	0.98	1.15	0.64
0.82	0.93	1.7	0.97	1.45	0.92	1.09	0.60
0.72	0.81	1.64	0.94	1.26	0.8	0.95	0.52
0.44	0.65	1.44	0.8	0.79	0.51	0.59	0.33
0.55	0.7	1.34	0.5	0.99	0.63	0.74	0.41
		1.1	0.62				